Neutrophils in Respiratory Syncytial Virus Infection

A thesis submitted for the degree of Doctor of Philosophy

to

Imperial College London

Freja Kirsebom

Section of Respiratory Infections

National Heart and Lung Institute

Imperial College London

Declaration of Originality

This is to certify that to the best of my knowledge, the content of this thesis is my own work. This thesis has not been submitted for any degree or other purposes. I certify that the intellectual content of this thesis is the product of my own work and that all the assistance received in preparing this thesis and sources have been acknowledged.

Copywrite Declaration

Acknowledgements

First of all, my greatest thanks go to my supervisor Cecilia Johansson for her guidance and support throughout my PhD. Cecilia's positivity and enthusiasm provided constant momentum and I feel very fortunate to have been able to undertake my PhD in a such a supportive and encouraging environment where I have always been able to ask for advice and help - scientific and otherwise.

I also want to thank the present and past members Cecilia's group, especially Fahima Kausar and Rinat Nuriev whose experimental work contributed to these studies. Thank you to all the other students who I have shared office and laboratory space with; in particular David Swieboda, Sophie Sagawe, Kornelija Suviezdyte, Kate Strong, Anabel Guedán and Inne Nauwelaers.

I also wish to thank my internal thesis committee assessors Rob Snelgrove and James Harker for their constructive feedback and scientific suggestions during my early and late stage assessments. Especially thank you to James for sharing the FTY720 protocol. I wish to thank Max Habibi, Ryan Thwaites, Chris Chiu and Peter Openshaw for the opportunity to contribute to their study of airway neutrophilia in a human challenge model of RSV infection.

Thank you to everyone in the department of respiratory medicine for the scientific input and contributions which have shaped this work.

I am particularly grateful to Seema Vekaria, Sasha Ashbourne-Lewis and Susanna Soler for all their help with practical aspects in the laboratory, Yanping Guo at the St Mary's FACS facility for her flow cytometry advice and expertise and to the staff at St Mary's CBS for their involvement in the animal studies.

I would also like to thank the Wellcome Trust for funding these studies.

Finally, great thanks go to my family and friends for all their support over the years.

Abstract

Respiratory syncytial virus (RSV) is a leading cause of lower respiratory tract infections, especially in infants. In clinical studies of RSV infection, neutrophils have long been implicated as drivers of disease severity as they make up the vast majority of the cellular composition of the airways of infants hospitalised with severe disease. Furthermore, a transcriptomic analysis found that genes related to neutrophil function were over-expressed in infants hospitalised with severe RSV infections. Although airway neutrophilia is a hallmark of severe RSV disease, the mechanisms underlying neutrophil recruitment and activation in the lung are not yet well understood. Furthermore, it is unclear whether airway neutrophilia during RSV infection contributes to viral control and/or drives disease severity. Mechanistic studies into the role of neutrophils during RSV infection in murine and bovine models of disease have suggested that neutrophils may release NETs in response to RSV but whether this causes lung pathology in a manner which affects the outcome of disease is unknown. In these studies, the innate immune signalling pathways underlying neutrophil recruitment and activation in RSV-infected mice were investigated. MyD88/TRIF signalling was found to be essential for lung neutrophil recruitment while MAVS signalling, leading to type I IFN production, was necessary for neutrophil activation. Furthermore, antibody mediated neutrophil depletion was used to investigate the role of neutrophils during RSV infection. Neutrophils were not required for the production type I interferons (IFNs) in response to RSV, nor did neutrophils contribute to viral control. Neutrophil depletion also demonstrated that neutrophil recruitment during primary RSV infection was not required for the formation of memory T cell responses during RSV re-challenge. Neither neutrophil removal nor the enhancement of airway neutrophilia, by administration of the chemoattractant CXCL1 following RSV infection, affected disease severity as measured by weight loss. However, increased airway neutrophilia pre-infection, as established by administration of CXCL1, enhanced disease severity as measured by weight loss during RSV infection. This was associated with an enhanced recruitment of $CD8^+$ T cells to the lung at the peak of disease. This study found that two distinct pathogen sensing pathways must collaborate for neutrophil recruitment and activation during RSV infection. Furthermore, although neutrophil recruitment in response to RSV does not appear to drive disease in mice, pre-existing infections or conditions which heighten airway neutrophilia may contribute to disease severity during RSV infection.

Table of Contents

Abbreviations

$^1O_2$	Singlet oxygen
ACK buffer	Ammonium chloride potassium buffer
AF	Alexa Fluor
AMs	Alveolar macrophages
ANOVA	Analysis of variance
AP-1	Activator protein 1
APC	Antigen presenting cell
APC	Allophycocyanin
APRIL	A proliferation-inducing ligand
ATII	Alveolar type II
ATP	Adenosine triphosphate
AWERB	Animal Welfare and Ethical Review Body
BAFF	B cell activating factor
BAL	Broncho-alveolar lavage
BPI	Bactericidal/permeability-increasing protein
BSA	Bovine serum albumin
BUV	Brilliant Ultra-Violet
BV	Brilliant Violet
CXCL1/KC	C-X-C motif ligand 1
CXCL2/MIP2	C-X-C motif ligand 2
CXCL5	C-X-C motif ligand 5
CXCL9	C-X-C motif ligand 9
CXCL10	C-X-C motif ligand 10
CXCL12	C-X-C motif ligand 12
C/EBP	CCAAT-enhancer-binding proteins
C3a	Complement component 3
C5a	Complement component 3
CARD	Caspase activation and recruitment domains
CCL2	C-C motif chemokine ligand 2
CCL5	C-C motif chemokine ligand 5
CD	Cluster of differentiation
cDCs	Conventional dendritic cell
cDMEM	Complete Dulbecco's Modified Eagle Medium
cDNA	Complementary DNA
cGAS	Cyclic GMP-AMP synthase
Cit H3	Citrullinated histone 3
CLR	C-type lectin receptor
COX-2	Cyclooxygenase 2

CR1	Complement receptor type 1
CT	Cycle threshold
DAB	3,3'-diaminobenzidine
DAMP	Damage associated molecular pattern
DAPI	4',6-Diamidine-2'-phenylindole dihydrochloride
DC	Dendritic cell
DEG	Differentially expressed gene
DMEM	Dulbecco's Modified Eagle Medium
DMSO	Dimethylsulfoxide
DNA	Deoxyribonucleic acid
dsDNA	Double stranded deoxyribonucleic acid
EDTA	Ethylenediaminetetraacetic acid
ELISA	Enzyme-linked immunosorbent assay
Eomes	Eomesodermin
EpCAM	Epithelial cell adhesion molecule
ERK1/2	Extracellular signal-regulated protein kinases 1 and 2
FACS	Fluorescence-activated cell sorting
FAM	6-carboxyfluorescein
FCS	Foetal calf serum
FcγR	Fc γ receptor
FFU	Focus forming units
FITC	Fluorescein isothiocyanate
fMLP	N-Formylmethionine-leucyl-phenylalanine
FMO	Fluorescence minus one
FoxP3	Forkhead box P
F	Fusion protein
g	Gram
g	Gravity
G	Glycoprotein
GAPDH	Glyceraldehyde 3-phosphate dehydrogenase
GFP	Green fluorescent protein
GM-CSF	Granulocyte-macrophage colony-stimulating factor
G-CSF	Granulocyte colony-stimulating factor
GPCR	G protein coupled receptor
GrzmB	Granzyme B
H&E	Hematoxylin and eosin
H^+	Proton
H_2O	Water
H_2O_2	Hydrogen peroxide
HDN	High-density neutrophil
HEp-2	Human epithelial cell line

HIV	Human immunodeficiency virus
HMGB1	High mobility group box 1 protein
HOCl	Hypochlorous acid
hRSV	Human respiratory syncytial virus
HRP	Horse radish peroxidase
i.n.	Intranasal
i.p.	Intraperitoneal
i.v.	Intravenous
ICAM	Intercellular adhesion molecule
IFITM	Interferon-induced transmembrane protein 1
IFN	Interferon
IFNAR	Interferon-α receptor
Ig	Immunoglobulin
IgA	Immunoglobulin A
IgG	Immunoglobulin G
IKK	IκB kinase
IL	Interleukin
ILC	Innate lymphoid cell
IRAK	Interleukin-1 receptor associated kinase
IRF	Interferon regulatory factor
ISG	Interferon stimulated gene
JAK1	Janus kinase 1
JNK	c-Jun N-terminal kinases
LDN	Low-density neutrophils
LFA-1	Lymphocyte function-associated antigen 1
LN	Lymph node
LPS	Lipopolysaccharide
LRTI	Lower respiratory tract infection
LTB4	Leukotriene B4
M	Molar
Mab	Monoclonal antibody
MACS	Magnetic-activated cell sorting
MAPK	Mitogen-activated protein kinases
MAVS	Mitochondrial antiviral-signalling protein
MDA-5	Melanoma differentiation-associated protein 5
MHC	Major histocompatibility complex
MLN	Mesenteric lymph nodes
MMP	Matrix metalloproteinase
MPO	Myeloperoxidase
mTOR	Mammalian target of rapamycin
MyD88	Myeloid differentiation primary response 88

NADPH	Nicotinamide adenine dinucleotide phosphate
NE	Neutrophil elastase
NEMO	NF-κB essential modulator
NETs	Neutrophil extracellular traps
NFKB	Nuclear factor κ-light-chain-enhancer of activated B cells
NK cell	Natural killer cell
NLR	NOD-like receptor
NOD	Nucleotide-binding oligomerization domain
NS1	Non-structural protein 1
NS2	Non-structural protein 2
NSP4	Rotavirus non-structural protein 4
O_2	Oxygen
$O_2^{\cdot -}$	Superoxide radical
OAS	2′,5′-oligoadenylate synthetase
OCT	Optimal cutting temperature
P	RSV phosphoprotein
P value	Probability value
p.i.	Post infection
PAD4	Peptidylarginine deiminase 4
PAF	Platelet activating factor
PAMP	Pathogen associated molecular pattern
PBS	Phosphate buffered saline
PCR	Polymerase chain reaction
pDCs	Plasmacytoid dendritic cell
PE	Phycoerythrin
PerCP	Peridinin chlorophyll protein complex
PGE_2	Prostaglandin E2
PGSL-1	P-selectin glycoprotein ligand-1
PKR	Protein kinase R
PMA	Phorbol 12-myristate 13-acetate
PRR	Pattern recognition receptor
PVM	Pneumonia virus of mice
RBCs	Red blood cells
rCXCL1	Recombinant CXCL1
rIFN-α	Recombinant IFN-α
RIG-I	Retinoic acid-inducible gene I
RIP-1	Receptor-interacting serine/threonine-protein kinase 1
RLR	RIG-I like receptor
RNA	Ribonucleic acid
ROS	Reactive oxygen species
RSV	Respiratory syncytial virus
RT	Room temperature
RT-qPCR	Quantitative reverse transcription PCR

S1P	Sphingosine 1-phosphate
S1PR1	Sphingosine 1-phosphate receptor 1
SCAMP	Secretory carrier-associated membrane protein
SEM	Standard error of mean
SH	Small hydrophobic protein
SNP	Single nucleotide polymorphism
ssRNA	Single stranded ribonucleic acid
STAT2	Signal transducer and activator of transcription 2
STING	Stimulator of interferon genes
TAK1	Mitogen-activated protein kinase kinase kinase 7
TAMRA	Tetramethylrhodamine
TANK	TRAF family member-associated NF-κB activator
TBK1	TANK binding kinase 1
T_{CM}	Central memory T cell
TCR	T cell receptor
T_{EM}	Effector memory T cell
TGF-β	Transforming growth factor beta 1
Th1	Type 1 T helper
Th17	Type 17 T helper
Th2	Type 2 T helper
Th9	Type 9 T helper
TLR	Toll-like receptor
TMB	3,3',5,5'-Tetramethylbenzidine
TNF	Tumor necrosis factor α
TRAF	TNF receptor associated factors
Treg	Regulatory T cell
TRIF	TIR-domain-containing adapter-inducing interferon-β
TRIM	T cell receptor interacting molecule
T_{RM}	Resident memory T cell
tSNE	t-Distributed Stochastic Neighbor Embedding
U/ml	Enzymatic units per ml
UV	Ultra-violet
UV-RSV	UV-inactivated RSV
VAMP	Vesicle-associated membrane protein
VEGF	Vascular endothelial growth factor
VVN2	Vanin-2
Wt	Wild-type
ZAP1	Zinc-finger antiviral protein 1

Table Index

Figure Index

1 Introduction

1.1 Respiratory Syncytial Virus

1.1.1 Epidemiology

Respiratory syncytial virus (RSV) is a major global respiratory pathogen which causes annual epidemics worldwide (Nair *et al.* 2010). In temperate climates the RSV season spans the winter months (Rose *et al.* 2018), while in tropical climates incidences of RSV peak during the rainy season (Weber *et al.* 1998). The World Health Organisation (WHO) has estimated that RSV affects 64 million people each year. It is further estimated that there are 33 million cases of severe disease which result in 3.2 million hospital admissions per annum in children under the age of 5 (Shi *et al.* 2017). RSV is classically considered as a severe pathogen of infants; healthy adults who become infected with RSV are typically either asymptomatic or will develop mild disease of the upper respiratory tract with cold-like symptoms (Openshaw *et al.* 2017). Despite the fact that >90% of children will have encountered RSV by the age of 2 (Glezen *et al.* 1986; Simoes 1999), only a minority go on to develop severe lower respiratory tract infections resulting in bronchiolitis or pneumonia. As such, RSV is the leading cause of infant hospitalisations in the developed world (Nair *et al.* 2010), although the disease burden is thought to be much higher in resource poor settings (Shi *et al.* 2017; Shi *et al.* 2019). Furthermore, severe RSV infection has serious long term respiratory health implications - hospitalisation with RSV during infancy is associated with wheeze (Henderson *et al.* 2005; Escobar *et al.* 2010) and asthma (Sigurs *et al.* 2010; Thomsen *et al.* 2009; Stein *et al.* 1999) in later life.

The ability of RSV to cause repeat infections throughout life means RSV infection of adults is also a huge economic burden. The National Office of Statistics estimated that in 2016 almost a quarter of the school and work days that were lost to sickness were due to mild diseases such as the common cold. In the US, the cost of the common cold has been estimated at $25 million per year (Bramley *et al.* 2002). Furthermore, it is increasingly well recognised that RSV does cause severe disease in certain vulnerable adult populations such as the immunocompromised (Hijano *et al.* 2018; Science *et al.* 2019) and the elderly (Openshaw *et al.* 2017; Shi *et al.* 2019; Falsey and Walsh 2005). It has been estimated that up to 78% of RSV-associated deaths occur in individuals aged 65 and older (Thompson *et al.* 2003). The

factors determining propensity to developing severe as opposed to mild disease are not yet well understood but both viral and host factors have been implicated as drivers of disease severity (Siezen *et al.* 2009; Openshaw and Chiu 2013; Lukacs *et al.* 2006; Collins and Graham 2008). Efforts to create a formalin-inactivated vaccine in the 1960s disastrously resulted in enhanced disease and even in the deaths of two of the infant participants who mounted a heightened immune response after vaccination in response to a natural RSV infection (Kim *et al.* 1969). Currently, there is no vaccine available and the only prevention is prophylactic therapy with a RSV-specific monoclonal antibody - the use of which is restricted to susceptible infants, largely for economic reasons.

1.1.2 Virology

RSV was first isolated from a chimpanzee in 1956 (Blount *et al.* 1956) and later identified in human infants (Chanock *et al.* 1957). It is a linear, non-segmented, single stranded, negative sense RNA virus originally classified in the family of *Paramyxoviridae* but later reclassified as a member of the *Pneumoviridae* family in 2016 (Afonso *et al.* 2016). Unlike influenza virus, there are no animal hosts for human RSV (hRSV), however, there are similar viruses found in other species including bovine RSV in cows and pneumonia virus in mice (PVM) (Altamirano-Lagos *et al.* 2019). There are two major strains of hRSV in global circulation, RSV A and RSV B (Mufson *et al.* 1985), of which subtype A induces more severe disease in infants (Papadopoulos *et al.* 2004). RSV is named after its unique ability to induce the merging of infected cells into syncytia as a mechanism of cell to cell transmission which avoids exposure to the extracellular environment (Shigeta *et al.* 1968). The formation of syncytia causes airway epithelial cell destruction in the respiratory tract and contributes to disease severity (Villenave *et al.* 2012; Tian *et al.* 2013). *In vivo*, RSV is found in both spherical and filamentous forms (Liljeroos *et al.* 2013; Bächi 1988) but viral spread between cells beyond the formation of syncytia is thought to be dependent on the formation of filamentous viral particles (Kiss *et al.* 2014; Mitra *et al.* 2012).

The genome of RSV is roughly 15.2 kb in length and contains ten open reading frames encoding two non-structural proteins and nine structural proteins. In order of transcription, first encoded are the non-structural proteins (NS1 and NS2), followed by the structural proteins; the nucleoprotein (N), phosphoprotein (P), matrix protein (M), small hydrophobic protein (SH), attachment glycoprotein (G), fusion glycoprotein (F), the transcription anti-termination protein

M2-1 and RNA synthesis regulatory protein M2-2 (both encoded in the M2 open reading frame), and the RNA polymerase (encoded by the L gene) (Fig. 1.1).

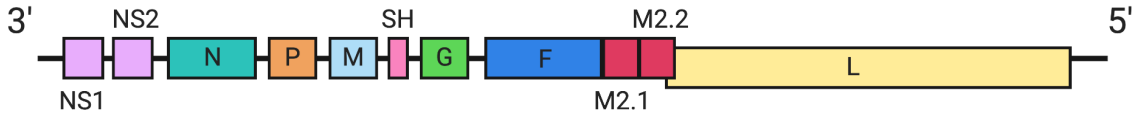

Figure 1.1. Schematic illustrating the genomic structure of RSV. RSV is a 15.2kb, single stranded, negative sense, enveloped RNA virus. As encoded from the 3' end to the 5' end; the NS1, NS2, N, P, M, SH, G, F, M2.1, M2.2 and L genes. Created with BioRender.

RSV is an enveloped virus, and the virion is coated in a lipid bilayer derived from the host plasma membrane during budding and exit from the host cell (Canedo-Marroquín *et al.* 2017; Battles and McLellan 2019). The RSV genome is coated with the helical nucleoprotein N as part of the ribonucleoprotein complex (Bakker *et al.* 2013). Also associated with this complex is the RNA-dependent RNA polymerase complex, made up of the large polymerase subunit L along with the phosphoprotein P which directly interacts with N in the ribonucleoprotein complex (García *et al.* 1993). In addition to acting as a co-factor for the RNA polymerase during transcription, P protein can act as a chaperone to prevent newly synthesised RNA from associating with the N protein (Canedo-Marroquín *et al.* 2017). Similarly located within the viral capsid are the M2-1 and M2-2 proteins. M2-1 acts as a transcription elongation factor (Fearns and Collins 1999) and enhances polymerase activity by suppressing transcription termination while M2-2 aids the transition from viral transcription to viral genome replication (Bermingham and Collins 1999). M2-1 also physically associates with the M protein which together form a protective protein lining underneath the viral envelope, encasing the ribonucleoprotein and polymerase complexes (Battles and McLellan 2019). The non-structural proteins NS1 and NS2 are not required for RSV viral replication *in vitro* but inhibit the cellular antiviral response of the host *in vivo* and impair the induction or signalling of type I IFNs in response to RSV (Ling *et al.* 2009; Bossert and Conzelmann 2002; Bossert *et al.* 2003).

The F, G and SH glycoproteins are all located in the envelope of the RSV virion. The SH protein is less abundant and its role is less well characterised than both F and G proteins. However, it is known that SH proteins form pentameric ion channels in the envelope (Gan *et al.* 2012; Fuentes *et al.* 2007). The G protein is present both as a transmembrane protein as well as in a soluble form (Battles and McLellan 2019; Canedo-Marroquín *et al.* 2017; Hendricks *et al.* 1987; Hendricks *et al.* 1988). In its transmembrane form, it is the major RSV protein

responsible for attachment of the virion to host cells prior to entry (Battles and McLellan 2019). G protein is the most genetically diverse RSV protein and distinguishes the two major RSV subtypes, RSV A and RSV B (Sullender 2000). G protein is thought to be a possible vaccine target and recently crystal structures were obtained of G protein bound to neutralising antibody (Jones *et al.* 2018; Fedechkin *et al.* 2018). As a soluble protein, G has been shown to act as a decoy by binding antibodies targeted to transmembrane G (Bukreyev *et al.* 2008; Bukreyev *et al.* 2012). RSV F protein is required for fusion of the viral membrane with the host cell membrane during viral entry and required for epithelial cells to fuse forming syncytia (Ito *et al.* 1997). Prior to entry, monomers of F must trimerise on the surface of the virion and form the pre-fusion complex. This complex is immunogenic yet highly unstable (Liljeroos *et al.* 2013). During protein folding into the post-fusion conformation, F peptides will insert into nearby host membrane if present and mediate viral entry to the host cell. Formation of the post-fusion complex is irreversible, and this conformation is very stable (Colman and Lawrence 2003). Unlike G protein, there is little antigenic variation in F between RSV A and RSV B strain. Furthermore, unlike influenza virus, there is not much seasonal antigenic drift between RSV epidemics (Ascough *et al.* 2018). This lends hope to the possibility of developing a universal RSV vaccine (Battles and McLellan 2019).

1.2 Initiation of innate immunity to RSV

The importance of innate immunity in protection against RSV disease is increasingly well recognised and has been especially highlighted by *in vivo* models of RSV infection (Johansson 2016). After inhalation of the virus into the airways, physical barriers such as mucus provide the first line of defence against infection (Zanin *et al.* 2016), along with protection induced by anti-microbial peptides (Currie *et al.* 2013; Currie *et al.* 2016) and surfactants in the lung (Barreira *et al.* 2011; LeVine *et al.* 2004). The microbiome in the airways also likely provides a line of innate protection against invading pathogens. The lung microbiome has been less studied than the gut microbiome, however it is clear that the total bacterial biomass of the lung is much lower than that of the gut (Savage 1977; O'Dwyer *et al.* 2016). Nonetheless, many bacterial, viral and fungal species are known to transiently colonise the respiratory tract without causing pathogenesis and likely prevent the growth of other, pathogenic species (Man *et al.* 2017; Dickson *et al.* 2016). Furthermore, it is also increasingly well appreciated that the gut microbiome can influence immunity in the lung via the gut-lung axis (Marsland *et al.* 2015; Dang and Marsland 2019; Dumas *et al.* 2018). However, the role of this in immunity to RSV is not yet well understood and remains an important area of research.

The second line of defence is mediated by the resident cells of the respiratory tract. This includes stromal cells, such as different types of epithelial cells, as well as immune cells such as alveolar macrophages (AMs), dendritic cells (DCs) and various subtypes of innate lymphoid cells. In order to trigger an immune response, resident lung cells must detect the virus – this occurs by the binding of pathogen associated molecular patterns (PAMPs) on the virus to pattern recognition receptors (PRRs) on the host cell (Kawai and Akira 2010; Takeuchi and Akira 2010). RSV infection can also cause extensive cell death and tissue damage in the lungs (Bohmwald *et al.* 2019; Liesman *et al.* 2014) and it is widely appreciated that damage associated molecular patterns (DAMPs) released by host cells during cellular stress and death can also trigger PRRs and other receptors to further induce immunity (Schaefer 2014; Johansson 2016). PRRs are germline encoded innate receptors which act as cellular sensors of external and internal non-self molecules (Kawai and Akira 2010; Takeuchi and Akira 2010). They are constitutively expressed in many cell types and their expression can also be up and downregulated during infection. Several classes of PRRs have been described including Toll-like receptors (TLRs), C-type lectin receptors (CLRs), RIG-I-like receptors (RLRs), NOD-like receptors (NLRs) and cytosolic DNA sensors (Akira *et al.* 2006; Kawai and Akira 2010; Takeuchi and Akira 2010; Wu *et al.* 2013; Sun *et al.* 2013). Following the binding of PAMPs

to PRRs, downstream signalling cascades drive the upregulation genes encoding pro-inflammatory immune mediators which orchestrate innate immune responses and mediate pathogen killing (Kawai and Akira 2010; Takeuchi and Akira 2010). During viral infections, PRR driven expression of interferons (IFNs) is especially important to mediate antiviral immunity (Sen 2001).

1.2.1 Membrane-bound pattern recognition receptor signalling

Several membrane bound PRRs have been implicated in the detection of RSV in the lung (Kim and Lee 2014; Johansson 2016; Marr *et al.* 2013). Of the TLRs; TLR2, TLR3, TLR4, TLR6 and TLR7 are all thought to be involved in the initiation of immune responses to RSV. TLR2 is expressed on the cell surface and dimerises with either TLR1 or TLR6 to recognise a plethora of ligands with diacyl and triacylglycerol moieties, proteins and polysaccharides (Oliveira-Nascimento *et al.* 2012). It is not known precisely how TLR2/TLR6 heterodimers recognise RSV but depletion of TLR2 and TLR6 in peritoneal macrophages resulted in reduced cytokine production in response to RSV and *Tlr2*$^{-/-}$ and *Tlr6*$^{-/-}$ mice had higher viral loads during RSV infection (Murawski *et al.* 2009). TLR2/TLR6 complexes signal through the myeloid differentiation primary response 88 (MyD88) adaptor protein to upregulate pro-inflammatory mediators. TLR4 is also expressed on the cell surface and is thought to recognise RSV F protein (Kurt-Jones *et al.* 2000). However, it is not clear how this recognition contributes to immunity to RSV (Kim and Lee 2014). TLR4 mutations have been associated with disease severity in infants with RSV-induced bronchiolitis (Tal *et al.* 2004; Awomoyi *et al.* 2007). However *in vivo* studies using TLR4-deficient strains of mice do not agree on whether TLR4 deficiency impairs inflammatory cytokine production and viral control (Kurt-Jones *et al.* 2000; Ehl *et al.* 2004; Haynes *et al.* 2001) and as yet, the mechanism by which TLR4 may mediate immunity to RSV remains unclear. TLR4 can signal via both the MyD88 and TIR-domain-containing adapter-inducing interferon-β (TRIF) adapter proteins. TLR3 and TLR7 are both expressed on the membrane of the endosome and signal via the adaptor proteins TRIF and MyD88, respectively (Kim and Lee 2014). TLR3 recognises dsDNA while TLR7 detects ssRNA. The RSV genome exists in both these forms at different stages of viral replication and it is likely direct detection of the RSV genome by these TLRs in the endosome initiates downstream immune responses (Johansson 2016; Marr *et al.* 2013; Kim and Lee 2014). TLR3 and TLR7 deficient mice both have T helper cell 2 (Th2) screwed immune responses to RSV (Rudd *et al.* 2006; Lukacs *et al.* 2010), implying recognition of the virus by these TLRs may initiate a protective, Th1 skewed immune response. As yet, the relative importance of RSV

detection via these pathways is unclear as heightened disease or loss of viral control has not been demonstrated *in vivo* in TLR3 or TLR7 deficient mice.

Binding of the relevant ligand to TLRs triggers signalling via either the adaptor proteins MyD88 or TRIF, which induces a downstream signalling cascade to switch on immune gene expression (Fig. 1.2). Upon activation, MyD88 forms a complex termed the Myddosome; this is made up of units of interleukin 1 receptor associated kinase 1 (IRAK1) and IRAK4 (Kawasaki and Kawai 2014). IRAK4 activates IRAK1 by phosphorylation which releases it from MyD88 (Li *et al.* 2002). IRAK1 is then able to associate with TNF receptor associated factor 6 (TRAF6), a member of the mitogen-activated protein kinases (MAPK) family. TRAF6 promotes the ubiquitination and activation of the transforming growth factor-β-activated kinase 1 (TAK1) complex (Ajibade *et al.* 2013). TAK1 is then able to activate two distinct pathways to induce gene expression; the MAPK pathway and the nuclear factor κ-light-chain-enhancer of activated B cells (NF-κB) pathway (Ajibade *et al.* 2013; Kawasaki and Kawai 2014). TAK1 activation activates MAPK family members extracellular signal-regulated protein kinases 1 and 2 (ERK1/2), c-Jun N-terminal kinase (JNK) and p38 which in turn activate the activator protein 1 (AP-1) family of transcription factors (Burotto *et al.* 2014). TAK1 activation also allows it to bind to the IκB kinase (IKK) complex, phosphorylating and activating IKKβ (Ajibade *et al.* 2013; Kawasaki and Kawai 2014). The IKK complex targets the NF-κB inhibitor IκBα for degradation, thereby allowing NF-κB to translocate to the nucleus and induce the gene expression of pro-inflammatory mediators (Kawasaki and Kawai 2014). Activation of TRIF leads to interactions between TRIF and TRAF6 and TRAF3 (Fig. 1.2). Activation of TRAF6 recruits receptor-interacting serine/threonine-protein kinase 1 (RIP-1) which then activates the TAK1 complex (Kawai and Akira 2010), driving MAPK and NF-κB dependent gene expression, as explained above (Meylan *et al.* 2004; Burotto *et al.* 2014). Activation of TRAF3 recruits TANK binding kinase 1 (TBK1), IKKi and NF-κB essential modulator (NEMO) which induces the phosphorylation of interferon regulatory transcription factor (IRF3). This causes dimerization of IRF3 and facilitates its translocation into the nucleus where it acts as a transcription factor to induce the transcription of the type I IFNs; IFN-α and IFN-β (Kawai and Akira 2010; Kawasaki and Kawai 2014; Akira *et al.* 2006). During RSV infection however, MyD88/TRIF signalling is not thought to be required for IFN production. Instead, cytosolic detection of the virus which triggers signalling via mitochondrial antiviral-signalling protein (MAVS) is required for IFN-α/β production and viral immunity (Goritzka, Makris, *et al.* 2015; Bhoj *et al.* 2008; Demoor *et al.* 2012).

1.2.2 Cytoplasmic pattern recognition receptor signalling

When RSV fuses with the plasma membrane of the host cell, the virus enters into the cytoplasm of the cell. Here, innate sensors such as nucleotide-binding oligomerisation domain-containing protein 2 (NOD2), melanoma differentiation-associated protein 5 (MDA-5) and retinoic acid-inducible gene I (RIG-I) can detect RSV and signal through the adaptor protein MAVS (Seth *et al.* 2005) to trigger the expression of IFNs (Johansson 2016). NOD2 is more considered as a sensor during bacterial infections, however ssRNA was found to be a NOD2 ligand which can induce IFN-β production during RSV infection by signalling through MAVS (Sabbah *et al.* 2009). Furthermore, NOD2 deficient mice produce less IFN-β, have higher viral loads and develop more severe RSV disease (Sabbah *et al.* 2009). MDA-5 is thought to recognise longer dsRNA intermediates formed when ssRNA viruses replicate (Triantafilou *et al.* 2012). It is not known how MDA-5 interacts with RSV, but a child deficient in MDA-5 was found to get severe recurrent respiratory viral infections, including RSV infections (Lamborn *et al.* 2017). Silencing of MDA-5 in A549 epithelial cells did not influence RSV viral replication but did decrease the production of IFN-regulated transcripts (Lamborn *et al.* 2017). RIG-I preferentially binds to short dsRNA with a 5'-triphosphate (Rehwinkel *et al.* 2010), formed when RSV replicates or when the ssRNA RSV genome forms panhandles (Marr *et al.* 2013). RIG-I is thought to be a more important sensor of RSV in the cytosol than MDA-5 as RIG-I was essential for the production of ISGs in mouse fibroblasts cultured *in vitro* with RSV, while MDA-5 was dispensable for this (Loo *et al.* 2008). There is cross-talk and overlap between the signalling pathways downstream of the TLRs and the RLRs (Marr *et al.* 2013) however silencing of RIG-I and TLR3 in A549 epithelial cells *in vitro* showed that TLR3 was dispensable for IFN-β induction in response to RSV while RIG-I was essential for IFN-β production (Liu *et al.* 2007).

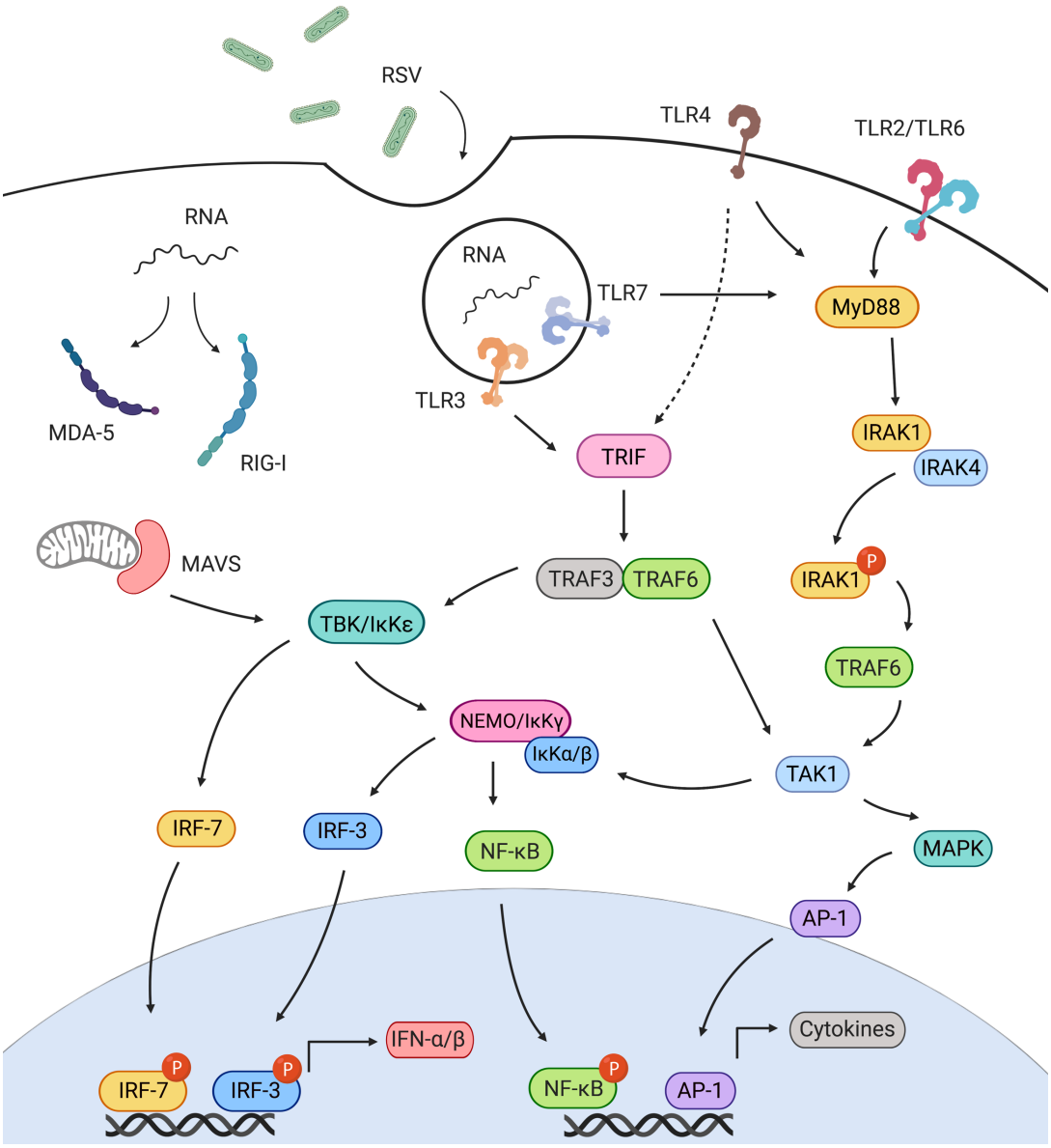

Figure 1.2. Viral recognition drives signalling via the adaptor proteins MAVS, MyD88 and TRIF to induce the production of type I IFNs and pro-inflammatory mediators, initiating innate immunity. Viral recognition by MDA-5 and RIG-I in the cytosol activates MAVS signalling. Activated MAVS associates with the TBK complex, driving the translocation of IRF3 and IRF7 to the nucleus. This induces the transcription of type I IFNs. MAVS signalling can also facilitate NF-κB translocation to the nucleus to induce the expression of pro-inflammatory cytokines. TLR3 and TLR4 activation can trigger signalling via TRIF. This activates TRAF3 and TRAF6. TRAF3 activation can further activate the TBK complex to induce downstream gene expression. TRAF6 activation induces signalling by TAK1, which can signal through both the IKK complex and the MAPK pathway to induce the transcription of cytokines via NF-κB and the API family of transcription factors. TLR4, TLR2 and TLR6 also induce gene expression via TRAF6 activation by activating the intermediate signalling components IRAK1 and IRAK4. Created using BioRender.

Following ligand binding to the RLRs, the MDA-5 and RIG-I receptors undergo K63-linked polyoligomerisation mediated by E3 ubiquitin ligases (Gack *et al.* 2007). Caspase activation and recruitment domains (CARD) on RLRs interact with MAVS which is situated in the mitochondrial membrane (Takeuchi and Akira 2010) (Fig. 1.2). Following CARD-CARD interactions between activated RLRs and MAVS, MAVS can trigger IFN production via two pathways. MAVS can drive NF-κB translocation to the nucleus by activating the IKK complex, as described above. MAVS can also trigger IFN production by interacting with TRAFs. This induces the recruitment of TBK1 and IKKε which phosphorylate IRF3 and IRF7 in the cytoplasm of the cell. Phosphorylated IRF3 and IRF7 are able to form homodimers and this allows them to translocate to the nucleus where they act as transcription factors to induce the expression of IFN-α and IFN-β (Jin *et al.* 2017).

While the importance of PRR signalling, particularly via the RLRs, has been demonstrated for type I IFN production and antiviral immunity during RSV infection (Demoor *et al.* 2012; Bhoj *et al.* 2008; Goritzka, Makris, *et al.* 2015), it is interesting to note that mice deficient in MAVS, MyD88 and TRIF are still able to mount adaptive immune responses (Goritzka, Pereira, *et al.* 2015). These mice recruit RSV-specific $CD8^+$ T cells to the lung and are able to survive RSV infection (Goritzka, Pereira, *et al.* 2015). It is likely that DAMPs such as heat shock proteins, HMGB1, uric acid, and ATP might also play an underappreciated role in mediating adaptive immunity to RSV in the absence of direct pathogen sensing mechanisms. It is possible that the cyclic GMP-AMP synthase/stimulator of interferon genes (cGAS/STING) pathway normally involved in sensing DNA viruses might also be involved in immunity to RSV (Schoggins *et al.* 2014; Goritzka, Pereira, *et al.* 2015).

1.3 Innate immune responses to RSV

1.3.1 Interferons

IFNs were the first cytokines discovered and were named after their ability to interfere with viral replication (Isaacs and Lindemann 1957; Sen 2001). It is now well established that IFNs play an important role in immunity to most, if not all, pathogenic viruses. There are three classes of IFNs; type I, type II and type III IFNs. Type I and III IFNs are mainly important in innate, antiviral immunity. The type II IFN group consists only of IFN-γ; an important mediator in natural killer (NK) cell responses and during adaptive $CD4^+$ and $CD8^+$ T cell responses (Schroder *et al.* 2004). The type I IFN family consists of multiple distinct IFN-α genes (13 in man and 14 in mice), IFN-β (1 in man) as well as IFN-κ, IFN-δ, IFN-ε, IFN-τ, IFN-ω and IFN-ζ (Randall and Goodbourn 2008). IFN-κ, IFN-δ, IFN-ε, IFN-τ, IFN-ω and IFN-ζ have less defined roles in immunity to viruses, but IFN-α/β are induced directly in response to viral detection downstream of PRR signalling, as described above. Type III IFNs consist of three IFN-λ (IFN-λ1, IFN-λ2 and IFN-λ3) (Kotenko *et al.* 2003). During influenza virus infection, IFN-λ has been demonstrated to impair viral replication while limiting tissue damaging inflammation (Davidson *et al.* 2016; Crotta *et al.* 2013; Wack *et al.* 2015). The role of IFN-λ is less well understood in RSV infection; it is hard to detect in the mouse model of infection but it was shown in a clinical study of infants with bronchiolitis that IFN-λ levels correlated with disease severity (Selvaggi *et al.* 2014)

During RSV infection, it is well established that the type I IFNs (IFN-α/β) are very important in initiating protective antiviral immune responses. Polymorphisms in genes involved in the induction of IFNs are associated with the development of severe disease in infants (Janssen *et al.* 2007; Tal *et al.* 2004; Awomoyi *et al.* 2007). Furthermore, studies in mice have shown that MAVS deficient mice which cannot induce the production of type I IFNs develop more severe RSV disease and are less able to control viral replication (Bhoj *et al.* 2008; Demoor *et al.* 2012; Goritzka, Makris, *et al.* 2015). Type I IFNs are produced transiently and act by binding to the interferon-α/β receptor (IFNAR), which is expressed on all nucleated cells and consists of two subunit chains; IFNAR1 and IFNAR2 (Randall and Goodbourn 2008; Johansson 2016). Ligand-receptor interactions of the IFNAR activates Janus kinase 1 (JAK1) and tyrosine kinase 2 (TYK2), which phosphorylate the cytoplasmic factors signal transducer and activator of transcription 1 (STAT1) and STAT2 (Ivashkiv and Donlin 2014). Phosphorylated STAT1

and STAT2 form homodimers and translocate to the nucleus where they interact with IRF9 to induce the gene expression of hundreds of interferon stimulated genes (ISGs), thereby amplifying the original antiviral signal induced by IFN-α/β production (Ivashkiv and Donlin 2014). IFNAR deficient mice do not mount pro-inflammatory immune responses during RSV infection, have higher viral loads and have more severe disease as measured by weight loss (Goritzka *et al.* 2014).

Hundreds of ISGs are induced downstream of IFNAR binding. ISGs can have multiple functions in both intrinsic and extrinsic manners; some act to enhance pathogen detection, while others encode for mediators which can be directly antiviral (Ivashkiv and Donlin 2014; Schoggins 2018; Schneider *et al.* 2014). Proteins such as the myxovirus resistance (Mx) proteins, cholesterol-25-hydroxylase, oxysterols, the interferon-induced transmembrane (IFITM) family of proteins and tripartite motif (TRIM) family of proteins are thought to directly inhibit viral entry into cells (Boo and Yang 2010). Other ISGs such as the zinc-finger antiviral protein (ZAP), the oligoadenylate synthetase (OAS)-RNase L pathway and protein kinase R (PKR) are antiviral by inhibiting protein translation (Boo and Yang 2010). Cell extrinsic effects of ISGs include the initiation of innate immunity by the production of cytokines, chemokines and pro-inflammatory mediators (Ivashkiv and Donlin 2014; Schoggins 2018; Schneider *et al.* 2014). During RSV infection of IFNAR1 deficient mice, IFN-α, IFN-β, IFN-λ, IFN-γ, CXCL10, RIG-I, Mx-1, IL-6, IL-1β, IL-1α, TNF-α, GM-CSF, IL-5, IL-12p40, CXCL9 and CCL3 are all downregulated on either the gene expression level or the protein level or both, as compared to wt RSV infected mice (Goritzka *et al.* 2014). It is also increasingly appreciated that ISGs drive the recruitment of other arms of the immune response; for example during RSV infection IFN-α signalling induces CCL2 production which recruits antiviral monocytes to the lung (Goritzka, Makris, *et al.* 2015).

1.3.2 Epithelial cells

RSV is thought to primarily infect and replicate in the epithelial cells (Zhang *et al.* 2002; Johansson 2016; Openshaw *et al.* 2017). These cells line the respiratory tract and are the first cells encountered by the virus (Zhang *et al.* 2002; Johansson 2016; Openshaw *et al.* 2017). There are likely to be several mechanisms of viral entry into epithelial cells. Binding of the G and F proteins on RSV is known to mediate entry into the epithelial cells. G, the attachment protein, binds to host receptors including the fractalkine receptor (CX3CR1) (Johnson *et al.* 2015) and nucleolin (Tayyari *et al.* 2011). Studies of RSV infection in mice have shown that

mice deficient in CX3CR1 are less susceptible to infection (Johnson *et al.* 2015) while nucleolin knockdown in mice inhibits the ability of the virus to replicate (Tayyari *et al.* 2011), highlighting the contribution of these receptors for entry *in vivo*. After initial entry, RSV is able to spread between epithelial cells by inducing cell fusion or syncytia formation; this is mediated by the RSV F protein (Openshaw *et al.* 2017; Ito *et al.* 1997). RSV infection of epithelial cells induces the production of many pro-inflammatory cytokines and chemokines, including CXCL10, CCL5, IL-6 and CXCL8 (Villenave *et al.* 2012; Noah and Becker 1993; Das *et al.* 2005; Becker *et al.* 1993). These pro-inflammatory responses likely contribute to both host defence but also to tissue damage. Epithelial cells cultured from patients with RSV induced bronchiolitis have been demonstrated to express B cell activating factor (BAFF) mRNA and protein (McNamara *et al.* 2013), suggesting that the airway epithelia may play a role in mediating antibody and B cell immunity in the lung.

1.3.3 Alveolar macrophages

AMs are long-lived resident immune cells with important roles in maintaining homeostasis in the lung during health as well as acting as a first line of defence to protect against invading pathogens (Hussell and Bell 2014). AMs are also one of the first cells to encounter RSV along with the epithelial cells however, although RSV can be detected inside AMs, RSV does not replicate productively in these cells (Makris *et al.* 2016). AMs have a crucial role in initiating innate immune responses to RSV as they are the major producers of antiviral type I IFNs (Goritzka *et al.* 2014; Goritzka, Makris, *et al.* 2015). This is in contrast with influenza virus infection, where plasmacytoid dendritic cells (pDCs) have been demonstrated to be a major producer of type I IFNs (Jewell *et al.* 2007; Thomas *et al.* 2014; Killip *et al.* 2015). In addition to IFN-α/β, AMs are also major producers of cytokines and chemokines during RSV infection including but not restricted to; CXCL10, TNF-α, IL-6, CCL3 as well as the ISGs viperin, OAS-1 and PKR (Makris *et al.* 2016; Pribul *et al.* 2008). The production of these mediators is dependent on signalling via both MAVS and IFNAR (Makris *et al.* 2016). The production of type I IFNs by AMs during RSV infection is essential for viral control and protection against severe disease in the murine model (Goritzka *et al.* 2014; Goritzka, Makris, *et al.* 2015). It is important to note that there are many pro-inflammatory cytokines and chemokines not produced by AMs during RSV infection (Makris *et al.* 2016), and that cooperation is required between the stromal cells and the AMs to initiate the first early, pro-inflammatory antiviral immune responses during RSV infection.

1.3.4 Monocytes

Inflammatory monocytes are recruited early to the lung during RSV infection where they peak at day 2 post infection (p.i.) in the mouse model (Goritzka, Makris, *et al.* 2015). The recruitment of monocytes is dependent on the production of type I IFNs by AMs; *Mavs*$^{-/-}$ mice which do not produce IFN-α during RSV infection are not able recruit monocytes to the lung (Goritzka, Makris, *et al.* 2015; Goritzka *et al.* 2014). Monocytes are thought to have an important antiviral function during RSV infection; *Mavs*$^{-/-}$ mice have higher viral loads early and at the peak of viral replication and develop more severe disease as measured by weight loss. When monocytes are recruited back into *Mavs*$^{-/-}$ mice by treatment with the chemokine CCL2, control of viral replication is restored and mice do not develop more severe disease than wild-type (wt) mice (Goritzka, Makris, *et al.* 2015). However, the mechanism by which monocytes are antiviral is still not well understood; this could either be via a direct effect on infected cells or via the secretion of inflammatory mediators which influence other aspects of the immune response.

1.3.5 Innate lymphoid cells

Innate lymphoid cells (ILCs) comprise a group of innate immune cells which belong to the lymphoid lineage but do not express antigen-specific B or T cell receptors. ILCs are largely classified into three major groups; group 1 ILCs (ILC1s), group 2 ILCs (ILC2s) and group 3 ILCs (ILC3s), based on the transcription factors regulating their development, their cell surface markers and by the cytokines they produce (Vivier *et al.* 2018; Hildreth and O'Sullivan 2019). The group 1 ILCs includes both tissue resident ILC1s, characterised by the expression of CD127, as well as the circulating Natural Killer (NK) cells which can be recruited into tissues during inflammation. While very little is known about the role of lung tissue resident ILC1s during RSV infection, the role of NK cells has been better characterised. NK cells are recruited to the lung early following RSV infection, in a manner which is at least in part dependent on AMs (Pribul *et al.* 2008). Severe RSV disease in infants is associated with an immune response skewed towards a Th2 response (Openshaw *et al.* 2017), and NK cell depletion in mice has shown that NK cells have a role in driving a protective Th1-driven response (Kaiko *et al.* 2010). NK cell depletion in BALB/c mice demonstrated that the skewed Th2 responses observed in their absence was dependent on IL-25 production by epithelial cells which induced Jagged1 upregulation on DCs (Kaiko *et al.* 2010). During RSV infection, NK cells are able to directly kill RSV infected cells and produce protective IFN-γ (Hussell and Openshaw 1998; Li

et al. 2012). Further support of their role in disease protection comes from studies of fatal RSV cases where almost no NK cells were detected (Welliver *et al.* 2007; De Weerd *et al.* 1998). However, studies in mice have also suggested that NK cell activation and IFN-γ production must be carefully regulated as this can have a role in mediating acute lung injury during RSV infection (Li *et al.* 2012). The role of the other major groups of ILCs, ILC2s and ILC3s, in RSV has not been well studied. However, RSV infection has been suggested to induce the proliferation of IL-13 producing ILC2 cells in a mouse model of disease although it is not clear whether this influences viral load or disease severity (Stier *et al.* 2016).

1.3.6 Dendritic cells

DCs provide a critical link between the innate and adaptive immune response by acting as antigen-presenting cells to facilitate the activation and proliferation of antigen specific T cells in the lymph nodes (LNs) which are then recruited to the lung (Neyt and Lambrecht 2013). Although RSV can be detected inside DCs, it is not thought that productive viral replication occurs within these cells (Tognarelli *et al.* 2019). The two major subsets of DCs, $CD11c^{+}$ conventional DCs (cDCs) and $CD11c^{low}$/mPDCA-1^{+} plasmacytoid DCs (pDCs), are both important during immunity to RSV and are recruited to the lung early during RSV infection of both infants and mice (Openshaw *et al.* 2017; Johansson 2016; Gill *et al.* 2005). To induce antigen-specific T cell responses during RSV infection, cDCs express both major histocompatibility complexes I and II which are required to present RSV antigen derived epitopes to $CD8^{+}$ and $CD4^{+}$ T cells, respectively (Schmidt 2018). Several subsets of cDCs exist; these cells reside in tissues and following infection they become activated and migrate to the draining LN where they act as the link between the innate and the adaptive immune responses to drive antigen-specific T cell responses.

During RSV infection, two major subtypes of lung-derived cDCs were shown to be important in presenting RSV antigens in the context of both MHC-I and MHC-II in the mesenchymal lymph nodes (MLNs); subepithelial $CD103^{+}$ $CD11b^{low}$ cDCs and the parenchymal $CD103^{-}$ $CD11b^{high}$ cDCs (Lukens *et al.* 2009). Furthermore, $CD103^{+}$ cDCs were shown to be able to induce $CD8^{+}$ T cell proliferation *in vitro* (Ruckwardt *et al.* 2014). During respiratory viral infections, $CD103^{+}$ cDCs are superior over $CD11b^{+}$ cDCs in their ability to activate antigen-specific cytotoxic $CD8^{+}$ T cells; this is thought to be due to their enhanced capacity to cross-present antigens taken up in the lung (Desch *et al.* 2011; Kim and Braciale 2009; Ho *et al.* 2011). In addition to their ability to either directly present or cross-present antigen to $CD4^{+}$ and

$CD8^+$ T cells, cDCs must provide co-stimulation for T cell activation (Braciale *et al.* 2012; Chen and Flies 2013). This is mediated by interactions between CD80 and CD86 on the surface of DCs with CD28 on the surface of T cells (Chen and Flies 2013; Braciale *et al.* 2012). During RSV infection, CD80 and CD86 are both upregulated on mouse and human DCs (Ruckwardt *et al.* 2014; Guerrero-Plata *et al.* 2006). Furthermore, antibody-mediated blocking of CD80 and CD86 during RSV infection of mice blocked the recruitment of $CD8^+$ T cells to the lung during the adaptive phase of the immune response (Ruckwardt *et al.* 2014). Finally, as part of the three-signal T cell activation paradigm, cDCs can also provide the third signal in the form of cytokines such as IL-12 which are required for full T cell activation (Curtsinger *et al.* 1999; Curtsinger *et al.* 2005). These cytokine signals however can also be provided by other cells to fully activate antigen specific T cells (Curtsinger *et al.* 2005).

Unlike cDCs, pDCs are morphologically similar to plasma cells and are classically distinguished by their ability to secrete IFN-α in response to many viral stimuli (Colonna and Trinchieri 2004). *In vitro* studies using human pDCs stimulated with RSV have suggested DCs can produce type I IFN in response to RSV (Hornung *et al.* 2004) however during RSV infection *in vivo*, AMs are the major source of type I IFNs and DCs are not thought to be major contributors (Goritzka, Makris, *et al.* 2015). Nonetheless, antibody-mediated depletion of pDCs during RSV infection of mice resulted in reduced viral clearance and heightened lung pathology, underlining the importance of these cells in early protection against disease (Wang *et al.* 2006).

1.4 Adaptive and memory immune responses to RSV

The innate immune response is required to control early viral replication during RSV infection (Goritzka, Makris, *et al.* 2015; Bhoj *et al.* 2008; Demoor *et al.* 2012) however adaptive T and B cell immunity is essential for viral clearance, disease resolution and the formation of virus-specific immunological memory responses (Chiu and Openshaw 2015; Openshaw *et al.* 2017). Despite this, T cell responses have the potential to be highly pathogenic in the lung during RSV infection and therefore must be tightly regulated to prevent immunopathology (Openshaw and Chiu 2013). Both $CD4^+$ and $CD8^+$ T cell responses have been implicated in viral control and in lung immunopathology during RSV infection. However, the $CD8^+$ T cell response is thought to be both more important in RSV clearance from the lungs as well as more capable of driving tissue damage and immunopathology (Graham *et al.* 1991; Tregoning *et al.* 2008; Openshaw and Chiu 2013; Openshaw *et al.* 2017).

1.4.1 $CD4^+$ T lymphocytes

RSV antigen-specific $CD4^+$ T cells are recruited to the lung following activation by DCs presenting extracellular peptide antigens in the context of MHC-II molecules in the LNs. There are several subsets of $CD4^+$ T helper (Th) cells including Th1, Th2, Th17, Th9 and regulatory T cells (Tregs) (Hirahara *et al.* 2013; O'Shea and Paul 2010). RSV infection of mice is characterised by a pro-inflammatory Th1 driven response and depletion of $CD4^+$ T cells in this model results in less severe disease, as measured by weight loss, indicating that these cells can contribute to disease severity (Graham *et al.* 1991; Tregoning *et al.* 2008). Severe RSV infection of infants is characteristically skewed towards a type 2 immune responses. Clinical data suggest that both Th1 and Th2 $CD4^+$ T cells are present in the lungs of infants infected with RSV, but that severe disease may be associated with decreased Th1 responses and increased Th2 responses (Christiaansen *et al.* 2014; Legg *et al.* 2003). Several groups have reportedly detected Th2 cytokines, which can be produced by $CD4^+$ T cells, such as IL-4, IL-5 and IL-13 in RSV infected infants (Legg *et al.* 2003; Garofalo *et al.* 2001). However these mediators are only present at low concentrations and undetectable using some assays (Tabarani *et al.* 2013) so it is not yet clear whether these cytokines contribute to disease. In mice, $CD4^+$ $FoxP3^+$ Tregs have been shown to have a beneficial role in modulating the immune response to RSV (Lee *et al.* 2010; Durant *et al.* 2013; Fulton and Meyerholz 2010; Liu *et al.* 2009; Loebbermann *et al.* 2012). Specific depletion of $FoxP3^+$ Tregs in the mouse model of RSV infection demonstrated that these cells have an important role in limiting disease

by suppressing overall $CD4^+$ and $CD8^+$ T cell recruitment, and in particular the recruitment of $GATA3^+$ Th2 $CD4^+$ T cells, as well as by inhibiting airway eosinophilia (Durant *et al.* 2013; Loebbermann *et al.* 2012).

1.4.2 $CD8^+$ T lymphocytes

To generate virus-specific cytotoxic $CD8^+$ T cell responses in the lung during RSV infection, DCs must present intracellular peptide antigens in the context of MHC-I molecules to naïve $CD8^+$ T cells in the lymph nodes. It has long been known that $CD8^+$ T cells are critical in viral control during RSV infection (Cannon *et al.* 1987; Cannon *et al.* 1988; Schmidt 2018; Openshaw *et al.* 2017; Morabito *et al.* 2016; Graham *et al.* 1991). However, studies in both mice and humans also indicate that an overexuberant $CD8^+$ T cell response can cause pathogenesis (Tregoning *et al.* 2008; Graham *et al.* 1991; Lukens *et al.* 2010). $CD8^+$ T cells mediate their antiviral effects by activation and secretion of effector molecules and pro-inflammatory cytokines such as TNF-α, IFN-γ and Granzyme B (GrzmB) (Schmidt 2018) or by directly killing virus-infected cells (Chen and Kolls 2013). Intranasal treatment of mice with IFN-γ has been shown to be sufficient to reduce viral load and improve disease severity, as measured by weight loss without increasing the recruitment of $CD4^+$ or $CD8^+$ T cells (Empey *et al.* 2012).

In mice, $CD8^+$ T cell recruitment peaks at day 7-8 following primary RSV infection; this correlates with the peak of disease severity as measured by weight loss (Tregoning *et al.* 2008; Graham *et al.* 1991). It has been harder to establish the precise timing of $CD8^+$ T cell recruitment during primary infection in humans, however studies in infants have shown that activated effector T cells peak at day 9-12 in the blood during primary RSV infection (Heidema *et al.* 2007). It has been suggested that a delayed $CD8^+$ T cell response in infants might be the cause of the heightened disease severity as observed in infants compared to adults, as the effector $CD8^+$ T cells peak in the airways during disease resolution in infants (Heidema *et al.* 2007). During experimental human challenge with RSV, healthy adult volunteers mount $CD8^+$ T cell responses but do not develop severe disease (Jozwik *et al.* 2015). It should be considered however that all adults are expected to have encountered RSV in their lives and so these immune responses are highly unlikely to represent a primary immune response to RSV.

1.4.3 Humoral responses

The fact that RSV is a ubiquitous pathogen, able to cause annual, seasonal epidemics worldwide, is in part due to the fact that very similar strains of RSV cause repeat infections throughout life (Openshaw *et al.* 2017). Unlike influenza virus, which has high mutation rates driving high antigenic variation between infectious seasons, people are able to become re-infected with genetically similar strains of RSV throughout life (Melero and Moore 2013; Ascough *et al.* 2018). This is thought to be mediated by selective immune amnesia induced by the virus and remains one of the major unanswered questions in the field of immunity to RSV (Chiu and Openshaw 2015).

Although people do produce RSV-specific antibodies following RSV infection, the antibodies produced are neither well maintained nor are they thought have a high neutralising capacity (Openshaw *et al.* 2017; Chiu and Openshaw 2015). During natural infection, maternal antibody levels provide some protection from severe disease; maternal antibody levels correlate inversely with disease in infants however this does not provide complete protection (Stensballe *et al.* 2009). In an experimental human challenge model of RSV infection, RSV-specific nasal IgA correlated more strongly with protection than serum neutralising IgG antibody (Habibi *et al.* 2015). However, this also did not provide complete protection and over half of the volunteers in the RSV challenge study became infected following RSV inoculation, despite all volunteers having moderate levels of pre-existing antibody (Habibi *et al.* 2015). These data suggest that although RSV can induce antibody production, the antibody is not of high enough quality to provide good protection. Furthermore, although experimental RSV infection of human volunteers induced the production of both serum and nasal RSV-specific antibody as measured 4 weeks after inoculation, this was not well maintained at 180 days post inoculation. This suggests there may also be a defect in the production of long-lived plasma B cells (Habibi *et al.* 2015). Unlike humans, mice are able to mount long-lasting, antigen-specific humoral responses to RSV which protect against re-infection (Shafagati and Williams 2018; Kinnear *et al.* 2018; Chiu and Openshaw 2015) and as such the immunological mechanism behind the humoral immune amnesia in humans has been challenging to investigate.

1.4.4 Memory T lymphocytes

In light of the fact that memory immunity mediated by B cell production of antibody is impaired during RSV infection, virus-specific memory T cell responses are thought to have an elevated importance in protection against re-infection (Kinnear *et al.* 2018; Jozwik *et al.* 2015). Various subtypes of $CD4^+$ and $CD8^+$ memory T cells exist; traditionally the major subtypes are central memory T (T_{CM}) cells, effector memory T (T_{EM}) cells and the more recently discovered resident memory T (T_{RM}) cells (Jameson and Masopust 2018; Lefrançois and Marzo 2006; Mueller *et al.* 2013; Sallusto *et al.* 2004). However, within the T_{CM} and T_{EM} subtypes many other subpopulations exist and there is plasticity between some of these populations (Wherry *et al.* 2003; Sallusto *et al.* 2004; Jameson and Masopust 2018). T_{CM} cells are present in both the circulation and in the T cell areas of the LNs (Sallusto *et al.* 1999). These cells are defined by the expression of CD62L, which facilitates their homing to the LNs (Sallusto *et al.* 1999). T_{EM} cells are found in the circulation as well as in non-lymphoid organs and lack the expression of CD62L (Sallusto *et al.* 1999). T_{EM} cells can rapidly respond to re-encounter of antigen and become activated to secrete cytokines such as IFN-γ, GrzmB, IL-4 and IL-5 (Sallusto *et al.* 2004). Conversely, although T_{CM} cells are less dependent on co-stimulation and therefore can respond to antigen more rapidly than naïve T cells, they do not respond as effectively as T_{EM} cells (Sallusto *et al.* 1999). They are, however, more capable of proliferation than T_{EM} cells upon stimulation with cytokines (Geginat *et al.* 2003). Upon T cell receptor (TCR) stimulation, T_{CM} cells initially produce IL-2 but can then go on to differentiate into T_{EM} cells which produce IFN-γ and IL-4 (Sallusto *et al.* 2004). As T_{CM} cells have high proliferation capacities these cells are very important in protective immunity and some T_{EM} cells can even go on to differentiate into T_{CM} cells (Wherry *et al.* 2003).

1.4.5 Resident memory T lymphocytes

T_{RM} cells are formed during a primary infection and are defined by their localisation in the peripheral tissue following disease resolution (Schenkel and Masopust 2014). T_{RM} cells are similar to T_{EM} cells in terms of function; both have innate-like characteristics in that they can respond rapidly upon pathogen re-encounter in the tissues, mounting a specific and cytotoxic memory immune response to prevent pathogen establishment (Pizzolla *et al.* 2017; Schenkel and Masopust 2014). However, unlike T_{EM} cells, T_{RM} cells are not thought to re-enter the circulation (Jiang *et al.* 2012; Masopust *et al.* 2010; Masopust *et al.* 2001). Therefore, they can respond much more rapidly upon pathogen re-encounter. The biological importance of

T_{RM} mediated memory immunity was demonstrated using local vaccinia virus infection of parabiotic mice (Jiang *et al.* 2012). Mice with both T_{RM} and circulating T_{EM} cleared 10^4 times more virus after 6 days than mice with circulating T_{EM} cells alone (Jiang *et al.* 2012).

Seminal studies which connected the vasculature of mice by parabiosis showed that distinct populations of both $CD4^+$ and $CD8^+$ memory T cells of an effector cell phenotype are maintained in peripheral tissues including the skin epidermis, the female reproductive tract and the lungs where they reside following disease resolution without re-entering the circulation (Iijima and Iwasaki 2014; Jiang *et al.* 2012; Schenkel *et al.* 2013; Teijaro *et al.* 2011). For ease, in most studies, $CD4^+$ T_{RM} cells are characterised by the cell surface expression of CD69 while $CD8^+$ T_{RM} cells are defined by the additional presence of cell surface CD103 (Masopust and Soerens 2019). However, both $CD69^-$ and $CD103^-$ T_{RM} populations have been reported *in vivo* (Masopust and Soerens 2019; Steinert *et al.* 2015) and so these markers are not definitive of memory T cell residency status. CD69 is a transmembrane lectin-protein and is also a T cell activation marker (Ziegler *et al.* 1994). CD69 inhibits S1P-mediated T cell migration into the blood by binding the receptor S1PR1, also expressed on the surface of T cells. This drives the internalisation and degradation of S1PR1 from the cell surface membrane, retaining T cells in the peripheral tissues by preventing their migration towards S1P gradients in the blood (Mackay *et al.* 2015; Shiow *et al.* 2006; Bankovich *et al.* 2010). CD103 (integrin αE) is a receptor for E-cadherin which therefore tethers T cells to the epithelium (Karecla *et al.* 1995; Cepek *et al.* 1994).

Although the origin and developmental regulation of T_{RM} cells is not yet fully understand, it is known that a specific inflammatory milieu is required for their persistence in peripheral tissues (Schenkel and Masopust 2014; Masopust and Soerens 2019). T_{RM} cells are thought to develop locally from uncommitted memory precursor cells (Schenkel and Masopust 2014; Mani *et al.* 2019). Cytokines such as transforming growth factor β (TGF-β) help to form T_{RM} cell populations (Schenkel and Masopust 2014) when precursor cells acquire the ability to respond to TGF-β by down-regulation of T-bet and eomesodermin (Eomes) (Mackay *et al.* 2015). It was shown *in vivo* that the formation of T_{RM} cells in the epidermis of the skin is dependent on interaction with DCs which activate and present TGF-β to memory precursors (Mani *et al.* 2019). The biological mechanisms which regulate the maintenance of T_{RM} cell populations locally in tissues are thought to be highly dependent on both the tissue and the infectious agent (Masopust and Soerens 2019). As T_{RM} cells remain in a specific anatomical compartment, they need to be well adapted to unique local oxygen and metabolite concentrations. Furthermore, cell-cell interactions between T_{RM} cells and neighbouring

stromal cells and extracellular matrix proteins also likely play a role in their maintenance (Masopust and Soerens 2019). These are all factors which can vary greatly between tissues. It is thought that the maintenance of T_{RM} cell populations is not dependent on antigen (Hogan *et al.* 2001), although it has been suggested that this could also vary between tissues (Lee *et al.* 2011).

T_{RM} cell mediated immunity has been described in viral, bacterial, fungal and parasitic infections (Muruganandah *et al.* 2018) and the importance of immunity mediated by T_{RM} cells during RSV infection has been demonstrated in both mouse and man (Jozwik *et al.* 2015; Kinnear *et al.* 2018). Experimental human challenge of healthy volunteers with RSV found that pre-existing RSV-specific memory $CD8^+$ T cells was associated with better symptom scores and reduced viral load during RSV challenge (Jozwik *et al.* 2015). Furthermore, in mice, transfer of airway $CD8^+$ T cells from previously RSV infected mice to RSV-naïve mice was sufficient to ameliorate disease severity as measured by weight loss during primary RSV infection (Kinnear *et al.* 2018). Together these findings imply that vaccine design may benefit from targeting local memory immunity in the lung and provide an optimistic outlook on the possibility of developing antigen-specific $CD8^+$ T cell immunity which may confer protection in the absence of antibody.

1.5 Animal models of RSV infection

Clinical studies of infants hospitalised with severe RSV infection have been essential for our basic understanding of the immune responses which occur in the lung during human disease. However, there are many challenges associated with clinical RSV research. First of all, RSV-infected infants typically only present at a healthcare centre when symptoms have become severe. As such, it is difficult to establish the time point at which the infection occurred and therefore impossible to precisely determine the kinetics of the ensuing immune response. It is also difficult to study innate immunity to RSV in humans as these transient events have passed at the point at which children present with symptomatic disease. Furthermore, it is often very difficult to obtain ethical approval for observational studies in infants, and infant airway and blood samples can be challenging to collect. Complimentary studies in animal models have therefore been essential for our current understanding of RSV immunity.

Many different animal models have been used to study hRSV infection (Taylor 2017; Sacco *et al.* 2016; Bern *et al.* 2011). Models using species-specific pneumoviruses related to hRSV, such as bovine RSV infection of cows and PVM infection of mice, have the advantage that they are highly permissive for viral replication and cause lung pathology and disease (Bern *et al.* 2011). The major disadvantage of these models is that the disease caused by related pneumoviruses may not exactly replicate the immunology of and disease caused by hRSV. Therefore, the animal model which has been used most extensively to further our understanding of immunity to RSV is infection of adult mice with hRSV (Taylor 2017; Sacco *et al.* 2016; Bern *et al.* 2011). Although BALB/c mice are more permissive for viral replication (Jessen *et al.* 2011), hRSV is also able to replicate productively in C57BL/6 mice and causes disease in both strains as measured by weight loss (Cannon *et al.* 1988; Graham *et al.* 1991; Goritzka *et al.* 2014; Goritzka, Makris, *et al.* 2015). The major advantage of studying RSV in C57BL/6 mice over BALB/c mice is the existence of more genetic knock-out strains on the C57BL/6 background. Both these models have limitations; mice must be infected with a very high titre viral inoculum for productive viral replication and disease to occur. Additionally, not all aspects of disease are recapitulated – hRSV disease in infants is characterised by the production of mucus plugs in the airways (Aheme *et al.* 1970; Johnson *et al.* 2007). Infection of mice with hRSV typically does not induce a pathological mucus response, although this can be modulated using infection with more mucus-inducing strains of hRSV (Moore *et al.* 2009; Stokes *et al.* 2011).

Overall, the adult mouse model is considered to be a good model in which to study RSV infection as the major immunological responses which have been observed in infants are also observed in mice (Fig. 1.3). The kinetics of the immune response in mice is understood much more precisely than in infants as the exact timing of the infection can be clearly established. In infants, it is thought that RSV viral load peaks in the lung prior to the onset of symptomatic disease however RSV can still be detected by PCR at variable loads throughout disease (DeVincenzo *et al.* 2005; Houben *et al.* 2010; Garcia-Mauriño *et al.* 2019). In mice, the viral load peaks in the lung on day 4 p.i., also prior to the onset of disease, yet viral loads are very low during the peak of disease (Goritzka *et al.* 2014). It is likely that hRSV is more easily detectable in infants during RSV disease than in mice as humans are the natural host for RSV and the lungs are therefore more permissive to viral replication.

RSV infection of mice induces an immediate, protective type I IFN response which peaks at 6 h p.i. (Bhoj *et al.* 2008; Demoor *et al.* 2012; Goritzka *et al.* 2014; Goritzka, Makris, *et al.* 2015). Type I IFNs also play an important role in RSV disease of infants; polymorphisms in genes related to IFN production are associated with disease severity (Janssen *et al.* 2007; Tal *et al.* 2004; Awomoyi *et al.* 2007). Neutrophils are the first recruited cells to the lungs of mice during RSV infection and peak at 18-24 h p.i. (Goritzka *et al.* 2014). Inflammatory monocytes are recruited on day 2 p.i. in mice (Goritzka, Makris, *et al.* 2015), while NK cells peak on day 4 p.i. (Hussell and Openshaw 1998). Evidence from fatal RSV cases suggest that NK cells are also important in preventing severe disease in infants (Welliver *et al.* 2007; De Weerd *et al.* 1998), however the kinetics of the NK cell response in humans is not known. The major immunological events which occur during symptomatic disease have been better studied in infants than the early immune responses. A hallmark of RSV-induced bronchiolitis is extreme airway neutrophilia at the height of disease severity (McNamara 2003; Everard *et al.* 1994). In contrast, in the murine model, neutrophil recruitment to the lung peaks earlier, prior to the onset of disease (Fig. 1.3). Neutrophils are also detected in the murine lung on day 7 p.i., but to a lesser extent than the influx observed during the incubation period (Tregoning *et al.* 2008). In mice, it is well known that cytotoxic $CD8^+$ T cells are major drivers of disease (Graham *et al.* 1991; Cannon *et al.* 1988; Tregoning *et al.* 2008). $CD4^+$ T cells also contribute to disease, yet to a lesser extent than $CD8^+$ T cells (Tregoning *et al.* 2008). Activated $CD4^+$ and $CD8^+$ T cells are also detected in both the airways and circulation of infants hospitalised with severe disease (Heidema *et al.* 2007). This suggests that the mouse model likely recapitulates this aspect of human disease, although the exact kinetics of T cell recruitment and activation in the infant lung are unknown. One aspect of RSV immunity which cannot be modelled in adult

mice are the humoral responses. Unlike humans, mice are able to mount protective and long-lasting antigen-specific antibodies in response to RSV (Shafagati and Williams 2018; Kinnear *et al.* 2018; Chiu and Openshaw 2015).

As with all animal disease models, the adult mouse model of RSV infection has certain limitations. As mice are not the natural host for hRSV, not all aspects of disease or the immune response are fully recapitulated. Nonetheless it is broadly considered to be a good model to use for mechanistic studies of RSV infection, especially to investigate the events which occur during the incubation period which are so challenging to study in humans.

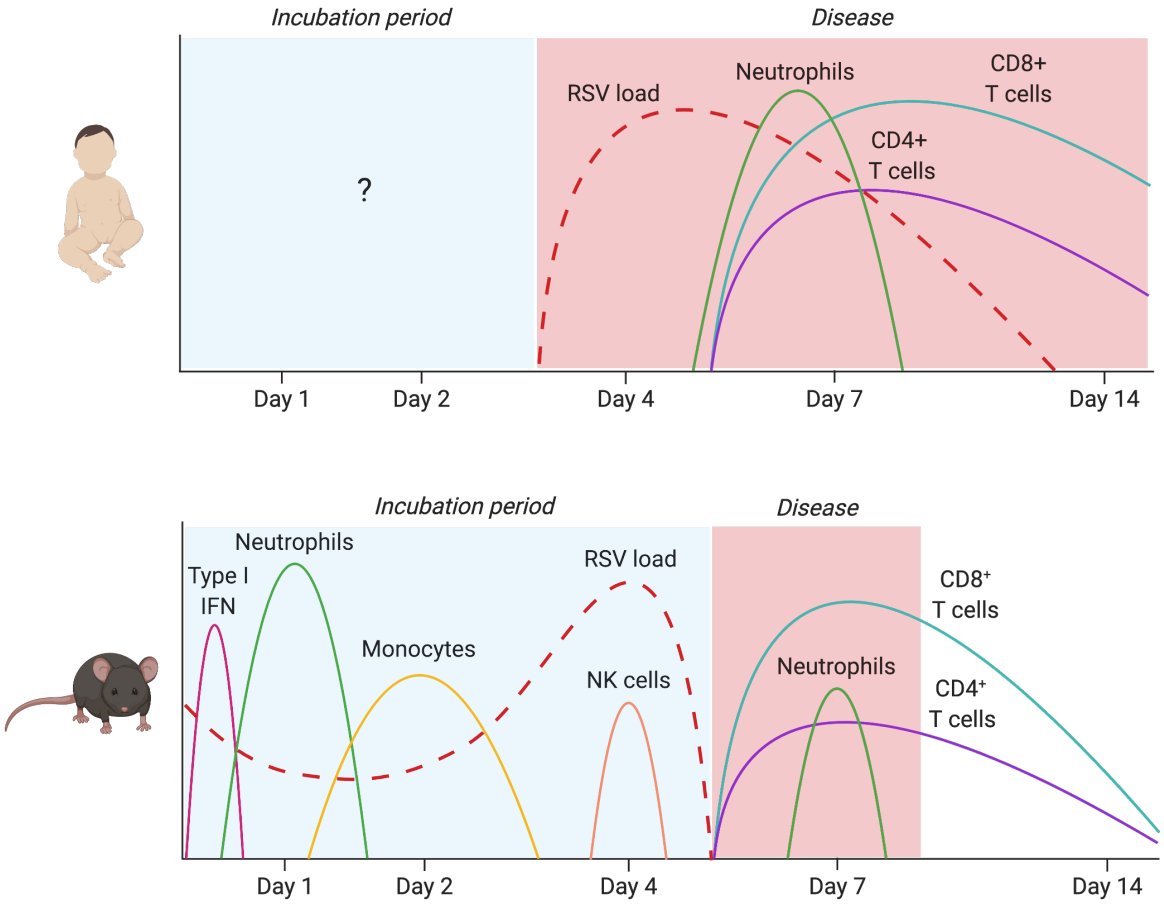

Figure 1.3. The kinetics of the immune response to RSV in infants versus in mice. During RSV infection of infants, very little is known about the immune responses which occur during the incubation period following infection (days 0-3). Infants typically present at a healthcare setting after symptoms develop from days 3-6 p.i.. Viral load is thought to peak around day 4-6 in infants but can still be detected at variable loads throughout disease, dependent in part on disease severity and the timing after the initial infection. Airway neutrophilia is thought to peak at the height of disease severity. $CD8^+$ and $CD4^+$ T cells can also be detected in the airways and circulation during severe disease. Experimental RSV infection of mice is characterised by the immediate production of type I IFNs and the recruitment of neutrophils and monocytes to the lungs during the incubation period. Viral load peaks at day 4 p.i., during this period NK cell recruitment also peaks in the lungs. Disease, as measured by weight loss, ensues from days 5-8 p.i. in mice. The peak of disease severity coincides with the recruitment of $CD8^+$ and $CD4^+$ T cells to the lungs as well as, to a lesser extent, a second wave of recruited neutrophils.

1.6 Neutrophils

1.6.1 Origin and development

Neutrophils, an important innate immune cell, are the most abundant cell type in the circulation of the human body. During steady state, it is estimated that 1 billion neutrophils are produced per kilo of body weight daily – this can increase to 10 billion during an infection (Ley *et al.* 2018). The vast proportion of neutrophils reside in the bone marrow while a large number of mature neutrophils are also detected in the circulation; these can respond rapidly to infection or injury. Notably, the lungs of both mice and humans are enriched in a population of neutrophils which reside in the pulmonary vasculature and perivascular space (Nicolás-Ávila *et al.* 2017). It is thought that these neutrophils are retained in the lung actively, by upregulation of CXCR4 which binds CXCL12, a ligand expressed by a subset of lung endothelial cells (Devi *et al.* 2013). The role of these resident lung neutrophils is not yet well understood, but it is thought that they exist to supply the circulation and/or to be positioned for rapid responses to pulmonary pathogens (Nicolás-Ávila *et al.* 2017). Neutrophils are short-lived, although their precise life span is debated. Lowest estimates range from 4 hours (Summers *et al.* 2010) up to 5.4 days for circulating human neutrophils (Simon and Kim 2010; Pillay *et al.* 2010). However, the methods used in this latter study may also have labelled bone marrow neutrophils and this is therefore likely an over-estimate (Tofts *et al.* 2011; Kolaczkowska and Kubes 2013). As the most abundant and short-lived cell in the circulation, neutrophil turnover must be tightly regulated during both homeostasis and disease.

During haematopoiesis in the bone marrow, haematopoietic stem cells give rise to common myeloid progenitor cells which can go on to differentiate to become both megakaryocyte/erythroid and granulocyte/macrophage lineages (Lawrence *et al.* 2018). Granulocyte-colony stimulating factor (G-CSF) is a major regulator of neutrophil production; G-CSF drives haematopoietic stem cells to commit to the common myeloid progenitor line (Richards *et al.* 2003) and G-CSF knock out mice are highly neutropenic (Liu *et al.* 1996). The C/EBP family of transcription factors is in part responsible for determining differentiation to the neutrophil lineage; C/EBP-ε acetylation and GFI-1 expression drives differentiation into neutrophils and eosinophils while loss of GATA1 expression differentiates neutrophils from eosinophils (Lawrence *et al.* 2018). Upon maturation, neutrophils upregulate CXCR2 to facilitate migration into the circulation towards gradients of CXCL2 whilst they downregulate

CXCR4; a receptor which mediates neutrophil retention in the bone marrow (Nauseef and Borregaard 2014). Multiple different inflammatory signals have been demonstrated to increase neutrophil lifespan including IFN-γ, G-CSF and lipopolysaccharide (LPS) (Colotta *et al.* 1992). During disease, secretion of IL-17 by Th17 cells can promote neutrophil production (Cua and Tato 2010), in part via the upregulation of G-CSF (Stark *et al.* 2005), Conversely, the production of pre-B cell colony enhancing factor can inhibit neutrophil apoptosis thereby inhibiting neutrophil production in the bone marrow (Jia *et al.* 2004).

The development and maturation of the neutrophil granules, granulopoiesis, occurs over a period of 4-6 days in the bone marrow (Lawrence *et al.* 2018). Neutrophil granules contain >1200 unique proteins pre-stored in membrane bound vesicles the cytoplasm (Rørvig *et al.* 2013). These include proteolytic enzymes, antimicrobial proteins, components of the respiratory burst oxidase as well as membrane-bound receptors for endothelial adhesion molecules, extracellular matrix proteins, bacterial products and soluble mediators of inflammation (Faurschou and Borregaard 2003). Azurophilic granules first form in myoblasts and promyelocytes, during which time the nucleus is large and rounded. Specific or secondary granules form next, followed by gelatinase granules and finally neutrophil maturation ends with the formation of ficolin-1 granules and secretory granules. At this point the neutrophils have acquired the characteristic segmented nucleus (Lawrence *et al.* 2018).

1.6.2 Neutrophil granules

Azurophilic granules were originally defined as staining positive for peroxidase due to their high content of myeloperoxidase (MPO). These granules are filled with a multitude of proteolytic enzymes including the serine proteases proteinase 3, cathepsin G, neutrophil elastase (NE), and neutrophil serine protease 4 (NSP4) (Rørvig *et al.* 2013). These factors can degrade the extracellular matrix thereby facilitating neutrophil migration as well as have direct anti-microbial effects on pathogens (Rørvig *et al.* 2013). Neutrophil elastase, for example, has been shown to have an important role in host defence against gram negative bacteria (Belaaouaj *et al.* 1998). Furthermore, excluding NSP4, these factors can induce the activation of macrophages, lymphocytes and platelets (Faurschou and Borregaard 2003). Azurophilic granules also contain antimicrobial peptides such as α-defensin, azurocidin and bactericidal/permeability-increasing protein (BPI). Neutrophil defensins can have direct effects on pathogens including bacteria, fungi and enveloped viruses by inducing pore formation in the protective lipid bilayers (Wimley *et al.* 1994). Furthermore, defensins can act on other

branches of the immune response including DCs and T cells (Yang *et al.* 2000). Azurophilic granules are most characteristically the granules which carry MPO. MPO is the most abundant enzyme pre-stored in neutrophil granules and makes up 5% of the dry weight of neutrophils (Odobasic *et al.* 2016). By fusing with phagolysosomes, MPO collaborates with nicotinamide adenine dinucleotide phosphate (NADPH) oxidase to drive the production of reactive oxygen species (ROS) during the oxidative burst in phagolysosomes where destruction of the pathogen can be carried out without damaging the host (Lawrence *et al.* 2018). First NADPH oxidase in the membrane of the phagolysosome catalyses the reaction between NADPH and O_2 to generate $NADP^+$, H^+, and superoxide radicals ($O_2^{\cdot-}$). $O_2^{\cdot-}$ is rapidly converted to hydrogen peroxide (H_2O_2). MPO then catalyses the reaction between H_2O_2 and chloride to form anti-microbial hypochlorous acid (HOCl) and hydroxyl radicals (·OH), as well as singlet oxygen ($^1O_2$). MPO activity within the neutrophil is also required to enhance chromatin decondensation during the final stages of neutrophil extracellular trap (NET) release (Papayannopoulos *et al.* 2010). Finally, MPO can be released into the extracellular milieu during neutrophil degranulation.

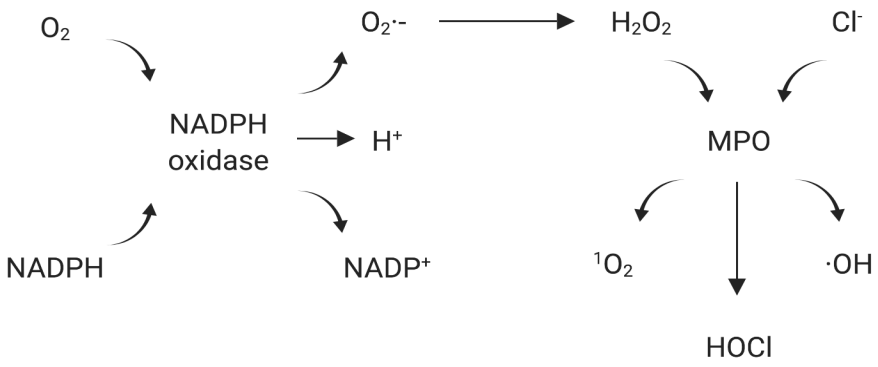

Figure 1.4. NADPH oxidase and MPO drive oxidative burst in neutrophils. In the membrane of the phagolysosome, NADPH oxidase catalyses the reaction between NADPH and O_2 to generate $NADP^+$, H^+, and $O_2^{\cdot-}$. $O_2^{\cdot-}$ is rapidly converted to H_2O_2 by superoxide dismutase. MPO in the azurophilic granules catalyses the reaction between H_2O_2 and chloride to form HOCl, ·OH and $^1O_2$. Created using BioRender.

Specific granules, also known as secondary granules, generally contain proteins more important as secreted arsenal during degranulation in contrast to azurophilic granules which have classically been considered as more important in the defence against ingested particles and pathogens (Borregaard and Cowland 1997). These granules contain anti-microbial peptides such as lysozyme and lactoferrin, cathelicidins, proteinases such as collagenase (MMP-8) and complement activators as well as cytoplasmic membrane receptors for

neutrophil chemoattractants such as N-formylmethionyl-leucyl-phenylalanine (fMLP) and laminin receptors (Rørvig *et al.* 2013; Borregaard and Cowland 1997; Faurschou and Borregaard 2003; Sørensen *et al.* 2001). In contrast to the protein content of azurophilic granules which is largely fully processed, the mediators and enzymes stored in specific granules are stored as inactive zymogens and need to be processed in order to be active (Cowland and Borregaard 2016). There is some overlap in mediator content between the specific granules and gelatinase granules; also known as tertiary granules. These granules are defined by their lack of peroxidase and lactoferrin as well as by containing gelatinase (MMP-9) (Kjeldsen *et al.* 1994). These granules are formed after the azurophilic and secretory granules during neutrophil maturation. Gelatinase granules also contain membrane receptors which are thought to be important for neutrophil migration and extravasation into inflamed tissues such as CD11b/CD18, CD67, CD177, SCAMP, and VAMP2 (Lawrence *et al.* 2018; Borregaard and Cowland 1997).

Originally, three types of pre-stored neutrophils granules were defined in addition to the secretory vesicles. However, more recently a fourth type of granule was identified; the ficolin-1-rich granules (Rørvig *et al.* 2013). In terms of content, these are very similar to neutrophil secretory vesicles and they are also formed in the final stages of neutrophil development (Lawrence *et al.* 2018). Ficolin-1 granules and secretory vesicles are both secreted with minimal stimulation and contain factors such as human serum albumin, CR1, vanin-2 (VNN2), LFA-1, actin and several cytoskeleton-binding proteins (Lawrence *et al.* 2018). Secretory vesicles, which are not true granules, also contain a plethora of membrane-bound receptors. The contents of ficolin-1-rich granules and secretory vesicles are both important for neutrophil interactions with the vascular endothelium and for migration through to infected tissues.

1.6.3 Subtypes

In recent years experimental evidence has suggested that there may be various subtypes of neutrophils with different roles in infection, cancer and autoimmunity (Ng *et al.* 2019). In a murine model of cancer N1 and N2 subtypes of neutrophils were first described, defined by their pro-tumorigenic (N1) or anti-tumorigenic roles (N2) (Fridlender *et al.* 2009). In these studies, TGF-β promoted neutrophils to take on an N2 phenotype; these neutrophils expressed less immune-activating cytokines and were impaired in their ability to kill tumour cells *ex vivo*. More recently, N1 and N2 neutrophils were characterised in the circulation (Arnardottir *et al.* 2012) and in the lungs of mice (Peñaloza *et al.* 2018). N1 lung neutrophils

are thought to be smaller and less granular than N2 cells. During infection with *Streptococcus pneumoniae* both N1 and N2 cells were recruited to the lung (Peñaloza *et al.* 2018) and it is not yet clear whether these subtypes have differing functions in host defence against this respiratory pathogen. It is also still unclear whether the phenotypic differences between N1 and N2 cells represent true subtypes or whether these differences can be attributed to differences in the priming, maturation status and/or activation status of these neutrophils.

It has also been suggested that neutrophils can be subtyped by their density; phenotypic differences between low-density neutrophils (LDNs) and high-density neutrophils (HDNs) have been observed in a variety of solid cancer, inflammatory conditions including systemic lupus erythematosus and infectious diseases including HIV (Hong 2017; Carmona-Rivera and Kaplan 2013). Furthermore, both immunosuppressive and pro-inflammatory LDNs have been described (Hong 2017; Carmona-Rivera and Kaplan 2013). Immunosuppressive LDNs have been found to suppress T cell proliferation and IFN-γ production and may have a more immature phenotype in some situations (Hong 2017). CD10 is thought to be a stable and relevant marker of neutrophil maturity on both human LDNs and HDNs, and was found to be upregulated on neutrophils with a suppressive phenotype (Brandau and Hartl 2017; Marini *et al.* 2017). This would suggest that the functional differences may be due to the maturation status of the neutrophils. It is also possible that LDNs represent exhausted neutrophils which have become low-density after degranulating and expelling their granular contents (Hong 2017). Furthermore, it is known that neutrophils can tailor their responses depending on the signals in the inflammatory environment (Branzk *et al.* 2014). Therefore, as with N1 and N2 cells, it is not clear whether LDNs and HDNs are true subtypes and future work is needed to define the transcriptional profiles and cell surface markers of possible neutrophil subtypes.

1.6.4 Recruitment, priming and activation

A defining feature of neutrophils is their ability to infiltrate tissues early and rapidly during both infection and sterile injury. For neutrophil recruitment to occur, PAMPs and DAMPs must trigger their respective receptors in order to initiate the production of pro-inflammatory mediators and neutrophil chemoattractants (Williams *et al.* 2011). Major neutrophil chemoattractants induced downstream of PRR signalling include interleukin-8 (IL-8) (humans), KC/CXCL1 (mice), MIP2/CXCL2 (mice), CXCL5, complement component 5a (C5a), fMLP, platelet activating factor (PAF), leukotriene B4 (LTB4) while some of the DAMPs which can trigger neutrophil recruitment include hyaluronan, heparin sulfate, heat shock proteins,

and adenosine triphosphate (ATP) (Williams *et al.* 2011; Chen and Nuñez 2010). Many DAMPs act to recruit neutrophils indirectly by inducing the production of pro-inflammatory mediators including neutrophil chemoattractants and by upregulating cell adhesion molecules on the endothelium (Pittman and Kubes 2013). However, ATP and factors released from the mitochondria of necrotic cells can act directly on migrating neutrophils, enhancing their recruitment into damaged tissues (Pittman and Kubes 2013). During inflammation, neutrophils must undergo a series of steps in order to transmigrate through to the affected tissue; this process is known as the leukocyte adhesion cascade (Kolaczkowska and Kubes 2013). The key steps in this cascade are tethering to the endothelium, rolling, firm adhesion, crawling and finally transmigration through the vascular endothelium (Kolaczkowska and Kubes 2013).

Initially, inflammation induces endothelial cells to upregulate cell adhesion molecules such as E-selection (Lawrence *et al.* 1994; Lawrence and Springer 1993) and P-selectin (Petri *et al.* 2008; Bevilacqua *et al.* 1989). This facilitates the primary interactions between circulating neutrophils with the endothelial barrier and is the first step in slowing down the rapid flow of neutrophils through the vasculature. PGLS-1 on circulating neutrophils binds P-selectin to mediate the initial adherence to the vascular walls while the binding of ESL-1 on neutrophils to E-selectin is required for neutrophil rolling across the endothelial cells (Hidalgo *et al.* 2007). During rolling, neutrophils must form new interactions with the endothelium at the leading edge while releasing contacts at the back (Kolaczkowska and Kubes 2013); this is in part mediated by CD44 interactions (Hidalgo *et al.* 2007). During arrest and adhesion, further interactions between CD11b and LFA1 on neutrophils with ICAM-1 and ICAM-2 on the endothelial cells slows down the rolling and begins to mediate tighter interactions between the vascular wall and the neutrophils (Kolaczkowska and Kubes 2013). These initial interactions begin the process of priming neutrophils for activation in the tissue. Interactions with chemokines associated with the endothelium further drives neutrophil extravasation into tissues and also contributes to priming. ELR-CXC chemokines including IL-8, CXCL1, CXCL2 and CXCL5 amongst others have been particularly well studied in this context (McColl and Clark-Lewis 1999; Herbold *et al.* 2010; Ludwig *et al.* 1997; Kolaczkowska and Kubes 2013). It was originally hypothesised that chemokines diffuse from the tissue through intracellular gaps to the lumen of the vasculature. However, it has been shown that IL-8 can also be endocytosed and actively transported through endothelial cells to the apical side in order to facilitate neutrophil recruitment (Middleton *et al.* 1997). Chemokines associate with the vascular endothelium through interactions with factors such as heparan sulphate to prevent being washed away by the velocity of the circulation (Massena *et al.* 2010).

Following firm adhesion, neutrophils either migrate between cell-cell junctions (paracellular migration) or are transported through the endothelial cells (transcellular migration) (Kolaczkowska and Kubes 2013). During both processes, neutrophils move to the site of tissue entry by crawling along the endothelium; a process not thought to be mediated by chemokines (Kolaczkowska and Kubes 2013) but which is dependent on β2 and α4 integrins (Harding *et al.* 2014). During migration, neutrophils must move against the chemokine gradient/s which initiated their recruitment from the circulation into a site saturated with non-orientating concentrations of these chemokines. It has been proposed that there are hierarchies of neutrophil chemoattractants and that certain chemokine gradients can override others so that neutrophils migrate against these early chemokine gradients in order to reach the site of inflammation (Foxman *et al.* 1997). For example, factors such as fMLP and the complement component C5a are thought to override CXC-motif chemokines (Kolaczkowska and Kubes 2013; Foxman *et al.* 1997). These factors also drive further activation of primed neutrophils. During paracellular migration, neutrophils must first cross between endothelial cells by breaking cell-cell junction bonds which maintain the structure of the vascular wall, then cross the basement membrane and migrate between pericytes to reach the inflamed tissue. Transcellular migration is thought to be slower and involves neutrophils passing through a pore in an individual endothelial cell; this maintains cell-cell junctions (Carman 2009; Feng *et al.* 1998; Phillipson *et al.* 2008).

A unique pattern of neutrophil recruitment termed swarming was first described in 2008 in a murine model of *Toxoplasma gondii* infection (Chtanova *et al.* 2008). Neutrophil swarming refers to the phenomenon of neutrophils moving as a group in a highly coordinated manner, named as a nod to the behavioural dynamics observed in insects (Lämmermann 2016). Since, neutrophil swarming has been observed in sterile inflammation, bacterial, fungal and parasitic infections (Kienle and Lämmermann 2016). Two types of neutrophil swarms have been described; transient swarms typically consist of groups of 10-150 neutrophils forming smaller clusters, which are dispersed within 10-40 minutes (Lämmermann 2016; Kienle and Lämmermann 2016). Persistent swarms describe larger clusters containing >300 cells which persist for over 40 minutes (Lämmermann 2016; Kienle and Lämmermann 2016). Neutrophil swarming is initiated by “pioneer” cells which respond to the inflammatory signal. This signal is then amplified by cell death and by the release of LTB4 by neutrophils which recruits more interstitial neutrophils. Accumulating neutrophils remodel the extracellular matrix in order to from aggregates; this is dependent on signalling through multiple chemokine receptors. The final stage is swarm resolution, which is in part mediated by other myeloid cells (Lämmermann

2016; Kienle and Lämmermann 2016; Lämmermann *et al.* 2013). The type of organ, the size of the tissue damage, the presence of pathogens, the induction of secondary cell death and the number of recruited neutrophils are all thought to be factors contributing to swarm formation (Lämmermann 2016). However, it is still not well understood why swarming occurs under certain inflammatory conditions and not under others.

Neutrophil activation is a process which occurs over time, starting during recruitment and priming by inflammatory mediators and chemoattractants (Amulic *et al.* 2012). In order to become fully activated to degranulate and undergo oxidative burst, neutrophils must first undergo a series of priming steps. Neutrophil activation can be highly destructive and cause local damage to host tissues, thereby driving immunopathology (Bardoel *et al.* 2014). Therefore, the multi-step priming process acts as a mechanism to regulate these potentially damaging effector functions. Once in the tissue, pro-inflammatory host factors such as TNF-α, IL-1β and GM-CSF can contribute further to neutrophil recruitment, priming and activation (Condliffe *et al.* 1998; Buckle and Hogg 1989; Kato and Kitagawa 2006), as can pathogen derived factors such as LPS, LTB4, C5a and fMLP (Amulic *et al.* 2012). Binding of these factors to their respective receptors (often G-protein coupled receptors) on neutrophils triggers a downstream signalling cascade often via the MAPK/ERK pathway (Selvatici *et al.* 2006; Kato and Kitagawa 2006), which then induces neutrophil effector functions such as oxidative burst and neutrophil degranulation. In the inflammatory tissue micro-environment, host-derived compounds can drive neutrophil activation (Graça-Souza *et al.* 2002). Heme, released abundantly from damaged cells, was shown *in vitro* to potently trigger oxidative burst in human neutrophils in a dose dependent manner (Graça-Souza *et al.* 2002). The concentration of host chemokines can also impact the effect these mediators have on neutrophil activation status; for example, IL-8 induces shedding of L-selectin and upregulation of certain integrins at low concentrations while at higher concentrations it can induce oxidative burst (Amulic *et al.* 2012; Ley 2002). Binding of IL-1β can directly induce ROS production in human neutrophils in a MAPK dependent manner while stimulation with GM-CSF can activate neutrophils in an ERK dependent manner (Suzuki *et al.* 2001). Notably, stimulation of human neutrophils with both IL-1β and GM-CSF had an additive effect, resulting in activation of both MAPK and ERK pathways, and demonstrating how activation can be enhanced by the presence of multiple stimuli (Suzuki *et al.* 2001). Pathogen-derived neutrophil activating factors can also act synergistically on neutrophils; for example, LPS can induce assembly of the cellular machinery required for oxidative burst on the membrane of neutrophils while recognition of fMLP provides the final signal to drive the production of ROS (Guthrie *et al.* 1984; El-Benna *et al.* 2008). The

triggering of activating receptors can often lead to receptor internalisation; this has the effect of sensitising neutrophils to the same activating signal thereby regulating their activation within the tissues (Amulic *et al.* 2012).

1.6.5 Effector functions

Activation is required for neutrophils to exert their anti-microbial functions and contribute to host defence. Historically, neutrophils were considered as unsophisticated responder cells, yet it is increasingly evident that the role of neutrophils in inflammation is more complex than has previously been appreciated. Neutrophils can respond differentially to harmful stimuli (Warnatsch *et al.* 2017; Branzk *et al.* 2014), interact with other arms of the immune response and can also have roles in wound healing and the resolution of inflammation (Castanheira and Kubes 2019). Degranulation, the secretion of neutrophil granules, is a critical effector function of neutrophils and starts to be initiated early during neutrophil recruitment. Degranulation occurs in a sequential manner; first to be released are the secretory vesicles while azurophilic granules require the most potent activation signals for their release. The proteomic arsenal of the granule contents can have widespread effector functions. Gelatinases and collagenases such as MMP-8 and MMP-9 are thought to aid neutrophils in their migration through the extracellular matrix (Bradley *et al.* 2012; Keck *et al.* 2002). Other proteins are thought to be directly anti-microbial, such as NE and MPO, and can either act proteolytically or by catalysing ROS production (Borregaard and Cowland 1997). Other families of anti-microbial peptides include the cathelicidins (e.g. LL-37) and the α-defensins. Cathelicidins are activated by cleavage by proteinase 3 (Sørensen *et al.* 2001) and can be directly anti-microbial, or contribute to host defence by inducing or modulating chemokine and cytokine production (Bowdish *et al.* 2005; Kościuczuk *et al.* 2012). α-defensins have anti-microbial activity against a wide range of bacteria, fungi and enveloped viruses; the mechanism of action is thought to be via disruption of the plasma membrane by pore formation or by covering the pathogen (Wimley *et al.* 1994). The extent of neutrophil degranulation must be carefully balanced against the potential harm caused by the pathogen as the dysregulated release of proteolytic enzymes by neutrophils can cause immunopathology (Bardoel *et al.* 2014).

As professional phagocytes, another important way neutrophils contribute to host defence is by clearing up pathogens, dead cells and other debris during inflammation by engulfment (Mayadas *et al.* 2014; Kolaczkowska and Kubes 2013). Pathogens opsonised with complement and antibody can be engulfed following interactions with their respective

receptors on neutrophils; the complement receptors and FcγRs (Teng *et al.* 2017). Neutrophils also express a broad repertoire of PRRs, including TLRs (TLR1/2, TLR2/6, TLR4, TLR5, TLR7, TLR8, TLR8), RLRs (RIG-I, MDA-5), CLRs and NLRs which can directly sense microbes (Thomas and Schroder 2013). Following encapsulation of the phagocytic vacuole, pre-formed granules in the cytoplasm of the neutrophil containing hydrolytic enzymes and NADPH oxidase will fuse to make a phagosome (Mayadas *et al.* 2014). The pathogen can either be destroyed enzymatically or be destroyed by ROS in the mature phagosome. It has been suggested that phagocytosis can cause bystander damage to local host tissues when granules fuse with the phagocytic vacuole before the vacuole is fully encapsulated within the neutrophil – thereby releasing the granular contents into the extracellular milieu (Mayadas *et al.* 2014). Additionally, it was suggested that this could occur in a process termed frustrated phagocytosis when neutrophils try to engulf matter spread across large surfaces (Mayadas *et al.* 2014). More recently, however, it has been demonstrated that large microbes selectively induce extracellular ROS production (Branzk *et al.* 2014) and therefore whether frustrated phagocytosis occurs in an unregulated manner is disputed. Nonetheless, the release of proteolytic enzymes and ROS into the extracellular environment must be regulated to avoid bystander damage to host tissues (Mayadas *et al.* 2014; Bardoel *et al.* 2014).

Although capable of causing bystander damage to the host, oxidative burst via the production of ROS is a powerful tool to eliminate pathogens. In neutrophils, this is largely mediated by the enzyme NADPH oxidase (Nguyen *et al.* 2017). NADPH oxidase is made up of five protein subunits. The catalytic core ($cytb_{558}$) is made of two subunits; $gp91^{phox}$ and $gp22^{phox}$, which reside on the membranes of granules. The regulatory subunits ($p40^{phox}$, $p47^{phox}$, and $p67^{phox}$) are localised in the cytosol of the neutrophil (Nguyen *et al.* 2017). During neutrophil priming, certain changes prepare the cellular machinery for oxidative burst. GM-CSF and TNF-α can lead to the phosphorylation of $tp47^{phox}$ regulatory subunit (Dang *et al.* 2006). Furthermore, signals from G protein coupled receptors (GPCRs) and TLRs can lead to conformational changes in the three regulatory subunits, supporting their binding to the catalytic core; other signals induce the translocation of the catalytic core to the plasma membrane (Nguyen *et al.* 2017). Some stimuli, including fMLP, are also able to directly activate the NADPH oxidase in neutrophils so they can undergo oxidative burst (Dang *et al.* 2001). Assembly of a functional NADPH oxidase is required to catalyse the transfer of electrons from NADPH to O_2, producing $NADP^+$, H^+, and $O_2^{\cdot-}$. Superoxide dismutase converts $O_2^{\cdot-}$ to H_2O_2 – this can be converted by MPO, localised in the azurophilic granules, to HOCl and free radicals such as ·OH (Fig. 1.3).

ROS are thought to be damaging to pathogens in multiple ways; directly by causing damage to the pathogen as well as indirectly by inducing autophagy, inhibiting mTOR kinase to trigger an antiviral response, promoting NETosis and by promoting the cell death of infected groups of cells acting as pathogen reservoirs (Paiva and Bozza 2014). It was recently demonstrated using different physical forms of the fungal pathogen *Candida albicans* that ROS localisation can act as a mechanism for neutrophils to sense microbe size and that this influences the ensuing neutrophil response (Branzk *et al.* 2014; Warnatsch *et al.* 2017). In this study, spores of "small" *C. albicans* induced intracellular ROS production in phagosomes while "large" *C. albicans* hyphae induced extracellular ROS. The induction of intracellular ROS in response to "small" pathogens suppressed IL-1β production and restricted the recruitment of more neutrophils to the site of infection while extracellular ROS in response to a "large" pathogen had the opposite effect on IL-1β production and neutrophil recruitment (Branzk *et al.* 2014; Warnatsch *et al.* 2017). These findings suggest that the induction of ROS, in addition to the well-known role in pathogen removal, also has an important role in directing the ensuing neutrophil response.

A more recently described effector function of neutrophils is their ability to secrete NETs (Papayannopoulos 2015; Brinkmann *et al.* 2004; Branzk and Papayannopoulos 2013; Papayannopoulos *et al.* 2010; Papayannopoulos 2018). NETs are large extracellular structures of modified, decondensed chromatin and DNA decorated with the protein contents of neutrophil granules (Papayannopoulos 2018). NETs have been shown to be induced during infections with bacteria (Brinkmann *et al.* 2004), fungi (Urban and Nett 2019), parasites (Kho *et al.* 2019) and viruses (Schönrich and Raftery 2016). The induction of NETs is thought to be especially beneficial in host defence against larger pathogens which cannot be removed by phagocytosis (Papayannopoulos 2018; Branzk *et al.* 2014; Warnatsch *et al.* 2017). Multiple factors can trigger neutrophils to secrete NETs and several molecular pathways regulate their secretion (Papayannopoulos 2018). The main way NETs are thought to be induced is via a form of cell death termed NETosis, which is distinct from apoptosis and necrosis, and dependent on ROS production by NADPH oxidase (Fuchs *et al.* 2007). Protein-arginine deiminase type 4 (PAD4) is activated to citrullinate arginine residues on chromatin histones, a process which may contribute to chromatin decondensation (Papayannopoulos 2018). NE is required to translocate from granules to the nucleus where it degrades specific histones to further decondense the chromatin. This is enhanced by MPO, albeit not via its enzymatic activity (Papayannopoulos *et al.* 2010). Later the nuclear membrane disintegrates and finally

the plasma membrane breaks to release the chromatin into the extracellular environment (Fuchs *et al.* 2007).

Alternatively, NETs can be induced in a manner which doesn't kill the neutrophil in a process termed non-lytic NETosis (Yipp *et al.* 2012; Pilsczek *et al.* 2010). This is independent of ROS and occurs by exocytosis of vesicles filled with nuclear DNA (Pilsczek *et al.* 2010). Interestingly, this leaves behind cytoplasts with both diffuse, intracellular cytoplasmic DNA and completely anucleated cytoplasts; neutrophil "ghosts" (Wills-Karp 2018; Bird 2018). During infection with *Staphylococcus aureus*, these anucleated cytoplasts still retained granules in the cytoplasm suggesting they may still be able kill bacteria (Yipp *et al.* 2012). In further support of this, anucleated cytoplasts also contained bacteria implying that phagosome maturation and NET release can be regulated independently and that NET release does not necessarily also cause the release of phagocytosed bacteria (Yipp *et al.* 2012). Although NETosis can aid in host defence, it was shown recently that NETs and cytoplasts may contribute to pathological neutrophilic inflammation in asthma (Krishnamoorthy *et al.* 2018; Toussaint *et al.* 2017). In this study, the presence of NETs and cytoplasts in asthmatics positively correlated with levels of IL-17, an important mediator in neutrophil recruitment (Krishnamoorthy *et al.* 2018). NETs are thought to contribute to pathogen control by limiting microbial spread; and it is unclear how NETs might benefit the host in antiviral defence where the pathogen is largely intracellular (Schönrich and Raftery 2016). Histones have been shown to be able to neutralise H3N2 and H1N1 seasonal influenza virus (Hoeksema *et al.* 2015). However, *in vivo*, NETs were detected in areas of tissue injury in the lung during infection with a mouse adapted influenza strain (PR8) (Narasaraju *et al.* 2011; Pillai *et al.* 2016), and it is not clear overall whether NETs are beneficial or detrimental to the host during influenza virus infection.

In recent years it is increasingly well appreciated that neutrophils also play a role in directing aspects of adaptive immunity (Minns *et al.* 2019). During influenza virus infection, antibody mediated neutrophil depletion demonstrated that neutrophil recruitment to the lung is required for the later recruitment of adaptive $CD8^+$ T cells (Tate *et al.* 2012). Formation of antigen-specific T cells is dependent on the presentation of antigen to naïve T cells in the lymph nodes by DCs. In other inflammatory contexts, it has been suggested that neutrophils enhance this process by interacting directly with DCs (Schuster *et al.* 2013; van Gisbergen *et al.* 2005), as well as indirectly by secreting granule contents, which then act on DCs (Bennouna and Denkers 2005; Charmoy *et al.* 2010). In some contexts, neutrophils have also been shown to act directly as antigen presenting cells (APCs) themselves (Potter and Harding 2001; Culshaw

et al. 2008). Finally, there is evidence that neutrophils directly guide the recruitment of T cells to the lung in influenza virus infection by leaving behind trails of the T cell attracting chemokine CXCL12 (Lim *et al.* 2015). Conversely, it has also been suggested that $CD11b^+$ neutrophils suppress T cells to limit T cell mediated lung pathology during influenza virus infection (Tak *et al.* 2018) and it is possible that neutrophils may have dual roles in balancing T cell immunity versus T cell driven tissue damage during influenza virus infection. Neutrophils have also been suggested to contribute to B cell help and thereby contribute to the development of antibody responses (Cerutti *et al.* 2013; Costa *et al.* 2019; Leliefeld *et al.* 2015), in part by producing the cytokines BAFF and APRIL; regulators of B cell survival and activation (Puga *et al.* 2012). However, whether this contributes to the functionality of antibody responses during respiratory viral infections is not well known.

Neutrophils are also increasingly appreciated for having a role in the resolution of inflammation (Wang 2018; Peiseler and Kubes 2019). One mechanism is by phagocytosing and clearing up dead cells and debris from the site of inflammation (Hyde *et al.* 1999; Wang 2018). This prevents extended inflammation by removing DAMPs, which can trigger pro-inflammatory immune responses, and facilitates the wound healing response. Neutrophils also contain many factors stored in the granules which can contribute to resolution; for example, vascular endothelial growth factor (VEGF) which can drive revascularisation of damaged tissues (Gaudry *et al.* 1997). In a model of corneal injury, neutrophil depletion significantly impaired angiogenesis (Gong and Koh 2010). Finally, neutrophils can contribute to the resolution of inflammation by regulating their own recruitment by a negative feedback loops; for example, lactoferrin release during neutrophil activation inhibits further neutrophil recruitment (Bournazou *et al.* 2009). Furthermore, dying neutrophils actively attract scavenger cells to remove them from the site of inflammation (Soehnlein and Lindbom 2010). The uptake of apoptotic neutrophils by macrophages can, in turn, further suppress the inflammatory response by increasing the production of TGF-β, IL-10 and PGE_2 (Soehnlein and Lindbom 2010). During homeostasis, it has been well described that some aged neutrophils will migrate back to the bone marrow where they are cleared (Rankin 2010; Furze and Rankin 2008). Recently, it was also shown in a model of sterile injury that following activation in the tissue, neutrophils can migrate back to the bone marrow where they undergo apoptosis (Wang *et al.* 2017).

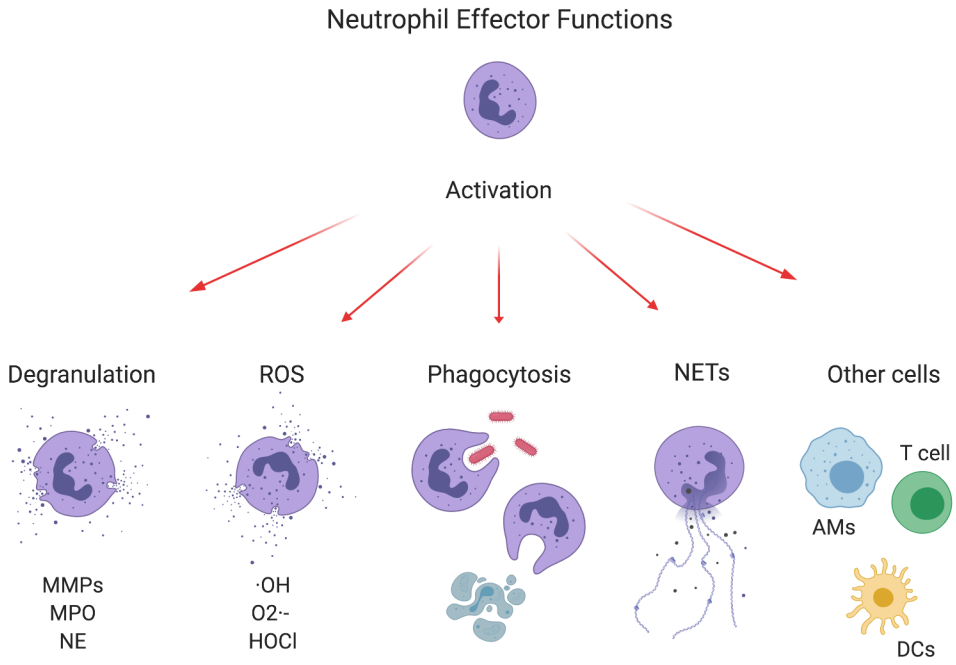

Figure 1.5. Neutrophil activation can drive a plethora of effector functions. Upon activation, neutrophils exert their effector functions to mediate pathogen killing. This must be carefully regulated to avoid contribution to disease. Neutrophil activation can trigger degranulation whereby neutrophils secrete mediators and proteolytic enzyme such as MMPs, MPO and NE which are pre-stored in cytoplasmic granules. Neutrophils can also mediate pathogen clearance by ROS production - this can either occur intracellularly in the phagolysosome to kill internalised microbes or extracellularly, to combat larger pathogens. Phagocytosis is an important effector function of neutrophils. Phagocytosis of pathogens can limit microbial spread while phagocytosis of cellular debris and apoptotic material can contribute to the resolution of inflammation. Neutrophils can also restrict microbial spread by secreting their DNA as NETs, trapping pathogens. Finally, it is increasingly appreciated that neutrophils can have direct and indirect interactions with other cells which can contribute to both innate and adaptive immunity.

1.6.6 Neutrophils in RSV infection

The role of neutrophils is better understood in bacterial and fungal infections where it is more obvious how the extracellular defence arsenal of neutrophils can contribute to host immunity. During viral infections, where the pathogen is replicating intracellularly, it is less clear how neutrophil recruitment and activation might benefit the host (Galani and Andreakos 2015; Schönrich and Raftery 2016). During influenza virus infection, neutrophil depletion studies do not agree on whether neutrophils drive disease or contribute to host defence (Peiró *et al.* 2018; Ichinohe *et al.* 2009; Tate *et al.* 2009; Tate *et al.* 2012). This is in part due to influenza strain-specific differences. The mouse adapted PR8 strain induces more severe disease, which is in part mediated by neutrophils, while infection of mice with influenza strains which cause less disease does not appear to induce neutrophil driven pathology to the same extent (Tate *et al.* 2011). Influenza virus infection has been shown to induce NETosis in mice (Pillai *et al.* 2016), likewise rhinovirus infection in a mouse model of allergic airway hypersensitivity was also

shown to be able to induce NETs (Toussaint *et al.* 2017). However, it is not clear whether the induction of NETs is beneficial or whether it causes disease by driving excessive tissue damage in either influenza virus or rhinovirus infection.

Clinical studies of RSV infection have long implicated neutrophils in disease pathogenesis (McNamara 2003; Everard *et al.* 1994; Marguet *et al.* 2008; Lukens *et al.* 2010). During severe disease of infants with RSV induced bronchiolitis, neutrophils can make up >90% of the cellular composition of the broncho-alveolar lavage (BAL) (McNamara 2003; Everard *et al.* 1994). In line with this, high levels of the neutrophil chemoattractant IL-8 are detected in the airways of infants hospitalised with severe RSV disease (Abu-Harb *et al.* 1999). A clinical investigation of infants with acute bronchiolitis in France found that levels of IL-8 were associated with more severe disease as measured by the respiratory rate and the duration of their hospital stay (Marguet *et al.* 2008). While not all infants in this study will have been infected with RSV, the authors estimated that 90% of the cases will have been RSV infected (Marguet *et al.* 2008). NE has been detected in the serum and airways of infants hospitalised with RSV, however the levels of NE did not correlate with disease severity (Emboriadou *et al.* 2007; Abu-Harb *et al.* 1999). The detection of NE, stored in the azurophilic granules and requiring the most potent activating signals for secretion, indicates neutrophils recruited to the lung during RSV infection are indeed of an activated phenotype. However, the relationship between this and their role in disease protection/pathogenesis is not clear from this study. In further support of the notion that neutrophils contribute to disease severity, it was found that the frequency of an allele containing a single nucleotide polymorphism (SNP) upstream of the *IL8* gene was significantly increased in infants who had been hospitalised with RSV-induced bronchiolitis (Hull *et al.* 2000). This allele was associated with heightened IL-8 production following stimulation of whole blood with LPS, suggesting that there is a genetic factor which contributes to the likelihood of developing severe disease during RSV infection which may act by driving increased neutrophil recruitment (Hull *et al.* 2000). However, a causal relationship is yet to be established. A prospective observational study found in a whole blood transcriptomic analysis that genes related to neutrophil function were amongst the over-expressed genes in infants hospitalised with RSV (Mejias *et al.* 2013), further supporting the notion that neutrophil dysregulation may be involved in disease susceptibility or severity.

It has been suggested that mass neutrophil recruitment to the lung early during infection might provide RSV with cellular sites for viral replication to take place. One study did indeed detect RSV mRNA transcripts in neutrophils isolated from infants with RSV induced bronchiolitis (Halfhide *et al.* 2011). However, it remains to be fully investigated whether RSV can replicate

productively in neutrophils; the finding that neutrophil depletion does not alter viral loads *in vivo* suggests this is unlikely (Stokes *et al.* 2013). It has also been suggested that RSV induced neutrophil activation delays apoptosis *in vitro* but whether this would be beneficial or detrimental to disease outcome during infection *in vivo* remains unclear (Lindemans *et al.* 2006). *In vitro* studies of the potential of RSV to activate neutrophils should be carefully considered as the inflammatory mediators produced by epithelial cells during virus propagation are also able to drive neutrophil activation (Bataki *et al.* 2005). A study using RSV "washed" of pro-inflammatory mediators to stimulate neutrophils *in vitro* significantly reduced activation as compared to neutrophils stimulated with "unwashed" RSV (Bataki *et al.* 2005).

Our current understanding of the role of neutrophils in RSV infection has also been shaped by animal models; neutrophils are also abundantly recruited to the airways of mice and calves during RSV infection (Goritzka, Makris, *et al.* 2015; van Schaik *et al.* 1998; Hägglund *et al.* 2017; Cortjens *et al.* 2016). In mice, neutrophil depletion during RSV infection revealed no change in viral load at day 4, the peak of viral replication in the mouse model, suggesting that neutrophils do not have a beneficial role in the immune response to RSV (Stokes *et al.* 2013). In this study it was also found that neutrophil depletion reduced the production of the pro-inflammatory mediator TNF-α as well as the production of airway mucin, known to cause airway obstruction during RSV infection (Stokes *et al.* 2013). Nonetheless, the cathelicidin LL-37, produced primarily by neutrophils and epithelial cells, was found to be antiviral against RSV *in vitro* in epithelial cell cultures, in mice and in humans (Currie *et al.* 2016; Currie *et al.* 2013), suggesting a possible beneficial role for neutrophils during RSV infection. Several groups have tried to investigate whether RSV infection causes neutrophils to secrete NETs (Cortjens *et al.* 2016; Funchal *et al.* 2015; Hägglund *et al.* 2017; Geerdink *et al.* 2017; Muraro *et al.* 2018). Neutrophils isolated from the airways of patients with RSV induced bronchiolitis and cultured *ex vivo* secreted strands of DNA, as stained with Hoechst and SYTOX (Geerdink *et al.* 2017). However, the possibility that this represents neutrophil cell death cannot be excluded as a specific NETs stain for citrullinated histone 3 (cit H3) was not used. Cit H3 was however detected by mass spectrometry in the airways of non-vaccinated RSV infected calves (Hägglund *et al.* 2017). Furthermore, cit H3 fluorescent microscopy staining was used to visualise the formation of NETs in lung tissue sections from RSV infected calves (Cortjens *et al.* 2016). In mice, the two major studies which have tried to visualise NETs *in vivo* during RSV infection in tissue sections are limited by the use of a generic DNA stain to visualise NETs, as opposed to the specific cit H3 staining (Muraro *et al.* 2018; Funchal *et al.* 2015). Therefore, it cannot be excluded that these studies are not just detecting cell death in the lung in response

to RSV infection. Nonetheless, RSV was found to induce possible NETs in the lung and, more specifically, RSV F protein alone was sufficient to induce possible NET secretion *in vivo* in mice (Funchal *et al.* 2015).

The molecular mechanisms regulating neutrophil recruitment and activation during RSV infection are not known. Neither is it well understood what the role of neutrophils are in the immune response against RSV. It is not yet clear whether neutrophils benefit the host and/or whether they contribute to disease severity. In this study, the regulation and role of neutrophils in RSV infection was investigated *in vivo*. *Mavs*$^{-/-}$ mice, unable to respond to RLR signalling, and *Myd88/Trif*$^{-/-}$ mice, unable to respond to the TLRs, IL-1R and IL-18R, were used to investigate the role of PRR signalling in neutrophil recruitment and activation. Furthermore, neutrophil removal by antibody mediated neutrophil depletion as well as the heightening of lung neutrophilia during RSV infection by treatment of mice with CXCL1 was used to fully explore the role of neutrophils during RSV infection *in vivo.*

2 Hypothesis & Aims

2.1 Hypotheses

- Neutrophils have an anti-viral role during RSV infection either directly by inhibiting infection or indirectly by recruiting and/or activating other cells of the immune system.
- Neutrophil recruitment to the lung during RSV infection drives disease severity.

2.2 Aims

- To investigate the mechanisms regulating neutrophil recruitment during RSV infection.
- To determine the signals which activate neutrophils in the lung during RSV infection.
- To investigate the anti-viral capabilities of neutrophils and the mechanisms by which neutrophils may be anti-viral during RSV infection.
- To explore whether neutrophil recruitment and activation drives disease severity during RSV infection.

3 Materials

3.1 Mice

Wt C57BL/6 and BALB/c mice were purchased from Charles River, UK. *Ifna6gfp*$^{+/-}$, *Ifna6gfp*$^{+/-}$ *Myd88Trif*$^{-/-}$ and *Ifna6gfp*$^{+/-}$ *Mavs*$^{-/-}$ mice were bred in-house (obtained from S. Akira, Japan). Knock-out mice are on a mixed 129/C57BL6 background and were all backcrossed for at least 6 generations. The mice were continuously screened to maintain the genotype by Transnetyx Inc. (Cordova, TN, USA). The GFP signal has not been quantified in this work so the mice are noted as wt, *MyD88/Trif*$^{-/-}$ and *Mavs*$^{-/-}$ mice, respectively, throughout. All mice were bred and housed in specific pathogen-free conditions. Different strains of mice were not co-housed but kept in the same breeding room. The breeders of *MyD88/Trif*$^{-/-}$ mice were kept on Septrin in the drinking water because of their immunocompromised status. Animals were not randomised but were gender and age-matched (7-12 weeks) between control and experimental groups. Experiments were not blinded. The total number of animals used per experiment and the number of experimental and control groups are indicated in the figure legends throughout. Each experimental unit is a single animal. To determine group sizes, a power of 0.8 was used to calculate experimental group size. 0.8 was chosen on grounds of reduction and refinement. It is the power that gives the best ratio of likelihood of success in the context of the smallest group size. A group size of 5 is sufficient to yield significant data according to power calculations based on our previous studies of murine RSV infection (example calculation; a major readout of inflammation in mice is the presence of IFN-γ^+CD8$^+$ T cells in the airways. Typical responses in inflammation were found to be 20% cytokine producing cells, with a SD of 5. Power calculations reveal that for an 80% power to detect a 2-fold change in the percentage of IFN-γ^+ T cells at a 5% significance level, a group size of 5 is required). All animal experiments were reviewed and approved by the Animal Welfare and Ethical Review Board (AWERB) within Imperial College London and approved by the UK Home Office in accordance with the Animals (Scientific Procedures) Act 1986 and the ARRIVE guidelines.

3.2 Chemicals

Table 3.1. Chemicals.

Chemical	**Supplier**
Acetone	Sigma-Aldrich, Dorset, UK
Agarose	Sigma-Aldrich, Dorset, UK
Dimethyl sulfoxide (DMSO)	Sigma-Aldrich, Dorset, UK
Ethanol	VWR, Leicestershire, UK
Isopropanol	VWR, Leicestershire, UK
$KHCO_3$	Sigma-Aldrich, Dorset, UK
Methanol	VWR, Leicestershire, UK
Na_2EDTA	Sigma-Aldrich, Dorset, UK
NH_4CL	Sigma-Aldrich, Dorset, UK
PBS tablets	Sigma-Aldrich, Dorset, UK
Sulphuric acid	Sigma-Aldrich, Dorset, UK
Tween 20	Sigma-Aldrich, Dorset, UK
β-Mercaptoethanol	Sigma-Aldrich, Dorset, UK

Table 3.2. Anaesthetics.

Anaesthetics	**Supplier**
Isofluorane	Centaur, Somerset, UK
Pentobarbital	Centaur, Somerset, UK

3.3 Reagents and kits

3.3.1 Reagents

Table 3.3. Reagents.

Reagents	Supplier	Catalogue No.
α-Ly6G MAb (1A8)	Bio X Cell, Lebanon, NH, USA	BE0075-1
Isotype rat Ig2A MAb (2A3)	Bio X Cell, Lebanon, NH, USA	BE0089
0.4% Trypan Blue	Sigma-Aldrich, Dorset, UK	T8154
0.5% Trypsin-EDTA (10x)	Gibco, Paisley, UK	59418C-100ML
CompBeads; anti-mouse	BD Bioscience, Oxford, UK	552843
CompBeads; anti-hamster anti-rat	BD Bioscience, Oxford, UK	552845
Biotin-conjugated Goat α-RSV Antibody	Bio-Rad, Watford, UK	ab19986
BSA	Sigma-Aldrich, Dorset, UK	A2058
Collagenase D	Roche, Welwyn Garden City, UK	11088882001
DAB substrate for plaque assay	Sigma-Aldrich, Dorset, UK	11718096001
DNAse I from bovine pancreas	Sigma-Aldrich, Dorset, UK	D5025
Dispase	Roche, Welwyn Garden City, UK	04942078001
Dulbecco's Modified Eagle Medium	Sigma-Aldrich, Dorset, UK	SLM-020
ELISA grade streptavidin	Biosource, Paisley, UK	MBS689542
Extravidin-peroxidase for plaque assay	Sigma-Aldrich, Dorset, UK	E2886
FCS	Sigma-Aldrich, Dorset, UK	F2442
Fixation buffer	BioLegend, Cambridge, UK	420801
FTY720	Enzo Life Sciences, Exeter, UK	BML-SL233-0025
GolgiPlug Protein Transport Inhibitor	BD Bioscience, Oxford, UK	555029
Hydrogen peroxide solution 30%	Sigma-Aldrich, Dorset, UK	216763
L-glutamin (100x)	Gibco, Paisley, UK	25030081
LIVE/DEAD Fixable Aqua Dead Cell Stain	Thermo Fisher Scientific, MA, USA	L34966
LPS from *E. coli*	Invitrogen, Paisley, UK	L23352
Nuclease free water	Promega, Southampton, UK	P1193

OCT	VWR, Leicestershire, UK	00411243
PBS solution (sterile)	Sigma-Aldrich, Dorset, UK	806552
Penicillin-Streptomycin (100x)	Gibco, Paisley, UK	10378016
Permeabilization Buffer (10X)	eBioscience, Hatfield, UK	00-8333-56
PMA	Sigma-Aldrich, Dorset, UK	P8139
ProLong Gold Anti-fade with DAPI	Thermo Fisher Scientific, MA, USA	P36931
Purified Rat Anti-Mouse CD16/CD32	BD Bioscience, Oxford, UK	553141
Pyruvate free DMEM	Thermo Fisher Scientific, MA, USA	11965-084
Recombinant CXCL1	BioLegend, Cambridge, UK	573708
Recombinant G-CSF	BioLegend, Cambridge, UK	574604
Recombinant GM-CSF	BioLegend, Cambridge, UK	576304
Recombinant IFN-α	Miltenyi Biotec, Surrey,UK	752804
Recombinant IFN-γ	BioLegend, Cambridge, UK	752804
RNAse AWAY	Molecular BioProducts, San Diego, USA	10666421
RSV $M_{187-195}$ peptide	Synthetic Biomolecules, San Diego, USA	n/a
SYTOX Blue Dead Cell Stain	Invitrogen, Paisley, UK	S34857
Taq PCR Master Mix Kit	Qiagen, Crawley, UK	201445
TMB Single Solution	Invitrogen, Paisley, UK	00-2023
TRIzol Reagent	Invitrogen, Paisley, UK	15596026
UltraPure 0.5M EDTA, pH 8	Thermo Fisher Scientific, MA, USA	15575020

Table 3.4. Reagents for IFN-α ELISA.

Reagent	**End Conc.**	**Supplier**	**Catalogue No.**
Capture Ab F18	1 µg/ml	Cambridge Bioscience, Cambridge, UK	HM1001
1st Detection Ab Rabbit-Anti-IFN-α	0.2 µg/ml	PBL Biomedical Laboratories, NJ, USA	32100-1
2nd Detection Ab Mouse-Anti-Rabbit biotinylated	1:1000	Jackson ImmunoResearch, Suffolk, UK	211-065-109
Standard Recombinant IFN-α		Cambridge Bioscience, Cambridge, UK	HC1040-10

Table 3.5. Reagents for IL-6 ELISA.

Reagent	End Conc.	Supplier	Catalogue No.
Capture Ab MP520F3	4 µg/ml	BD Pharmingen, Oxford, UK	554400
1st Detection Ab MP5-32C11 biotinylated	1 µg/ml	BD Pharmingen, Oxford, UK	554402
Standard Recombinant IL-6		BD Pharmingen, Oxford, UK	554582

3.3.2 Kits

Table 3.6. ELISA kits.

ELISA kits	Supplier	Catalogue No.
Cell Death Detection ELISA	Sigma-Aldrich, Dorset, UK	11544675001
Mouse IL-1β	eBioscience, Hatfield, UK	15500997
Mouse KC (CXCL1)	R&D systems, MN, USA	DY453
Mouse MMP-9	R&D systems, MN, USA	DY6718
Mouse MPO	R&D systems, MN, USA	DY3667
Mouse NE	R&D systems, MN, USA	DY4517-05
Mouse TNF-α	R&D systems, MN, USA	DY410
Serum Albumin	Bethyl Laboratories, TX, USA	E99-134

Table 3.7. Other kits

Other kits	Supplier	Catalogue No.
High Capacity RNA-to-cDNA kit	Applied Biosystems, Paisley, UK	4387406
Neutrophil Isolation Kit, mouse	Miltenyi Biotec, Surrey, UK	130-097-658
REASTAIN Quick Diff kit	GENTAUR Ltd, London, UK	102164
RNAeasy Micro Kit	Qiagen, Crawley, UK	74004
RNAeasy Mini Kit	Qiagen, Crawley, UK	74104
RNAse-Free DNase set	Qiagen, Crawley, UK	79254

3.3.3 Primers and probes

Table 3.8. qPCR primers and probes.

Primer/Probe	Sequence (5'-3')	Supplier	Catalogue No.
L-gene (fwd)	GAACTCAGTGTAGGTAGAATGTTTGCA	Invitrogen, UK	n/a
L-gene (rev)	TTCAGCTATCATTTTCTCTGCCAAT	Invitrogen, UK	n/a
L-gene probe	TTTGAACCTGTCTGAACATTCCCGGTT	Eurofins, GER	n/a
Tnfa forward	CATCTTCTCAAAATTCGAGTGACAA	Invitrogen, UK	n/a
Tnfa reverse	TGGGAGTAGACAAGGTACAACCC	Invitrogen, UK	n/a
Tnfa probe	CACGTCGTAGCAAAC	Eurofins, GER	n/a
Ifnb forward	CCATCATGAACAACAGGTGGAT	Invitrogen, UK	n/a
Ifnb reverse	GAGAGGGCTGTGGTGGAGAA	Invitrogen, UK	n/a
Ifnb probe	CTCCACGTGCGTCCTGCTGTG	Eurofins, GER	n/a
Ifng forward	TCAAGTGGCATAGATGTGGAAGAA	Invitrogen, UK	n/a
Ifng reverse	TGGCTCTGCAGGATTTTCATG	Invitrogen, UK	n/a
Ifng probe	TCACCATCCTTTTGCCAGTT	Eurofins, GER	n/a
Areg	Sequence not revealed by supplier	Applied Biosystems	Mm01354339_m1
Csf2	Sequence not revealed by supplier	Applied Biosystems	Mm01290062_m1
Cxcl1	Sequence not revealed by supplier	Applied Biosystems	Mm04207460_m1
Cxcl10	Sequence not revealed by supplier	Applied Biosystems	Mm00445235_m1
Cxcl12	Sequence not revealed by supplier	Applied Biosystems	Mm00445553_m1
Cxcl2	Sequence not revealed by supplier	Applied Biosystems	Mm00436450_m1
Cxcl5	Sequence not revealed by supplier	Applied Biosystems	Mm00436451_g1
Cxcl9	Sequence not revealed by supplier	Applied Biosystems	Mm00434946_m1
Gapdh	Sequence not revealed by supplier	Applied Biosystems	Mm99999915_g1
Ifna5	Sequence not revealed by supplier	Applied Biosystems	Mm00833976_s1
Il1b	Sequence not revealed by supplier	Applied Biosystems	Mm00434228_m1

Il33	Sequence not revealed by supplier	Applied Biosystems	Mm00505403_m1
Ptgs2	Sequence not revealed by supplier	Applied Biosystems	Mm00478374_m1

3.3.4 Antibodies

Table 3.9. Antibodies for innate immune cells panel.

Antigen	**Clone**	**Fluorochrome**	**Isotype**	**Supplier**	**Cat. No.**	**Conc. (µg/ml)**
CD45	30-F11	APC-eF780	Rat IgG2b,κ	eBioscience	47-0451-82	0.5
	30-F11	BV605	Rat IgG2b,κ	BioLegend	103140	0.5
CD11c	HL3	PE-CF594	Armenian Hamster IgG1, λ2	BD Biosciences	562454	1
CD11b	M1/70	AF-700	Rat IgG2b,κ	BioLegend	101222	1.25
Ly6C	HK1.4	eFluor450	Rat IgG2c,κ	eBioscience	48-5932-82	0.5
	HK1.4	BV711	Rat IgG2c,κ	BioLegend	128037	0.5
	HK1.4	BV421	Rat IgG2c,κ	BioLegend	128032	0.5
Ly6G	1A8	BV570	Rat IgG2a,κ	BioLegend	127629	1
	1A8	BV785	Rat IgG2a,κ	BioLegend	127645	1
CD64	X54-5/7.1	APC	Mouse IgG1,κ	BioLegend	139306	1
	X54-5/7.1	FITC	Mouse IgG1,κ	BioLegend	139316	2.5
MHC II	M5/114.15.2	APC eF780	Rat IgG2b,κ	eBioscience	47-5321-82	1
CD3	17A2	FITC	Rat IgG2b,κ	BioLegend	100204	1
CD19	6D5	FITC	Rat IgG2a,κ	BioLegend	115506	2.5
CD69	H1.2F3	Per CP Cy5.5	Armenian Hamster IgG	BioLegend	104522	1
CD62L	MEL-14	BV421	Rat IgG2a,κ	BioLegend	104436	1
CD182	SA044G4	PE	Rat IgG2a,κ	BioLegend	149304	1
Siglec-F	S17007L	PE	Rat IgG2a,κ	BioLegend	155506	1

Table 3.10. Antibodies for stromal lung cell panel.

Antigen	Clone	Fluorochrome	Isotype	Supplier	Cat. No.	Conc. (µg/ml)
EpCAM	G8.8	PerCP-Cy5.5	Rat IgG2a,κ	BioLegend	118220	2
CD31	MEC13.3	PE	Rat IgG2a,κ	BioLegend	102508	2
CD45	30-F11	APC-eF780	Rat IgG2b,κ	eBioscience	47-0451-82	0.5
CD11c	HL3	PE-CF594	Armenian Hamster IgG1, λ2	BD Biosciences	562454	1

Table 3.11. Antibodies/tetramer for T cell panel.

Antigen	Clone	Fluorochrome	Isotype	Supplier	Cat. No.	Conc. (µg/ml)
CD45	30-F11	BV605	Rat IgG2b,κ	BioLegend	103140	0.5
	30-F11	BUV395	Rat IgG2b,κ	BD Biosciences	564279	0.5
CD103	2E7	PerCP-Cy5.5	Armenian Hamster IgG1, λ2	BioLegend	121416	2
CD4	GK1.5	PE	Rat IgG2b,κ	eBioscience	12-0041-82	1
CD8	53-6.7	eFluor780	Rat IgG2a,κ	eBioscience	47-0081-82	0.5
CD62L	MEL-14	BV421	Rat IgG2a,κ	BioLegend	104436	1
CD69	H1.2F3	BUV737	Armenian Hamster IgG1, λ3	BD Pharmingen	612793	2
CD3	17A2	AF-700	Rat IgG2b,κ	eBioscience	56-0032-82	2
CD19	6D5	FITC	Rat IgG2a,κ	BioLegend	115506	2.5
Ly6G	1A8	FITC	Rat IgG2a,κ	BioLegend	127606	5
CD44	IM7	PE-Cy7	Rat IgG2b,κ	BioLegend	103030	2
GrzmB	GB11	PE-CF594	Mouse IgG1,κ	BD Pharmingen	562462	2
IFN-γ	XMG1.2	BV711	Rat IgG1, κ	BioLegend	505836	2
M-Tetramer	Epitope: $M_{187-195}$ tetramers (H-2D^b/ NAITNAKII)	AF-647		NIH Tetramer Core Facility (Emory University, Atlanta, GA)	n/a	2

Table 3.12. Antibodies for fluorescent microscopy.

Antigen	Clone	Fluorochrome	Isotype	Supplier	Cat. No.	Conc. (µg/ml)
Ly6G	1A8	-	Rat IgG2a,κ	Abcam	Ab236484	2
Anti-Rat IgG H+L	[polyclonal]	AF-647	Donkey IgG	Abcam	Ab150155	2

3.4 Consumables

Table 3.13. Consumables.

Consumables	Supplier
0.2 ml Natural Thin walled tubes	Bioquote Ltd., York, UK
1.7 ml Safe Seal Tubes	Bioquote Ltd., York, UK
96-well ELISA microplate	Greiner Bio One, Stonehouse, UK
96-well U-bottomed polypropylene plate	Corning Inc, New York, NY, USA
AcroPrep 96-well filter plates	PALL Life Sciences, Hoegaarden, Belgium
BD Plastipak Syringe	BD, Oxford, UK
CELLSTAR 96-well flat-bottom plate	Greiner Bio One, Stonehouse, UK
CELLSTAR 96-well V-bottom plate	Greiner Bio One, Stonehouse, UK
Cover slips	VWR, Leicestershire, UK
Cryovials	Applied Biosystems, Paisley, UK
Cytospin microscope slides	Tharmac, Weisbaden, Germany
EASYstrainer cell sieve (70/100 μm)	Greiner Bio One, Stonehouse, UK
Falcon tubes	Greiner Bio One, Stonehouse, UK
FastRead counting slides	Immune Systems, UK
Filter cards for Shandon Cytospin	Thermo Fisher Scientific, MA, USA
gentleMACS™ C-tubes	Miltenyi Biotec, Surrey, UK
Large tissue moulds	VWR, Leicestershire, UK
LS column	Miltenyi Biotec, Surrey, UK
MACS separator	Miltenyi Biotec, Surrey, UK
MicroAmp Optical Adhesive film	Applied Biosystems, Paisley, UK
PAP pen	Sigma-Aldrich, Dorset, UK
Phase Lock Gel Eppendorf	VWR, Leicestershire, UK
Scalpel	Swann-Morton Ltd., Sheffield, UK
Sterile needles	BD, Oxford, UK
SuperFrost Plus Adhesive slides	VWR, Leicestershire, UK

3.5 Media, solutions and buffers

Table 3.14. Media, solutions and buffers.

Name	Contents	Final concentration	Final pH
ACK	Distilled water	-	7.2
	NH_4Cl	0.15 M	
	$KHCO_3$	1.0 mM	
	Na_2EDTA	0.1 mM	
BAL media	EDTA	0.5 mM	-
	PBS	1x	
cDMEM	DMEM (500 ml)	1x	-
	FCS (heat inactivated from Gibco)	10%	
	L-glutamine (Invitrogen)	2 mM	
	Penicillin (Sigma-Aldrich)	100 U/ml	
	Streptomycin (Sigma-Aldrich)	100 µg/ml	
Wash buffer	Tween 20	0.5%	
(ELISA)	PBS	1x	
FACS buffer	PBS	1x	-
	BSA	1%	
	EDTA	5 mM	
MACS buffer	PBS	1x	7.2
	BSA	0.5%	
	EDTA	2 mM	

3.6 Instruments

Table 3.15. Instruments

Instruments	Supplier
7500 Fast Real-Time PCR system	Applied Biosystems, Paisley, UK
BD FACSAria	BD Bioscience, Franklin Lake, NJ, USA
BD Fortessa	BD Bioscience, Franklin Lake, NJ, USA
Cryostat	Leica Biosystems, Wetzlar, Germany
CX-2000 UV cross-linker	Analytik Jena AG, Jena, DE
Cytospin 4 Cytocentrifuge	Thermo Fisher Scientific, MA, USA
FLUOstar OMEGA plate reader	BMG LABTECH, Aylesbury, UK
gentleMACS dissociator	Miltenyi Biotec, Surrey, UK
Hera Safe Microbiological Safety Cabinet	Thermo Scientific, Wilmington, Germany
Heraeus Megafuge 40R	Thermo Scientific, Wilmington, Germany
Heraeus Pico17 microcentrifuge	Thermo Scientific, Wilmington, Germany
Incubator	Binder Inc., Bohemia, NY, USA
Inverted Widefield Microscope	Zeiss, Cambridge, UK
NanoDrop 1000 Spectrophotometer	Thermo Scientific, Wilmington, Germany
Optical Light Microscope	Zeiss, Cambridge, UK
TissueLyser LT	Qiagen, Crawley, UK

3.7 Software

Table 3.16. Software.

Software	Supplier
7500 Fast System SDS v1.4	Applied Biosystems, Paisley, UK
Adobe Illustrator	Adobe Systems Europe, Berkshire, UK
BioRender	BioRender, Toronto, ON, Canada
FACSDiVa	BD Bioscience, Paisley, UK
Fiji (ImageJ)	https://imagej.net/Fiji/Downloads
FlowJo v.10	Tree Star, Ashland, OR, USA
GraphPad Prism v6.0h	GraphPad Software Inc, La Jolla, CA, USA
MARS data analysis software	BMG LABTECH, Aylesbury, UK
Microsoft Office Package	Microsoft Corporation, Washington, USA
Omega/MARS	BMG LABTECH, Aylesbury, UK
Zeiss ZEN	Zeiss, Cambridge, UK

4 Methods

4.1 RSV stock

4.1.1 Growing RSV

Plaque-purified human RSV (originally A2 strain from ATCC, US) was grown in HEp-2 cells (Lee *et al.* 2010). 10^7 HEp-2 cells in a total volume of 30 ml were seeded into 175 cm^2 flasks and left to grow to 80% confluence overnight at 37^0C in 5% CO^2 in antibiotic-free cDMEM. HEp-2 monolayers were washed with 10 ml serum-free DMEM and infected with RSV at a multiplicity of infection (MOI) of 0.1 in 4 ml serum-free DMEM for 2 h at 37^0C in 5% CO^2. Flasks were rotated 90^0 every 15 min to counteract uneven surfaces. 26 ml antibiotic-free cDMEM was added and flasks were incubated for 24 h at 37^0C in 5% CO^2. FCS was reduced to 2% by removing 25 ml of medium and centrifuging the medium at 500×g for 5 min at 4^0C. The pellet was resuspended in 25 ml serum-free DMEM and added back to the flask. Flasks were incubated for 48 h and the cytopathic effect of the virus was regularly assessed. Cells were harvested with a cell scraper when 80% were detached. Harvested cells were sonicated for 2 min in an ice-cold water bath and centrifuged at 500×g for 5 min at 4^0C. Supernatant containing live RSV was pooled to eliminate batch variability, aliquoted into cryovials, snap frozen in liquid nitrogen and stored in liquid nitrogen.

4.1.2 Immunoplaque assay of RSV stock

RSV titre was assessed in RSV viral stocks by immunoplaque assay. HEp-2 monolayers were cultured in cDMEM in 96 well plates overnight. HEp-2 monolayers were washed once with 200 µl serum-free cDMEM. Duplicates of serial dilutions of the viral stock diluted in serum-free cDMEM (top dilution, 1:100) were incubated in 50 µl on HEp-2 cell monolayers for 2 h at 37^oC. 150 µl pyruvate-free DMEM (2% heat inactivated FCS) was added. Plates were incubated for 20 h at 37^oC before washing once with 100 µl PBS and then fixed for 20 min using methanol containing 2% hydrogen peroxide. Monolayers were washed twice in 1% BSA/PBS and stored in the fridge overnight. Monolayers were incubated with biotin-conjugated goat anti-RSV antibody (1:500 in 1% BSA/PBS) for 2 h. Infected cells were stained using streptavidin-HRP (1:500 in 1% BSA/PBS) and DAB (3,3'-diaminobenzidine) substrate

and the assay was developed in the dark at room temperature until the desired coloration was achieved. Immunoplaques were enumerated by light microscopy and the titre of the stock was calculated as focus forming units (FFU)/ml. Focus forming units (FFU)/ml were calculated as: (number of plaques x dilution factor)/volume of the inoculum (ml).

4.1.3 Immunoplaque assay of whole lung

RSV titre was assessed in mouse lungs by immunoplaque assay, optimised from (Loebbermann *et al.* 2012). One lung lobe was homogenised in 350 µl cDMEM for 4 min using TissueLyser LT and then sonicated for 2 min. Samples were centrifuged for 3 min at 21,100×g and the supernatant removed from the cell debris. Duplicates of the lung homogenate supernatant diluted in serum-free cDMEM (top dilution, 1:2) in 50 µl were incubated on HEp-2 cell monolayers for 2 h at 37°C, and an immunoplaque assay was performed as described above. FFU/g of lung tissue was calculated as: (number of plaques x dilution factor x (350/50))/weight of lung lobe(g).

4.1.4 Ultraviolet inactivation of RSV

RSV was inactivated by exposing virus to UV light for 2 min (UV-RSV) in a CX-2000 UV cross-linker.

4.2 Murine RSV infection model

4.2.1 Infection with RSV

Mice were lightly anaesthetised with isofluorane before intranasal (i.n.) administration of 100 µl containing up to 10^6 FFU RSV or PBS control, as indicated in figure legends. In some cases, mice were re-challenged with mock (PBS) or RSV 21 days later.

4.2.2 Immune-modulation

In some instances, infection was preceded or followed by i.n. administration of 100 µl of the immune mediators CXCL1 (5-10 µg/mouse) or IFN-α (1 µg/mouse) under light anaesthesia, as indicated in figure legends. To remove T cells from the circulation, 25 µg FTY720 (fingolimod) was administered by intra-peritoneal injection (i.p) in a volume of 250 µl to mice every day in a total of 6 doses, starting from two days prior to RSV re-challenge. FTY720 was initially dissolved in DMSO and diluted in H_2O (1:50) for administration to mice.

4.2.3 Antibody mediated neutrophil depletion

Two regimes were used to deplete neutrophils in mice, as indicated in figure legends. Mice were either given 200 µg i.n. and 500 µg i.p. α-Ly6G MAb (1A8; Rat IgG2a, κ) or isotype control MAb (2A3; Rat IgG2a, κ) one day pre-infection or mice were given 150 µg i.p. one day pre-infection and then every other day throughout the infection as indicated in the figure legends (Tate *et al.* 2009; Peiró *et al.* 2018; Lim *et al.* 2015).

4.3 Harvest of murine tissues

Mice were culled by fatal overdose of the anaesthetic pentobarbital to preserve the structure of the respiratory tract for performing BAL. Death was confirmed by severing the femoral artery. In some cases, circulating leukocytes were stained by intravenous (i.v.) injection of 200 µl CD45-BUV395 (2 µg/mouse) 5 min prior to culling.

4.3.1 Whole blood

Whole blood was harvested from the femoral or carotid arteries. At least 100 µl was collected in 1 ml PBS + 5 mM EDTA to prevent clotting. Red blood cells (RBCs) were removed by lysis in 15 ml ACK (Table 3.13) for 5 min, followed by the addition of 15 ml cDMEM. Cells were centrifuged at 500×g for 5 min at 4^0C and washed once with 1 ml FACS buffer (Table 3.13) Blood cells were resuspended in FACS buffer for antibody staining for flow cytometry (Chapter 4.4).

4.3.2 Airway cells and mediators

Airway cells were isolated from mouse lungs by BAL. A small incision was made in the trachea using a scalpel and the lungs were flushed three times with the same 1 ml BAL media (Table 3.14) with a 2 ml needle with plastic tubing attached. The BAL was centrifuged at 3500×g for 5 min and the supernatant was collected and stored at -80°C for analysis of mediators. To remove RBCs, the BAL cell pellet was resuspended in 100 µl ACK for 2 mins, and then 400 µl cDMEM was added. Cells were centrifuged at 3500×g for 5 min and BAL cells were enumerated on counting slides using 0.1% Trypan Blue Solution to exclude dead cells. BAL cells were resuspended in media for cytospins and differential cell counts (Chapter 4.3.7) or in FACS buffer for antibody staining for flow cytometry (Chapter 4.4).

4.3.3 Lung tissue for analysis of leukocytes by flow cytometry

The lungs were perfused by injecting the heart with at least 5 ml PBS to flush the blood out of the lungs. The superior lobe was harvested in a cryovial and immediately flash frozen in liquid nitrogen for RNA extraction and gene expression analysis by RT-qPCR (Chapter 4.6.1). The remaining lung lobes were harvested into cDMEM in gentleMACS™ C-tubes. Lungs were

processed using the gentleMACS dissociator according to the manufacturer's instructions and incubated for 1 h at 37^{0}C in 5% CO^2 in cDMEM supplemented with 30 µg/ml DNAse I from bovine pancreas and collagenase D (1 mg/ml). Cells were further processed using the gentleMACS dissociator according to the manufacturer's instructions, supplemented with 5 ml PBS and centrifuged at 500×g for 5 min at 4^{0}C. RBCs were removed by incubation with 5 ml ACK for 5 min then the cell suspension was supplemented with 5ml cDMEM and cells were centrifuged at 500×g for 5 min at 4^{0}C. Cells were resuspended in 5ml PBS and filtered through a 100 μm cell strainer to obtain a single cell suspension. Cells were enumerated on counting slides using 0.1% Trypan Blue Solution to exclude dead cells and resuspended in FACS buffer for antibody staining for flow cytometry (Chapter 4.4).

4.3.4 Lung tissue for analysis of stromal cells by flow cytometry

The lungs were perfused by injecting the heart with at least 5 ml PBS to flush the blood out of the lungs. The small incision was made in the trachea and the lungs were inflated with 3 ml 37^{0}C dispase (5 mg/ml) using a needle with plastic tubing attached. Lungs were then inflated with 0.5 ml agarose at 45^{0}C and covered with ice for 2 min. The lung was removed and incubated in 2 ml 37^{0}C dispase (5 mg/ml) at room temperature (RT) for 45 min. Lungs were processed in C-tubes containing 5 ml cDMEM (supplemented with 1 mg/ml DNase) using the gentleMACS dissociator according to the manufacturer's instructions. Cell suspensions were filtered through 100 μm cell strainers and the cell suspension was centrifuged at 200×g for 10 min. RBCs were removed by lysis with 5ml ACK for 5 min, followed by addition of 5 ml cDMEM and cells were centrifuged at 200×g for 10 min. The cell pellet was resuspended in 5 ml cDMEM and centrifuged at 200×g for 10 min. The cell pellet was resuspended in 5 ml PBS and filtered through 70 μm cell strainers. Mice were pooled prior to antibody staining for FACS (Chapter 4.4.3).

4.3.5 Isolation and stimulation of bone marrow neutrophils *ex vivo*

Bone marrow was harvested from the femur and tibia and neutrophils were isolated by magnetic activated cell sorting (MACS) using Neutrophil Isolation Kit according to the manufacturer' instructions (Miltenyi Biotech). Cells were flushed from the bone marrow using a needle and PBS. Cells were enumerated on counting slides using 0.1% Trypan Blue Solution to exclude dead cells and centrifuged at 300×g for 10 min. Cells were resuspended

in 200 µl MACS buffer (Table 3.13) per 5×10^7 total cells. 50 µl Neutrophil Biotin-Antibody Cocktail was added per 5×10^7 total cells, and cells were incubated for 10 min at 4°C. Cells were washed using 10 ml MACS buffer per 5×10^7 cells and centrifuged at 300×g for 10 min. The cell pellet was resuspended in 400 µl MACS buffer per 5×10^7 total cells and 100 µl anti-Biotin MicroBeads was added per 5×10^7 total cells. Cells were incubated for 15 min in the dark at 4°C. Cells were washed using 10 ml MACS buffer per 5×10^7 cells and centrifuged at 300×g for 10 min. 10^8 cells were resuspended 500 µl MACS buffer. A LS column was placed in the magnetic field of a MACS separator and the column was rinsed with 3 ml MACS buffer. The cell suspension was added to the column, the column was washed three times with 3 ml MACS buffer and the flow through was collected. Neutrophil purity was assessed by differential cell counts (Chapter 4.3.7) or by flow cytometry (Chapter 4.4).

1.25×10^5 cells were seeded in 96-well plates and stimulated with RSV, UV-RSV, phorbol myristate acetate (PMA), LPS, recombinant IFN-α, recombinant IFN-γ, recombinant G-CSF, recombinant GM-CSF and various combinations of these mediators, as indicated in figure legends, for 4 h at 37^{0}C in 5% CO^2 in a total volume of 200 µl. Supernatants were filtered using AcroPrep 96-well filter plates prior to mediator analysis by enzyme-linked immunosorbent assay (ELISA) (Chapter 4.6.5).

4.3.6 Inflation of whole lung for cryo-sectioning

A small incision was made in the trachea using a scalpel and the lungs were slowly inflated with 1 ml 50% OCT/PBS with a 2 ml needle with plastic tubing attached. The trachea was tied with sewing thread and lungs were removed from the chest cavity. Each lobe was removed, blotted dry and placed in the centre of a large mould containing 100% OCT. Inflated lungs in moulds were frozen on dry ice and stored in airtight bags at -80°C prior to sectioning on a cryostat.

4.3.7 Differential cell counts

The cellular composition of the BAL and of the isolated bone marrow neutrophils was determined by adding 100 µl media containing $1\text{-}2\times10^5$ cells into funnels attached to a cytospin microscope slide with a Shandon filter card in between to absorb excess liquid. Cells were spun onto slides at 450 rpm for 5 min using Cytospin 4 Cytocentrifuge. Slides were fixed and H&E stained using Reastain Quick-Diff kit, according to the manufacturer's instructions

(Gentaur). Cells were classified as alveolar macrophages, lymphocytes/monocytes, neutrophils or eosinophils using a microscope and ≥300 cells were counted/slide.

4.4 Flow cytometry

4.4.1 Cell surface antibody stain

2.5×10^6 cells were transferred into 96-well U-bottomed polypropylene plates. Additional wells were included for the unstained control, live/dead control and fluorescence minus one (FMO) controls. Cells were first incubated for 20 min at 4°C with Fc block (rat IgG2b anti–mouse CD16/CD32 receptor antibody). For RSV M Tetramer staining, Alexa Fluor 647-conjugated $M_{187\text{-}195}$ tetramers (H-2Db/NAITNAKII) were obtained from the NIH Tetramer Core Facility (Emory University, Atlanta, GA, USA). Tetramer staining was performed in FACS buffer for 30 min at RT following Fc block and prior to surface staining. For surface staining, cells were washed with PBS and stained with fluorochrome-conjugated antibodies (Chapter 3.3.4) and LIVE/DEAD™ Fixable Aqua Dead Cell Stain (1:500) in PBS for 30 min in the dark at 4°C. Cells were fixed by incubation with 100 µl Cytofix™ Fixation Buffer for 20 min at 4°C and stored in FACS buffer in the dark at 4°C. After fixation, analysis was performed on a BD Fortessa using the FACSDiVa software. Acquisition was set to at least 200,000 single, live, $CD45^+$ cells.

4.4.2 Intracellular cytokine stain

For intracellular staining the cells were re-stimulated with 5 µg/ml RSV $M_{187\text{-}195}$ peptide or 5 µg/ml LPS diluted in cDMEM in a total volume of 190 µl for 1 h at 37°C. After the addition of 10 µl Golgi Plug diluted in media (1:1000) the samples were incubated for another 3 h, stained for surface marker expression as described above and fixed by incubation with 10 µl Cytofix™ Fixation Buffer for 20 min and stored in FACS buffer in the dark at 4°C. Next day, cells were permeabilized in 150 µl 1X Permeabilization Buffer (eBioscience) for 10 min and stained with fluorochrome-conjugated antibodies against cytokines in the presence of Fc block (rat IgG2b anti–mouse CD16/CD32 receptor antibody) for 1 h in the dark at 4°C. Samples were washed once with 150 µl 1X Permeabilization Buffer, once with 150 µl FACS buffer and resuspended in FACS buffer for analysis on a BD Fortessa using the FACSDiVa software, as described above.

4.4.3 Fluorescence-activated cell sorting

Aliquots of cells were taken for the FMO controls (1×10^6 cells/FMO) and for the presort (5×10^6 cells/presort). Cells were first incubated with Fc block (rat IgG2b anti–mouse CD16/CD32 receptor antibody) (1:100) for 20 min on ice. Cells were then washed with FACS buffer and centrifuged at 200×g for 10 min. For surface staining, cells were stained with fluorochrome-conjugated antibodies (Table 3.10) for 30 min in the dark on ice, washed with FACS buffer and centrifuged at 200×g for 10 min. Cells were resuspended in 5 ml FACS buffer, filtered through 70 μm cell strainers and enumerated on counting slides using 0.1% Trypan Blue Solution to exclude dead cells. Dead cells were stained with SYTOX Blue Dead Cell Stain (1:8000) before running on a BD FACSAria III using FACSDiVa software. Stromal cells were defined as described in the gating strategy (Fig. 4.3). Sorted stromal cells were reanalysed to confirm purity, spun down and resuspended in 1 ml TRIzol™ reagent (Invitrogen, UK) and stored at -80°C. Purity was always >95%.

4.4.4 Analysis and gating strategies

Flow cytometry data were analysed with FlowJo software version 10 (Tree Star). Manual gates were set according to staining observed in FMO controls and gating strategies are shown below. Different panels and strategies were used to identify AMs, monocytes and neutrophils (Fig. 4.1), stromal cells (Fig. 4.2) and T cells during RSV infection and re-challenge (Fig. 4.3). tSNE analysis was performed using the FlowJo plugin. For each sample, the DownSample plugin was used to reduce the total number of events to 5000 $CD45^+$ events or 2000 $CD8^+$ events. Samples were then concatenated and the tSNE algorithm was run at 1000 iterations, perplexity = 20, eta (learning rate) = 20 and theta = 0.5 (van der Maaten and Hinton 2008). Manual gates were overlaid on tSNE clusters to identify known cell populations and the analysis was stratified by treatment group, each containing the same number of total events, to visualise differences. To calculate the total number of cell populations, populations were quantified as the whole lung count × (%population of $CD45^+$ cells) × (%$CD45^+$ cell of live cells) × (proportion of lung tissue sampled).

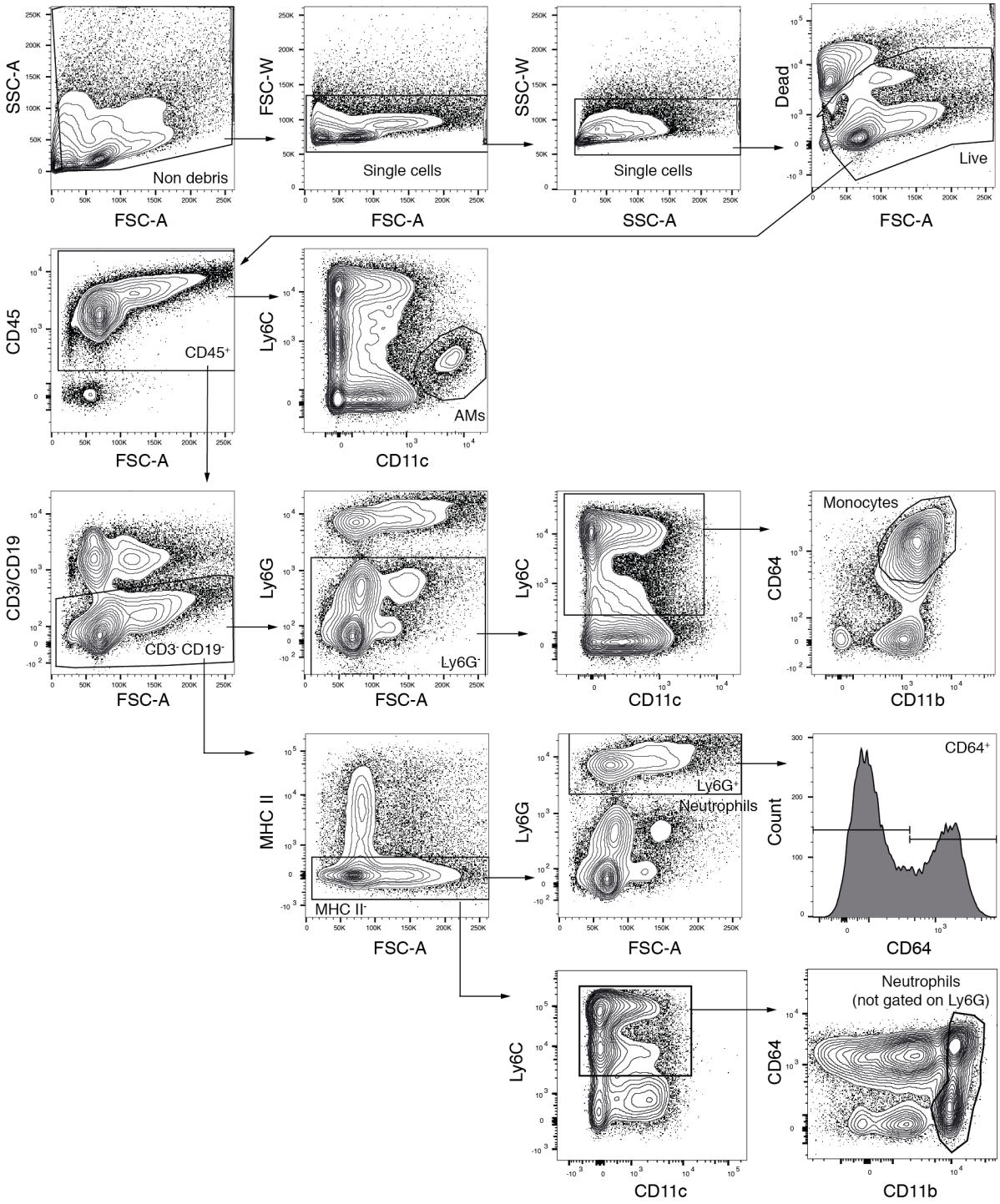

Figure 4.1. Gating strategies to identify airway and lung innate immune cells. Mice were intranasally infected with RSV. **a.** Airway/lung innate immune cells were obtained by collagenase digestion and stained for the indicated cell surface molecules, full details of panel in Table 3.9. After excluding debris and gating on single, live, CD45$^+$ cells, the depicted gates were used to identify AMs, monocytes and neutrophils. Ly6G$^+$ neutrophils were further gated to determine cell surface activation marker expression. During neutrophil depletion with α-Ly6G, neutrophils were quantified without gating on Ly6G.

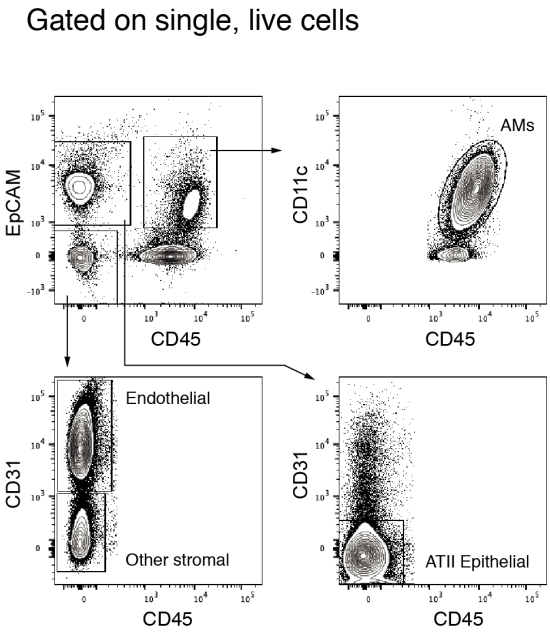

Figure 4.2. Gating strategies to identify lung stromal cells. Mice were intranasally infected with RSV. Lung cells, including stromal cells, were obtained by dispase digestion and stained for the indicated cell surface molecules, full detail of panel in Table 3.10. After excluding debris and gating on single and live cells, the depicted gates were used to identify and sort AMs, ATII epithelial cells, endothelial cells and other stromal cells.

a T cells - Intracellular cytokine stain (single, live)

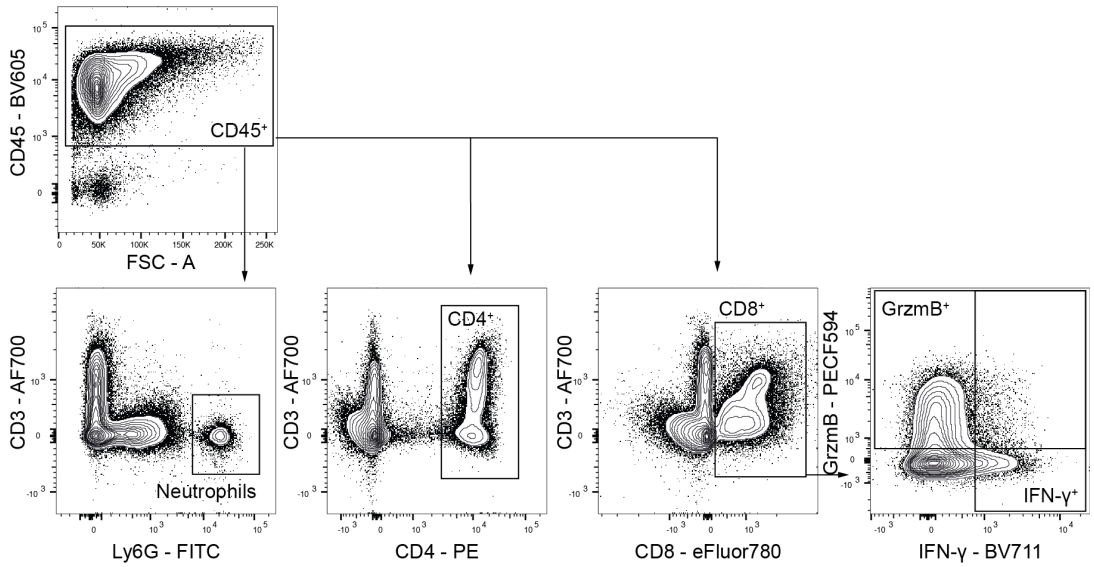

b CD8+ tetramer stain (single, live)

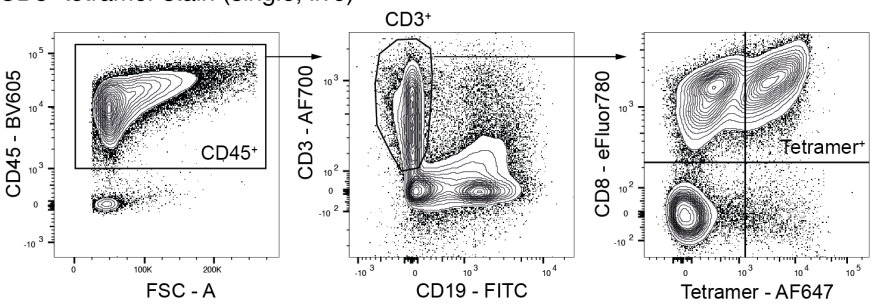

c Memory T cells (single, live, CD45+)

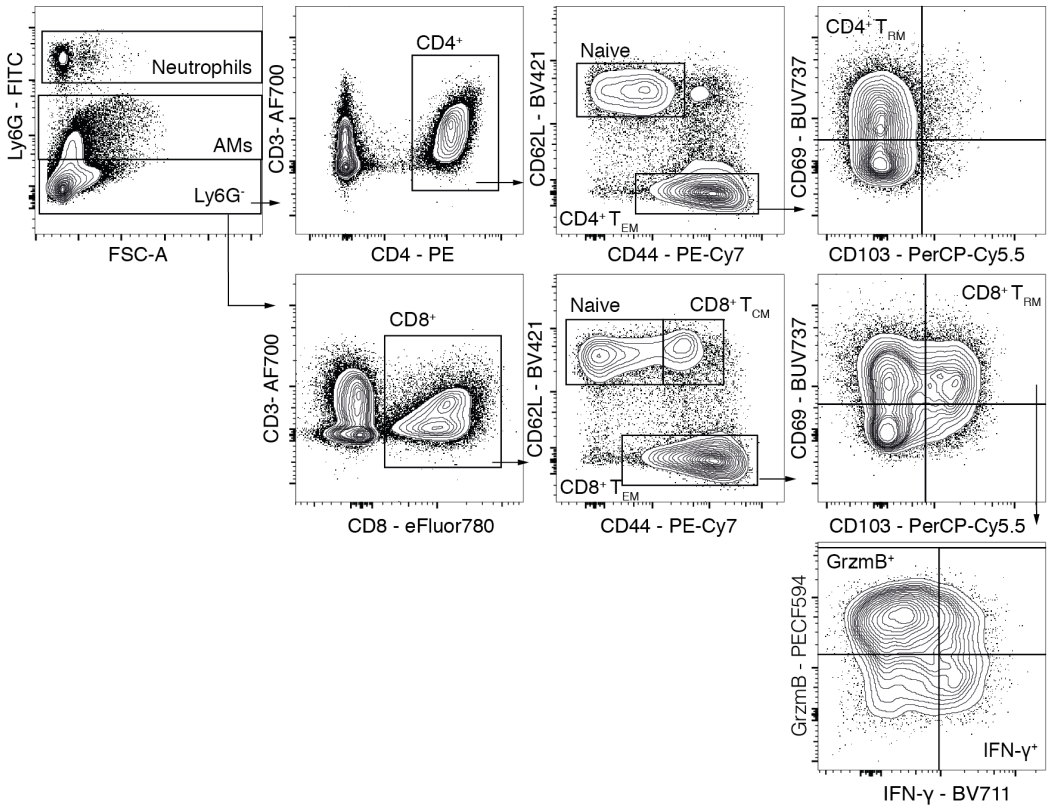

Figure 4.3. Gating strategies to identify T cells during RSV infection. Mice were intranasally infected with RSV. In some cases re-infected with RSV 21 days p.i.. Lung cells were obtained by collagenase digestion and stained for the indicated cell surface molecules, full details of panel in Table 3.11. **a.** After excluding debris and gating on single, live, $CD45^+$ cells, the depicted gates were used to identify neutrophils, $CD4^+$ and $CD8^+$ T cells as well as $GrzmB^+$ and IFN-γ^+ $CD8^+$ T cells. **b.** The depicted gates were used to identify RSV $tetramer^+$ $CD8^+$ T cells. **c.** The depicted gates were used to identify subsets of memory T cells and GrzmB and IFN-γ producing $CD8^+$ T_{RM} cells.

4.5 Fluorescence microscopy

4.5.1 Lung tissue sectioning

To visualise neutrophils in the lung, 10 μm lung sections were cut using a cryostat (Leica), adhered onto SuperFrost Plus Adhesion slides and stored at -80°C.

4.5.2 Fluorescence microscopy

Tissue sections were fixed in acetone at RT for 10 min. Sections were then rehydrated by washing twice in PBS for 5 min. Sections were circled by a water repellent film using a PAP pen, and sections were blocked with Fc block (rat IgG2b anti–mouse CD16/CD32 receptor antibody) (1:50 in 1% BSA) for 30 min. Sections were then stained with rat anti-mouse α-Ly6G diluted in 1% BSA (1:800) at 4°C overnight with gentle rocking. Sections were washed twice in PBS for 5 min and incubated with fluorochrome conjugated secondary antibody (donkey anti-rat IgG) for 2 h at RT. Sections were washed twice in PBS for 5 min and mounted in ProLong Gold Antifade Mountant with DAPI. Slides were stored flat at 4°C for at least 12 h prior to imaging, and the edges were sealed for long term storage. Zeiss Axio Observer inverted microscope on a 20x lens with a fully motorised stage controlled by Zen acquisition software was used for obtaining images. All analysis was performed on Fiji, an open-source image processing software (ImageJ, USA).

4.6 Measurement of mediators

4.6.1 RNA extraction of whole lung

Lung lobes were homogenised using a TissueLyser LT (Qiagen). Total RNA was extracted from homogenised lung tissue supernatant using RNeasy Mini kit (Qiagen), including the optional DNA digestion step, as per the manufacturer's instructions. RNA was eluted in 40 µl nuclease-free H_2O (Promega). RNA concentrations and quality were determined by NanoDrop spectrophotometer (Thermo Fisher Scientific).

4.6.2 RNA extraction of sorted cells

Sorted cells in TRIzol™ reagent (Invitrogen, UK) were transferred into Phase Lock Gel Eppendorf tubes (VWR). 200 µl chloroform was added and tubes were shaken vigorously for 15 s. Samples were centrifuged for 10 min at 12000×g at 4°C. The aqueous phase was isolated, and RNA was extracted using either RNeasy Mini kit (Qiagen) or RNeasy Micro kit (Qiagen), depending on cell number, including the optional DNA digestion step as per the manufacturer's instructions. RNA was eluted in 14 µl nuclease-free H_2O (Promega).

4.6.3 RNA to cDNA conversion

From whole lung, 2 µg of RNA was converted to cDNA using High Capacity RNA-to-cDNA kit (Applied Biosystems), as per the manufacturer's instructions. For sorted cells, either 0.5 µg or 9 µl of RNA was converted to cDNA using High Capacity RNA-to-cDNA kit (Applied Biosystems), as per the manufacturer's instructions.

4.6.4 Real time quantitative polymerase chain reaction (RT-qPCR)

For mRNA analysis of L gene, *Tnfa* and *Ifng*, gene specific primers and probes were used (Table 3.7) in the reaction mix in Tables 4.1 and 4.2. For mRNA analysis of *Gapdh*, *Cxcl1*, *Cxcl2*, *Cxcl5, Cxcl9*, *Cxcl10, Cxcl12*, *Ifna5, Ifnb, Il1a, Il1b, Il33, Areg, Ptgs2* and *Csf2* gene specific primers and probes were used (Table 3.7; all Applied Biosystems) in the reaction mix in Table 4.3. The probes were all tagged with a double-dye (FAM-fluorophore, TAMRA-

quencher), except for the *Gapdh* probe which was tagged with VIC-fluorophore and no quencher. RT-qPCR was performed using the 7500 Fast Real-Time PCR System (Applied Biosystems). Analysis was performed using 7500 Fast System SDS Software (Applied Biosystems). To quantify the relative mRNA expression, the mean ΔCT (cycle threshold difference) was calculated for each target gene relative to *Gapdh* (encoding glyceraldehyde-3-phosphate dehydrogenase) and expressed as $2^{-\Delta CT}$. For exact quantification, copy numbers were calculated using a plasmid DNA standard curve and normalised to *Gapdh* (L gene, *Tnfa* and *Ifng*). Data were normalised *Gapdh* as previous studies from the lab found RSV infection had no effect on the expression level of *Gapdh* in murine lung tissues (data not shown).

Table 4.1. Reaction mix for RSV L gene.

Reagent	**Volume/(µl/well)**
Master Mix	6.25
Forward primer (5 µM)	1.00
Reverse primer (5 µM)	0.33
Probe (5 µM)	0.2
Nuclease-free water	3.72
cDNA	1.00

Table 4.2. Reaction mix for *Tnfa, Ifnb, Ifng*.

Reagent	**Volume/(µl/well)**
Master Mix	6.25
Forward primer (5 µM)	2.25
Reverse primer (5 µM)	2.25
Probe (5 µM)	0.4375
Nuclease-free water	0.3125
cDNA	1.00

Table 4.3. Reaction mix for relative mRNA expression.

Reagent	**Volume (µl/well)**
Master Mix	6.25
Target PP	0.63
Nuclease-free water	4.62
cDNA	1.00

4.6.5 Enzyme-linked Immunosorbent Assay (ELISA)

Protein concentrations in BAL and cell culture supernatant were measured by ELISA. Samples were tested in duplicate. For mediators with commercial kits available (CXCL1, CXCL2, MMP-9, MPO, NE, TNF-α, IL-1β, serum albumin and histone-bound DNA), 50 µl sample were tested following the manufacturer's instructions (Table 3.6) in 96-well plates (Greiner Bio One). IFN-α and IL-6 ELISAs were performed using the reagents in Table 3.4 and Table 3.5, respectively, as previously described (Asselin-Paturel *et al.* 2001; Goritzka *et al.* 2014). In brief, the capture antibody was diluted 1:100 (IFN-α)/1:125 (IL-6) in 0.2 M $NaHCO_3$ and was bound to the ELISA plate by incubation overnight at 4°C. The plate was washed using ELISA wash buffer (Table 3.13), blocked with 300 µl diluent (1% BSA/PBS) for 1 h. Plates were washed and 50 µl of standards and samples diluted in 1% BSA/PBS was incubated on the plate for 2 h. The protein standard stocks were diluted to create standard curves ranging from 19.5 pg/ml - 5000 pg/ml (IL-6) or 39 U/ml - 20,000 U/ml (IFN-α). Plates were washed and in incubated with detection antibody, diluted 1:500 in 1% BSA/PBS (IL-6)/1:3500 (IFN-α), for 1 h (IL-6, IFN-α – first detection antibody). Plates were washed and incubated with 100 µl second detection antibody, diluted in 1% BSA/PBS, for 1 h (IFN-α). Plates were washed and 100 µl Streptavidin-HRP (Thermo Fisher Scientific) diluted 1:1000 in 1% BSA/PBS was added for 30 min (IL-6, IFN-α). Plates were washed and 100 µl tetramethylbenzidin (TMB) (Sigma Aldrich) was added per well to induce a colorimetric change. The colour change reaction was stopped by the addition of 50 µl 2 M H_2SO_4. The fluorescence was determined at 450 nm, on a FLUOstar OMEGA plate reader (BMG Labtech) and analysed using Omega/MARS and MARS data analysis software (BMG Labtech).

4.7 Statistical Analysis

Statistical analysis was performed using Prism (GraphPad software) version 6. Data are presented as the mean ± SEM. As indicated in figure legends, one-way ANOVA followed by Tukey's post hoc was used to compare multiple groups. To compare genotypes during mock and RSV infection, a two-way ANOVA followed by Bonferroni's post hoc test was used. For repeated measures, a two-way ANOVA followed by Bonferroni's post hoc test was used to determine statistical significance between groups. Statistical significance of differences between two groups was analysed by unpaired, two-tailed Student's *t* test. p values < 0.05 were considered statistically significant for all tests. *, $p < 0.05$; **, $p < 0.01$; ***, $p < 0.001$.

5 Results

5.1 Neutrophil recruitment and activation in RSV infection

5.1.1 Introduction

RSV is the greatest cause of infant hospitalisations in the developed world (Smyth and Openshaw 2006; Borchers *et al.* 2013; Hall *et al.* 2009). Airway neutrophilia has long been clinically associated with disease severity during severe RSV induced lower respiratory tract infections (LRTIs) of infants (Abu-Harb *et al.* 1999; Emboriadou *et al.* 2007; Hull *et al.* 2000; Marguet *et al.* 2008) and neutrophils are abundant in the lungs of both mice and humans during RSV infection (McNamara 2003; Goritzka, Makris, *et al.* 2015). Clinical studies implicate neutrophils as likely drivers of disease severity in infants yet the immunological mechanisms regulating neutrophil recruitment and activation in the lung during RSV infection are not known.

In this chapter, the data presented are adapted from a recently published article (Kirsebom *et al.* 2019). In brief, the innate signalling pathways which regulate neutrophil recruitment and activation in the lung during RSV infection were investigated using PRR knock-out mice deficient in the adaptor proteins MAVS and MyD88/TRIF. *Mavs*$^{-/-}$ mice, unable to signal via MDA-5 or RIG-I, and *Myd88/Trif*$^{-/-}$ mice, unable to signal via the TLRs, IL-1R and IL-18R, were infected with RSV. Neutrophil recruitment to the lung in response to RSV was largely independent of signalling via MAVS but was dependent on MyD88/TRIF signalling. However, neutrophil activation in the lung during RSV infection was dependent on the pro-inflammatory environment induced downstream of MAVS signalling. Restoring the pro-inflammatory environment in the lungs of *Mavs*$^{-/-}$ mice during RSV infection by treating mice with rIFN-α was sufficient to at least partially activate lung neutrophils. Furthermore, neutrophils recruited into the lungs of *Myd88/Trif*$^{-/-}$ mice during RSV infection where the MAVS driven pro-inflammatory environment was intact were able to become fully activated. These data demonstrate that neutrophil recruitment and activation are differentially regulated by distinct innate signalling pathways. These pathways must collaborate to drive neutrophil responses in the lung during RSV infection.

5.1.2 Neutrophil recruitment and activation peaks early in the lung during RSV infection

Initially, neutrophil recruitment to the lung in the C57BL/6 murine model of RSV disease was investigated over time (Fig. 5.1). Mice were infected intranasally (i.n.) with mock (PBS) or 10^6 FFU of plaque purified RSV of the A2 strain. AMs, $CD64^+$ inflammatory monocytes and neutrophils were quantified in the airways, from the BAL, and in the lungs by flow cytometry (Fig. 4.1 for gating strategy). At the early time points measured, from 6 h to 36 h p.i., there was no major difference in the number of AMs detected in the airways, although fewer AMs were detected following RSV infection at 12, 24 and 36 h p.i. as compared to mock infected mice (Fig. 5.1a). Monocyte recruitment was observed in the airways from 36 h p.i., and in the lungs from 12 h p.i. (Fig. 5.1b). Neutrophil recruitment peaked in both the airways and the lung at 18 – 24 h p.i. (Fig. 5.1c and Fig. 5.1d). From 12 h p.i. there were significantly more neutrophils in the lungs of RSV infected mice than there were in the lungs of mock infected mice (Fig. 5.1d). Lung neutrophilia occurred rapidly and transiently during RSV infection; by 36 h p.i. there was no difference in the number of neutrophils in either the airways or the lungs between mock and RSV infected mice (Fig. 5.1c and Fig. 5.1d). $Ly6G^+$ cells were imaged in the lung using fluorescent microscopy at 24 h p.i. to investigate the localisation of neutrophils throughout lung tissue at the peak of recruitment (Fig. 5.1e). $Ly6G^+$ cells were evenly distributed throughout the lungs and did not appear to cluster at distinct sites.

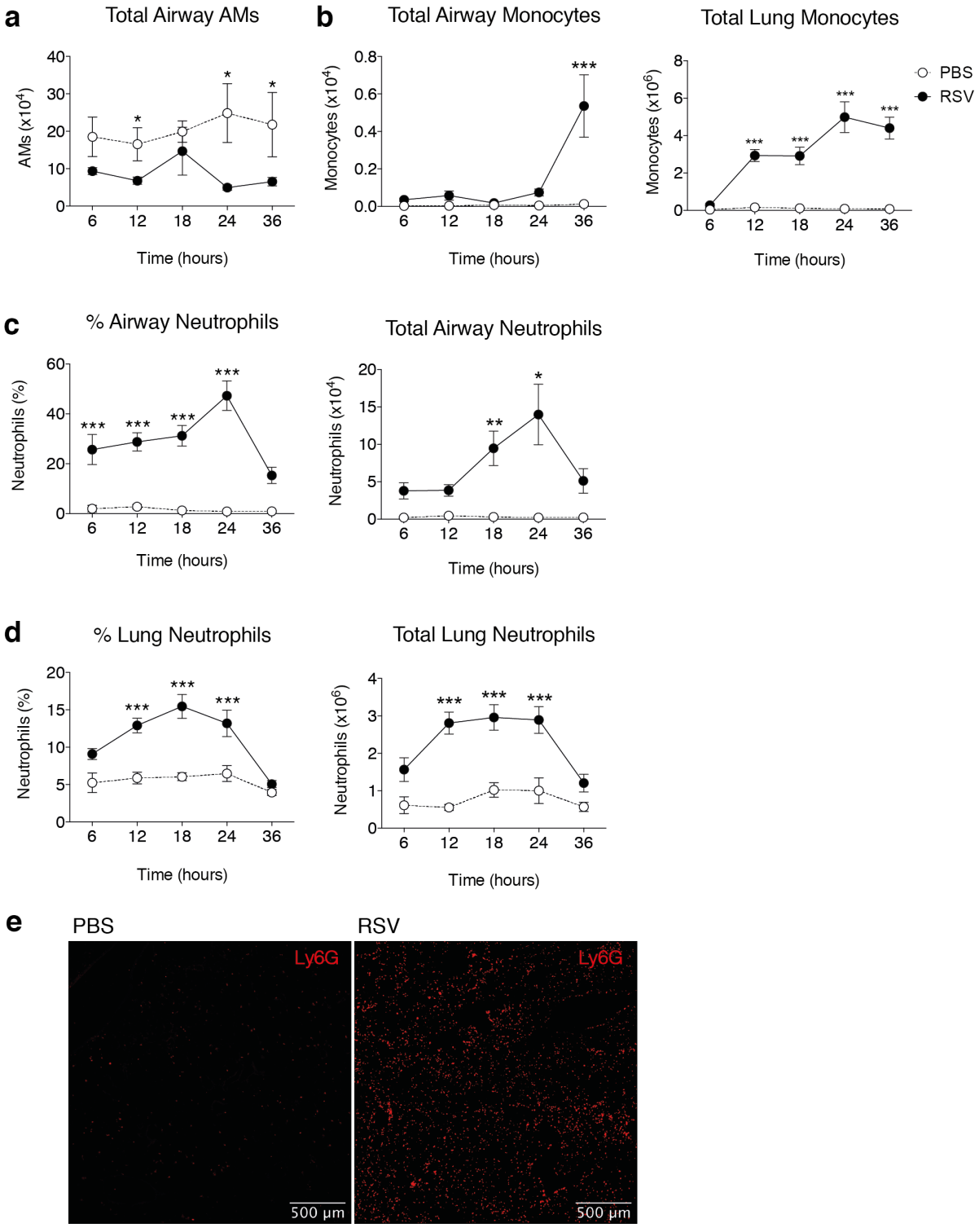

Figure 5.1. Neutrophil recruitment to the lung during RSV infection *in vivo.* Wt mice were intranasally mock (PBS) or RSV infected and immune cells were quantified by flow cytometry (Fig. 4.1 for gating strategy). **a.** Total numbers of CD45$^+$, CD11c$^+$ AMs were quantified in the airways using flow cytometry at the indicated time points. **b.** Total numbers of CD45$^+$, CD3$^-$, CD19$^-$, Ly6G$^-$, Ly6C$^+$, CD64$^+$, CD11b$^+$ monocytes were quantified in the airways and lung using flow cytometry at the indicated time points. **c-d.** Frequencies and total numbers of CD45$^+$, CD3$^-$, CD19$^-$, MHC-II$^-$, Ly6G$^+$ neutrophils were quantified in the airways and lung using flow cytometry at the indicated time points. **e.** Images show representative immunostaining of Ly6G$^+$ neutrophils (red) in lung cryosections at 24 h p.i. from 3 mice per group. In a-d the data are presented as the mean±SEM of 3-5 (PBS), or 8-13 (RSV) individual mice, pooled from at least two independent experiments. Statistical significance of differences between mock and RSV infection was determined by one-way ANOVA with Tukey's post hoc test. * $p \leq 0.05$, ** $p \leq 0.01$, *** $p \leq 0.001$.

The gene expression of the neutrophil chemoattractants CXCL1 and CXCL2 was also assessed over time during RSV infection *in vivo* (Fig. 5.2). *Cxcl1* and *Cxcl2* peaked in the lungs at 12 h p.i., just prior to the peak of neutrophil recruitment (Fig. 5.2a). This was confirmed at the protein level for CXCL1, which also peaked at 12 h p.i. (Fig. 5.2b).

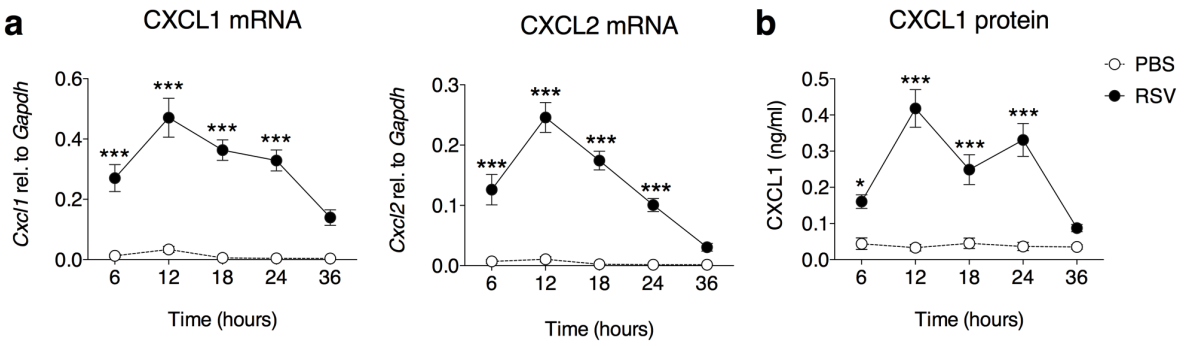

Figure 5.2. The gene expression and protein production of neutrophil chemoattractants peaks early in the lung during RSV infection *in vivo*. Wt mice were intranasally mock (PBS) or RSV infected at the indicated time points. **a.** *Cxcl1* and *Cxcl2* were quantified relative to *Gapdh* by RT-qPCR from RNA isolated from lung tissue. **b.** CXCL1 was detected in the BAL fluid by ELISA. Data are presented as the mean±SEM of 3-5 (PBS), or 8-13 (RSV) individual mice, pooled from at least two independent experiments. Statistical significance of differences between mock and RSV infection was determined by one-way ANOVA with Tukey's post hoc test. * $p \leq 0.05$, *** $p \leq 0.001$.

To gain an insight into neutrophil functionality during RSV infection, the activation status of neutrophils in the lungs was also assessed over time (Fig. 5.3 – 5.5). During activation, neutrophils degranulate to secrete a plethora of effector molecules including MMP-9, MPO and NE (Rørvig *et al.* 2013). The production of MMP-9, MPO and NE in the airways all peaked at 24 h p.i., as assessed in the BAL fluid, demonstrating that neutrophils recruited to the lung during RSV infection do become activated to degranulate and secrete effector molecules (Fig. 5.3).

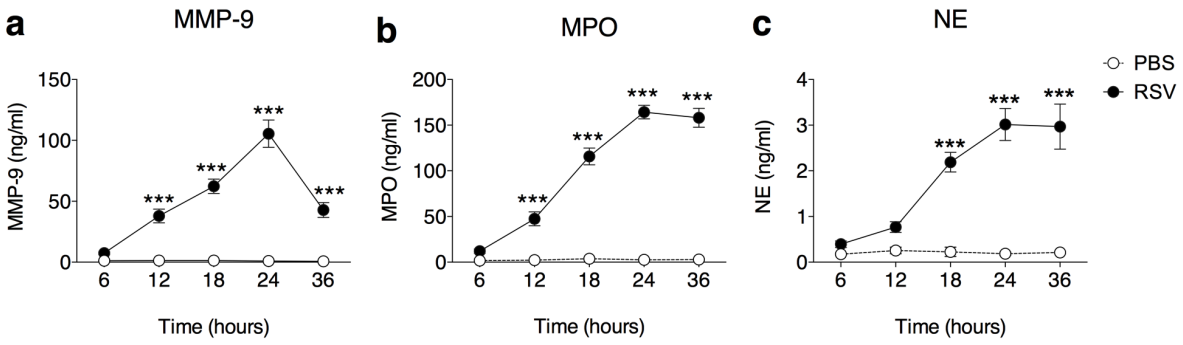

Figure 5.3. Neutrophil degranulation products MMP-9, MPO and NE are produced in the lung during RSV infection *in vivo*. Wt mice were intranasally mock (PBS) or RSV infected at the indicated time points. **a-c.** MMP-9, MPO and NE were detected in the BAL fluid by ELISA. Data are presented as the mean±SEM of 3-5 (PBS), or 8-13 (RSV) individual mice, pooled from at least two independent experiments. Statistical significance of differences between mock and RSV infection was determined by one-way ANOVA with Tukey's post hoc test. *** $p \leq 0.001$.

To further characterise neutrophil activation status in the lung during early RSV infection, the expression of cell surface markers associated with neutrophil activation in other inflammatory conditions were investigated at 18 h post RSV infection (Fig. 5.4). The cell surface expression of CD69, CD11b, CD62L, CD182 and CD64 was quantified on neutrophils in the lung, airway and blood using flow cytometry (Fig. 5.4). The cell surface expression of these markers on airway and lung neutrophils from mock (PBS) and RSV infected mice were compared to circulating neutrophils in the blood. CD69 and CD182 were not upregulated on neutrophils in the lungs, BAL or blood at 18 h p.i. although CD69 is upregulated on activated neutrophils during influenza virus infection (Tate *et al.* 2008). The expression level of CD11b, the upregulation of which is also associated with neutrophil activation (Borjesson *et al.* 2002), was high on neutrophils in all compartments during both mock and RSV infection, and therefore not a relevant marker of activation (Fig. 5.4). CD62L downregulation has also been associated with neutrophil activation (Smolen *et al.* 2000). BAL and lung neutrophils downregulated CD62L as compared to blood neutrophils, however this was not specific to RSV infection as neutrophils from mock infected mice displayed similar expression levels of CD62L (Fig. 5.4). Of the activation markers tested, only CD64 was a specific marker of neutrophil activation during RSV infection; CD64 expression levels were low on blood neutrophils and high on lung neutrophils specifically during RSV infection but not during mock infection (Fig. 5.4 and Fig. 5.5). Notably lung neutrophils had an increased upregulation of cell surface CD64 as compared to airway neutrophils (Fig. 5.4). The total number of $CD64^+$ neutrophils peaked in the lung at 18-24 h p.i. at which time >40% of lung neutrophils were $CD64^+$ (Fig. 5.5).

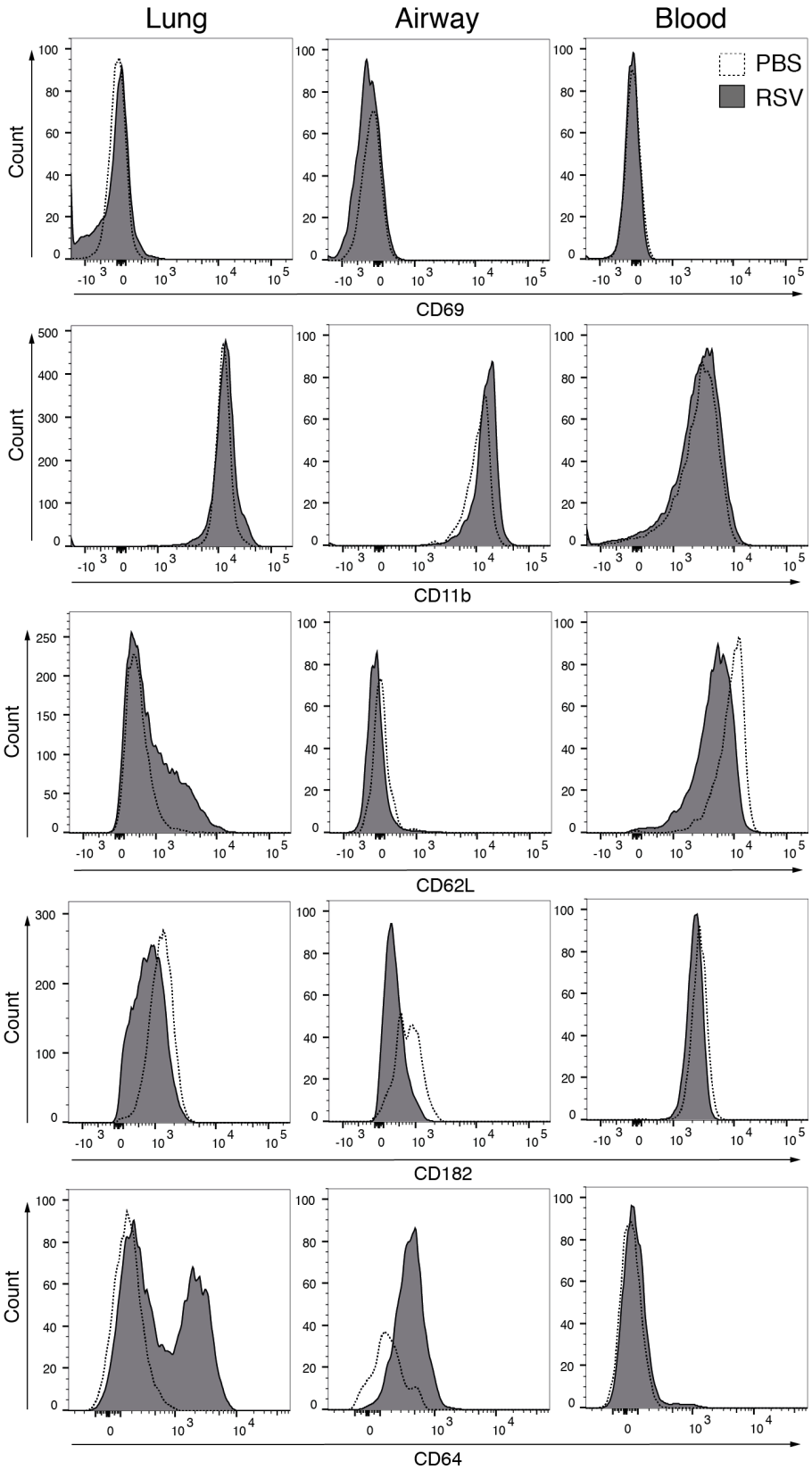

Figure 5.4. CD64 upregulation is a marker of lung neutrophil activation during RSV infection *in vivo*. Wt mice were mock (PBS) or RSV infected for 18 h. Representative histograms of CD69, CD11b, CD62L, CD182 and CD64 expression on $CD45^+$, $CD3^-$, $CD19^-$, MHC-II^-, $Ly6G^+$ neutrophils in the lung, airways and blood.

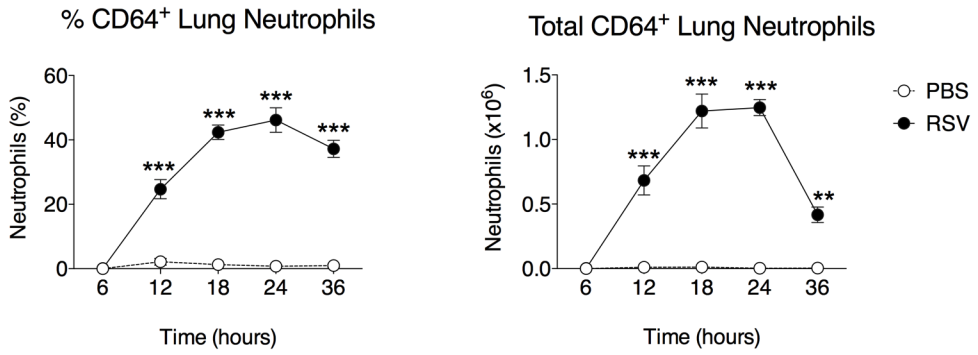

Figure 5.5. CD64 cell surface expression peaks on lung neutrophils at 18-24 h post RSV infection *in vivo.* Wt mice were intranasally mock (PBS) or RSV infected at the indicated time points and neutrophils were analysed by flow cytometry (Fig. 4.1 for gating strategy). Frequencies and total numbers of $CD64^+$ lung neutrophils ($CD45^+$, $CD3^-$, $CD19^-$, MHC-II^-, $Ly6G^+$). Data are presented as the mean±SEM of 3-5 (PBS) or 8-13 (RSV) individual mice pooled from two independent experiments. Statistical significance of differences were determined by one-way ANOVA with Tukey's post hoc test. ** $p \leq 0.01$, *** $p \leq 0.001$.

To confirm that neutrophil recruitment and activation in response to RSV was dependent on live virus, mice were infected for 18 h with UV inactivated RSV (UV RSV; Fig. 5.6). UV RSV did not recruit neutrophils to either the airways or the lungs (Fig. 5.6a). Likewise, UV RSV infection did not drive neutrophil activation; UV RSV infected mice did not produce MMP-9, MPO or NE in the airways (Fig. 5.6b) or upregulate cell surface expression of CD64 on lung neutrophils (Fig. 5.6c and 5.6d). To confirm that neutrophils are the cellular source of MMP-9, MPO and NE in the airways during RSV infection and therefore that this is an appropriate measure of neutrophil activation status, antibody mediated (α-Ly6G) neutrophil depletion was used to block neutrophil recruitment to the lung in response to RSV (Fig. 5.7). Neutrophils were depleted systemically at day -1 pre-infection and MMP-9, MPO and NE production in the airways was assessed at 18 h p.i. (Fig. 5.7a). The α-Ly6G dose given was confirmed to be sufficient to inhibit the recruitment of neutrophils to the lung during RSV infection as no neutrophils were detected in the airways following RSV infection of α-Ly6G treated mice (Fig. 5.7b). Neutrophil depletion confirmed that neutrophils are the cellular source of MMP-9 and NE during RSV infection; the production of MMP-9 and NE in the airways was completely abrogated during infection of α-Ly6G treated mice (Fig. 5.7c). However, neutrophil depletion reduced but did not completely abrogate MPO production indicating there is likely another cellular source of this protein in the lung during RSV infection (Fig. 5.7c).

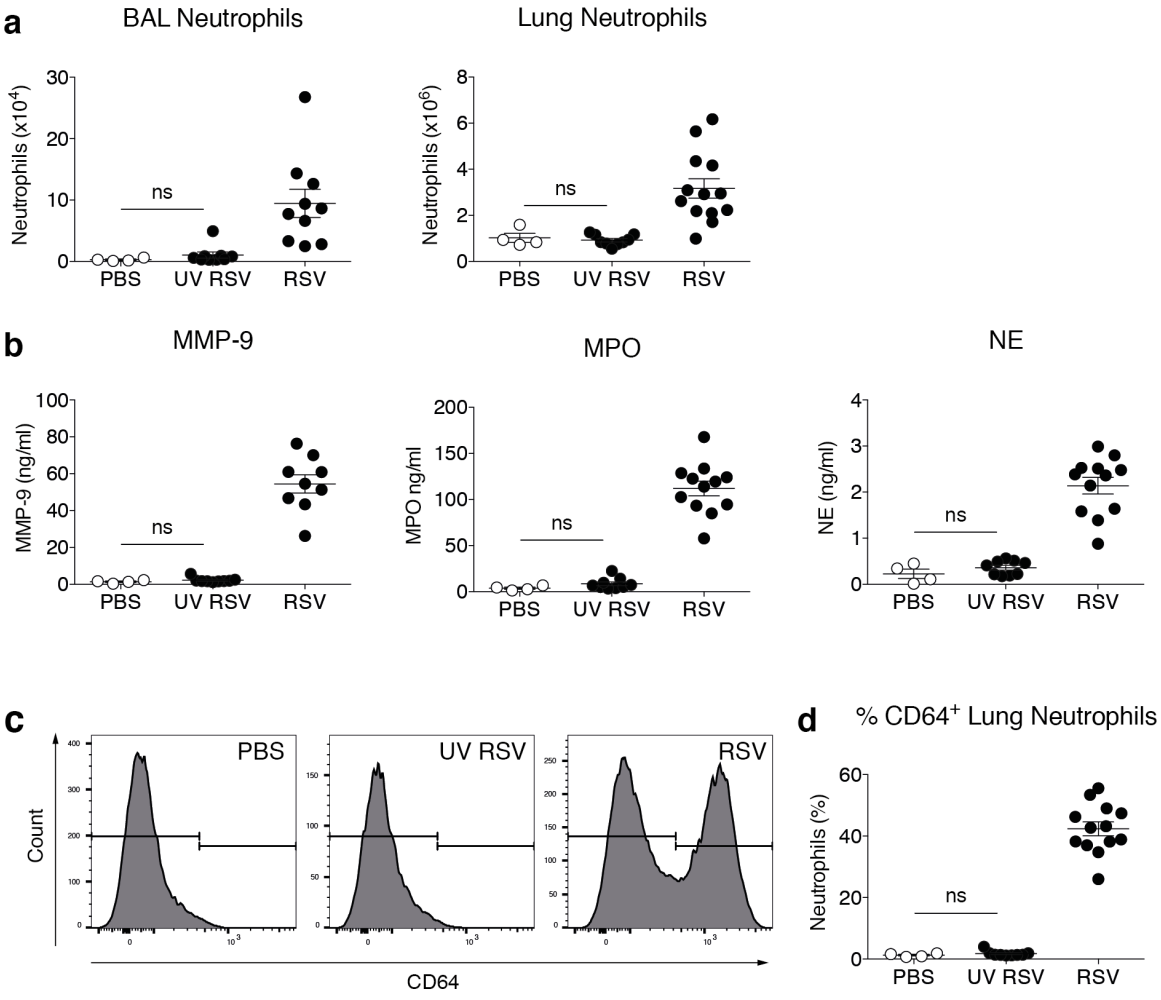

Figure 5.6. Live virus is necessary for neutrophil recruitment and activation during RSV infection. Wt mice were mock (PBS), UV RSV or RSV infected for 18 h. a. Total numbers of $CD45^+$, $CD3^-$, $CD19^-$, MHC-II^-, $Ly6G^+$ neutrophils were quantified in the airways and lung using flow cytometry (Fig. 4.1 for gating strategy). **b.** MMP-9, MPO and NE were detected in the BAL fluid by ELISA. **c.** Representative histograms of CD64 expression on $CD45^+$, $CD3^-$, $CD19^-$, $Ly6G^+$ neutrophils in the lung. **d.** Frequency of $CD64^+$ lung neutrophils, as quantified by flow cytometry. Data are presented as the mean±SEM of 4 (PBS), 9 (UV RSV) and 10-13 (RSV) individual mice, pooled from two independent experiments. Statistical significance of differences was determined by one-way ANOVA with Tukey's post hoc test. Only the statistical significance between PBS and UV RSV is shown.

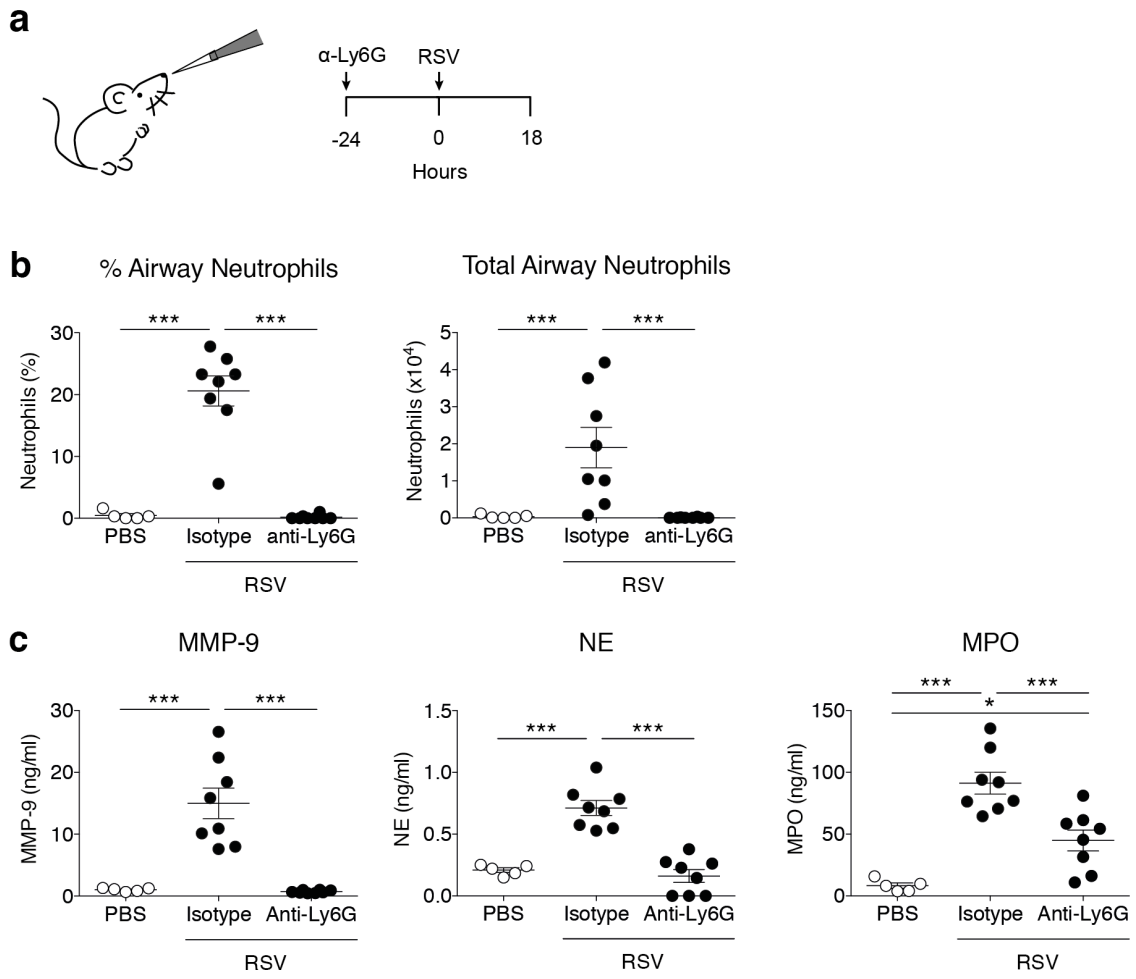

Figure 5.7. Neutrophil depletion using α-Ly6G prevents the recruitment of neutrophils to the lung during RSV infection *in vivo.* Wt mice were mock (PBS) or RSV infected for 18 h. To deplete neutrophils, mice were given 200 µg i.n. and 500 µg i.p. α-Ly6G or isotype control antibody one day before infection. **a.** Frequency and total number of neutrophils in the airways as quantified by differential counting of >300 cells on H&E stained cytospin slides **b.** MMP-9, NE and MPO were detected in the BAL fluid by ELISA. Data are presented as the mean±SEM from 4-5 (PBS) or 7-8 (RSV) individual mice, pooled from two independent experiments. Statistical significance of differences were determined by one-way ANOVA with Tukey's post hoc test. * $p \leq 0.05$, *** $p \leq 0.001$.

5.1.3 MyD88/TRIF signalling is required for neutrophil recruitment during RSV infection

PRRs are essential to detect invading pathogens and to initiate the immune response to protect the host (Takeuchi and Akira 2010). To investigate the role of two distinct pathogen sensing pathways in driving neutrophil recruitment and activation in the lung during RSV infection, *Mavs*$^{-/-}$ mice, unable to signal via MDA-5 or RIG-I, and *Myd88/Trif*$^{-/-}$ mice, unable to signal via the TLRs, IL-1R and IL-18R, were infected i.n. with mock (PBS) or with RSV for 18 h (Fig. 5.8). Neutrophils were recruited into the lungs of *Mavs*$^{-/-}$ mice during RSV infection, albeit significantly fewer were recruited than to the lungs of RSV infected wt mice (Fig. 5.8a). However, neutrophils were completely absent from the lungs of RSV infected *Myd88/Trif*$^{-/-}$ mice indicating that signalling via MyD88/TRIF is absolutely required for neutrophil recruitment to the lungs during RSV infection (Fig. 5.8a). The gene expression of the neutrophil chemokines CXCL1, CXCL2 and CXCL5 was investigated at early time points from 4 h p.i. to 18 h p.i. in wt, *Mavs*$^{-/-}$ and *Myd88/Trif*$^{-/-}$ mice (Fig. 5.8b). *Cxcl1*, *Cxcl2*, and *Cxcl5* was upregulated in wt mice early during RSV infection in the lung, but there was no difference in the expression level of these chemoattractants between *Mavs*$^{-/-}$ and *Myd88/Trif*$^{-/-}$ mice at any time point investigated; the expression level in both knock-out mice was comparable to uninfected wt mice (Fig. 5.8b).

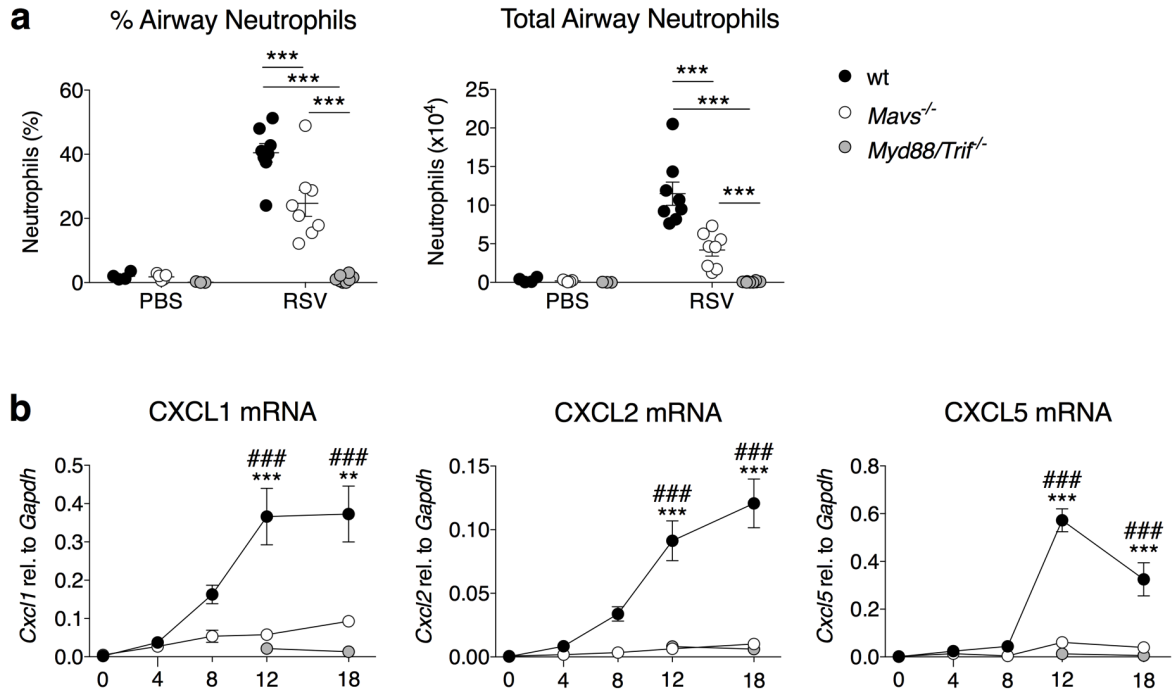

Figure 5.8. MyD88/TRIF is required for neutrophil recruitment to the lung during RSV infection. Wt, *Mavs*$^{-/-}$ and *Myd88/Trif*$^{-/-}$ mice were mock (PBS) or RSV infected for 18 h. **a.** Frequency and total number of neutrophils in the airways as quantified by differential counting of >300 cells on H&E stained cytospin slides. **b.** *Cxcl1, Cxcl2* and *Cxcl5* were quantified relative to *Gapdh* by RT-qPCR from RNA isolated from lung tissue. Data are presented as the mean±SEM from 4-10 individual mice from one or two independent experiments. Statistical significance of differences in **a** were determined by two-way ANOVA with Tukey's post hoc test. Statistical significance of differences in **b** were determined at 12 h and 18 h p.i. by one-way ANOVA with Tukey's post hoc test. * indicates differences between wt and *Mavs*$^{-/-}$ mice while # indicates differences between wt and *Myd88/Trif*$^{-/-}$ mice. ** $p \leq 0.01$, *** $p \leq 0.001$. Gene expression data were obtained in collaboration with Rinat Nuriev.

5.1.4 EpCAM^{-} CD31^{-} stromal cells are the cellular source of CXCL1 during RSV infection

To gain further insights into the mechanism of neutrophil recruitment during RSV infection, resident lung cells from wt and *Myd88/Trif*$^{-/-}$ mice were sorted at 12 h post RSV infection (Fig. 5.9; Fig. 4.2 for gating strategy). AMs, alveolar type II (ATII) epithelial cells (EpCAM^{+}), endothelial cells (CD31^{+}) and EpCAM^{-} CD31^{-} cells, termed "other stromal", were isolated by FACS and compared to a pre-sorted sample (total lung) (Fig. 5.9). Gene expression of RSV L gene, *Ifna5, Ifnb* and *Cxcl1* was analysed in the pre-sorted sample and FACS sorted lung cell populations by RT-qPCR (Fig. 5.9). Gene expression analysis revealed that viral load, as measured by quantification of RSV L gene, was similar in all resident lung cell types investigated in both wt and *Myd88/Trif*$^{-/-}$ mice during RSV infection (Fig. 5.9a). This confirmed

that RSV enters ATII epithelial cells, endothelial cells and other stromal cells, and that both wt and *Myd88/Trif*$^{-/-}$ mice were similarly infected with RSV at 12 h p.i. (Fig. 5.9a). The gene expression of IFN-α and IFN-β was enriched in sorted AMs from both wt and *Myd88/Trif*$^{-/-}$ mice as compared to total, unsorted lung cells from these mice during RSV infection (Fig. 9b and c). These experiments confirmed previously published findings from our group that AMs are the major source of the type I IFNs in response to RSV (Fig. 5.9b and Fig. 5.9c) (Makris *et al.* 2016; Goritzka, Makris, *et al.* 2015). To investigate the cellular source of the neutrophil chemoattractant CXCL1, *Cxcl1* expression was investigated in the sorted, resident lung cells (Fig. 5.9d). Notably only non-epithelial, non-endothelial, EpCAM^{-} CD31^{-} cells from wt mice had enriched *Cxcl1* expression during RSV infection, as compared to the presorted sample (Fig. 5.9d). CXCL1 was not detected at the mRNA level in RSV infected *Myd88/Trif*$^{-/-}$ mice (Fig. 5.9d), which did not recruit neutrophils to the lung (Fig. 5.8a).

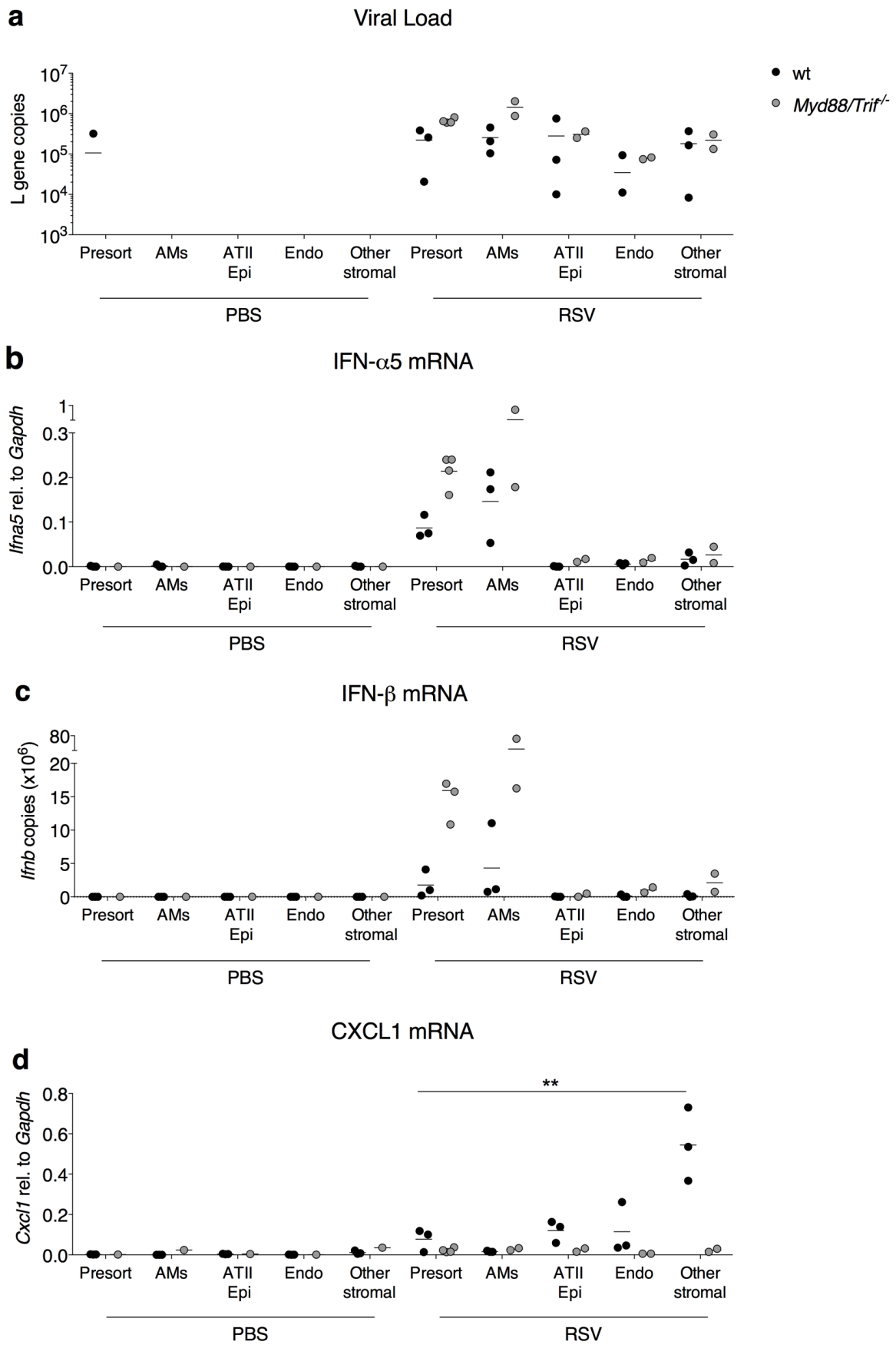
a
Viral Load
wt
Myd88/Trif-/-
L gene copies
Presort
AMs
ATII Epi
Endo
Other stromal
PBS
RSV
b
IFN-α5 mRNA
Ifna5 rel. to Gapdh
c
IFN-β mRNA
Ifnb copies (x10^6)
CXCL1 mRNA
d
Cxcl1 rel. to Gapdh
**

Figure 5.9. CXCL1 gene induction in stromal cells is dependent on MyD88/TRIF signalling during RSV infection. a-d. Wt and *Myd88/Trif*$^{-/-}$ mice were mock (PBS) or RSV infected for 12 h. RSV L gene copies, *Ifna5*, *Ifnb* and *Cxcl1* were quantified relative to *Gapdh* by RT-qPCR from RNA isolated from total lung cells (Presort) and fluorescence activated cell sorted: AMs (CD45^{+}, CD11c^{+}), ATII epithelial cells (CD45^{-}, EpCAM^{+}, CD31^{-}), endothelial cells (CD45^{-}, EpCAM^{-}, CD31^{+}) and other stromal cells (CD45^{-}, EpCAM^{-}, CD31^{-}; Fig. 4.2 for gating strategy). Data are presented as mean±SEM of 1-3 sorts per group (represented as individual dots), with 3-6 mice pooled per sort. Statistical significance of differences between wt sorted cell populations was determined by two-way ANOVA with Bonferroni's post hoc test. ** $p \leq 0.01$. Data for wt mice were obtained in collaboration with Fahima Kausar.

5.1.5 MAVS signalling is required for neutrophil activation in the lung during RSV infection

Previous work from our lab and others has demonstrated that the production of type I IFNs and other early pro-inflammatory mediators in the lung is dependent on *Mavs*$^{-/-}$ signalling during RSV infection (Goritzka, Makris, *et al.* 2015; Bhoj *et al.* 2008; Demoor *et al.* 2012). This was confirmed at 18 h post RSV infection in this project; *Mavs*$^{-/-}$ mice did not produce IFN-α or IL-6 in response to RSV (Fig. 5.10a). However, the production of these mediators was not dependent on MyD88/TRIF signalling as *Myd88/Trif*$^{-/-}$ mice did produce both IFN-α and IL-6 in the lungs at 18 h post RSV infection (Fig. 5.10a).

To further understand the pathways regulating neutrophil functionality in the lung during RSV infection, neutrophil activation status was assessed in the lungs of *Mavs*$^{-/-}$ and *Myd88/Trif*$^{-/-}$ mice (Fig. 5.10b-d). Despite recruiting neutrophils to the lung, RSV infected *Mavs*$^{-/-}$ mice did not produce MMP-9, MPO or NE in the airways; the concentrations of these mediators was comparable to mock-infected mice of all genotypes (Fig. 5.10b). RSV infected *Myd88/Trif*$^{-/-}$ mice, which did not recruit neutrophils to the lung, also did not produce MMP-9, MPO or NE in the airways (Fig. 5.10b). The activation status of neutrophils recruited into the lungs of RSV infected wt and *Mavs*$^{-/-}$ mice was further assessed by flow cytometry (5.10c and Fig. 5.10d). The activation marker CD64 was not upregulated on the cell surface of lung neutrophils from RSV infected *Mavs*$^{-/-}$ mice; the expression level of this marker was comparable to that on lung neutrophils from mock infected mice (Fig. 5.10c and Fig. 5.10d). Together, these data demonstrate that while neutrophil recruitment is dependent on signalling via MyD88/TRIF, neutrophil activation is dependent on signalling via MAVS during RSV infection. These observations in the context of previously published data demonstrating that MAVS signalling is required for the induction of a pro-inflammatory environment in the lung during RSV infection (Goritzka, Makris, *et al.* 2015; Bhoj *et al.* 2008; Demoor *et al.* 2012) formed the basis of the

hypothesis that pro-inflammatory factors induced downstream of MAVS signalling activate lung neutrophils after they are recruited into the lungs.

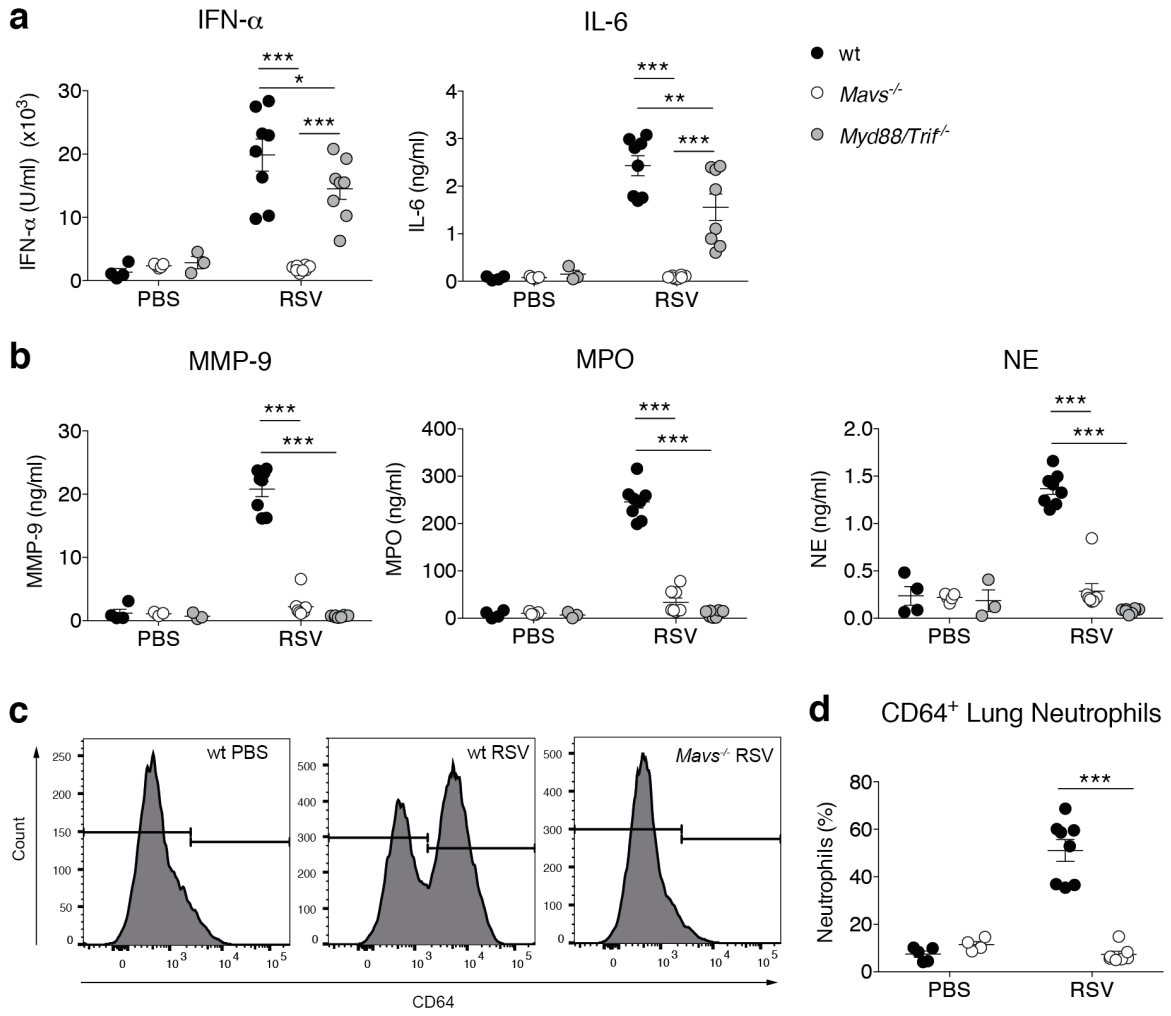

Figure 5.10. MAVS signalling is required for neutrophil activation in the lung during RSV infection. Wt, *Mavs*$^{-/-}$ and *Myd88/Trif*$^{-/-}$ mice were mock (PBS) or RSV infected for 18 h. **a-b.** IFN-α, IL-6, MMP-9, MPO and NE were detected in the BAL fluid by ELISA. **c.** Representative histograms of CD64 expression on CD45^{+}, CD3^{-}, CD19^{-}, Ly6G^{+} neutrophils in the lung. **d.** Frequency of CD64^{+} lung neutrophils, as quantified by flow cytometry (Fig. 4.1 for gating strategy). Data are presented as the mean±SEM from 3-5 (PBS) or 8 (RSV) individual mice (represented as individual dots) pooled from two independent experiments. Statistical significance of differences in **a-b** were determined by two-way ANOVA with Tukey's post hoc test. Statistical significance of differences in **d** were determined by one-way ANOVA with Tukey's post hoc test. * $p \leq 0.05$, ** $p \leq 0.01$, *** $p \leq 0.001$.

5.1.6 Recombinant IFN-α partially restores the pro-inflammatory environment in the lungs in the absence of MAVS signalling and is sufficient to drive at least partial neutrophil activation during RSV infection

To test this hypothesis, *Mavs*$^{-/-}$ mice were treated with rIFN-α i.n. after RSV infection to restore the type I IFN-driven pro-inflammatory environment in the lungs (Fig. 5.11– 5.13). Mice were first infected with RSV i.n., and then at 6 h p.i. mice were treated with 1 µg rIFN-α i.n.. This time point was chosen in order to mimic the natural kinetics of IFN-α induction in wt mice which starts to be produced from 4 h p.i. and peaks at 12 h p.i. (Goritzka *et al.* 2014). To confirm that the dose (1 µg) of rIFN-α was sufficient to induce an inflammatory environment in the lungs of *Mavs*$^{-/-}$ mice, the gene expression of a variety of pro-inflammatory mediators was assessed at 24 h p.i. (Fig. 5.11a). The gene expression levels of IL-6, TNF-α, IFN-γ and GM-CSF were all increased in RSV infected *Mavs*$^{-/-}$ mice treated with rIFN-α as compared to mock treated, RSV infected *Mavs*$^{-/-}$ mice (Fig. 5.11a). However, the gene expression of TNF-α, IFN-γ and GM-CSF in RSV infected *Mavs*$^{-/-}$ mice treated with rIFN-α was not restored to the same levels as observed in RSV infected wt mice (Fig. 5.11a). Our lab has previously shown that IFN-α production downstream of MAVS signalling is required for the upregulation of the monocyte chemoattractant CCL2 and therefore for monocyte recruitment to the lungs during RSV infection (Goritzka, Makris, *et al.* 2015). In these experiments, the dose of rIFN-α given to *Mavs*$^{-/-}$ mice was also sufficient to recruit comparable numbers of monocytes to the lung as in wt RSV infected mice at 24 h p.i.(Fig. 5.11b). This further confirmed that the timing and dose of rIFN-α given to *Mavs*$^{-/-}$ mice during RSV infection in these experiments was adequate to induce a pro-inflammatory environment in the lungs. During IFN-α treatment of RSV infected *Mavs*$^{-/-}$ mice, there was no overall change in the numbers of AMs detected in the airways at 24 h p.i. (Fig. 11c).

Mavs$^{-/-}$ mice are unable to produce type I IFNs but recruit neutrophils to the lung during RSV infection (Fig. 5.8). Treatment of *Mavs*$^{-/-}$ mice with rIFN-α following RSV infection did not influence the number of neutrophils detected in the airways or in the lung (Fig. 5.11d), confirming that type I IFNs do not regulate neutrophil recruitment during RSV infection. However, restoring the pro-inflammatory environment in the lung by treating RSV infected *Mavs*$^{-/-}$ mice with rIFN-α did result in neutrophil activation as measured by the upregulation of cell surface expression of CD64 (Fig. 5.12a and Fig. 5.12b). The frequency of CD64^{+} lung neutrophils observed in rIFN-α treated, RSV infected *Mavs*$^{-/-}$ mice was comparable to that observed during RSV infection of wt mice (Fig. 5.12a and Fig. 5.12b).

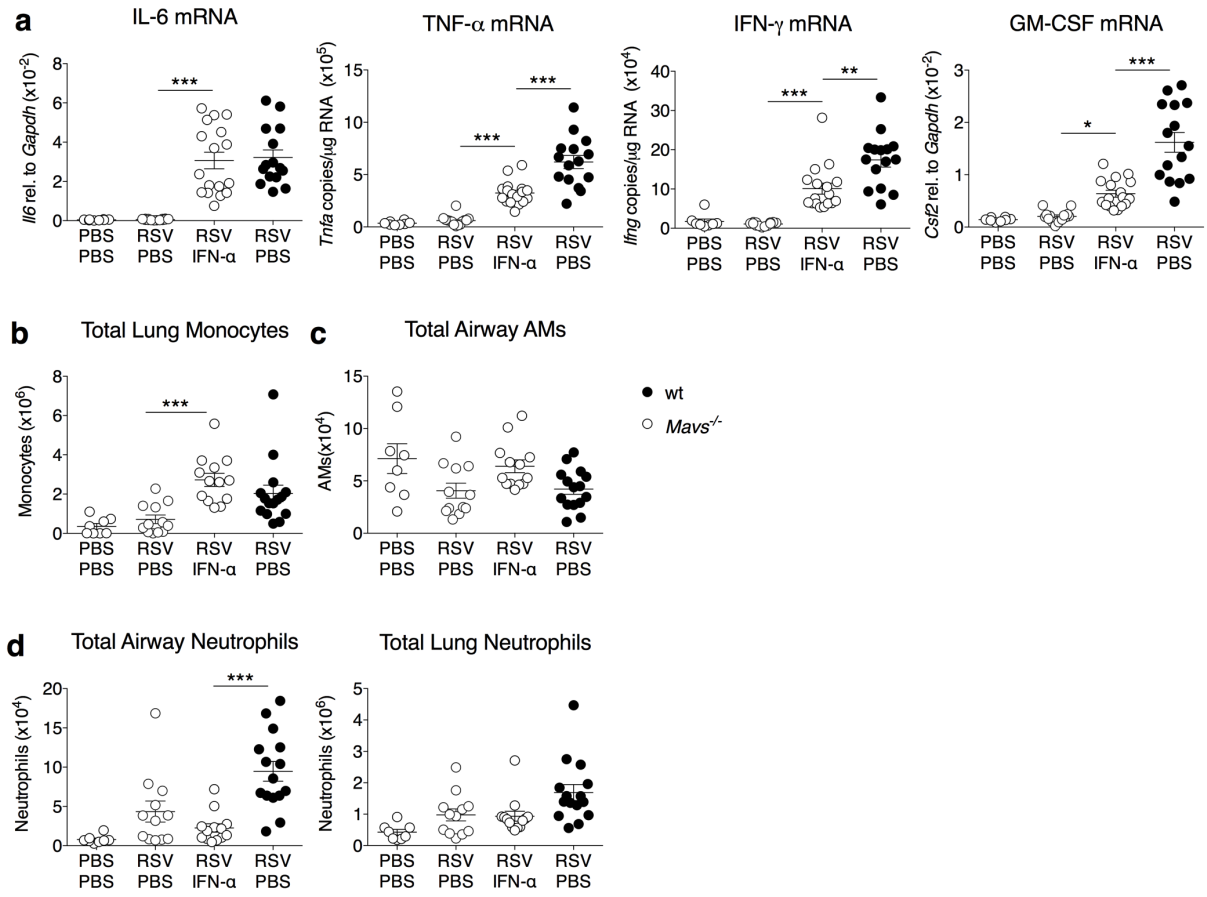

Figure 5.11. rIFN-α restores the pro-inflammatory environment in the lungs of *Mavs*$^{-/-}$ mice during RSV infection. Wt and *Mavs*$^{-/-}$ mice were mock (PBS) or RSV infected for 24 h. PBS or 1 µg rIFN-α was administered i.n. 6 h p.i.. **a.** mRNA was quantified by RT-qPCR from RNA isolated from the lung tissue. Expression levels of *Il6* and *Csf* were quantified relative to *Gapdh.* Absolute levels of *IFNg* and *Tnfa* were quantified using a plasmid standard and normalised to *Gapdh*. **b.** Total number of lung monocytes, **c.** total number of airway AMs and **d.** total number of airway and lung CD45^{+}, CD3^{-}, CD19^{-}, MHC-II^{-}, Ly6G^{+} neutrophils, as quantified by flow cytometry. Data are presented as mean±SEM of 8-17 mice (represented as individual dots) from each group, pooled from 3-4 independent experiments. Statistical significance of differences was determined by one-way ANOVA with Tukey's post hoc test. * $p \leq 0.05$, *** $p \leq 0.001$. Only differences between mock and IFN-α treated RSV infected *Mavs*$^{-/-}$ mice, and between IFN-α treated *Mavs*$^{-/-}$ and wt mice, are shown. Gene expression data were obtained in collaboration with Rinat Nuriev.

Furthermore, the activation status of neutrophils in the lungs of RSV infected *Mavs*$^{-/-}$ mice treated with rIFN-α was assessed by measuring the production of MMP-9, MPO and NE in the airways (Fig. 5.12c). There was a significant increase in the concentration of MPO in the airways of *Mavs*$^{-/-}$ mice when the pro-inflammatory environment was restored by treatment with rIFN-α (Fig. 5.12c). There was a trend for increased levels of airway MMP-9 and NE but this did not reach statistical significance (Fig. 5.12c). Neutrophil activation in *Mavs*$^{-/-}$ mice

during RSV infection was dependent on the effects of type I IFN signalling as treating RSV infected *Mavs*$^{-/-}$ mice with an unspecific protein control (1 µg BSA) i.n. after RSV infection did not result in monocyte or neutrophil recruitment into the lungs (Fig. 5.13a and Fig. 5.13b). Furthermore, BSA did not drive activation as measured by CD64 upregulation on lung neutrophils (Fig. 5.13b) nor did it result in the production of MMP-9, MPO or NE in the airways (Fig. 5.13c). Giving IFN-α on its own to wt mice in the absence of an RSV infection was also sufficient to drive CD64 cell surface upregulation on the <5% of lung neutrophils which are present in naïve mice (Fig. 5.13b).

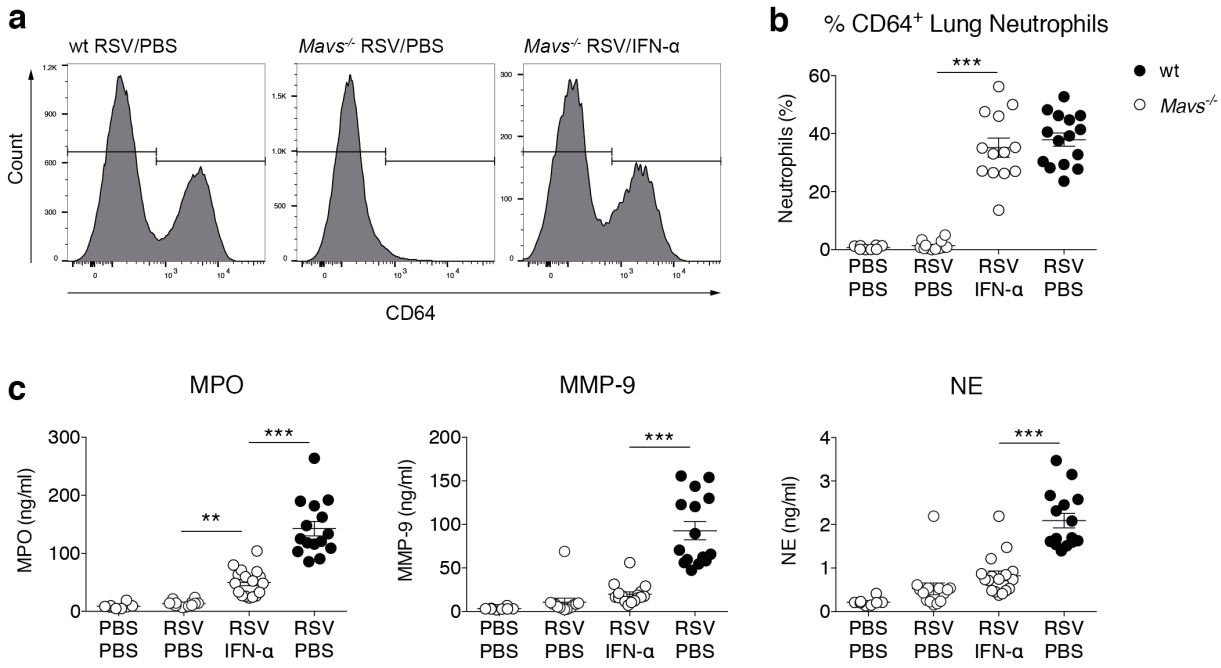

Figure 5.12. rIFN-α restores neutrophil activation in the lungs of *Mavs*$^{-/-}$ mice during RSV infection. Wt and *Mavs*$^{-/-}$ mice were mock (PBS) or RSV infected for 24 h. PBS or 1 µg rIFN-α was administered i.n. 6 h p.i. Immune cells were quantified by flow cytometry. **a.** Representative histograms of CD64 expression on CD45^{+}, CD3^{-}, CD19^{-}, Ly6G^{+} neutrophils in the lung. **b.** Frequency of CD64^{+} lung neutrophils. **c.** MMP-9, NE and MPO were detected in the BAL fluid by ELISA. Data are presented as mean±SEM of 8-17 mice (represented as individual dots) from each group, pooled from 3-4 independent experiments. Statistical significance of differences was determined by one-way ANOVA with Tukey's post hoc test. Only differences between mock and IFN-α treated RSV infected *Mavs*$^{-/-}$ mice, and between IFN-α treated *Mavs*$^{-/-}$ and wt mice, are shown. ** $p \leq 0.01$, *** $p \leq 0.001$.

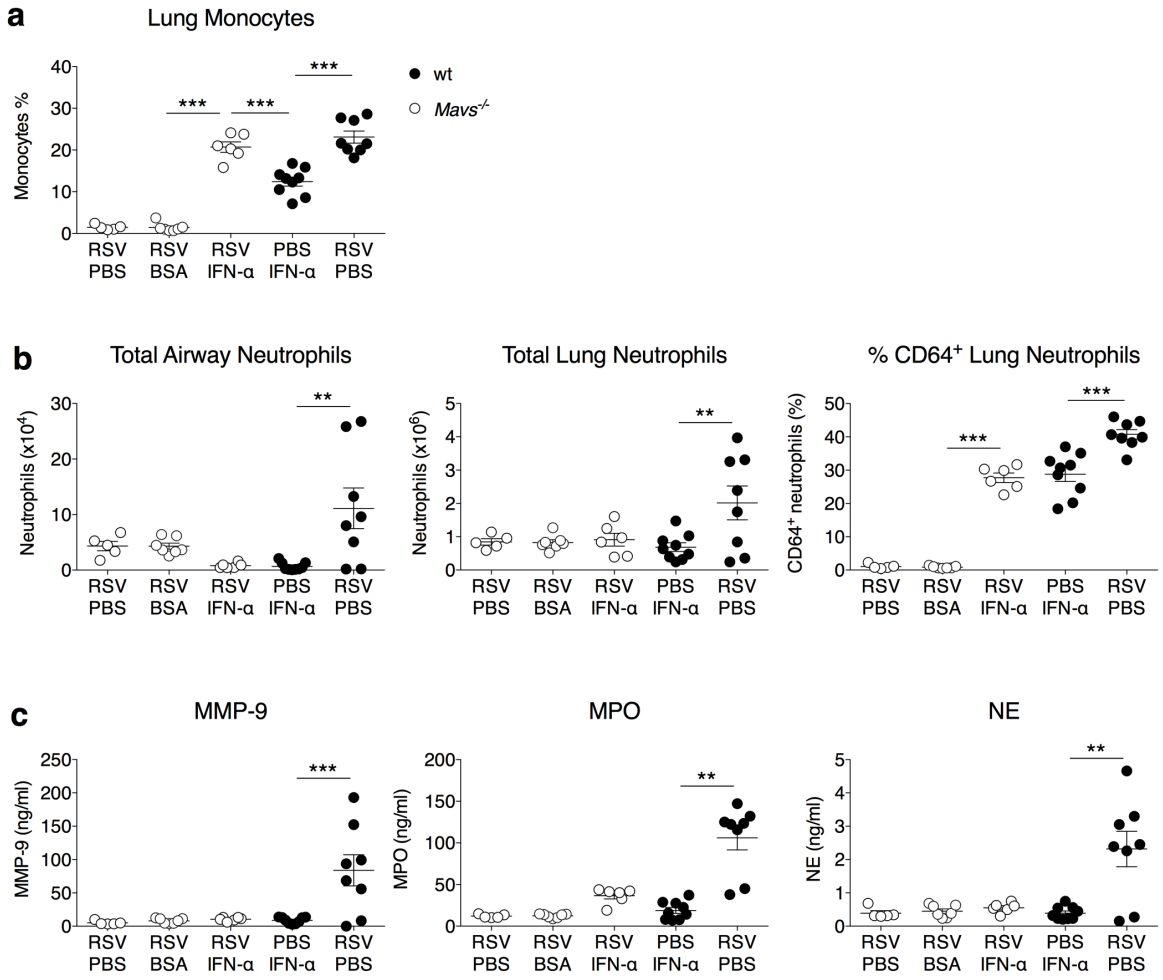

Figure 5.13. Figure 5.13. A protein control (BSA) does not activate lung neutrophils in *Mavs*$^{-/-}$ mice during RSV infecton. Wt and *Mavs*$^{-/-}$ mice were mock (PBS) or RSV infected for 24 h. PBS, 1 µg rIFN-α or 1 µg BSA was administered i.n. 6 h p.i.. Immune cells were quantified by flow cytometry (Fig. 4.1 for gating strategy). **a.** Frequency of CD45^{+}, CD3^{-}, CD19^{-}, Ly6G^{-}, Ly6C^{+}, CD64^{+}, CD11b^{+} monocytes were quantified in the lung. **b.** Total CD45^{+}, CD3^{-}, CD19^{-}, MHC II^{-}, Ly6G^{+} neutrophils were quantified in the airways and in the lung. The frequency of CD64^{+} lung neutrophils as quantified by flow cytometry. **c.** MMP-9, MPO and NE were detected in the BAL fluid by ELISA. Data are presented as the mean±SEM of 5-9 individual mice, pooled from two independent experiments. Statistical significance of differences was determined by one-way ANOVA with Tukey's post hoc test. ** $p \leq 0.0$, *** $p \leq 0.001$.

5.1.7 Recombinant CXCL1 drives neutrophil recruitment to the lungs of *Myd88/Trif*$^{-/-}$ mice where the pro-inflammatory environment activates neutrophils during RSV infection

An additional way to test the hypothesis that the pro-inflammatory environment induced downstream of MAVS signalling is required for neutrophil activation involved the use of *Myd88/Trif*$^{-/-}$ mice. As these mice are not deficient in MAVS signalling and can initiate a type I IFN driven pro-inflammatory cascade in response to RSV (Fig. 5.10a), the lung environment in these mice should contain the factor/s required for neutrophil activation if the hypothesis is correct. Therefore, to test this hypothesis in an alternative way, neutrophils were recruited into the lungs of *Myd88/Trif*$^{-/-}$ mice following RSV infection using recombinant CXCL1 (rCXCL1; Fig. 5.14). Mice were mock (PBS) or RSV infected, treated with 10 µg rCXCL1 6 h p.i. and the lungs were analysed at 18 h p.i. (Fig. 5.14). rCXCL1 treatment did not influence the number of airway AMs (Fig. 5.14a), nor did it drive the recruitment of monocytes to the lung (Fig. 5.14b), when given to *Myd88/Trif*$^{-/-}$ mice during mock or RSV infection. *Myd88/Trif*$^{-/-}$ mice treated with rCXCL1 in the absence of an RSV infection did not recruit any monocytes to the lung, while RSV infected *Myd88/Trif*$^{-/-}$ mice treated with rCXCL1 recruited comparable numbers of monocytes to the lung as wt RSV infected mice and mock treated, RSV infected *Myd88/Trif*$^{-/-}$ mice (Fig. 5.14b). RSV infection did not affect the number of neutrophils recruited to the lungs of *Myd88/Trif*$^{-/-}$ mice by rCXCL1; mock infected *Myd88/Trif*$^{-/-}$ mice treated with rCXCL1 recruited the same number of neutrophils as RSV infected *Myd88/Trif*$^{-/-}$ mice treated with rCXCL1 (Fig. 5.14c). This supported earlier findings that signalling via MyD88/TRIF drives neutrophil recruitment (Fig. 5.8). The dose and timing of rCXCL1 treatment was sufficient to induce a large recruitment of neutrophils to the airways and to the lung at 18 h p.i. (Fig. 5.14c). rCXCL1 treatment of RSV infected *Myd88/Trif*$^{-/-}$ mice confirmed that these mice are able to induce the factors required in the lung for neutrophil activation as lung neutrophils of RSV infected *Myd88/Trif*$^{-/-}$ mice upregulated cell surface expression of the activation marker CD64 (Fig. 5.14d). Furthermore, when neutrophils were recruited to the lungs of RSV infected *Myd88/Trif*$^{-/-}$ mice using rCXCL1, MMP-9, MPO and NE were detected in the airways (Fig. 5.14e).

To confirm that rCXCL1 alone did not induce neutrophil activation, *Myd88/Trif*$^{-/-}$ mice were treated with rCXCL1 following mock (PBS) infection. rCXCL1 treatment on its own, in the absence of an RSV infection, did not induce full neutrophil activation (Fig. 5.14). Mock infected, rCXCL1 treated mice did not upregulate CD64 on the cell surface of lung neutrophils (Fig.

5.14d). Treatment with rCXCL1 on its own did induce the production of significantly more MMP-9, MPO and NE in the airways than was observed in mock treated, RSV infected *Myd88/Trif*$^{-/-}$ mice (Fig. 5.14e). However, in the context of an RSV infection, *Myd88/Trif*$^{-/-}$ mice treated with rCXCL1 produced significantly more MMP-9, MPO and NE in the airways than mock infected, *Myd88/Trif*$^{-/-}$ mice treated with rCXCL1 (Fig. 5.14e). This demonstrated that the inflammatory environment in the lungs induced during RSV infection of *Myd88/Trif*$^{-/-}$ mice further activated the neutrophils recruited in by rCXCL1. Together these data support the hypothesis that neutrophil recruitment is dependent on signalling via MyD88/TRIF while neutrophil activation is dependent on MAVS signalling, which induces a type I IFN driven pro-inflammatory environment in the lungs.

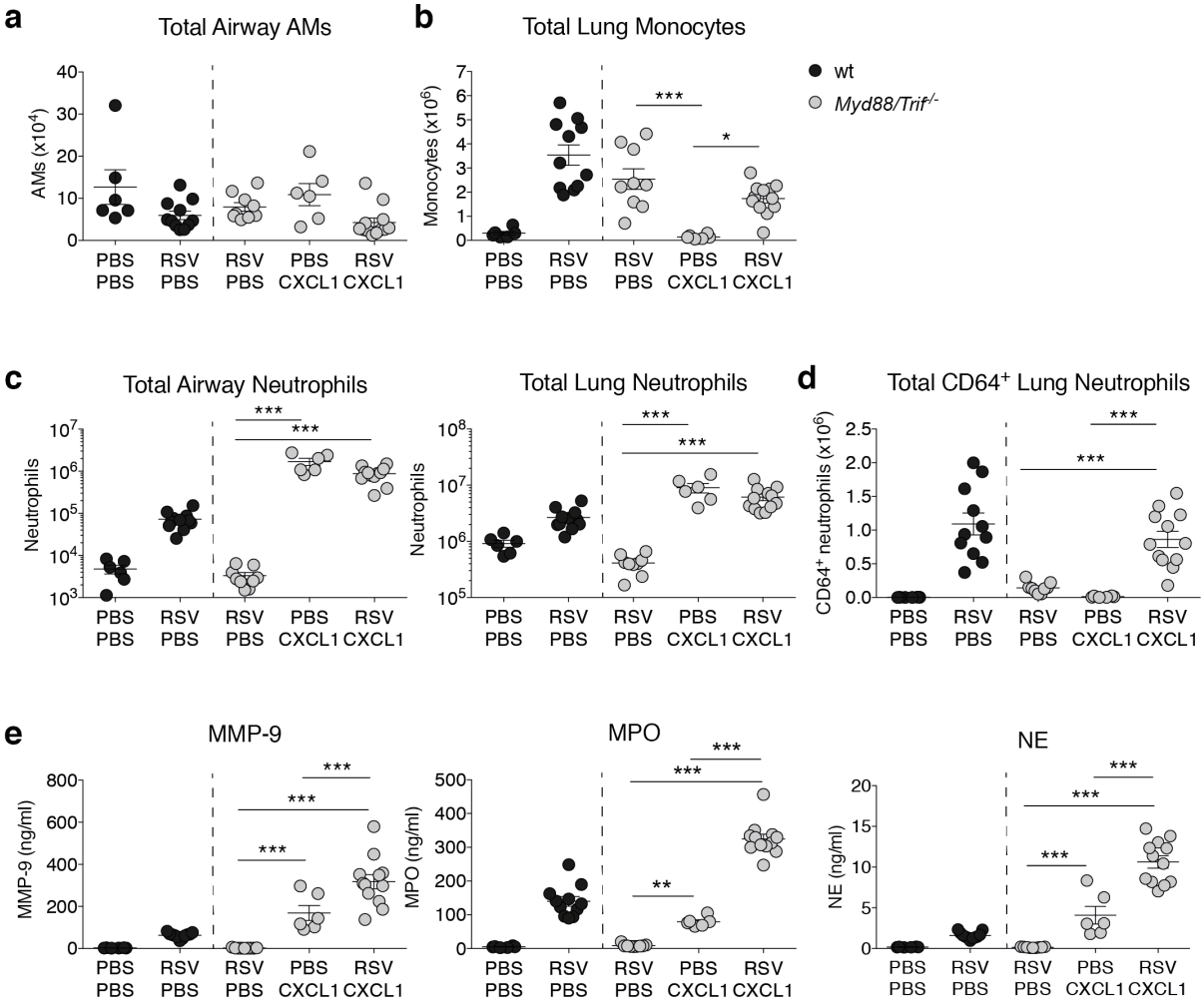

Figure 5.14. Neutrophil activation is not dependent on MyD88/TRIF signalling in the lung during RSV infection. Wt and *Myd88/Trif*$^{-/-}$ mice were mock (PBS) or RSV infected for 18 h. PBS or 10 µg rCXCL1 was administered i.n. 6 h p.i.. Immune cells were quantified by flow cytometry (Fig. 4.1 for gating strategy). **a.** Total numbers of CD45^{+}, Ly6C^{+}, CD11c^{+} AMs in the airways. **b.** Total number of CD45^{+}, CD3^{-}, CD19^{-}, Ly6G^{-}, Ly6C^{+}, CD64^{+}, CD11b^{+} lung monocytes. **c.** Total numbers of airway and lung CD45^{+}, CD3^{-}, CD19^{-}, MHC-II^{-}, Ly6G^{+} neutrophils. **d.** Total number of CD64^{+} lung neutrophils. **e.** MMP-9, MPO and NE were detected in the BAL fluid by ELISA. Data are presented as mean±SEM of 6-12 mice from each group (represented as individual dots), pooled from 2-3 independent experiments. Statistical significance of differences was determined by one-way ANOVA with Tukey's post hoc test. Only the statistical significances between groups of *MyD88/Trif*$^{-/-}$ mice are shown. * $p \leq 0.05$, ** $p \leq 0.01$, *** $p \leq 0.001$.

5.1.8 Activation of lung neutrophils cannot be investigated *ex vivo* in neutrophils isolated from murine bone marrow

PRR detection of RSV induces the production of type I IFNs, which act via a positive feedback loop to induce the expression of hundreds of anti-viral ISGs. While it is possible that IFN-α itself is required for neutrophil activation, it is more likely that neutrophils are activated by a factor or combination of factors induced downstream of IFN-α signalling during RSV infection. It is also possible that neutrophil activation is dependent on MAVS signalling occurring within the neutrophil itself. In order to investigate the inflammatory factors driving neutrophil activation during RSV infection and to investigate whether MAVS signalling is required in neutrophils, murine neutrophils were stimulated *ex vivo* (Fig. 5.15 and 5.16). Neutrophils were isolated from murine bone marrow by negative selection MACS (Fig. 5.15 and 5.16). The purity of the isolated neutrophils was assessed as >97% by H&E staining of cytospin slides as well as by flow cytometry (Fig. 5.15).

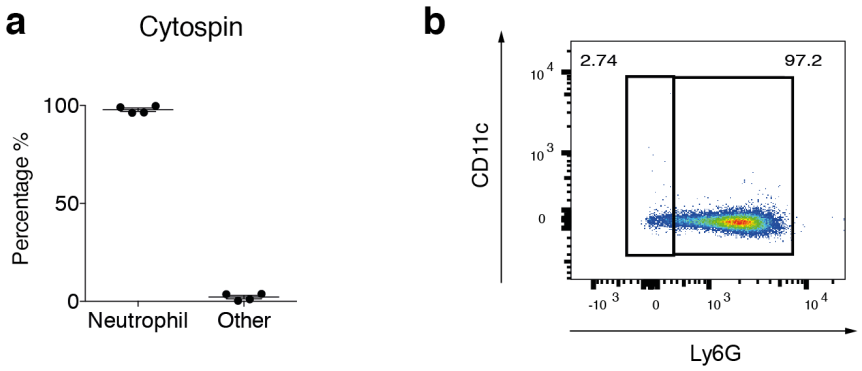

Figure 5.15. Negative selections MACS isolates a pure population of bone marrow neutrophils. Neutrophils were isolated from murine bone marrow from naïve wt mice by negative selection MACS. **a.** The frequency of neutrophils in the purified neutrophil fraction was determined after isolation by differential cell counting of >300 cells on H&E stained cytospin slides. **b.** The frequency of $CD45^+$, $Ly6G^+$ neutrophils in the purified neutrophil fraction, as quantified by flow cytometry.

Isolated neutrophils were stimulated with varying concentrations and combinations of PMA, IFN-α, IFN-γ, G-CSF and GM-CSF for 4 h *ex vivo* and the production of MMP-9, MPO and NE was measured in the cell culture supernatant (Fig. 5.16a). PMA, known to stimulate degranulation (Brown and Ganey 1995) potently induced MMP-9, MPO and NE secretion (Fig. 5.16a). However, none of the cytokines tested were able to induce neutrophil degranulation as measured by the secretion of these mediators (Fig. 5.16a). Bone marrow neutrophils were also incubated with RSV – both alone and in combination with the highest concentration of the above cytokines. No concentration of any mediator in any combination with RSV induced neutrophil degranulation (Fig. 5.16a). To test whether bone marrow neutrophils were able to become activated by a biologically relevant factor known to activate neutrophils in tissues, bone marrow neutrophils were also stimulated with LPS, which is known to drive MMP-9 secretion of blood neutrophils (Pugin *et al.* 1999), at varying concentrations for 4 h (Fig. 5.16b). Even at the highest concentration, LPS did not induce MPO or MMP-9 production by murine bone marrow neutrophils. The *ex vivo* neutrophil experiments did not further our understanding of which factor or combination of factors drives neutrophil activation during RSV infection and this experimental setup could not be used to model the final stage in neutrophil activation as it occurs *in vivo* following recruitment and priming in an organ.

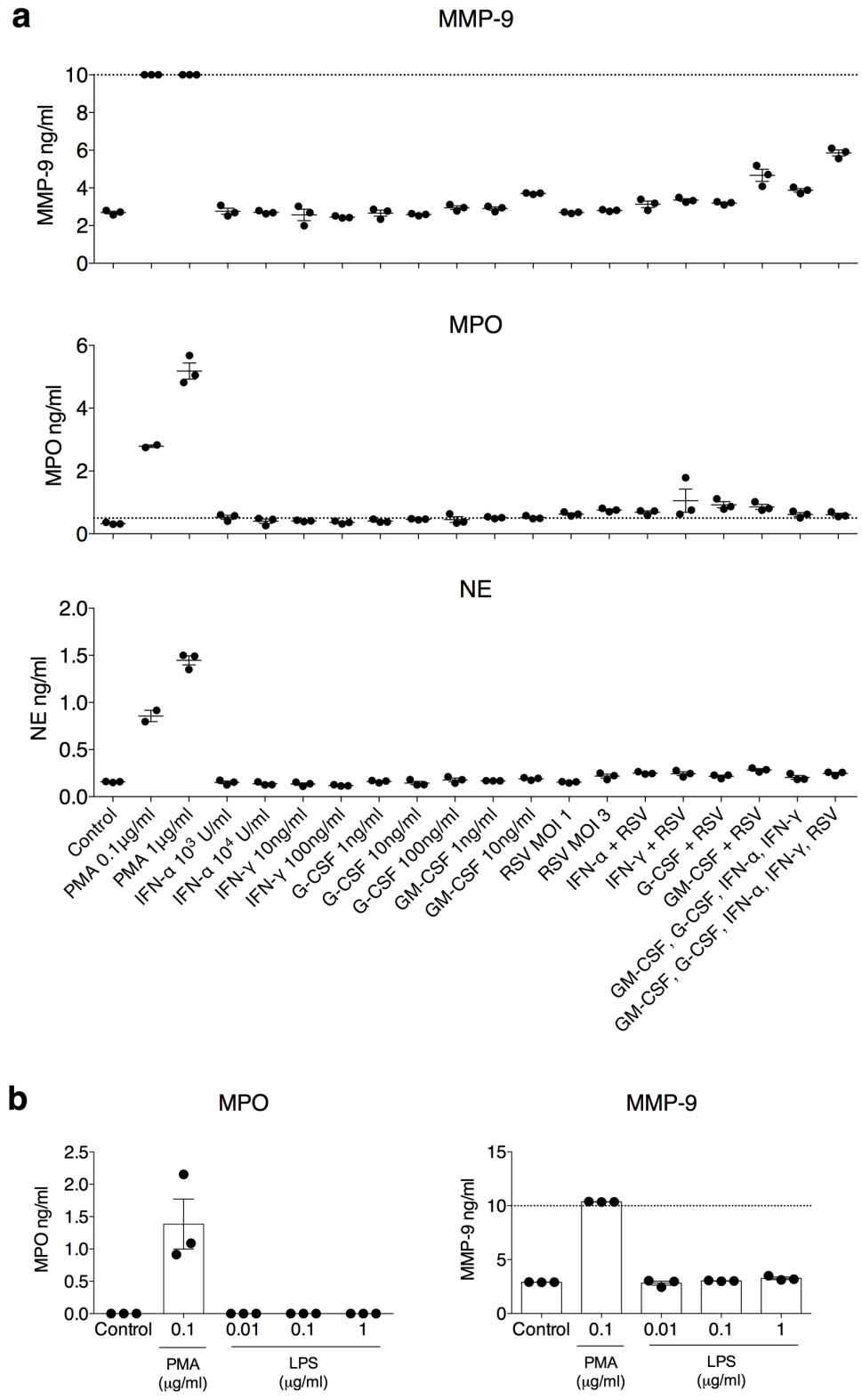

Figure 5.16. Neutrophils do not secrete MMP-9, MPO or NE after *ex vivo* stimulation with RSV, cytokines or LPS. Neutrophils were isolated from murine bone marrow from wt mice by negative selection MACS and exposed to PMA, LPS, IFN-α, IFN-γ, G-CSF, GM-CSF and RSV, individually and in combination, for 4 h. **a-b**. The secretion of MMP-9, MPO and NE was detected in filtered culture supernatant by ELISA. Data are presented as the mean mean±SEM from 3 individual cultures, from one experiment.

5.1.9 Discussion

Neutrophils are the most abundant cell type in the airways of infants with severe RSV disease and it is thought that neutrophils likely contribute to disease severity (McNamara 2003; Hull *et al.* 2000; Everard *et al.* 1994; Emboriadou *et al.* 2007; Marguet *et al.* 2008). However, the immunological mechanism by which neutrophils are recruited and activated in the lung remain poorly understood. In this study, the contribution of two major innate pathogen sensing pathways in the regulation of neutrophil recruitment and activation was investigated using mice deficient in the PRR signalling pathway adaptor proteins MAVS and MyD88/TRIF (Fig. 5.17) (Kirsebom *et al.* 2019). In this study using *Mavs*$^{-/-}$ mice, unable to signal via MDA-5 or RIG-I, and *Myd88/Trif*$^{-/-}$ mice, unable to signal via the TLRs, IL-1R and IL-18R, we found that MyD88/TRIF signalling was required for neutrophil recruitment to the lung. Non-epithelial, non-endothelial stromal lung cells were the major producer of the neutrophil chemoattractant CXCL1; this was abrogated in *Myd88/Trif*$^{-/-}$ mice, which did not recruit neutrophils during RSV infection. Meanwhile, MAVS signalling was required for the production of an IFN-α-driven pro-inflammatory environment in the lung which was at least partially required for neutrophil activation and degranulation (Fig. 5.17). Together these data demonstrate that two biologically distinct PRR signalling pathways must collaborate to achieve neutrophil recruitment and activation in the lung during RSV infection.

Neutrophils are classically considered as the first responders to an inflammatory scenario; this study also found that neutrophil recruitment to the lung in response to RSV occurs rapidly and transiently. Neutrophilia peaked very early in the lung at 18-24 h p.i., prior to the recruitment of inflammatory monocytes which occurs at 48 h p.i. (Goritzka, Makris, *et al.* 2015). This is similar to the kinetics of neutrophil recruitment during influenza virus infection in mice where lung neutrophilia also peaks early at 24 h p.i. (Peiró *et al.* 2018). Neutrophil activation in response to RSV was assessed in two ways; by quantifying the cell surface expression of markers associated with neutrophil activation in other inflammatory scenarios by flow cytometry as well as by measuring the production of the neutrophil degranulation proteins MMP-9, MPO and NE in the airways. Flow cytometry provides a sensitive readout of neutrophil activation as the expression level can be assessed on each cell individually. However, measurement of the production of neutrophil mediators in the airways provides a more global and functional readout of neutrophil activation status. NE is exclusively secreted by neutrophils and neutrophil depletion using α-Ly6G treatment prior to RSV infection confirmed that neutrophils are the only cellular source of NE during RSV infection.

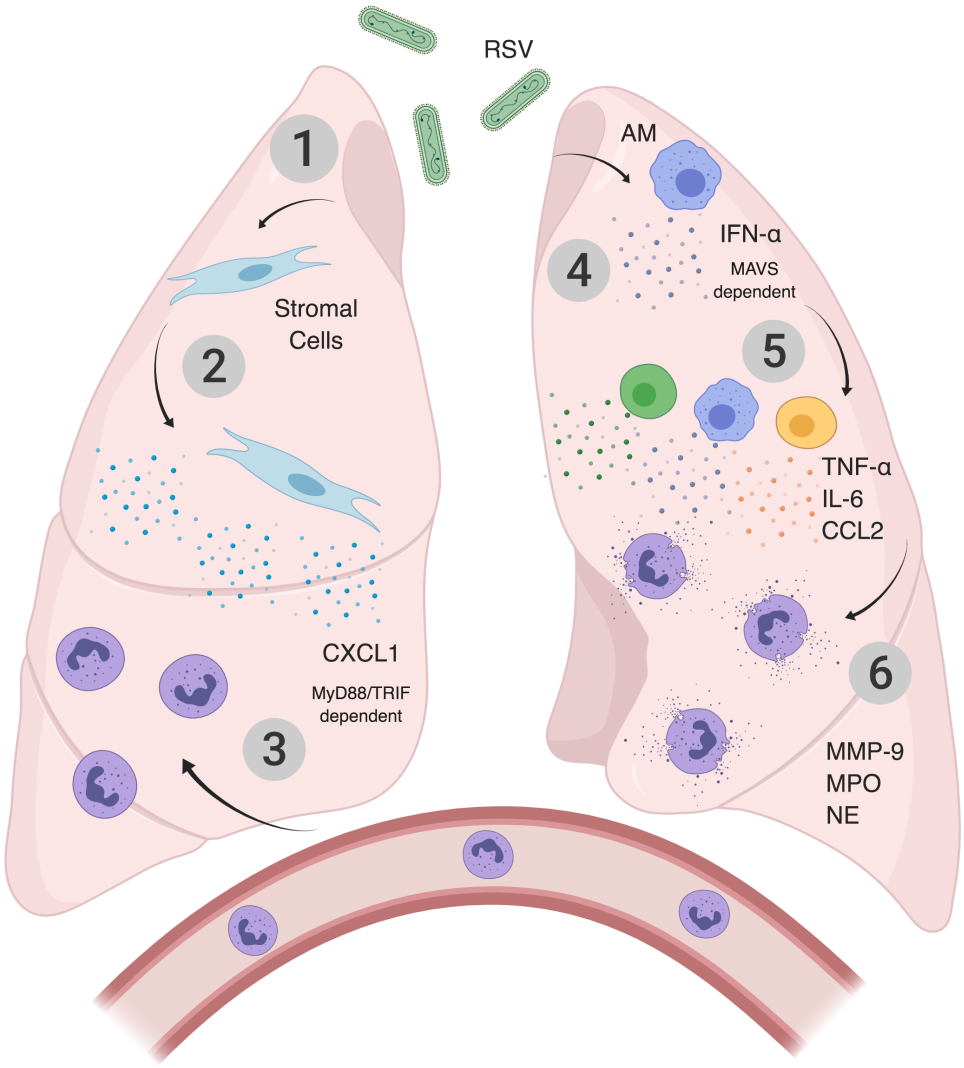

Figure 5.17. Schematic to illustrate the mechanism by which neutrophils are recruited and activated in the lung during RSV infection. RSV enters the airways and lung **(1)** and interacts either directly or indirectly with stromal cells to induce the production of CXCL1 via the MYD88/TRIF signalling pathway **(2)**. This drives the recruitment of neutrophils into the lungs from the vasculature **(3)**. Meanwhile, AMs produce type I IFNs in response to RSV via signalling through the MAVS signalling pathway **(4)**. Type I IFNs drive the induction of other pro-inflammatory mediators, such as TNF-α and IL-6, and chemokines such as CCL2 by multiple other cell types **(5)**. When neutrophils encounter this pro-inflammatory environment, they upregulate cell surface CD64 and become activated to secrete MMP-9, MPO and NE **(6)**. Created using BioRender.

Neutrophil depletion further confirmed that neutrophils are the exclusive cellular source of MMP-9 during RSV infection. In other inflammatory contexts, MMP-9 can also be secreted by epithelial cells (Hozumi *et al.* 2001; Hetzel *et al.* 2003), but this does not seem to occur early during RSV infection of the lung. However, neutrophil depletion did not entirely abolish MPO production, indicating there is likely another cellular source of this mediator in the lung during RSV infection. This could be monocytes as monocytes also start to be recruited at these early time points in response to RSV and human monocytes have been shown to contain intracellular MPO (Tay *et al.* 1998).

The cell surface expression of a number of markers associated with activation in other inflammatory contexts was also quantified on airway and lung neutrophils as an alternative measure of neutrophil activation status in the lung. Markers such as CD62L and CD11b were differentially expressed on lung neutrophils as compared to blood neutrophils, but there was no difference in the expression level of these markers between mock (PBS) and RSV infection. It is likely that some of the cell surface markers used as activation markers are merely markers of migration into tissues from the circulation. CD62L, or L-selectin, is shed when neutrophils transmigrate across the endothelium (Lee *et al.* 2007), which may contribute to neutrophil priming but, in itself, does not indicate cellular degranulation. CD69 has been demonstrated to be upregulated on BAL neutrophils specifically in response to influenza virus (Tate *et al.* 2008), however we did not observe CD69 upregulation on either lung or BAL neutrophils in response to RSV. These data suggest that neutrophils are differentially activated depending on the specific respiratory virus and supports recent literature that neutrophils can tailor their response during activation to specific pathogens (Branzk *et al.* 2014).

CD64 (high affinity FcγRI) was the only marker specifically upregulated on lung neutrophils in response to RSV. Triggering of CD64 drives an intracellular signalling cascade which leads to Ca^{2+} release, which has been suggested to drive actin polymerisation and facilitate phagocytosis in neutrophils (Melendez and Tay 2008). It would be interesting to investigate how CD64 upregulation might influence neutrophil functionality during RSV infection in future studies. Phagocytosis can benefit the host by restricting viral replication but as RSV spread largely occurs between cells via the formation of syncytia (Shigeta *et al.* 1968) this might not be a beneficial function during RSV infection. However, increased phagocytosis by neutrophils could have a role in clearing up damage or debris from dying cells in the lung, as has been reported in other inflammatory contexts (Wang 2018). Although roughly half of lung neutrophils were $CD64^{+}$ at the peak of their recruitment, airway neutrophils as detected in the BAL had a lower level of cell surface CD64 expression during RSV infection. In a cancer model, CD64

expression on neutrophils was dispensable for their migration towards tumours (Otten *et al.* 2012) so it does not seem likely that the differential CD64 expression observed on airway neutrophils as compared to lung neutrophils in this study was a consequence of migration into the airway lumen. It could also be that airway neutrophils have already been activated and have started to downregulate cell surface CD64. The kinetics of cell surface CD64 expression on neutrophils during neutrophil activation has not been well characterised and it would be interesting to better understand how this relates to neutrophil function in the lung during RSV infection.

Neutrophil recruitment to the lung was dependent on MyD88/TRIF signalling but largely independent of MAVS signalling. *Mavs*$^{-/-}$ mice did recruit neutrophils to the lung early during RSV infection albeit fewer than wt mice. MyD88/TRIF signalling is also essential for neutrophil recruitment to the lung during infections with influenza virus, *S. aureus* and *S. pneumoniae* (Dudek *et al.* 2016; Miller *et al.* 2006; Bradley *et al.* 2012). However the cell types which initiate neutrophil recruitment via MyD88/TRIF varies between pathogens; signalling in non-hematopoietic cells was shown to be required for neutrophil recruitment in influenza (Bradley *et al.* 2012) while during *S. pneumoniae* infection both hematopoietic and non-hematopoietic cells were required (Dudek *et al.* 2016). During RSV infection of *Myd88/Trif*$^{-/-}$ mice, the lack of neutrophil recruitment was in part explained by the loss of expression of the neutrophil chemoattractants CXCL1, CXCL2 and CXCL5.

Mavs$^{-/-}$ mice, however, also did not express these neutrophil chemoattractants at any early time point investigated, despite being able to recruit neutrophils to the lung. In a previous study by our lab, *Mavs*$^{-/-}$ mice recruited the same number of neutrophils to the lung as wt mice at 18 h p.i. and did produce CXCL1 early in the lungs during RSV infection, although not to the same levels as wt mice (Goritzka, Makris, *et al.* 2015). The disparity between the data from this study and the previous data from the lab could be explained by differences between batches of RSV. Notably, CXCL1, CXCL2 and CXCL5 are not the only chemokines regulating neutrophil recruitment to the lung. Many neutrophil chemoattractants have been described in addition to these factors including LTB4, IL-23, C5a, C3a, fMLF and PAF (Kolaczkowska and Kubes 2013; Sadik *et al.* 2011). It is likely that several of these factors regulate neutrophil recruitment in addition to CXCL1 during RSV infection and it would be interesting to quantify their production during RSV infection in wt and *Mavs*$^{-/-}$ mice.

While these data reveal the importance of MyD88/TRIF signalling in ensuring neutrophil recruitment to the lung during RSV infection, these data do not reveal which initial signal drives

neutrophil recruitment. This could be RSV itself or a host-derived DAMP. As neutrophil recruitment occurs very early before major tissue damage, it is likely that detection of RSV itself triggers the MyD88/TRIF-dependent downstream signalling cascade. TLR2 (Murawski *et al.* 2009), TLR3 (Kim and Lee 2014) TLR4 (Kurt-Jones *et al.* 2000) and TLR7 (Huang *et al.* 2009) have all been implicated in the initiation of the immune response to RSV but further work is needed to clarify exactly which PRR on which cell type initiates neutrophil recruitment. The gene expression of CXCL1 was investigated in sorted stromal cells to further our understanding of which resident lung cells drive neutrophil recruitment during RSV infection. Interestingly, CXCL1 was only expressed by $CD45^-$, non-epithelial, non-endothelial cells termed 'other stromal cells' during RSV infection. This upregulation was abrogated in *Myd88/Trif*$^{-/-}$ mice which did not recruit neutrophils. These data do not reveal which non-epithelial, non-endothelial cell type in the lung is the major producer of CXCL1 during RSV infection however data from the lab has shown that primary murine fibroblasts secrete CXCL1 when stimulated with RSV *ex vivo* (Fahima Kausar, unpublished). Further work is needed to clarify whether fibroblasts are indeed the major source of CXCL1 *in vivo*. It would be of interest to use the same FACS-based approach to investigate whether fibroblasts also produce the other chemoattractants driving neutrophil recruitment to the lung during RSV infection or whether different stromal cells collaborate to drive neutrophil recruitment to the lung in response to RSV.

While neutrophil recruitment was largely independent of MAVS signalling, MAVS was required for neutrophil activation during RSV infection. From previous work published by the lab and by others it is known that MAVS signalling is essential for the production of type IFNs from AMs (Goritzka, Makris, *et al.* 2015). This initiates a pro-inflammatory cascade amplified by signalling through the IFNAR receptor and induces an anti-viral immune environment in the lungs early during RSV infection (Goritzka *et al.* 2014; Goritzka, Makris, *et al.* 2015; Demoor *et al.* 2012; Bhoj *et al.* 2008). The recruitment of anti-viral monocytes to the lung is also dependent on the induction of this signalling cascade (Goritzka, Makris, *et al.* 2015). Restoring the pro-inflammatory environment in the lung by treating mice with rIFN-α after RSV infection was sufficient to at least partially restore neutrophil activation, as measured by the upregulation of the activation marker CD64 on lung neutrophils. Neutrophil activation was also assessed by the secretion of MMP-9, MPO and NE during rIFN-α treatment of RSV infected *Mavs*$^{-/-}$ mice. MPO was produced in the lung during rIFN-α treatment of *Mavs*$^{-/-}$ mice during RSV infection but there was no significant increase in the production of MMP-9 or NE in the airways. We suspect that a single dose of rIFN-α 6 h post RSV infection does not exactly

mimic the natural kinetics of rIFN-α induction during a natural RSV infection. The dose of rIFN-α given to RSV infected *Mavs*$^{-/-}$ mice was sufficient to upregulate the expression of multiple pro-inflammatory mediators, as has also previously been shown in wt mice (Goritzka *et al.* 2014). However, the gene expression levels of TNF-α, IFN-γ and GM-CSF was not as high in RSV infected *Mavs*$^{-/-}$ mice treated with rIFN-α as observed in RSV infected wt mice. This could explain why increased MMP-9 and NE production in the airways was not observed when RSV infected *Mavs*$^{-/-}$ mice were treated with rIFN-α.

This dose of IFN-α was, however, sufficient to upregulate CD64 on the neutrophils present at baseline in wt mice and was also sufficient to recruit monocytes to the lung, as previously described (Goritzka, Makris, *et al.* 2015). It is also possible that the defect in MMP-9 and NE production observed is because *Mavs*$^{-/-}$ mice did recruit slightly less neutrophils to the lung than wt mice in response to RSV. Therefore, the production of MMP-9, MPO and NE into the airways was not expected to be restored to equivalent levels to that observed during RSV infection of wt mice. Based on these data, the possibility that MAVS signalling is required in neutrophils themselves for neutrophil activation cannot be excluded. However, based on the fact that rIFN-α did induce the upregulation of CD64 on lung neutrophils to levels comparable to that observed on neutrophils from wt mice during RSV infection, we do not suspect that MAVS signalling is required within the neutrophils for their activation. In addition to our findings, a previous study found that RSV itself does not activate neutrophils *in vitro* (Bataki *et al.* 2005).

In further support of the hypothesis that neutrophil activation is dependent on MAVS signalling but not MyD88/TRIF signalling, neutrophils recruited by rCXCL1 into the inflammatory environment induced in the lungs of *Myd88/Trif*$^{-/-}$ mice during RSV infection did become fully activated. Cell surface expression of CD64 was upregulated on lung neutrophils and rCXCL1 treated RSV infected *Myd88/Trif*$^{-/-}$ mice produced comparable levels of MMP-9, MPO and NE in the airways to RSV-infected wt mice. Treatment of rCXCL1 to mock infected *Myd88/Trif*$^{-/-}$ mice did induce some MMP-9, MPO and NE production and it is known that CXCL1 has a role in both neutrophil recruitment and activation (Zeilhofer and Schorr 2000). However, RSV infection was required for full neutrophil activation in the lungs of *Myd88/Trif*$^{-/-}$ mice as this heightened the production of MMP-9, MPO and NE in the airways. Furthermore, rCXCL1 on its own did not induce CD64 cell surface expression on lung neutrophils. These data support the finding that while neutrophil recruitment is dependent on signalling via MyD88/TRIF, neutrophil activation does not require MyD88/TRIF and is instead dependent on the induction

of a pro-inflammatory environment induced downstream of MAVS signalling in the lung during RSV infection.

It is still not known which factor produced downstream of MAVS signalling activates lung neutrophils during RSV infection. It is possible that IFN-α itself activates neutrophils although it seems more likely that it is one or a combination of the hundreds of ISGs induced downstream of IFN-α may activate neutrophils during RSV infection. Factors such as IFN-γ, G-CSF and GM-CSF, which are induced downstream of type I IFN signalling during RSV infection (Goritzka *et al.* 2014), have been shown to activate neutrophils in other scenarios (Buckle and Hogg 1989; Fuxman Bass *et al.* 2008; Barreda *et al.* 2004). Very few lung neutrophils are detected in naïve mice and therefore it was not feasible to isolate neutrophils from the mouse lung to further investigate which factors drive their activation during RSV infection. Neutrophils were therefore isolated from the bone marrow *ex vivo* and stimulated with RSV, LPS and cytokines which have previously been demonstrated to induced neutrophil activation (Buckle and Hogg 1989; Fuxman Bass *et al.* 2008; Barreda *et al.* 2004). The only factor which induced neutrophil degranulation, as measured by MMP-9, MPO and NE secretion, was PMA. No biologically relevant factor induced neutrophil degranulation, including LPS at a high concentration. Isolated $Ly6G^+$ bone marrow neutrophils represent a diverse pool of neutrophils in different stages of their development; immature neutrophils still express Ly6G, albeit at lower levels than mature neutrophils (Deniset *et al.* 2017). In line with this, the Ly6G staining on bone marrow neutrophils as assessed by flow cytometry showed a bigger range in fluorescent intensity as compared to the Ly6G staining observed on lung neutrophils, illustrating that bone marrow neutrophils express differing levels of cell surface Ly6G. It is possible that bone marrow neutrophils were not mature enough to be activated to degranulate. It is known that neutrophils must undergo a series of priming steps in order to be able to become fully activated (Yao *et al.* 2015; Miralda *et al.* 2017; Potera *et al.* 2016; Bhattacharya *et al.* 2015), and this could explain why this not a suitable experimental model to investigate neutrophil activation in the lung in the context of an RSV infection.

Together these data demonstrate that neutrophil recruitment and activation in the lung are independently regulated by the triggering of PRRs which signal through the adaptor proteins MyD88/TRIF and MAVS, respectively. To our knowledge, this is the first study to demonstrate that biologically independent PRR signalling pathways must collaborate to ensure neutrophil recruitment and activation occur during a respiratory viral infection (Kirsebom *et al.* 2019). Clinical studies of infants with severe RSV induced bronchiolitis suggest neutrophils are likely drivers of disease severity (McNamara 2003; Everard *et al.* 1994; Emboriadou *et al.* 2007;

Marguet *et al.* 2008), however it is not known whether neutrophils can also be beneficial as part of the host immune response by contributing to viral control. Furthermore, the mechanisms by which neutrophils may drive severity during RSV infection are also not known. Following on from this study, the next step was to investigate how neutrophil recruitment and activation influences disease severity and outcome during RSV infection of mice.

5.2 The role of neutrophils in RSV infection

5.2.1 Introduction

Although neutrophils are highly abundant in the airways of children with severe RSV disease (McNamara 2003; Emboriadou *et al.* 2007; Abu-Harb *et al.* 1999), it is not known whether they contribute to viral control or whether they cause disease. It is well established that the host immune response is a determinant of disease severity during RSV infection (Openshaw *et al.* 2017) but the specific contribution of neutrophils to this is not known. Having determined the innate PRR signalling pathways which regulate neutrophil recruitment and activation in the lung, the next step was to investigate the role of neutrophils during RSV infection. This included investigating whether neutrophils benefit the host by contributing to the control of viral replication in the lung, and whether neutrophil recruitment and activation in the lung contributes to disease severity.

The role of neutrophils has been better characterised during bacterial and fungal infections than during viral infections (Galani and Andreakos 2015). The effector mechanisms by which neutrophils combat bacterial and fungal pathogens include phagocytosis, activation and degranulation, oxidative burst and by the secretion of their DNA in the form of NETs (Kolaczkowska and Kubes 2013; Rørvig *et al.* 2013; Brinkmann *et al.* 2004). Although neutrophils are recruited to the lungs during many respiratory viral infections, it is less clear how their recruitment may contribute to viral clearance as the intracellular nature of viruses make them inherently less susceptible to the extracellular defence arsenal of neutrophils (Galani and Andreakos 2015).

In this chapter, the data presented are adapted from two recently submitted articles (Kirsebom *et al.,* in review and Habibi, Thwaites *et al.,* in review). In brief, antibody mediated neutrophil depletion was used to investigate how a lack of neutrophils influences the early pro-inflammatory environment in the lungs, the control of viral replication and disease severity as measured by weight loss. Mice were also treated with rCXCL1 at different time points during RSV infection to heighten lung neutrophilia and to investigate the impact of this on disease severity. Finally, mice were pre-treated with rCXCL1 and then infected with RSV to investigate whether the presence of neutrophils in the lung at the time of RSV infection has an impact on disease severity.

5.2.2 Neutrophils are not required for the induction of a pro-inflammatory environment early in the lungs following RSV infection

Neutrophils were depleted using α-Ly6G on day -1 and mice were then infected with RSV i.n. on day 0 to investigate how neutrophils influence the early pro-inflammatory environment in the lungs during RSV infection (Fig. 5.18a). Neutrophil depleted, RSV infected mice were compared to isotype antibody control treated, RSV infected mice and untreated RSV infected mice (Fig. 5.18). The composition of cells in the blood and lungs was investigated at 18 h p.i. (Fig. 5.18), as this is when neutrophil recruitment and activation peaks in the lung during RSV infection (Fig. 5.1). A previously published dosing regime was used to deplete neutrophils (Akthar *et al.* 2015; Lim *et al.* 2015; Tate *et al.* 2008; Peiró *et al.* 2018) and it had been confirmed in earlier work that the timing and dose was sufficient to completely remove airway neutrophils at 18 h post RSV infection, as quantified by differential counts on H&E stained cytospin slides (Fig. 5.7a). This regime was also sufficient to remove neutrophils from the blood (Fig. 5.18b) and completely block neutrophil recruitment to the lung 18 h post RSV infection (Fig. 5.18c), as assessed by flow cytometry. As only one clone of α-Ly6G exists, neutrophils cannot be detected by staining for Ly6G during α-Ly6G-mediated neutrophil depletion. As such, an alternative gating strategy was used to quantify neutrophils in these experiments (Fig. 4.1 for gating strategy). As expected, there was a slight increase in the frequency of monocytes observed in the blood following neutrophil depletion (Fig. 5.18b). There was also an increase in both the frequency and total number of monocytes observed in the lungs of α-Ly6G treated, RSV infected mice as compared to isotype control treated mice (Fig. 5.18c). This suggests that neutrophil depletion using α-Ly6G may have an effect on the recruitment of inflammatory monocytes to the lung during RSV infection.

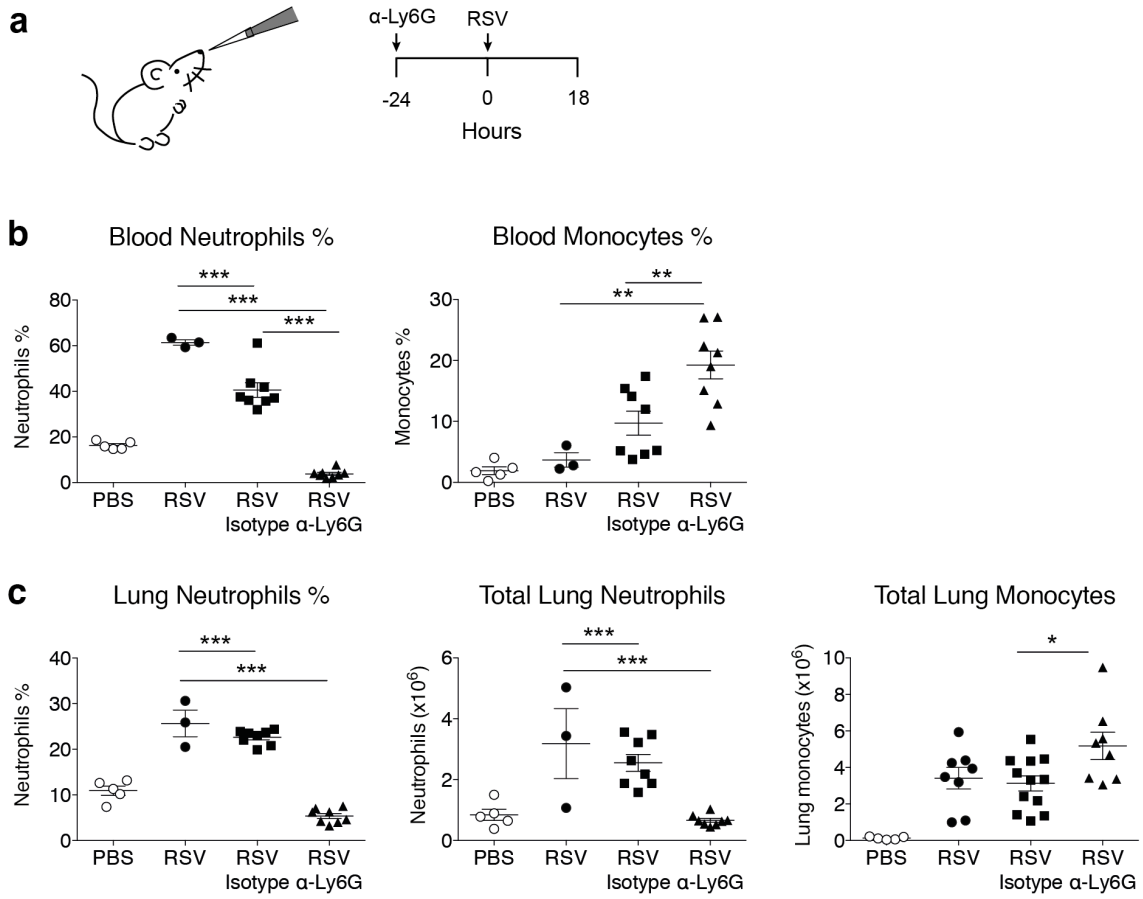

Figure 5.18. Antibody mediated (α-Ly6G) neutrophil depletion does not impair monocyte recruitment 18 h post RSV infection. a. Wt mice were given 200 µg i.n. and 500 µg i.p. α-Ly6G or isotype control antibody day -1 and were mock (PBS) or RSV infected for 18 h. Immune cells were analysed by flow cytometry (Fig. 4.1 for gating strategy). **b.** Frequencies of neutrophils and monocytes in the blood. **c.** Frequency and total number of neutrophils (not gated on Ly6G; see Fig 4.1 for gating strategy) and frequency of monocytes in the lung. Data are presented as the mean ±SEM from 5 (PBS) or 8-12 (RSV) individual mice pooled from two or three independent experiments. Each symbol represents an individual mouse. Statistical significance of differences was determined by one-way ANOVA with Tukey's post hoc test. Only the statistical significances between RSV infected groups are shown. * $p \leq 0.05$, ** $p \leq 0.01$, *** $p \leq 0.001$.

Next, the production of pro-inflammatory mediators and cytokines was examined in the lung following RSV infection of neutrophil depleted mice (Fig. 5.19). Neutrophil depletion did not affect the production of IFN-α, IL-6, TNF-α or IL-1β in the airways during RSV infection; there was no difference in the concentration of these mediators detected in the airways between isotype control treated and α-Ly6G treated, RSV infected mice (Fig. 5.19a-b). However, there was a difference between untreated and isotype control treated, RSV infected mice; isotype control treated mice produced less IFN-α and IL-6 than untreated mice during RSV infection (Fig. 5.19a). Neutrophil depleted mice had significantly higher concentrations of the neutrophil chemoattractant CXCL1 in the airways than isotype control treated, RSV infected mice (Fig.

5.19b). Serum albumin was also measured in the airways as a readout of lung damage at 18 h p.i. (Fig. 5.19c). Significantly less albumin was detected in the airways of α-Ly6G treated mice during RSV infection than was detected in untreated, RSV infected mice (Fig. 5.19c). However, there was no difference in the concentration of albumin detected in the airways of α-Ly6G treated mice as compared to isotype control treated mice during RSV infection (Fig. 5.19c). As a second readout of lung damage, the concentration of histone-bound DNA was also measured in the airways during neutrophil depletion of RSV infected mice (Fig. 5.19c). Interestingly, α-Ly6G treated mice had significantly lower levels of histone-bound DNA than both untreated and isotype control treated mice during RSV infection (Fig. 5.19c). Isotype control treated mice also had less detectable histone-bound DNA in the airways than untreated RSV infected mice at 18 h p.i. (Fig. 5.19c).

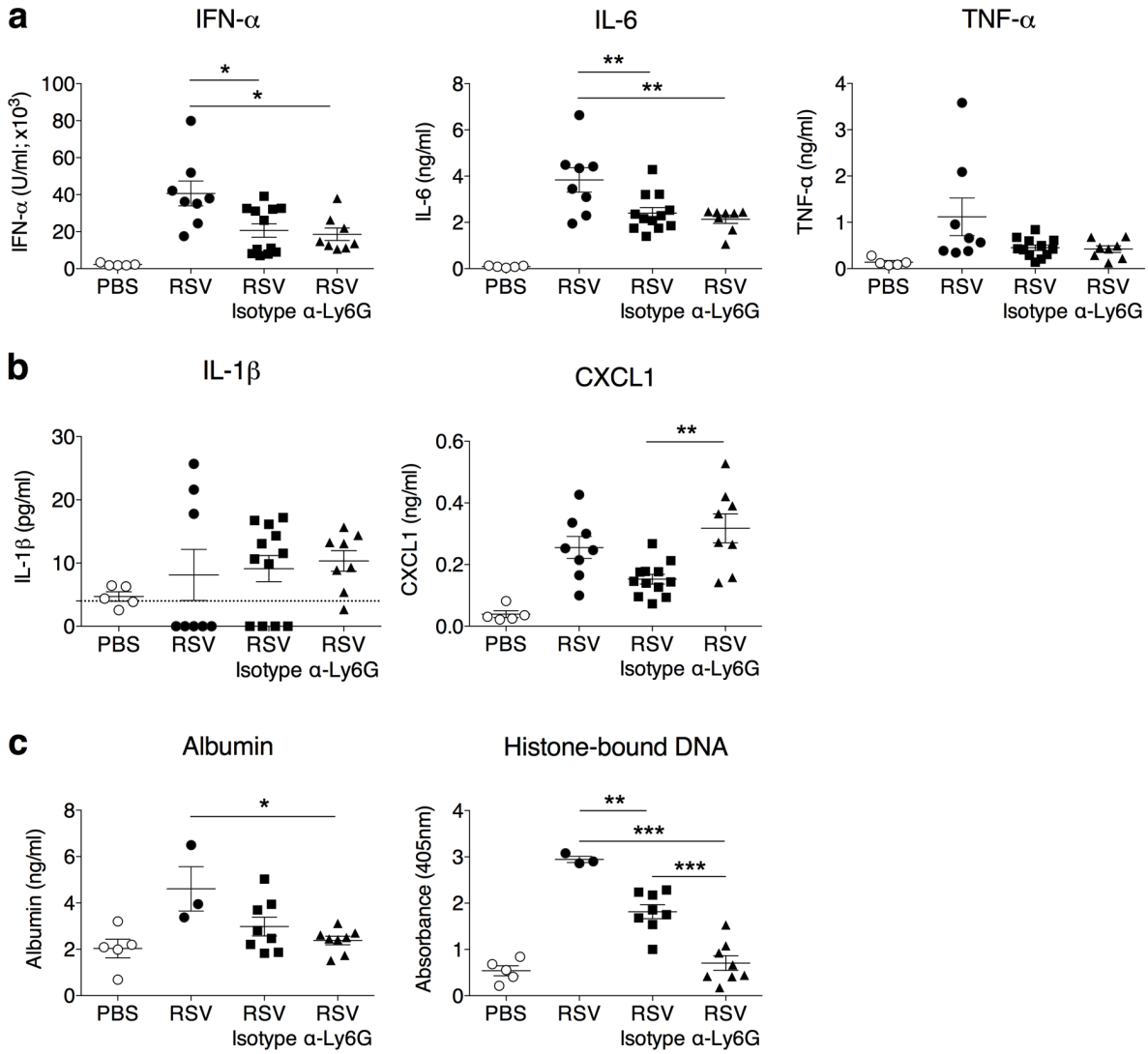

Figure 5.19. Neutrophils do not contribute to the induction of a pro-inflammatory immune environment in the lungs 18 h post RSV infection. To deplete neutrophils, wt mice were given 200 µg i.n. and 500 µg i.p. α-Ly6G or isotype control antibody day -1. Mice were mock (PBS) or RSV infected for 18 h. **a.** IFN-α, IL-6 and TNF-α were quantified in the BAL by ELISA. **b.** IL-1β and CXCL1 were quantified in the BAL by ELISA. **c.** Serum albumin and histone-bound DNA were quantified in the BAL by ELISA. Data from **a** and **b** are presented as the mean ±SEM from 5 (PBS) or 3-12 (RSV) individual mice pooled from two or three independent experiments. Data from **c** are presented as the mean ±SEM from 5 (PBS) or 3-8 (RSV) individual mice pooled from one or two independent experiments. Each symbol represents an individual mouse. Statistical significance of differences was determined by one-way ANOVA with Tukey's post hoc test. Only the statistical significances between RSV infected groups are shown. * $p \leq 0.05$, ** $p \leq 0.01$, *** $p \leq 0.001$.

The gene expression levels of numerous inflammatory immune mediators were also investigated at 18 h p.i. during neutrophil depletion of RSV infected mice (Fig. 5.20). *Cxcl1* was upregulated in α-Ly6G treated mice during RSV infection as compared to isotype control treated RSV infected mice (Fig. 5.20a). There was no difference in the gene expression levels of *Cxcl2*, *Cxcl12*, *Il1a* or *Il1b* (Fig. 5.20a-b). The expression level of mediators associated with

alarmins and tissue repair was also investigated during neutrophil depletion of RSV infected mice (Fig. 5.20c). There was also no significant difference in the expression level of *Il33*, *Areg* (Amphiregulin) or *Ptgs2* (COX-2) in the lungs between untreated, isotype control treated or α-Ly6G treated mice during RSV infection (Fig. 5.20c). Together these data demonstrate that neutrophils are dispensable for the induction of a pro-inflammatory environment in the lungs early during RSV infection.

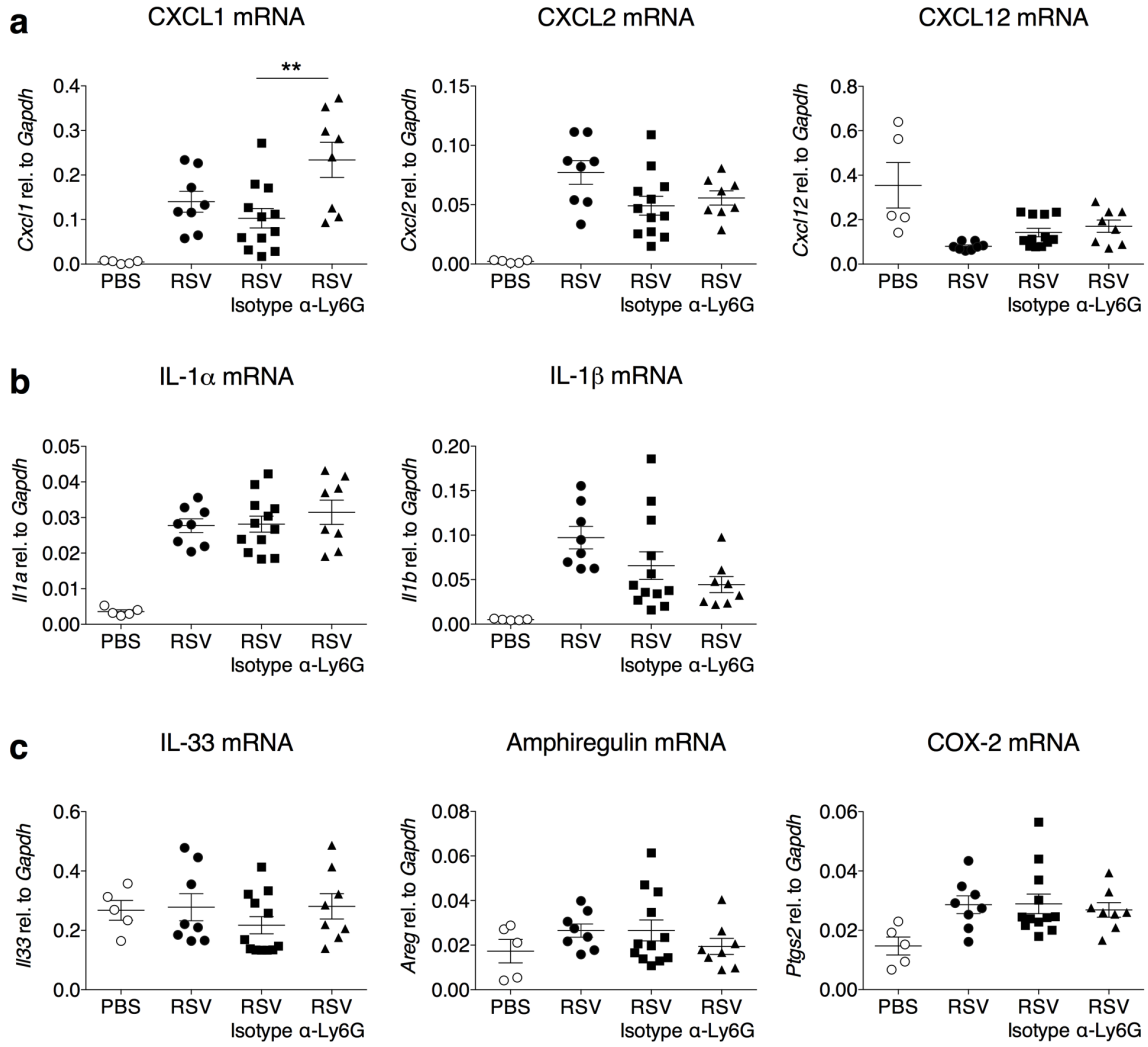

Figure 5.20. Neutrophils do not influence the gene expression of pro-inflammatory mediators in the lungs 18 h post RSV infection. To deplete neutrophils, wt mice were given 200 µg i.n. and 500 µg i.p. α-Ly6G or isotype control antibody day -1. Mice were mock (PBS) or RSV infected for 18 h. **a-c.** *Cxcl1, Cxcl2*, *Cxcl12, Il1a, Il1b, Il33, Areg* and *Ptgs2* mRNA was quantified in the lung by RT-qPCR and the relative expression ($2^{-\Delta CT}$) is expressed normalised to *Gapdh.* Data are presented as the mean±SEM from 5 (PBS) or 8-12 (RSV) individual mice pooled from two or three independent experiments. Each symbol represents an individual mouse. Statistical significance of differences was determined by one-way ANOVA with Tukey's post hoc test. Only the statistical significances between RSV infected groups are shown. ** $p \leq 0.01$.

5.2.3 Neutrophils do not restrict viral replication, nor do they contribute to disease severity as measured by weight loss during RSV infection

The primary aim of the immune response is to inhibit pathogen replication and therefore limit disease in the host. Neutrophils are classically considered as immediately responders in many bacterial and fungal infection where, as the first line of defence, they immediately exert their effector functions to restrict pathogen spread (Kolaczkowska and Kubes 2013). Much less is understood about how well neutrophils restrict the replication and spread of viruses (Galani and Andreakos 2015). It is particularly unclear how neutrophils would facilitate the restriction of RSV replication as RSV is able to infect new cells by forming syncytia, preventing exposure to the extracellular environment (Collins and Graham 2008; Shigeta *et al.* 1968).

Neutrophil depletion was used to investigate whether neutrophils have a beneficial role during the immune response to RSV by restricting viral replication during the infection (Fig. 5.21). In these experiments, an alternative neutrophil depletion regime was used to deplete neutrophils for up to 4 days p.i. (Peiró *et al.* 2018). In this regime, neutrophils were depleted every other day, starting from day -1, with 150 µg α-Ly6G i.p. (Peiró *et al.* 2018). We confirmed that this dose was also sufficient to block neutrophil recruitment during RSV infection; when mice were treated with 100 µg α-Ly6G i.p. on day -1 pre RSV infection lung neutrophils were not detected at 18 h p.i. (Fig. 5.21a), the time at which the next dose was given during when neutrophils were depleted for multiple days. To investigate whether a lack of neutrophil recruitment has an effect on the control of virus in the lungs during RSV infection, neutrophils were depleted every other day starting from day -1 (Fig. 5.21b). Viral load was assessed in the lungs by RT-qPCR at 18 h p.i. as well as on day 4 p.i. as this is when viral load peaks in the lung in the mouse model of RSV infection (Goritzka *et al.* 2014) (Fig. 5.21c). There was no difference in the viral load as measured by the copy number of RSV L gene detected in the lungs of α-Ly6G treated mice as compared to isotype control treated mice during RSV infection at either 18 h or on day 4 p.i. (Fig. 5.21c). RT-qPCR is extremely sensitive and does not discriminate between replication competent viral particles and damaged viral genomes which are replication incompetent. Therefore, viral load was also quantified on day 4 p.i. by immunoplaque assay (Fig. 5.21d). There was also no difference in the number of replication-competent RSV particles detected in the lungs of α-Ly6G treated mice as compared to isotype control treated mice during the peak of viral load on day 4 p.i. (Fig. 5.21d).

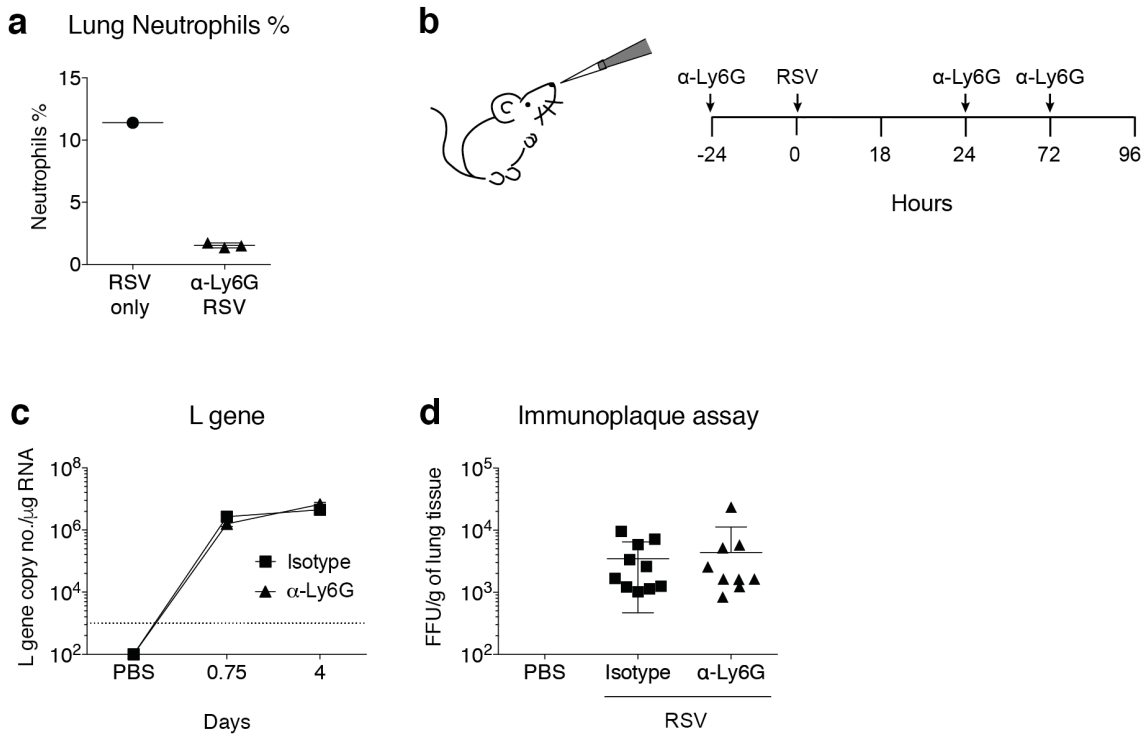

Figure 5.21. Neutrophils do not restrict viral replication during RSV infection *in vivo*. a. To deplete neutrophils, wt mice were given 100 µg i.p. α-Ly6G or isotype control antibody on day -1. Mice were infected with RSV for 18 h. Lung neutrophils were quantified by flow cytometry (not gated on Ly6G; see Fig. 4.1 for gating strategy). **b.** C57BL/6 or wt mice were mock (PBS) or RSV infected for 18 h or 4 days. To deplete neutrophils up to 18 h, mice were given 200 µg i.n. and 500 µg i.p. α-Ly6G or isotype control antibody day -1. To deplete neutrophils up to day 4, mice were given 150 µg i.p. α-Ly6G or isotype control antibody on day -1, day 1 and day 3 p.i.. **c.** RSV L gene copy number was quantified in lung tissue by RT-qPCR. Copy numbers were determined using a plasmid standard and the results were normalised to *Gapdh* levels. **d.** Infectious viral particles in the lung on day 4 were quantified by immunoplaque assay. Data from **a** are presented as the mean ±SEM from 1 (RSV) or 3 (α-Ly6G) individual mice from one experiment. Data from **c** are presented as the mean ±SEM from 5 (PBS and RSV day 4) or 8 (RSV 18 h) individual mice from one (day 4) or two (18 h) pooled independent experiments. Statistical significance of differences was determined by two-way ANOVA with Bonferroni's post hoc test. Data from **d** are presented as the mean ±SEM of 9 (PBS) or 10 (RSV isotype/α-Ly6G) individual mice from pooled from two independent experiments. Each symbol represents an individual mouse. Statistical significance of differences was determined by one-way ANOVA with Tukey's post hoc test.

Neutrophil recruitment and activation in the lung did not appear to benefit the host during RSV infection by preventing viral replication, so antibody mediated neutrophil depletion was used to assess whether neutrophils contribute to disease severity as measured by weight loss (Fig. 5.22 and Fig. 5.23). Weight loss is considered to be a good readout of disease severity in the murine model of RSV disease (Graham *et al.* 1991; Cannon *et al.* 1988). Initially, the early recruitment of neutrophils characterised in chapter 5.1 was depleted during the infection and weight loss was measured to day 9 p.i. (Fig 5.22). As previously described, mice were treated with α-Ly6G on day -1 pre RSV infection and on day 1 p.i. (Fig. 5.22a). There was no difference

in the weight loss of untreated, isotype control treated or α-Ly6G treated C57BL/6 mice during RSV infection (Fig. 5.22b). The same experiment was repeated using BALB/c mice which are more susceptible to severe RSV disease (Jessen *et al.* 2011) (Fig. 5.22c). Infection with the same number of RSV viral particles (10^6) lead to more severe weight loss in BALB/c mice as compared to C57BL/6 mice, which started from day 5 p.i. and peaked at day 7 p.i. (Fig. 5.22b). However, neutrophil depletion did not affect the timing or severity of disease as measured by weight loss in BALB/c mice (Fig. 5.22c).

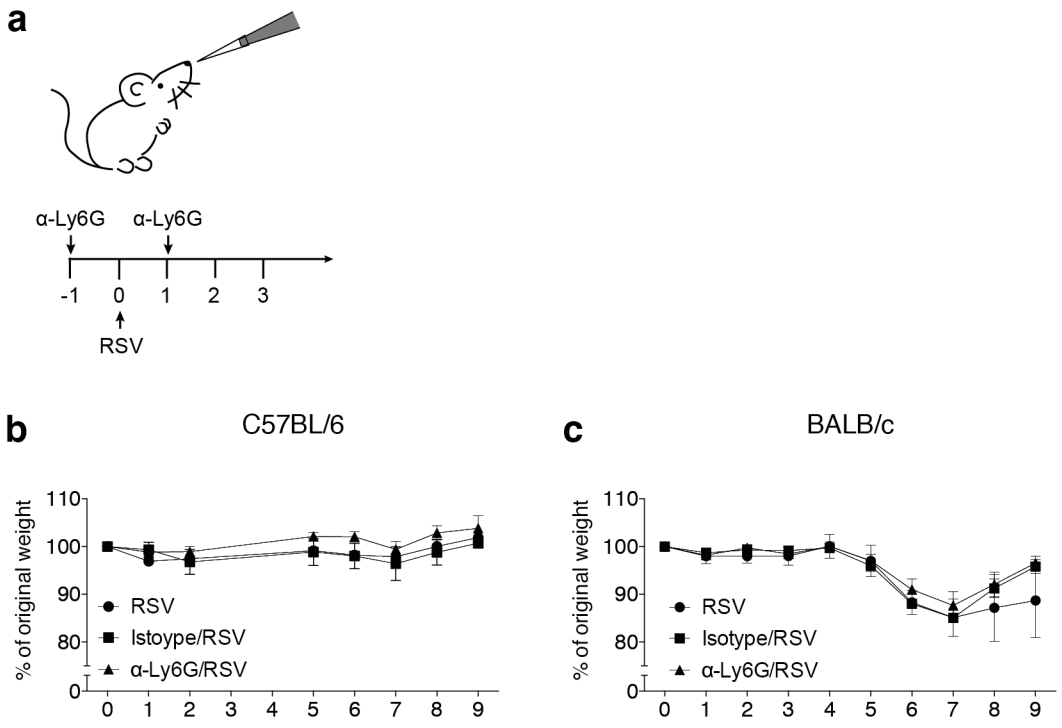

Figure 5.22. Neutrophils do not influence the weight loss of either C57BL/6 mice or BALB/c mice during RSV infection. a. C57BL/6 and BALB/c mice were mock (PBS) or RSV infected. To deplete neutrophils, 500 µg i.p. and 200 µg i.n. α-Ly6G or isotype control antibody was administered on day -1 and day 1 p.i.. **b-c.** Weight loss as percentage of original weight during RSV infection in C57BL/6 and BALB/c mice. Data are presented as the mean±SEM from 2 (RSV only) or 4 (C57BL/6), or 3-5 (BALB/c) individual mice from one experiment. Statistical significance of differences between α-Ly6G or isotype control treated mice was determined by two-way ANOVA with Bonferroni's post hoc test.

Although neutrophil recruitment to the lung primarily occurs early during RSV infection of mice, lung neutrophils are also detected in the lungs from days 5-7 p.i. when they are recruited along with the major influx of T cells during the adaptive immune response (Tregoning *et al.* 2008). To fully confirm that neither neutrophils recruited during the innate immune response nor during the adaptive immune response contribute to weight loss during RSV infection, neutrophils were depleted in C57BL/6 mice from day -1 pre-infection and then on every second day throughout the infection in a total of 5 doses (Fig. 5.23a). There was no difference in the timing or severity of weight loss between α-Ly6G treated mice and isotype control treated mice during RSV infection when neutrophils were removed throughout the entire infection (Fig. 5.23b). However, untreated mice lost slightly more weight on days 7 and 8 p.i. than either α-Ly6G treated or isotype control treated RSV infected mice (Fig. 5.23b). It is known that weight loss on days 5-8 is largely driven by the recruitment of $CD8^+$ T cells during the adaptive immune response to RSV (Graham *et al.* 1991; Cannon *et al.* 1988). Therefore, the recruitment of T cells to the lung was investigated on day 8 p.i. by flow cytometry following neutrophil depletion using α-Ly6G (Fig. 5.23c and Fig.5.23d; Fig. 4.3 for gating strategy). There was no difference in the frequency or number of $CD4^+$ or $CD8^+$ T cells in the lung on day 8 p.i. between α-Ly6G treated mice and isotype control treated mice (Fig. 5.23c-d). Furthermore, there was no difference in the frequency or number of RSV M peptide tetramer$^+$ $CD8^+$ T cells in the lung during neutrophil depletion. Untreated, RSV infected mice had a slightly higher frequency of $CD8^+$ T cells in the lungs as compared to both isotype control treated mice and α-Ly6G treated mice, but this difference was not detected in the total numbers of lung $CD8^+$ T cells (Fig. 5.23c and Fig.5.23d). Together these experiments demonstrate that the initial recruitment and activation of neutrophils in the lung during RSV infection does not induce weight loss in adult C57BL/6 or BALB/c mice (Fig. 5.22). Furthermore, neutrophil depletion did not affect the total number of $CD4^+$, $CD8^+$ or antigen-specific $CD8^+$ T cells in lung during the adaptive immune response to RSV (Fig. 5.23c-d).

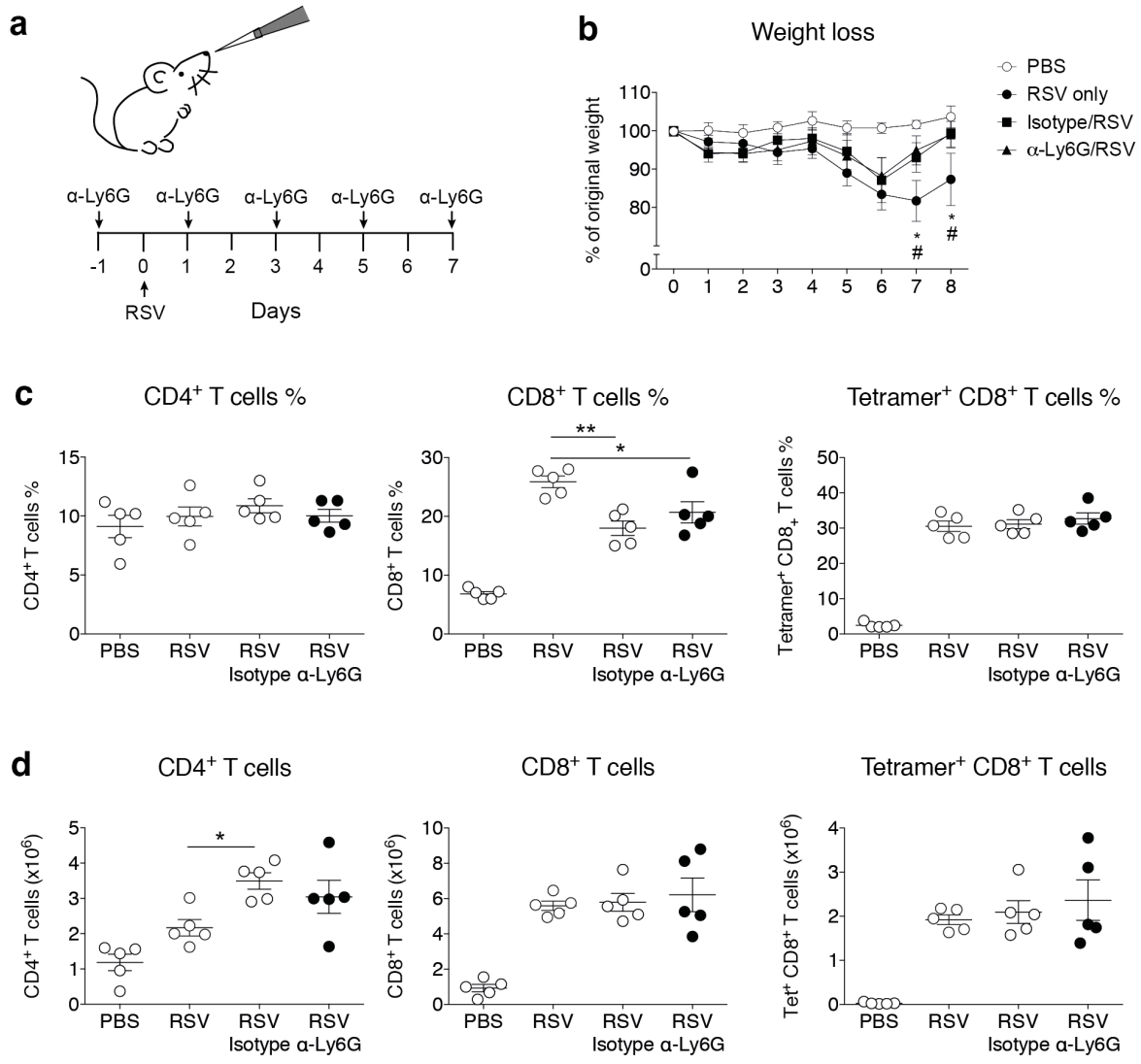

Figure 5.23. Neutrophils do not influence the recruitment of T cells to the lung on day 8 post RSV infection. **a.** C57BL/6 mice were mock (PBS) or RSV infected. To deplete neutrophils, 150 µg i.p. α-Ly6G or isotype control antibody was administered on day -1 and on every second day throughout the infection. Immune cells were analysed by flow cytometry (Fig. 4.3 for gating strategy). **b.** Weight loss shown as the percentage of original weight. Frequencies (**c**) and total numbers (**d**) of CD45$^+$ CD19$^-$ CD3$^+$ CD4$^+$ and CD45$^+$ CD19$^-$ CD3$^+$ CD8$^+$ T cells day 8 p.i.. RSV-specific CD8$^+$ T cells were detected by staining with $M_{187–195}$ tetramer. Each symbol represents an individual mouse. Data are presented as the mean ±SEM of 5 individual mice per group from one experiment. Statistical significance of differences was determined by one-way ANOVA with Tukey's post hoc test. Only the statistical significances between RSV infected groups are shown. * $p \leq 0.05$, ** $p \leq 0.01$.

5.2.4 Deficiency in MAVS signalling results in a higher viral load and in increased weight loss during RSV infection

Antibody mediated cell depletion is a powerful tool to investigate the role of specific cell types *in vivo*, however this approach has certain limitations. Earlier in this project it was observed that while *Myd88/Trif*$^{-/-}$ mice cannot recruit neutrophils to the lung, *Mavs*$^{-/-}$ mice can recruit neutrophils to the lung but they are not able to become activated during RSV infection (chapter 5.1). Therefore, these mice were used to further investigate viral control and disease severity in the absence of these signalling pathways during RSV infection (Fig. 5.24).

Myd88/Trif$^{-/-}$ mice, which do not recruit neutrophils to the lung during RSV infection, had the same viral load as wt mice at 18 h, day 4 and day 8 p.i. as measured by the copy numbers of RSV L gene in the lungs by RT-qPCR (Fig. 5.24a). *Mavs*$^{-/-}$ mice had a higher viral load at both 18 h p.i. and on day 4 p.i. than both wt and *Myd88/Trif*$^{-/-}$ mice (Fig. 5.24a). There was a trend for a higher viral load in *Mavs*$^{-/-}$ mice on day 8 p.i., but this difference was not statistically significant. To assess disease severity in the absence of MyD88/TRIF and MAVS signalling, *Mavs*$^{-/-}$ and *Myd88/Trif*$^{-/-}$ mice were infected with RSV and weight loss was measured throughout the RSV infection (Fig. 5.24b). Wt mice initially lost some weight early on day 1 p.i. which they recovered by day 2 p.i., and then lost weight again later during the infection from day 6 p.i. with the peak of disease as measured by weight loss occurring on day 7 p.i. (Fig. 5.24b). *Mavs*$^{-/-}$ mice did not lose weight on the first day of the infection, unlike wt mice, but had more severe disease during the later stage of the RSV infection than wt mice losing more weight than wt mice on days 7 and 8 p.i. (Fig. 5.24b). *Myd88/Trif*$^{-/-}$ mice lost slightly more weight than wt mice on day 6 p.i., but the weight loss pattern was overall more similar to wt mice than to *Mavs*$^{-/-}$ mice; *Mavs*$^{-/-}$ mice had more severe disease and lost more weight than both wt and *Myd88/Trif*$^{-/-}$ mice (Fig. 5.24b). Together these data support the earlier findings and suggest that neutrophils do not contribute to viral control, nor do they drive weight loss during RSV infection.

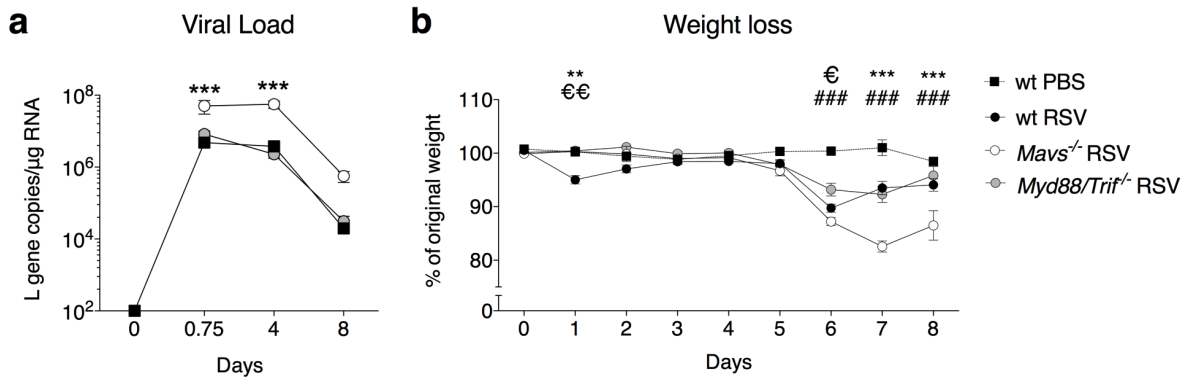

Figure 5.24. Signalling via MAVS is required for viral control and limitation of disease severity as measured by weight loss during RSV infection. Wt, *Mavs*$^{-/-}$ and *Myd88/Trif*$^{-/-}$ mice were mock (PBS) or RSV infected. **a.** RSV L gene copy number was quantified in lung tissue by RT-qPCR at 18 h p.i., and on day 4 and 8 post RSV infection. Copy numbers were determined using a plasmid standard and the results were normalised to *Gapdh* levels. **b.** Weight loss as percentage of original weight. Data from **a** are presented as mean±SEM of 5-10 individual mice pooled from one (day 8) or two (0, 18 h and day 4) individual experiments. Data from **b** are presented as mean±SEM of 6 (PBS) – 13 (RSV) infected mice pooled from two independent experiments. Weight loss on days 1, 2 and 8 are from one independent experiment only (3-7 mice per group). Statistical significance of differences was determined by two-way ANOVA with Tukey's post hoc test. For **a**, only RSV infected mice were compared. For **b,** * denotes differences between wt and *Mavs*$^{-/-}$ mice, € denotes differences between wt and *Myd88/Trif*$^{-/-}$ mice, # denotes differences between *Mavs*$^{-/-}$ and *Myd88/Trif*$^{-/-}$ mice. * $p \leq 0.05$, ** $p \leq 0.01$, *** $p \leq 0.001$.

5.2.5 Heightening lung neutrophilia with rCXCL1 does not increase disease severity as measured by weight loss of RSV infection

RSV infection of mice induces 50% airway neutrophilia early during the infection (Fig. 5.1). However, severe disease of infants hospitalised with RSV induced bronchiolitis is characterised by >90% airway neutrophilia (McNamara 2003). We postulated that perhaps the reason neutrophil depletion had no effect on disease severity as measured by weight loss was because the level of neutrophilia induced by RSV infection in mice does not accurately replicate the severity of neutrophilia as observed in severely ill, hospitalised infants. In order to better model severe RSV disease of infants in mice, lung neutrophilia was heightened early during RSV infection by treating mice with rCXCL1 (Fig. 5.25a). RSV infected wt mice were treated with 10 µg rCXCL1 i.n. 6 h p.i. and the composition of the airways was analysed 12 h later at 18 h post RSV infection (Fig. 5.25b). This dose of rCXCL1 was sufficient to induce >80% airway neutrophil recruitment in the context of an RSV infection (Fig. 5.25). Next, mice were treated with rCXCL1 6 h p.i. and weight loss was measured as a readout of disease severity (Fig. 5.25c). Increasing airway neutrophilia early during RSV infection did not influence weight lost by mice either early or later during RSV infection; there was no difference

at any time point in the weight loss between RSV/PBS treated mice and RSV/CXCL1 treated mice (Fig. 5.25c).

As well as the severity of airway neutrophilia, the kinetics of neutrophil recruitment differs between RSV infection of mice and humans. In mice, neutrophil recruitment peaks early during RSV infection (Fig. 5.1). Although neutrophils are also recruited later alongside T cells during the peak of disease (Tregoning *et al.* 2008) fewer are recruited than early at 18 h p.i. (Fig. 5.1). However, infants hospitalised with RSV typically have very high airway neutrophilia at the peak of disease severity (McNamara 2003). In order to adapt the mouse model to better replicate the timing of airway neutrophilia observed in RSV infected infants, mice were infected with RSV i.n. and then treated with 5 μg rCXCL1 i.n. on days 4, 5, 6 and 7 p.i. as this is when the peak of disease severity, as measured by weight loss, is observed in the mouse model of RSV (Fig. 5.25d). This, however, also did not exacerbate disease severity; there was no difference in the weight loss of RSV infected mice or RSV infected mice treated with rCXCL1 at any time point measured (Fig. 5.25e).

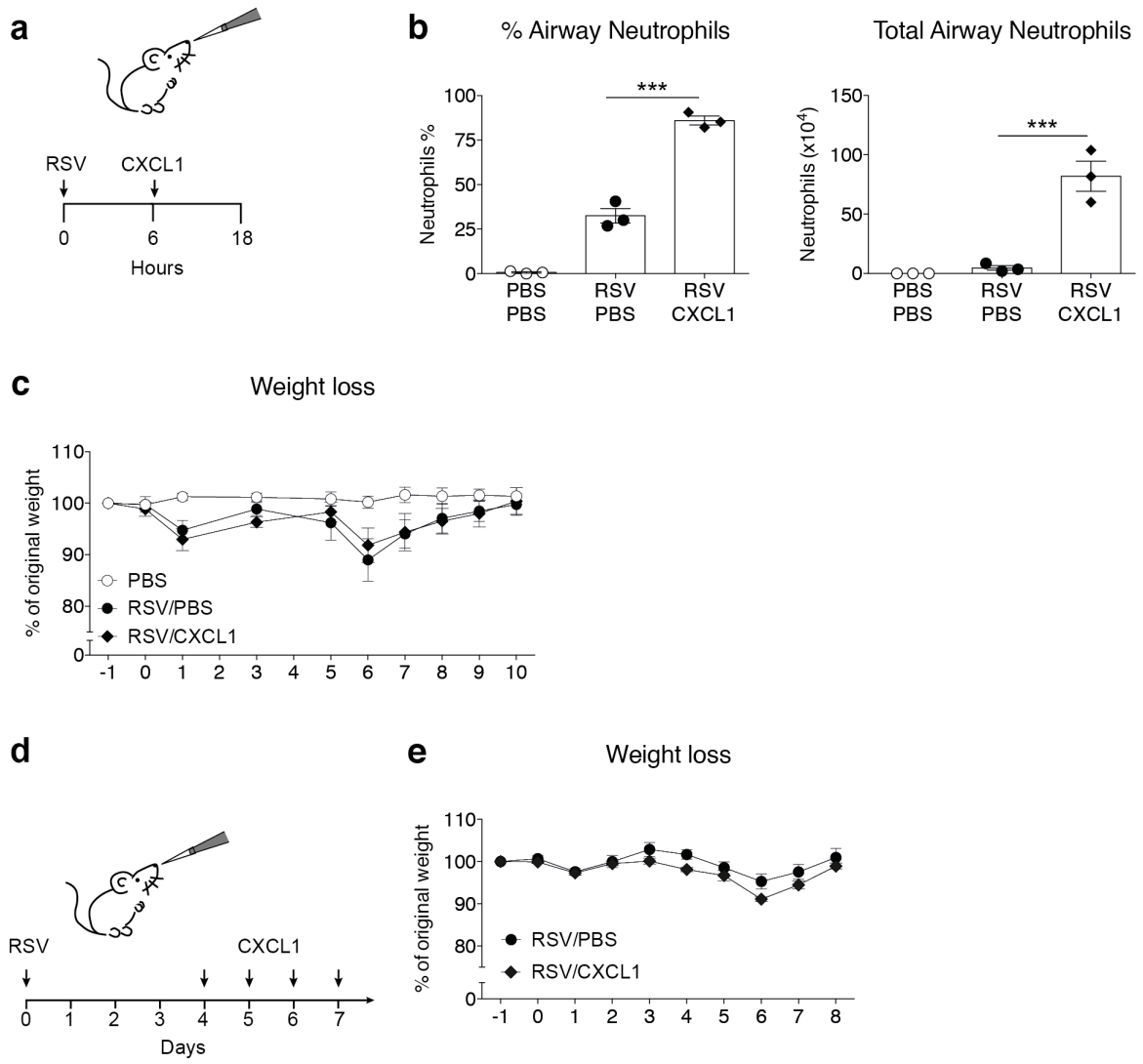

Figure 5.25. Augmentation of lung neutrophilia during RSV infection does not affect weight loss. C57BL/6 or wt mice were mock (PBS) or RSV infected. a. Lung neutrophilia was augmented by treatment with 10 µg CXCL1 i.n. 6 h p.i.. **b.** Frequency and total number of airway neutrophils 18 h p.i. (Fig. 4.1 for gating strategy). **c.** Weight loss as percentage of original weight. **d.** Lung neutrophilia was augmented by treatment with 5 µg CXCL1 i.n. day 4, 5, 6 and 7 p.i. **e.** Weight loss as percentage of original weight. Data from **b** are presented as mean±SEM of 3 individual mice per group from one independent experiment. Each symbol represents an individual mouse. Data from **c** are presented as mean±SEM of 4 (PBS and RSV/CXCL1) and 7 (RSV/PBS) individual mice from one experiment. Data from **e** are presented as mean±SEM of 4 (RSV/CXCL1) or 5 (RSV/PBS) individual mice from one experiment. For **b**, statistical significance of differences was determined by one-way ANOVA with Tukey's post hoc test. For **c** and **e,** statistical significance of differences was determined by two-way ANOVA with Bonferroni's post hoc test. Only the statistical significances between RSV infected groups are shown. *** $p \leq 0.001$.

5.2.6 Lung neutrophilia pre-RSV infection heightens $CD8^+$ T cell driven weight loss later during RSV infection

In vivo models of infection allow mechanistic studies, which are impossible to conduct in humans. Studying severe RSV infection of humans is especially challenging as the majority of severe cases occur in infants which are <2 years of age (Shi *et al.* 2017; Hall *et al.* 2009; Nair *et al.* 2010). Establishing when an individual became infected can be challenging and therefore it is difficult to know how advanced disease is when the infant presents at a GP clinic or hospital. Furthermore, it is extremely challenging to take clinical samples from the respiratory tract of infants which limits the quality of the data used for observational studies. A third approach to studying infections involves human challenge - exposing healthy volunteers to pathogens and systematically sampling throughout to gain a better insight into the kinetics of disease progression and resolution. While this approach also has limitations, strengths of this approach include the ability to take samples at defined time points before and after inoculation. This can facilitate an understanding of the kinetics of the immune response in the natural host.

Human challenge studies by Chris Chiu and Peter Openshaw's research teams, also in the Section of Respiratory Infections, Imperial College London, found that airway neutrophilia pre-RSV infection may heighten an individual's susceptibility to RSV disease (Habibi, Thwaites *et al.,* in review). In these studies, healthy adult volunteers were inoculated with the RSV strain Memphis 37. The nose was sampled prior to RSV inoculation as well as repeatedly throughout the infection. Of the inoculated individuals, some (n=23) went on to develop symptomatic RSV infections and were confirmed to be PCR positive for RSV (termed the "Cold" group). Other individuals (n=25) had no symptoms of a respiratory tract infection and were PCR negative for RSV (termed "No Cold" group), despite being inoculated in the same manner as the Cold group. Nasal tissue samples were taken at baseline (up to two weeks pre-inoculation). Gene expression differences between the Cold and No Cold groups were analysed by RNA sequencing. Of the differentially expressed genes (DEGs), 91% were upregulated in the Cold group as compared to the No Cold group. The gene clusters which were most significantly enriched in the Cold group versus the No Cold group involved genes relating to neutrophil immunity and activation. Notably, 16S sequencing revealed there were no differences in the bacterial load, diversity or composition in nasal samples between the Cold and No Cold groups at baseline suggesting that the differences observed were not due to underlying bacterial infections in the volunteers in the Cold group. Together, these findings suggested that airway

neutrophilia at baseline heightened the susceptibility of healthy adult volunteers to RSV disease (data not shown; Habibi, Thwaites *et al.,* in review).

To investigate the immunological mechanism behind the observation that neutrophilia in the respiratory tract pre-infection might enhance RSV disease susceptibility, we first tested whether this observation could be modelled in the murine model of RSV infection (Fig. 5.26 – Fig. 5.27). First, mice were treated with mock (PBS) or 10 µg rCXCL1 i.n. (Fig. 5.26a) and the cellular composition of the lungs was investigated 12 h later by flow cytometry (Fig. 5.26; Fig. 4.3 for gating strategy). Treatment of mice with 10 µg rCXCL1 for 12 h did not affect the overall number of AMs in the airways or in the lungs (Fig. 5.26b), nor did it affect the number of lung monocytes (Fig. 5.26c). This dose of rCXCL1 did however induce a high recruitment of neutrophils to the respiratory tract; neutrophils were abundant in both the airways and in the lung following treatment with rCXCL1 (Fig. 5.26d). Neutrophils recruited to the airways with rCXCL1 in the absence of RSV were activated to an extent as there were significantly higher levels of MMP-9, MPO and NE detected in the airways of rCXCL1 treated mice than in mock (PBS) treated mice after 12 h (Fig. 5.26e).

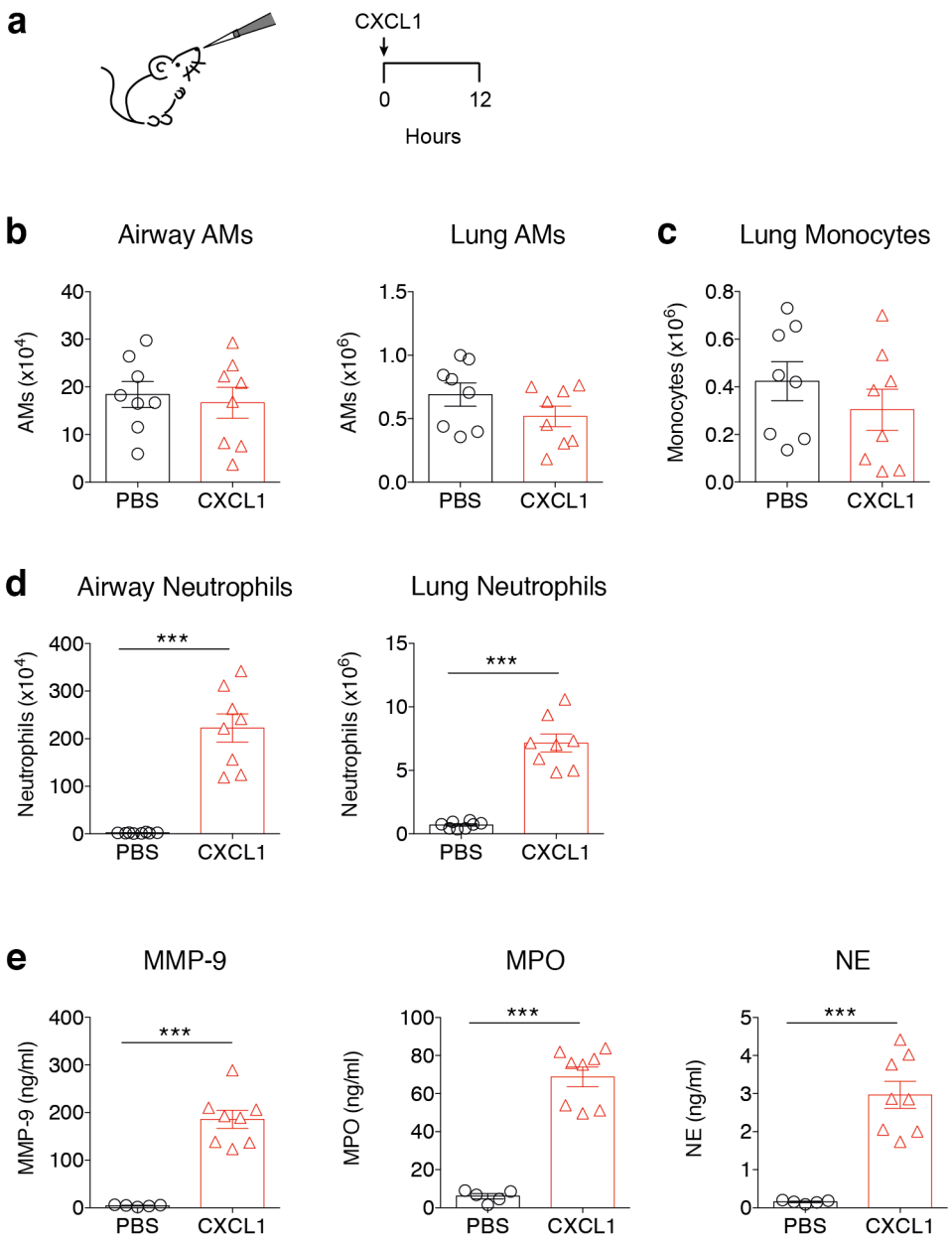

Figure 5.26. 10 µg rCXCL1 drives neutrophil recruitment to the lung at 12 h post instillation and does not influence the number of AMs or monocytes in the lungs. a. C57BL/6 mice were treated with mock (PBS) or 10 µg rCXCL1 i.n. and immune cells were analysed by flow cytometry 12 h post instillation (Fig. 4.1 for gating strategy). **b.** Total number of AMs in the airways and in the lung. **c.** Total number of monocytes in the lung. **d.** Total number of neutrophils in the airways and in the lung. **e.** MMP-9, MPO and NE were detected in the BAL by ELISA. Data are presented as mean±SEM of 5 - 8 individual mice per group from one (**e;** PBS/PBS) or two independent experiments. Statistical significance of differences was determined by unpaired, two-tailed Student's *t* test. *** $p \leq 0.001$.

To assess whether neutrophilia pre-infection influenced viral load and disease severity during RSV infection, mice were treated with mock (PBS) or rCXCL1 i.n. and then infected with mock (PBS) or RSV i.n. 12 h later (Fig. 5.27a). Treating mice with rCXCL1 pre-infection did not affect viral load as measured by quantification of RSV L gene in whole lung tissue by RT-qPCR on day 4 and day 8 p.i. (Fig. 5.27b). Interestingly however, this did influence disease severity as measured by weight loss (Fig. 5.27c). Mice which were treated with rCXCL1 prior to RSV infection, and therefore had airway neutrophilia upon exposure to the virus, lost significantly more weight than mock treated, RSV infected mice on days 5 – 8 p.i. (Fig. 5.27c). The observation that viral load was unchanged indicated that the heightened disease was not due to the virus but more likely due to host-driven immunopathology. Therefore, the cellular composition of the lungs was investigated on day 8 p.i. by flow cytometry during mock (PBS) and rCXCL1 pre-treatment of RSV infection (Fig. 5.28 and Fig. 5.29).

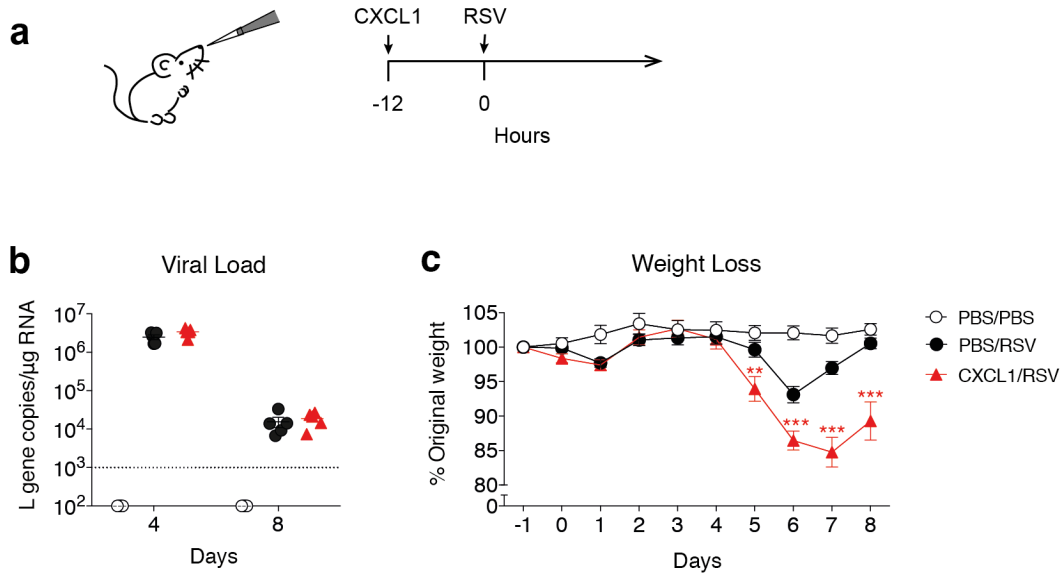

Figure 5.27. Treatment of mice with rCXCL1 prior to RSV infection heightens disease severity during the adaptive stage of the immune response, with no effect on viral load. a. C57BL/6 mice were treated with mock (PBS) or 10 µg rCXCL1 i.n. and after 12 h mice were infected with mock (PBS) or 7.5 x 10^5 FFU RSV. **b.** RSV L gene copy number was quantified on days 4 and 8 p.i. in lung tissue by RT-qPCR. Copy numbers were determined using a plasmid standard and the results were normalised to *Gapdh* levels. **c.** Weight loss as percentage of original weight. Data from **b** are presented as mean±SEM of 5 individual mice per group, representative of two independent experiments. Data from **c** are presented as mean±SEM of 10 (PBS/PBS) or 14-16 (RSV) individual mice pooled from 2 (PBS/PBS) or 3 (RSV) independent experiments. Statistical significance of differences in **b** was determined by one-way ANOVA with Tukey's post hoc test for each time point. Statistical significance of differences in **c** was determined by two-way ANOVA with Tukey's post hoc test. ** $p \leq 0.01$, *** $p \leq 0.001$.

On day 8 p.i. there was no difference in the frequency of lung neutrophils between mock treated mice and mice treated with rCXCL1 prior to RSV infection (Fig. 5.28a). However, the total number of neutrophils was slightly higher in the lungs of rCXCL1 treated, RSV infected mice as compared to mock treated, RSV infected mice (Fig. 5.28a). There was no difference in the number of $CD4^+$ T cells in the airways between mock treated or rCXCL1 treated, RSV infected mice (Fig. 5.28b), but there was a small but significant increase in the number of lung $CD4^+$ T cells detected during RSV infection when mice were pre-treated with rCXCL1 (Fig. 5.28b). However, there was a notable increase in the number of $CD8^+$ T cells detected in both the airways and in the lung on day 8 p.i. in RSV infected mice pre-treated with rCXCL1, as compared to mock treated mice (Fig. 5.28c). Using tetramers presenting RSV M peptide, we found there was no increase in the frequency of antigen-specific $CD8^+$ T cells when mice were treated with rCXCL1 prior to RSV infection (Fig. 5.29a and Fig. 5.29b), however because the total number of $CD8^+$ T cells was higher in these mice, the total number of RSV-specific $CD8^+$ T cells detected in the lung was also higher (Fig. 5.29b). To assess the functionality of the $CD8^+$ T cell response when mice were pre-treated with rCXCL1 and infected with RSV, the total lung cells were stimulated with RSV M peptide and intracellular cytokine staining for GrzmB and IFN-γ was performed (Fig 5.29c and Fig. 5.29d). This demonstrated that although mice pre-treated with rCXCL1 prior to RSV infection had a greater number of $CD8^+$ T cells in the lung on day 8 p.i., there was no difference in the ability of the $CD8^+$ T cells to produce either GrzmB or IFN-γ (Fig 5.29c and Fig. 5.29d).

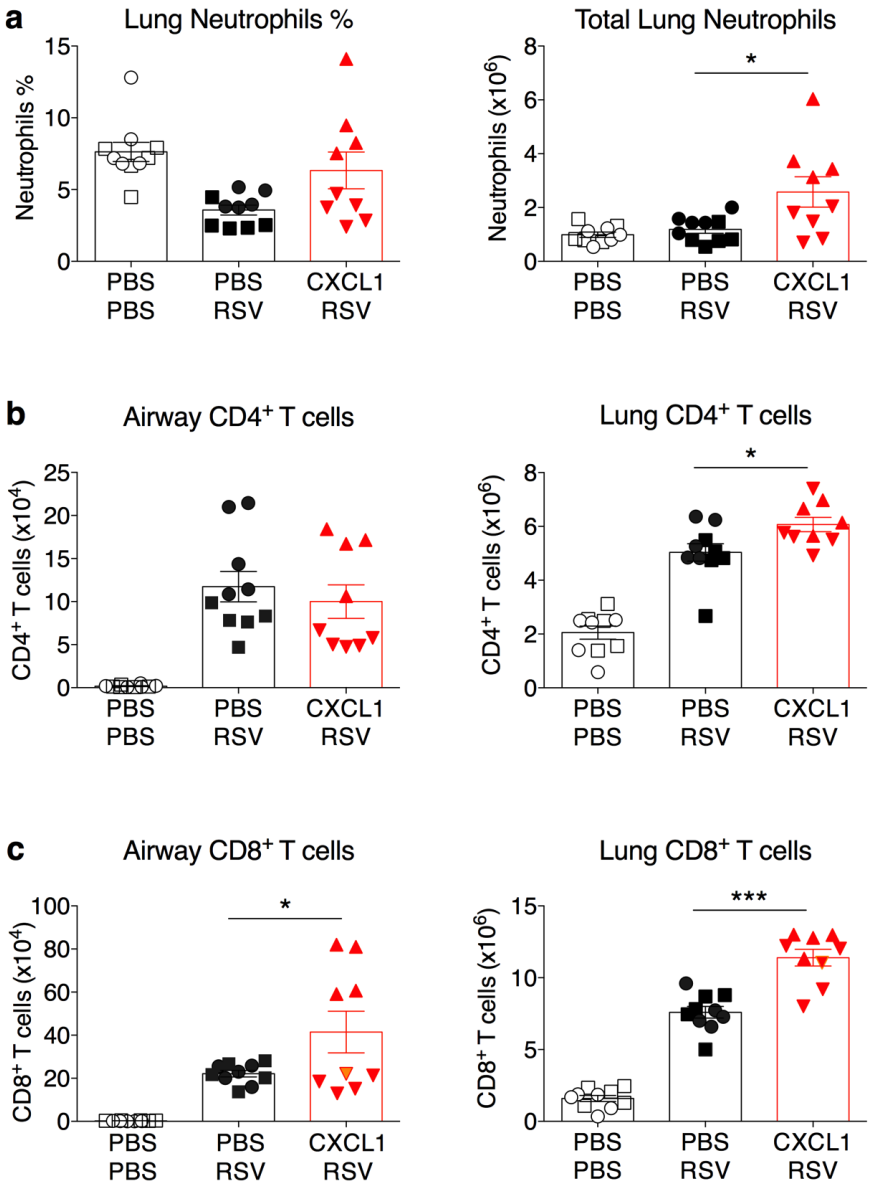

Figure 5.28. Treatment of mice with rCXCL1 prior to RSV infection enhances the recruitment of CD8⁺ T cells to the lung on day 8 p.i.. C57BL/6 mice were treated with mock (PBS) or 8-10 µg rCXCL1 i.n. and after 12 h mice were infected with mock (PBS) or 7.5 x 10^5 FFU RSV. Immune cells were analysed by flow cytometry on day 8 p.i. (Fig. 4.3 for gating strategy). **a.** Frequency and total number of lung neutrophils. **b.** Total number of airway and lung CD4⁺ T cells. **c.** Total number of airway and lung CD8⁺ T cells. Data from are presented as mean±SEM of 10 (PBS/PBS, PBS/RSV) or 9 (CXCL1/RSV) individual mice, pooled from two independent experiments - repeat 1 (10 µg CXCL1; ○, ●, ▲), repeat 2 (8 µg CXCL1; □, ■, ▼). Statistical significance of differences was determined by one-way ANOVA with Tukey's post hoc test. Only differences between RSV infected groups are shown. * $p \leq 0.05$, *** $p \leq 0.001$.

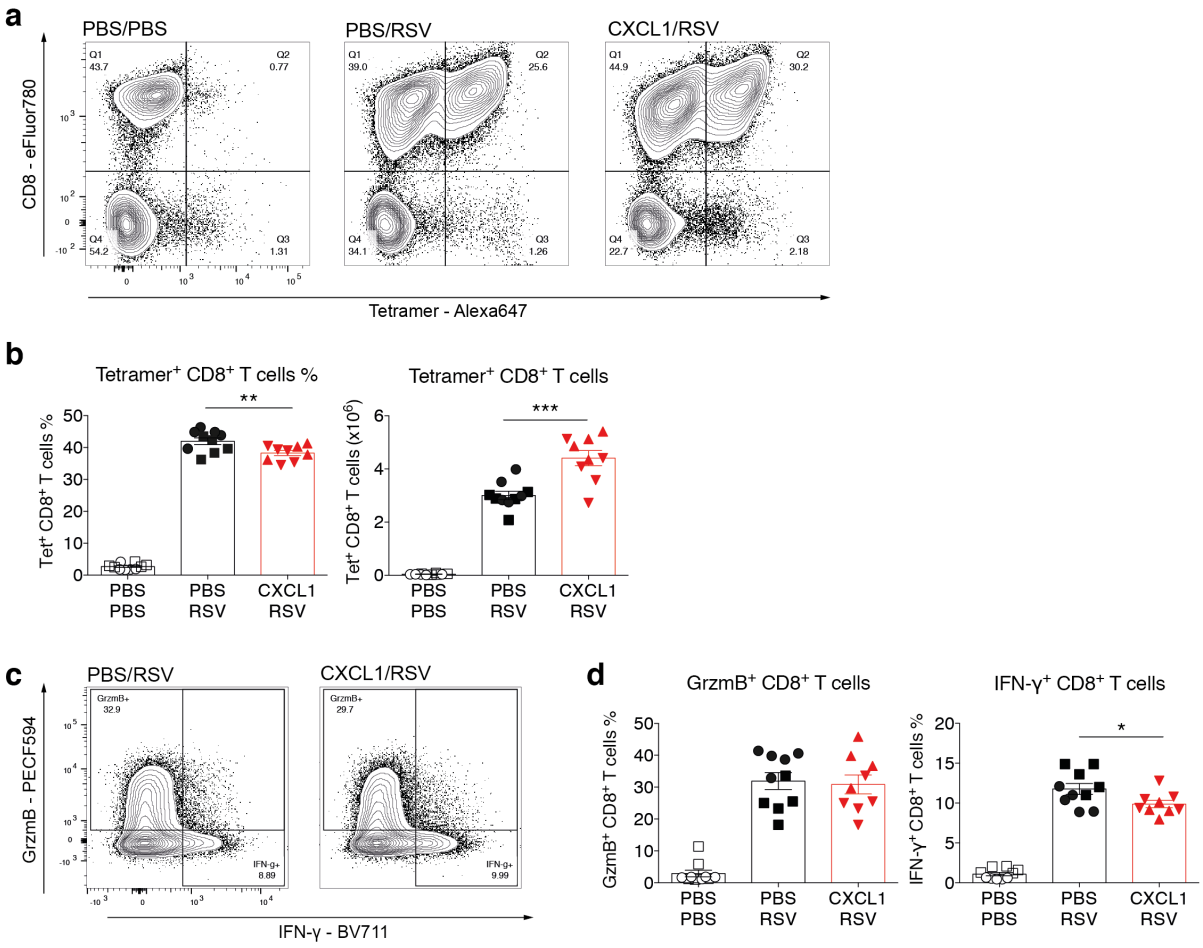

Figure 5.29. Treatment of mice with rCXCL1 prior to RSV infection does not influence the recruitment of antigen specific CD8+ T cells, nor their ability to produce GrzmB and IFN-γ on day 8 p.i.. C57BL/6 mice were treated with mock (PBS) or 8-10 µg rCXCL1 i.n. and after 12 h mice were infected with mock (PBS) or 7.5 x 10^5 FFU RSV. Immune cells were analysed by flow cytometry on day 8 p.i. (Fig. 4.3 for gating strategy). For detection of intracellular cytokines, lung cells were stimulated with RSV M peptide. **a.** Representative flow cytometry plots showing staining for CD8 and for RSV-specific $M_{187–195}$ tetramer on $CD19^-$, $CD3^+$ cells. **b.** Frequency and total number of RSV-specific $M_{187–195}$ $tetramer^+$ $CD8^+$ lung cells. **c.** Representative flow cytometry plots showing staining for GrzmB and IFN-γ on $CD8^+$ T cells. **d.** Frequency of $GrzmB^+$ and IFN-$γ^+$ $CD8^+$ T cells in the lung. Data from are presented as mean±SEM of 10 (PBS/PBS, PBS/RSV) or 9 (CXCL1/RSV) individual mice, pooled from two independent experiments - repeat 1 (10 µg CXCL1; ○, ●, ▲), repeat 2 (8 µg CXCL1; □, ■, ▼). Statistical significance of differences was determined by one-way ANOVA with Tukey's post hoc test. Only differences between RSV infected groups are shown. * $p \leq 0.05$, ** $p \leq 0.01$, *** $p \leq 0.001$.

5.2.7 Discussion

Neutrophils are largely assumed to be pathogenic during RSV infection based on their abundance in the airways of infants with severe disease (Abu-Harb *et al.* 1999; Emboriadou *et al.* 2007; Marguet *et al.* 2008; McNamara 2003; Everard *et al.* 1994). However, it is not yet clear what the role of neutrophils is during RSV infection and it remains unknown whether their recruitment and activation in the lung is of benefit or detriment to the host. In this chapter, data are presented from two submitted articles (Kirsebom *et al.,* in review and Habibi, Thwaites *et al.,* in review). Neutrophilia during RSV infection was modulated to investigate the contribution of neutrophils to the control of viral load as well as to disease severity as measured by weight loss. Neutrophils were removed by antibody-mediated neutrophil depletion and their numbers enhanced by treating mice with the neutrophil chemoattractant rCXCL1 during RSV infection. Neutrophils did not appear to be anti-viral, nor did their presence appear to drive the timing or severity of disease as measured by weight loss in the murine RSV infection model. However, in collaboration with members of our department studying RSV infection in a human challenge model, we found that airway neutrophilia at the time of RSV infection heightened disease severity in a manner likely driven by $CD8^+$ T cells during the adaptive phase of the immune response. The immunological mechanism behind this observation is yet to be understood.

Initially, neutrophils were depleted by α-Ly6G treatment early during RSV infection to investigate their contribution to the establishment of an anti-viral immune environment in the lungs. Earlier work had demonstrated that the peak of neutrophil recruitment and activation occurs at 18-24 h in the lung during RSV infection (Fig. 5.1 - Fig. 5.5; Kirsebom *et al.* 2019). Neutrophils were depleted prior to RSV infection, and the innate environment was investigated at 18 h p.i.. Overall no major differences in the gene expression or protein production of pro-inflammatory mediators were observed between α-Ly6G treated and isotype control antibody treated mice during RSV infection. Neutrophil depletion also did not impair the recruit of monocytes to the lung in response to RSV; in fact, more monocytes were detected in the lung during treatment with α-Ly6G highlighting the compensatory abilities of the immune response. A study of RSV infection in BALB/c mice found that on day 1 p.i. neutrophil depletion reduced the production of TNF-α in the lung (Stokes *et al.* 2013). There are not major differences between strains of RSV (Melero and Moore 2013) so this could indicate that there are some differences in the innate immune response to RSV between different mouse strains.

Our group and others have previously published that AMs are the major producers of type I IFNs (Makris *et al.* 2016; Goritzka, Makris, *et al.* 2015) and that type I IFN production is

required to initiate an anti-viral, pro-inflammatory environment in the lungs, which includes the production of CCL2 and the recruitment of anti-viral monocytes (Goritzka *et al.* 2014; Goritzka, Makris, *et al.* 2015; Bhoj *et al.* 2008; Demoor *et al.* 2012). As such it was not unexpected that neutrophils do not appear to be major producers of pro-inflammatory mediators in the lung during RSV infection, despite the fact that in other scenarios neutrophils are known to be major producers of a wide variety of immune mediators (Mantovani *et al.* 2011). Recently it has been shown in that neutrophils regulate the production of IL-1β by AMs during infection with influenza virus (Peiró *et al.* 2018), however during RSV infection neutrophils did not affect IL-1β production. IL-1β is produced at very low levels during RSV infection and is not thought to be major player in the host immune response. However, during influenza virus infection, IL-1β is critical in host protection (Ichinohe *et al.* 2009). This study highlights that the role of neutrophils varies between infections with different respiratory viruses. Neutrophil depletion studies typically compare α-Ly6G treatment with isotype control treatment. In this study, an untreated RSV infected control group was also included. This revealed there are some differences between untreated and isotype control treated mice during RSV infection – isotype control treated mice had significantly lower levels of IFN-α and IL-6 detectable in the airways at 18 h p.i.. These data demonstrate that the isotype control antibody may have some unspecific, off-target effects which, could influence the innate immune response in the lungs. This is an important consideration for researchers using α-Ly6G mediated neutrophil depletion as a tool and should be considered by those using α-Ly6G to study neutrophils in bacterial and fungal infections, during sterile inflammation, as well as in other viral infections.

At this early time-point, neutrophil depletion was also used to assess lung damage by measuring serum albumin as well as histone-bound DNA. Neutrophils are classically thought to cause tissue damage during inflammation (Bardoel *et al.* 2014), however this time point is likely too early to assess lung damage during RSV infection as the peak of disease occurs later during the adaptive stage of the immune response (Graham *et al.* 1991; Cannon *et al.* 1988). Nonetheless, there was a slight decrease in the concentration of albumin detected in the lungs of α-Ly6G treated mice as compared to untreated, RSV infected mice although there was no difference between untreated and isotype control treated mice, suggesting that neutrophils may cause some tissue damage at this early time point. This observation further highlights that the isotype control antibody may have some off-target effects on the immune response to RSV. Histone-bound DNA was measured in the BAL fluid as a second readout of possible cell death and tissue damage in the lung during neutrophil depletion early following RSV infection. Notably, there was indeed significantly less histone-bound DNA detected in the

airways in the absence of neutrophils during RSV infection, again suggesting neutrophils may be contributing to damage early during RSV infection. This could be a readout of cell death but could also be a readout of NETs. Neutrophils have been shown to secrete NETs during influenza virus infection (Pillai *et al.* 2016) as well as during rhinovirus infection in an allergic asthma mouse model (Toussaint *et al.* 2017). However, in an experimental model of the fungal pathogen *C. albicans*, it has also been shown that neutrophils selectively release NETs in response to large, extracellular pathogens and opt for phagocytosis in the defence against smaller pathogens (Branzk *et al.* 2014; Warnatsch *et al.* 2017). This study suggests that neutrophils would likely not secrete NETs in response to viruses. During RSV infection, one study found that RSV F protein binds TLR4 which induces NET formation (Funchal *et al.* 2015), while a study of bovine RSV found NETs staining in the lung of RSV infection calves (Cortjens *et al.* 2016). It is also possible that damaged cells trigger NETosis instead of the virus itself, or that different triggers in addition to pathogen size regulate whether neutrophils undergo NETosis during the host immune response. More work is underway to study this in more detail *in vivo*.

Neutrophil depletion is a powerful tool however it has the limitation that it removes all the effects of neutrophils, some of which may be beneficial and some of which may be detrimental to disease outcome. Neutrophil depletion eliminates all functions and therefore it could be that subtle effects of neutrophils are not observed. Neutrophil depletion did not alter viral load at the peak of viral replication in the mouse model; this is in agreement with a study which also found no effect of neutrophil depletion on viral load in BALB/c mice during RSV infection (Stokes *et al.* 2013). However, it is known that monocytes are anti-viral during RSV infection (Goritzka, Makris, *et al.* 2015) and monocyte recruitment was enhanced during neutrophil depletion in this study. It is possible that a subtle effect of neutrophils on the restriction of viral replication is masked by the increased presence of monocytes in the lung. However, *Myd88/Trif*$^{-/-}$ mice, which do not recruit neutrophils to the lung during RSV infection but do recruit comparable numbers of monocytes (Fig. 5.8 and Fig. 5.14), had a comparable viral load to wt mice on day 4 p.i.. This further supports the finding that neutrophils do not aid in the control of viral replication or spread during RSV infection. It has been suggested that RSV can replicate in neutrophils as RSV transcripts have been detected in neutrophils (Halfhide *et al.* 2011); however this has not been investigated fully and findings from this study do not support this. Overall, these data suggest that that neutrophil recruitment to the lung does not benefit the host.

Neutrophil depletion was also used to investigate whether neutrophil recruitment and activation in the lung during RSV infection is detrimental to the host. This was explored by measuring whether neutrophils contribute to disease severity as measured by weight loss. Neutrophil depletion did not affect the timing or severity of weight loss in mice, demonstrating that neutrophils do not seem to contribute to disease severity as measured by weight loss. It is known that the weight loss observed during RSV infection of mice is largely driven by $CD8^+$ T cells during the adaptive stage of the immune response (Graham *et al.* 1991; Cannon *et al.* 1988; Tregoning *et al.* 2008). In line with this, there was no change in the number of $CD4^+$, $CD8^+$ or RSV-specific $CD8^+$ T cells observed in the lung on day 8 p.i.. In influenza virus infection it was recently demonstrated that neutrophils can leave trails of the T cell chemokine CXCL12 in the lungs, which later guides the recruitment of $CD8^+$ T cells (Lim *et al.* 2015). Since we did not detect a difference in the expression of *Cxcl12* when neutrophils were removed early during RSV infection, nor a difference in $CD8^+$ T cell recruitment, these data further highlight how the role of neutrophils in the lung is not conserved between respiratory viruses. Together the data demonstrate that neutrophils themselves do not drive tissue pathology resulting in weight loss in mice, nor do they influence the recruitment of T cells to the lung during the adaptive immune response. In influenza virus infection, neutrophil depletion studies have shown that neutrophils can be important as a part of the host defence response yet can also mediate tissue damage (Lim *et al.* 2015; Peiró *et al.* 2018; Tate *et al.* 2009; Tate *et al.* 2012; Tate *et al.* 2011; Pillai *et al.* 2016). In contrast to RSV, influenza virus has great variability between strains (Ascough *et al.* 2018) and it is thought that differences in the pathogenicity of neutrophil recruitment to the lung during influenza virus infection is at least in part dependent on the virulence of the influenza strain (Tate *et al.* 2011). More recently, there is increasing evidence to demonstrate that neutrophils can aid in disease resolution and wound healing by clearing up debris by phagocytosis (Wang *et al.* 2017; Wang 2018; Castanheira and Kubes 2019). Removing neutrophils also did not alleviate weight loss so we do not suspect neutrophil recruitment has a beneficial role to the host during RSV disease resolution, but more detailed studies need to be performed to fully conclude this.

Some neutrophils are also observed in the lung during the adaptive stage of the immune response to RSV (Tregoning *et al.* 2008), however, in much smaller numbers than are recruited early during the innate immune response (Fig. 5.1). As complete neutrophil depletion throughout the entire infection did not influence weight loss, it does not seem likely that lung neutrophilia either early or late in response to RSV contributes to disease severity. In further support of this, *Myd88/Trif*$^{-/-}$ mice - which did not recruit neutrophils to the lung early during

RSV infection, lost a comparable percentage of their original body weight to wt mice during infection with RSV. Earlier work demonstrated that signalling via MyD88/TRIF is essential for neutrophil recruitment to the lung early during RSV infection (Fig. 5.8). However, it is possible that different signals regulate neutrophil recruitment during the innate and adaptive stages of the immune response and that recruitment later during RSV infection is not dependent on MyD88/TRIF signalling. On days 6-8 p.i. there is considerable lung damage and DAMPs also play an important role in neutrophil recruitment (Pittman and Kubes 2013). In comparison to wt and *Myd88/Trif*$^{-/-}$ mice, *Mavs*$^{-/-}$ mice lost significantly more weight during the adaptive phase of the response to RSV. *Mavs*$^{-/-}$ mice recruit neutrophils to the lung early during RSV infection (Fig. 5.8), but the neutrophils are not able to become activated as MAVS signalling is required for the establishment of an anti-viral immune environment driven by the production of type I IFNs (Goritzka *et al.* 2014; Goritzka, Makris, *et al.* 2015; Bhoj *et al.* 2008; Demoor *et al.* 2012). It is likely that the increased weight loss in *Mavs*$^{-/-}$ mice observed in this study is due to the fact that they have an increased viral load at day 4 p.i. (Goritzka, Makris, *et al.* 2015), and we suspect this leads to increased recruitment of CD8^{+} T cells later during the infection. In future work it would be interesting to characterise whether T cell recruitment is indeed heightened in *Mavs*$^{-/-}$ mice. It is known from previously published work that the lack of viral control in *Mavs*$^{-/-}$ mice is due to the lack of recruitment of anti-viral monocytes – restoration of monocyte recruitment by treating *Mavs*$^{-/-}$ mice with rCCL2 is sufficient to restore the control of viral load and prevent heightened disease as measured by weight loss (Goritzka, Makris, *et al.* 2015).

To complement neutrophil removal during RSV infection by α-Ly6G, neutrophil recruitment was also heightened by treating mice with rCXCL1 during RSV infection. This was in order to adapt the murine model of RSV disease to better mimic the kinetics of neutrophilia observed in infants hospitalised with severe RSV-induced bronchiolitis (McNamara 2003; Everard *et al.* 1994). Surprisingly, even a very high dose, which resulted in >80% airway neutrophilia early during the infection, did not influence disease severity as measured by weight loss during RSV infection. Neither did repeat doses of rCXCL1 during the adaptive phase of the immune response to heighten neutrophilia at the peak of disease severity. The effect of giving mice rCXCL1 during RSV infection on viral load was not investigated, but treatment with rCXCL1 12 h prior to RSV did not influence viral load or viral clearance. Lungs are very delicate tissue and the compromise of gas exchange can quickly have devastating consequences for the host. As such, it is interesting that the lungs seem able to tolerate such drastic recruitment of lung neutrophils and these data challenge the notion that a high level of tissue neutrophilia always exacerbates disease. This is relevant beyond respiratory viral infections and should

also be considered in the context of bacterial and fungal infections as well as during sterile inflammation.

While heightening neutrophil recruitment to the lung with rCXCL1 during RSV infection had no effect on weight loss, treating mice with rCXCL1 prior to RSV infection exacerbated disease; mice which were pre-treated with rCXCL1 lost more weight than mock treated mice following RSV infection. These studies in mice followed on from clinical studies of RSV challenge in human volunteers by Chris Chiu and Peter Openshaw's research teams, also in the Section of Respiratory Infections, Imperial College London. It was observed that when human volunteers were inoculated with RSV, the participants who became infected and went on to develop symptomatic disease had a transcriptomic signature associated with neutrophil activation in the nasal cavity prior to inoculation with RSV (Habibi, Thwaites *et al.,* in review). It is particularly interesting that giving rCXCL1 to mice 12 h prior to RSV infection had such a drastic effect on weight loss when treating mice with rCXCL1 just 6 h post RSV infection had no effect at all on disease severity. These data either suggest that neutrophils must be present in the lung at the point of infection or that the presence of neutrophil chemokine or neutrophils primes the lung in a manner which exacerbates disease. The enhanced RSV disease observed from day 5 p.i. in mice pre-treated with rCXCL1 was not due to an increase in viral load; there was no effect on viral load on day 4 or day 8 p.i., and disease is therefore more likely to be due to host-driven immunopathology. The observation that there was no change in viral load also lends support to the earlier finding that neutrophils are most likely not a cellular host for RSV replication in the lung.

It is known that neutrophil recruitment is highly transient and that neutrophils have a very short half-life (Castanheira and Kubes 2019; Kolaczkowska and Kubes 2013). The slightly elevated number of neutrophils observed in the lung on day 8 p.i. in rCXCL1 pre-treated, RSV infected mice is therefore more likely to be neutrophils recruited due to lung damage at this point in the infection than leftover neutrophils present from the initial treatment with rCXCL1. At day 8 p.i., there was an increase in the recruitment of $CD8^+$ T cells to the airways and lung in the rCXCL1 pre-treated mice during RSV infection. As $CD8^+$ T cells are known to be a major driver of disease severity (Tregoning *et al.* 2008; Cannon *et al.* 1988; Graham *et al.* 1991), it is likely that the increased weight loss observed was due to the increased recruitment of $CD8^+$ T cells. There was no change in the frequency of RSV-specific $tetramer^+$ $CD8^+$ T cells, but there was an increase in the total number. This most likely reflects the fact that there were more $CD8^+$ T cells in total. There was also no difference in the ability of lung $CD8^+$ T cells to produce GrzmB or IFN-γ when mice were pre-treated with rCXCL1 during RSV infection. These data together

suggest that pre-treatment with rCXCL1 affects the number of $CD8^+$ T cells recruited to the lung but does not influence the functionality of these cells.

From these data, it is yet unclear what the mechanism is behind the observation that treating mice with rCXCL1 prior to RSV infection drives disease severity during the adaptive stage of the immune response. CXCL1 potently recruits neutrophils (Kolaczkowska and Kubes 2013) and it is likely that the effect observed is due to increased neutrophilia in the airways and lung at the time of RSV infection. CXCR2, the main receptor for CXCL1, is found on neutrophils as well as epithelial cells and endothelial cells in the lung and CXCR2 signalling is well characterised to have a function in angiogenesis during cancer (Stadtmann and Zarbock 2012; Addison *et al.* 2000; Keane *et al.* 2004). Further investigation, possibly using antibody-mediated neutrophil depletion, is required to confirm that the effect observed is due to the recruitment of neutrophils by rCXCL1 and not due to an unrelated effect of this chemokine. As there was just a minimal increase in the recruitment of $CD4^+$ T cells to the lung on day 8 p.i., it is most likely due to a specific signal regulating $CD8^+$ T cell recruitment and not a side effect of the neutrophils causing tissue damage and therefore causing the lungs to be more easily infiltrated by all cell types later during the adaptive immune response. It is likely that the immunological mechanism is via an effect on cDCs; the major APC involved in generating antigen-specific $CD8^+$ T cell responses (Lukens *et al.* 2009). It would be particularly interesting to further investigate $CD103^+$ cDCs in this model as this subtype is more capable of cross-presenting antigens taken up in the lung and therefore superior in their ability to activate antigen-specific cytotoxic $CD8^+$ T cells (Desch *et al.* 2011; Kim and Braciale 2009; Ho *et al.* 2011). In future studies it will be interesting to characterise what this signal might be and how rCXCL1 affects the early immune environment in the lungs. In this study, there was no observed effect on the numbers of AMs or monocytes in the lung following treatment with rCXCL1 but it will be of great interest to investigate the innate immune environment more thoroughly to gain an insight into how the recruitment of $CD8^+$ T cells is heightened in the absence of increased virus.

Further work is also needed to understand the biological relevance of this observation. It is well known that respiratory viral infections can increase susceptibility to secondary bacterial infections (Thorburn *et al.* 2006; Hall *et al.* 1988; Hendaus *et al.* 2015) but the observations from this study suggest that bacterial or fungal infections might heighten the severity of a secondary viral infection. None of the healthy human participants who were inoculated with RSV reported any infections or symptoms at the time of the challenge study, so it is possible that an asymptomatic infection might be sufficient to drive RSV disease severity. It would be

interesting to investigate further whether this observation could also partially explain why some infants develop such severe RSV disease while the vast majority of children encounter the virus with few or no symptoms.

In summary, this study demonstrates that neutrophils do not appear to benefit the host by contributing to viral restriction or disease resolution during RSV infection *in vivo*. Neutrophils themselves do not appear to cause disease as measured by weight loss in the adult mouse model of RSV, but it is possible that this is because this aspect of RSV infection does not accurately mimic the disease as observed in infants. Yet to be explored is the possibility that neutrophilia during the primary RSV infection influences the memory immune response during RSV re-challenge.

5.3 Pattern recognition receptor signalling is required for resident memory T cell responses to RSV re-challenge

5.3.1 Introduction

RSV disease is a huge economic burden due to the ability of the virus to cause repeat infections throughout life (Openshaw *et al.* 2017). Unlike other respiratory viruses such as influenza and rhinovirus, RSV does not induce long-lasting, protective antibody responses (Chiu and Openshaw 2015; Hall *et al.* 1991; Openshaw *et al.* 2017; Ascough *et al.* 2018). As such, T cell mediated cellular immunity is of heightened importance during the memory response to RSV. Recent studies have shown the importance of T_{RM} cell responses in inducing rapid, protective memory responses locally in the lung during respiratory viral infections (Wakim *et al.* 2013; Pizzolla *et al.* 2017; Takamura *et al.* 2016; Wu *et al.* 2014). Studies in both mice and humans have shown that $CD8^+$ T_{RM} cells in the lung correlate with protection against RSV infection (Kinnear *et al.* 2018; Jozwik *et al.* 2015). There is increasing evidence that aspects of the innate immune response can shape T_{RM} cell mediated immunity during viral infections (Desai *et al.* 2018; Lim *et al.* 2015; Iborra *et al.* 2016). In this chapter, the relationship between lung neutrophilia and PRR signalling on the formation of T_{RM} cell responses was investigated *in vivo*. Neutrophil depletion experiments showed that neutrophil recruitment and activation during the primary RSV infection did not impair the development of functional T_{RM} cells. However, MAVS signalling was required for the formation of lung $CD8^+$ T_{RM} cells.

5.3.2 $CD4^+$ and $CD8^+$ T_{RM} cells peak in the lungs at day 4 post RSV re-challenge

To characterise the memory T cell response to RSV, mice were mock (PBS) or RSV infected i.n., and then re-challenged with mock (PBS) or RSV i.n. 21 days later (Fig. 5.30a). Mice were either mock infected twice (PBS/PBS), RSV infected then mock infected (RSV/PBS) or RSV infected twice (RSV/RSV) in order to compare mice with an activated memory T cell response (RSV/RSV), mice with present but inactive memory T cells (RSV/PBS) and completely naïve mice (PBS/PBS). First, viral load was assessed over time in the lungs by RT-qPCR to better understand the kinetics of viral control during the memory response to RSV. RSV L gene peaked at days 1-2 post re-challenge and by day 4 had decreased to similar levels as

RSV/PBS infected mice, which still had low levels of RSV genome detectable from the primary infection (Fig. 5.30b). The gene expression of the T cell chemoattractants CXCL9 and CXCL10 was also assessed over time during RSV re-challenge (Fig. 5.30c). Both *Cxcl9* and *Cxcl10* peaked early, at day 1 post RSV re-challenge, and had returned to baseline by day 3 post re-challenge (Fig. 5.30c).

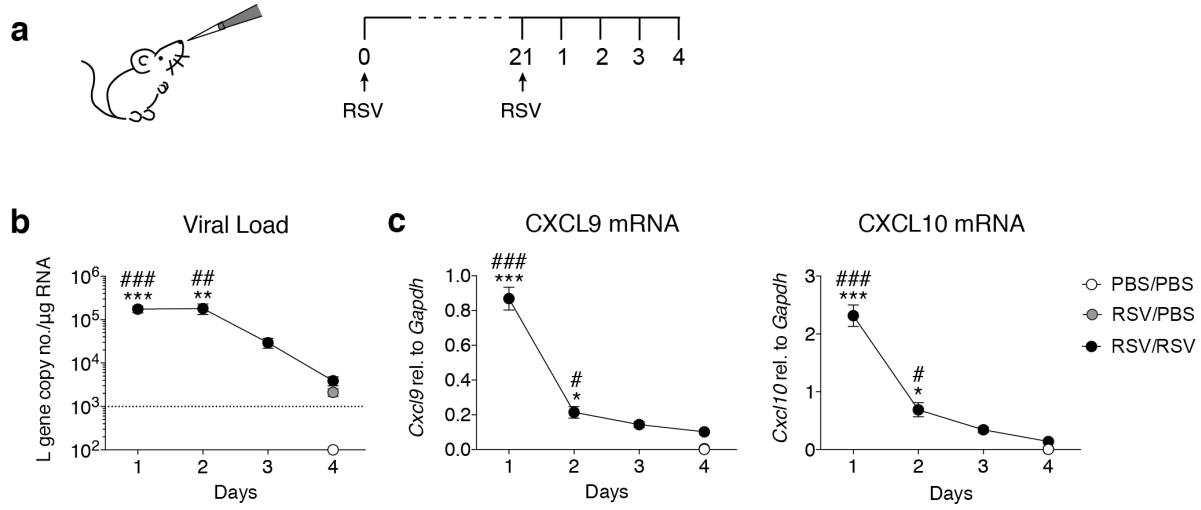

Figure 5.30. Viral load and expression of CXCL9 and CXCL10 peak early in the lung following RSV re-challenge. a. Mice were mock (PBS) infected or infected with 7.5 x 10^6 FFU RSV i.n.. At 21 days p.i. mice were re-challenged with mock (PBS) or RSV. RNA was isolated from lung tissue and gene expression was quantified by RT-qPCR at the indicated time points. PBS/PBS and RSV/PBS groups were only analysed on day 4 post re-challenge. **b.** RSV L gene copy number was quantified using a DNA plasmid standard and normalised to *Gapdh* expression. **c.** Expression levels of *Cxcl9* and *Cxcl10* were quantified relative to *Gapdh*. Data are presented as the mean ±SEM of 3 (PBS/PBS), 4 (RSV/PBS) or 4-6 (RSV/RSV) individual mice, from one independent experiment. Statistical significance of differences between groups was determined by one-way ANOVA with Tukey's post hoc test. * indicates differences between PBS/PBS (day 4) and RSV/RSV groups, # indicates differences between RSV/PBS (day 4) and RSV/RSV groups. * $p \leq 0.05$, ** $p \leq 0.01$, *** $p \leq 0.001$. The RT-qPCR data were obtained by Rinat Nuriev.

To determine the most appropriate time point to investigate memory T cells during the memory immune response, airway and lungs cell populations were analysed on days 1, 2, 3 and 4 post RSV re-challenge. Lung cell populations were defined by flow cytometry using a staining panel and gating strategy previously optimised in the lab (Michelle Paulsen, unpublished), allowing the separation of the following airway and lungs cell populations: AMs, neutrophils, naïve $CD4^+$ T cells, $CD4^+$ T_{EM} cells, $CD4^+$ T_{RM} cells, naïve $CD8^+$ T cells, $CD8^+$ T_{EM} cells, $CD8^+$ T_{CM} cells and $CD8^+$ T_{RM} cells (Fig. 4.3). In this work, the total effector memory T cells including T_{RM} cells were quantified as T_{EM}. There was no major difference in the total number of AMs in the

airways of RSV/RSV infected mice, as compared to RSV/PBS or PBS/PBS infected mice, during the first 4 days following RSV re-challenge (Fig. 5.31a). In both the airways and the lungs, neutrophil recruitment peaked at day 1 post RSV re-challenge (Fig. 5.31b). By day 3, the neutrophil response was cleared and there was no difference in the number of lung neutrophils between RSV/RSV infected mice and RSV/PBS or PBS/PBS control infected mice (Fig. 5.31b).

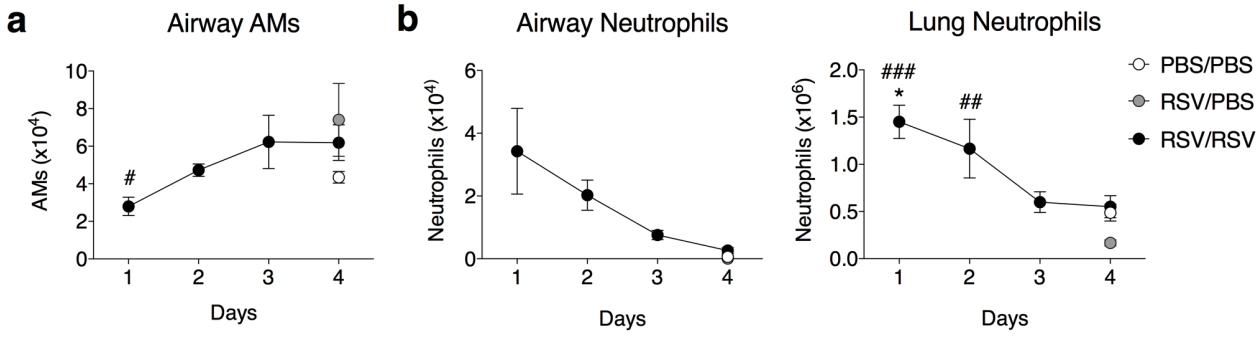

Figure 5.31. AMs and neutrophils in the airways and in the lung following RSV re-challenge. Mice were mock (PBS) infected or infected with 7.5 x 10^6 FFU RSV i.n.. At 21 days p.i. mice were re-challenged with mock (PBS) or RSV and airway and lung cells were analysed at the indicated time-points post re-challenge by flow cytometry (Fig. 4.3 for gating strategy). PBS/PBS and RSV/PBS groups were only analysed on day 4 post re-challenge. **a.** Total number of AMs in the airways. **b.** Total number of neutrophils in the airways and lungs. Data are presented as the mean ±SEM of 3 (PBS/PBS), 4 (RSV/PBS) or 4-6 (RSV/RSV) individual mice, from one independent experiment. Statistical significance of differences between groups was determined by one-way ANOVA with Tukey's post hoc test. * indicates differences between PBS/PBS (day 4) and RSV/RSV groups, # indicates differences between RSV/PBS (day 4) and RSV/RSV groups. * $p \leq 0.05$, ** $p \leq 0.01$, *** $p \leq 0.001$.

Next, $CD4^+$ and $CD8^+$ T cells were enumerated in the airways and the lungs over time following RSV re-challenge (Fig. 5.32). $CD4^+$ T cells peaked at day 4 post RSV re-challenge in both the airways and the lungs (Fig. 5.32a). There was no difference in the number of $CD4^+$ T cells in the airways or lungs of RSV/RSV infected mice until day 3 post re-challenge, after which there was an increase in the number of these cells in the airways and lungs (Fig. 5.32a). Likewise, there was a drastic increase in the number of $CD8^+$ T cells in the airways and the lungs of RSV/RSV infected mice on day 4 post RSV re-challenge compared to control RSV/PBS and PBS/PBS infected mice (Fig. 5.32b). There was no difference in the numbers of either $CD4^+$ or $CD8^+$ T cells in the airways or lungs between RSV/PBS mice or PBS/PBS (Fig. 5.32).

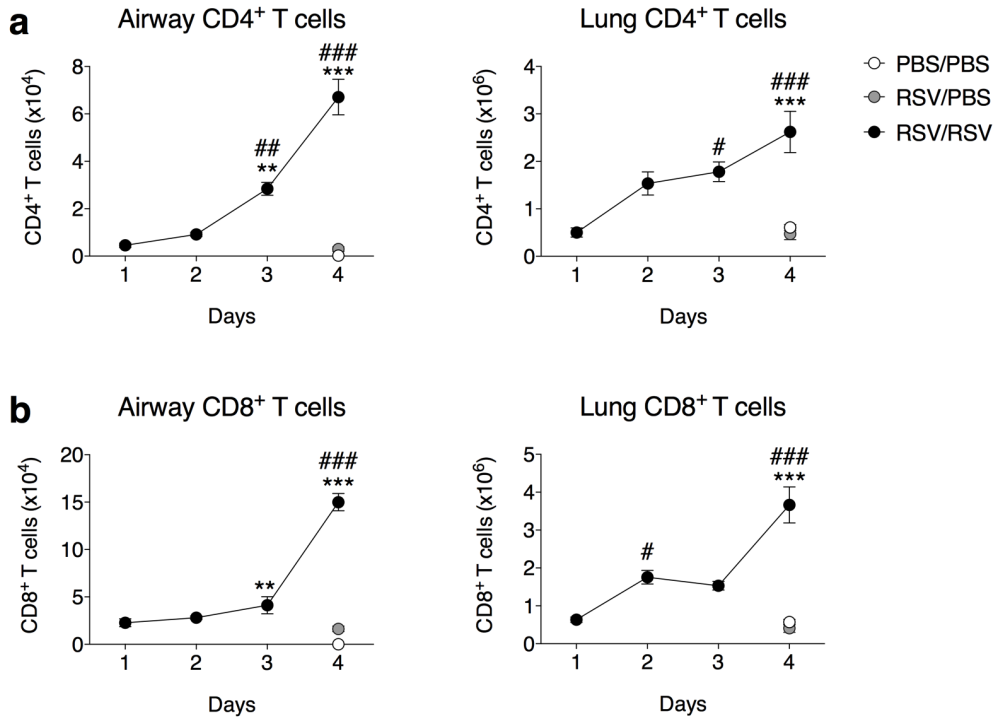

Figure 5.32. CD4+ and CD8+ T cell populations peak at day 4 in the airways and in the lung following RSV re-challenge. Mice were mock (PBS) infected or infected with 7.5 x 10^6 FFU RSV i.n.. At 21 days p.i. mice were re-challenged with mock (PBS) or RSV and airway and lung cells were analysed at the indicated time-points post re-challenge by flow cytometry (Fig. 4.3 for gating strategy). PBS/PBS and RSV/PBS groups were only analysed on day 4 post re-challenge. **a.** Total number of CD4+ T cells in the airways and in the lungs. **b.** Total number of CD8+ T cells in the airways and in the lungs. Data are presented as the mean ±SEM of 3 (PBS/PBS), 4 (RSV/PBS) or 4-6 (RSV/RSV) individual mice, from one independent experiment. Statistical significance of differences between groups was determined by one-way ANOVA with Tukey's post hoc test. * indicates differences between PBS/PBS (day 4) and RSV/RSV groups, # indicates differences between RSV/PBS (day 4) and RSV/RSV groups. * $p \leq 0.05$, ** $p \leq 0.01$, *** $p \leq 0.001$.

To investigate memory CD4$^+$ T cell subsets more closely, CD4$^+$ T_{EM} cells (CD45$^+$, CD3$^+$, CD4$^+$, CD62L$^-$, CD44$^+$) and CD4$^+$ T_{RM} cells (CD45$^+$, CD3$^+$, CD4$^+$, CD62L$^-$, CD44$^+$, CD69$^+$, CD103$^-$) were quantified in the airways and lungs over time (Fig. 5.33). In both compartments, the total number of CD4$^+$ T_{EM} cells increased from day 3 post RSV re-challenge, with the highest number observed on day 4 post re-challenge (Fig. 5.33a). There was no difference in the number of CD4$^+$ T_{EM} cells between RSV/PBS infected mice and PBS/PBS infected mice (Fig. 5.33a). Next, the expansion of CD4$^+$ T_{RM} cells, a subset of CD4$^+$ memory T cells which do not enter the circulation but remain in the tissue and proliferate upon pathogen re-encounter, was quantified over time following RSV re-challenge (Fig. 5.33b and Fig. 5.33d). CD4$^+$ T_{RM} cells are defined by the expression of CD69$^+$ on CD4$^+$ T_{EM} cells. There were no CD4$^+$ T_{RM} cells in the airways or lungs of control PBS/PBS infected mice (Fig. 5.33b and Fig. 5.33d). RSV/PBS infected mice had a small population of CD4$^+$ T_{RM} cells in the lungs which could be visualised on the flow cytometry plots (Fig. 5.33b), but as this population is very small there was no significant difference in the frequency or number of CD4$^+$ T_{RM} cells between RSV/PBS and PBS/PBS infected mice (Fig. 5.33c and Fig. 5.33d). In RSV/RSV infected mice, the frequency of CD4$^+$ T_{RM} cells in the lung increased from day 1 following RSV re-challenge, as compared to RSV/PBS and PBS/PBS infected mice (Fig. 5.33d). However, the total number of CD4$^+$ T_{RM} cells detected in the airways and lung only increased from day 3 following RSV re-challenge (Fig. 5.33c and Fig. 5.33d). This likely reflects the increase in the total number of CD4$^+$ T_{EM} cells at this time point as CD4$^+$ T_{RM} cells were defined as CD69$^+$ T_{EM} cells.

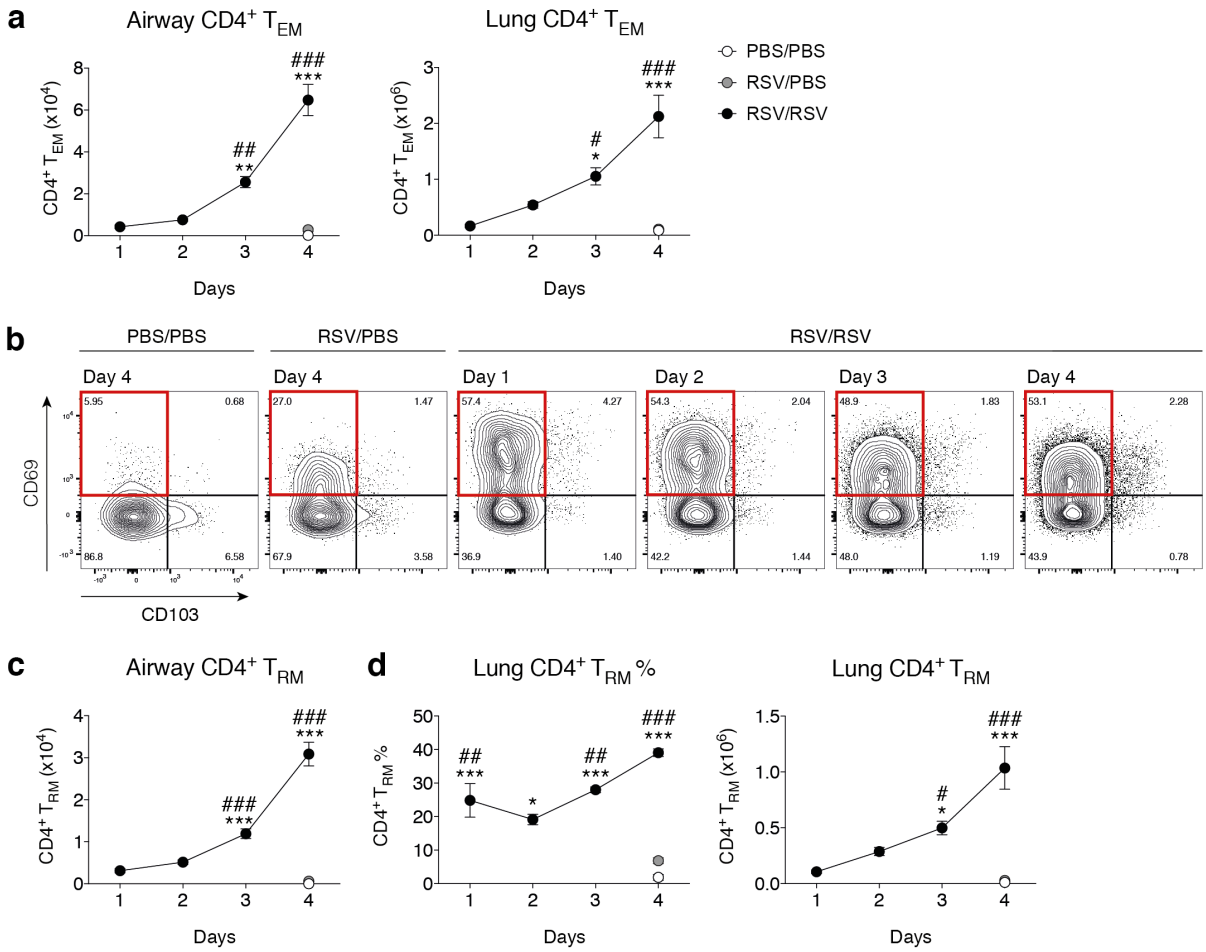

Figure 5.33. Memory CD4⁺ T cell subsets peak on day 4 in the airways and in the lung following RSV re-challenge. Mice were mock (PBS) infected or infected with 7.5 x 10^6 FFU RSV i.n.. At 21 days p.i. mice were re-challenged with mock (PBS) or RSV and airway and lung cells were analysed at the indicated time-points post re-challenge by flow cytometry (Fig. 4.3 for gating strategy). PBS/PBS and RSV/PBS groups were only analysed on day 4 post re-challenge. **a.** Total number of airway and lung CD4⁺ T_{EM} cells. **b.** Representative flow cytometry plots of CD69 expression on CD4⁺ T_{EM} cells (Fig. 4.3 for gating strategy) at the indicated time points, CD69⁺ CD103⁻ CD4⁺ T_{RM} highlighted in red. **c.** Total number of airway and lung CD4⁺ T_{RM} cells. Data are presented as the mean ±SEM of 3 (PBS/PBS), 4 (RSV/PBS) or 4-6 (RSV/RSV) individual mice, from one independent experiment. Statistical significance of differences between groups was determined by one-way ANOVA with Tukey's post hoc test. * indicates differences between PBS/PBS (day 4) and RSV/RSV groups, # indicates differences between RSV/PBS (day 4) and RSV/RSV groups. * $p \leq 0.05$, ** $p \leq 0.01$, *** $p \leq 0.001$.

Memory CD8+ T cells were also quantified after RSV re-challenge: CD8+ T_{EM} cells (CD45+, CD3+, CD8+, CD62L-, CD44+), CD8+ T_{CM} cells (CD45+, CD3+, CD8+, CD62L+, CD44+) and CD8+ T_{RM} cells (CD45+, CD3+, CD8+, CD62L-, CD44+, CD69+, CD103+) were quantified in the airways and the lung over time. (Fig. 5.34). The greatest number of CD8+ T_{EM} cells observed was on day 4 post RSV re-challenge in both the airways and the lung (Fig. 5.34a). This increase was drastic - there was no difference in the number of CD8+ T_{EM} cells in the lung between RSV/RSV infected mice and RSV/PBS or PBS/PBS infected mice on day 3 while on day 4 this difference was highly significant (Fig. 5.34a). CD8+ T_{CM} cells peaked on days 2-3 post re-challenge and by day 4 there was no difference in the number of T_{CM} cells between the lungs of RSV/RSV infected mice and RSV/PBS or PBS/PBS control infected mice (Fig. 5.34b). CD8+ T_{RM} cells, characterised by the cell surface expression of CD69 as CD4+ T_{RM} cells as well as by the additional cell surface expression of CD103, drastically increased in both frequency and number in the airways and the lungs on day 4 post RSV re-challenge (Fig. 5.34c – Fig.5.34e). We confirmed there were no CD8+ T_{RM} cells in the airways or lungs of PBS/PBS infected mice (Fig. 5.34c – Fig.5.34e). As with CD4+ T_{RM} cells, there was a small population of CD8+ T_{RM} cells RSV/PBS infected mice which could be observed in the flow cytometry plots but this population was so small there was no statistically significant difference detected in the number of CD8+ T_{RM} cells between RSV/PBS and PBS/PBS infected mice (Fig. 5.34c – Fig.5.34e).

Together, these time course experiments demonstrate that day 4 post RSV re-challenge is the most appropriate time point to further investigate both CD4+ and CD8+ T_{RM} cells during the memory immune response to RSV as this is when the greatest increase in both CD4+ and CD8+ T_{RM} cell populations was observed in the airways and in the lungs following RSV re-challenge.

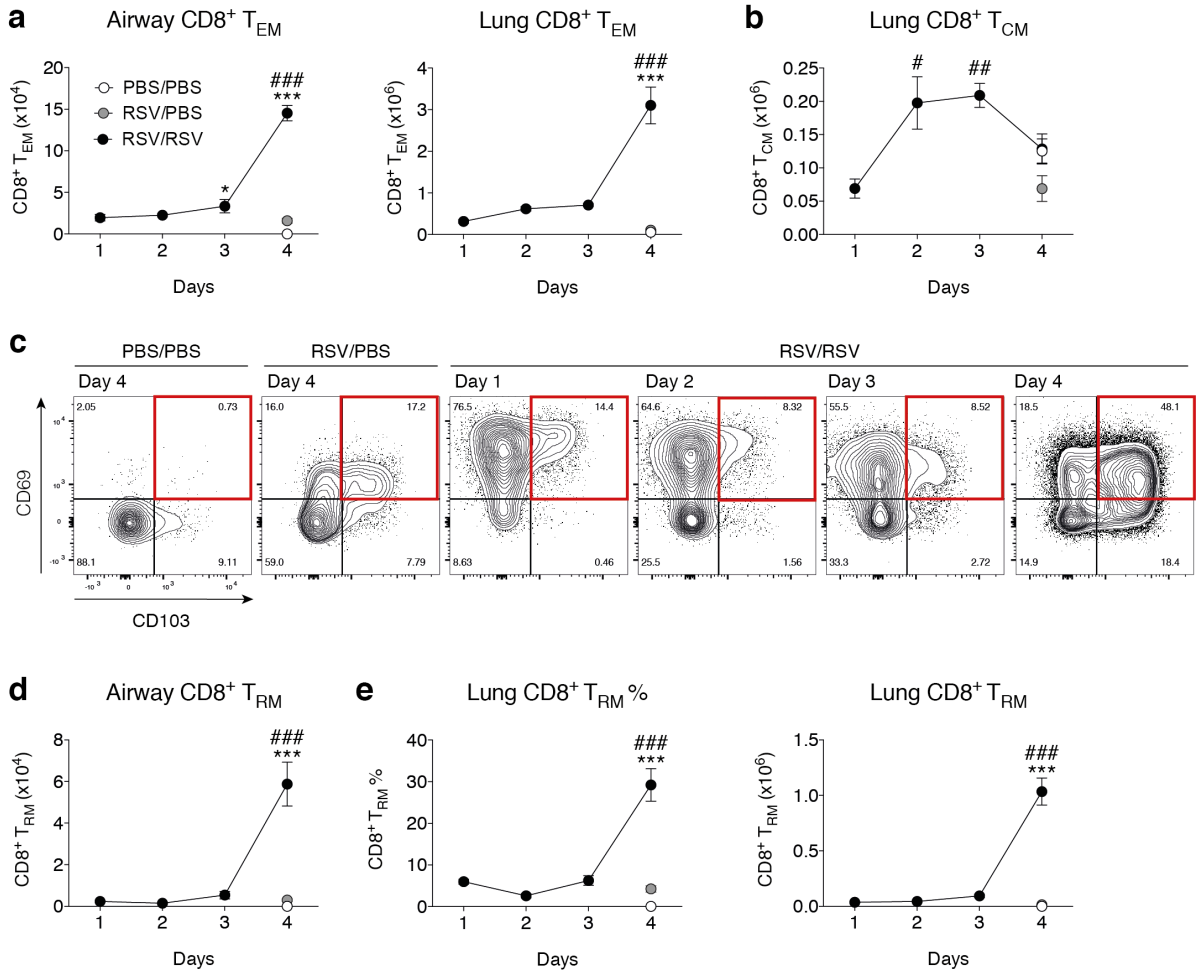

Figure 5.34. Memory CD8⁺ T cell subsets peak on day 4 in the airways and in the lung following RSV re-challenge. Mice were mock (PBS) infected or infected with 7.5 x 10^6 FFU RSV i.n.. At 21 days p.i. mice were re-challenged with mock (PBS) or RSV and airway and lung cells were analysed at the indicated time-points post re-challenge by flow cytometry (Fig. 4.3 for gating strategy). PBS/PBS and RSV/PBS groups were only analysed on day 4 post re-challenge. **a.** Total number of airway and lung CD8⁺ T_{EM} cells. **b.** Total number of lung CD8⁺ T_{CM} cells. **c.** Representative flow cytometry plots of CD69 and CD103 expression on CD8⁺ T_{EM} cells (Fig. 4.3 for gating strategy) at the indicated time points, CD69⁺ CD103⁺ CD8⁺ T_{RM} highlighted in red. **d.** Total number of airway CD8⁺ T_{RM} cells. **e.** Frequency and total number of lung CD8⁺ T_{RM} cells. Data are presented as the mean ±SEM of 3 (PBS/PBS), 4 (RSV/PBS) or 4-6 (RSV/RSV) individual mice, from one independent experiment. Statistical significance of differences between groups was determined by one-way ANOVA with Tukey's post hoc test. * indicates differences between PBS/PBS (day 4) and RSV/RSV groups, # indicates differences between RSV/PBS (day 4) and RSV/RSV groups. * $p \leq 0.05$, ** $p \leq 0.01$, *** $p \leq 0.001$.

5.3.3 FTY720 treatment of mice confirms the gating strategy correctly identifies $CD4^+$ and $CD8^+$ T_{RM} cells in the lungs during RSV re-challenge

There is considerable debate in the literature concerning the identification of T_{RM} cells based on their cell surface markers. It is suggested that the markers which classically define their residency status ($CD69^+$ for $CD4^+$ T_{RM} cells, $CD69^+$ and $CD103^+$ for $CD8^+$ T_{RM} cells) could be upregulated by T_{EM} cells which are recruited to the lungs from the circulation following pathogen re-exposure. CD69, for example, is used as a marker of T cell activation as well as a marker of tissue residency (Ziegler *et al.* 1994). To confirm that the gating strategy correctly identifies true T_{RM} cells in the lungs during the memory immune response to RSV, mice were treated with the drug FTY720 (fingolimod) during RSV re-challenge (Fig. 5.35a). FTY720 is used to treat multiple sclerosis and sequesters naïve T cells, T_{CM} cells and circulating T_{EM} cells in the lymph nodes (Chiba *et al.* 1998; Yanagawa *et al.* 1998; Henning *et al.* 2001) by internalising sphingosine 1-phosphate receptor 1 (S1PR1) on T cells and preventing sphingosine 1-phosphate (S1P) mediated T cell migration into the blood (Matloubian *et al.* 2004; Sykes *et al.* 2014). Mice were infected with RSV and re-challenged with RSV 21 days later (Fig. 5.35a). To prevent T cell migration to the lungs from the circulation, mice were treated with 6 doses of mock (PBS) or FTY720 starting from day 1 pre RSV re-challenge up to day 4 post RSV re-challenge and T_{RM} cells were analysed on day 4 post RSV re-challenge (Fig. 5.35a). To confirm that the FTY720 dosing regimen had successfully sequestered T cells from the circulation, T cells were first quantified in the blood (Fig. 5.35b). Very few $CD4^+$ or $CD8^+$ T cells were detected in the blood of mice treated with FTY720, confirming that the dose given was sufficient to remove all circulating T cells (Fig. 5.35b). To differentiate cells in the vasculature in the lungs from lung parenchyma cells, mice were given CD45-BUV395 i.v. 5 min prior to euthanasia. Circulating $CD45^+$ cells were thereby labelled with CD45-BUV395 and were double positive for CD45 during flow cytometry analysis (CD45-$BUV395^+$, CD45-$BV605^+$). Conversely, $CD45^+$ cells of the lung parenchyma were not stained by i.v. CD45-BUV395 and were therefore single positive for CD45 (CD45-$BUV395^-$, CD45-$BV605^+$) during analysis by flow cytometry. FTY720 treatment did not alter the number of lung AMs (Fig. 5.35c and Fig. 5.35d) or lung neutrophils on day 4 following RSV re-challenge (Fig. 5.35e and Fig. 5.35f). As expected, the majority of AMs were CD45-i.v.$^-$ as these are resident lung cells (Fig. 5.35c and Fig. 5.35d). Notably, the vast majority of lung neutrophils detected were in the vasculature of the lung at this time point during RSV re-challenge (Fig. 5.35e and Fig. 5.35f).

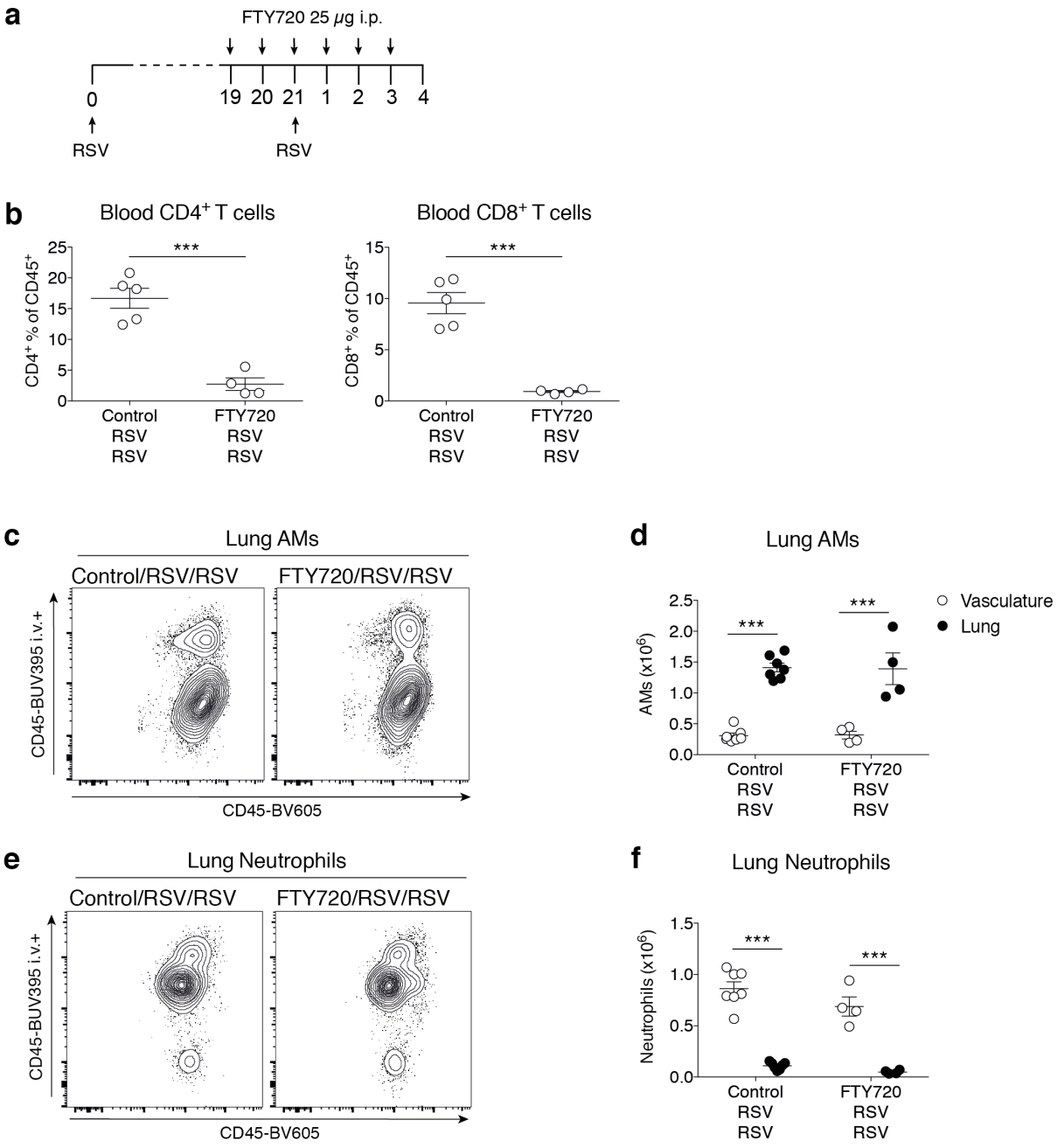

Figure 5.35. Retention of naïve T cells in the LN by FTY720 treatment abolishes circulating CD4⁺ and CD8⁺ following RSV re-challenge. a. Mice were infected with 7.5 x 10^6 FFU RSV i.n. and at 21 days p.i. mice were re-challenged with RSV. Mice were treated with 25 µg FTY720 i.p. administered daily from day -2 prior until day 3 post re-challenge. Mice were given CD45-BUV395 i.v. 5 min prior to euthanasia to distinguish cells in the vasculature of the lung (CD45-BUV395⁺) from resident lung cells (CD45-BUV395⁻). Blood and lung cells were analysed by flow cytometry on day 4 post re-challenge (Fig. 4.3 for gating strategy). **b.** Frequency of CD4⁺ and CD8⁺ circulating T cells. **c.** Representative flow cytometry plots of CD45-BUV395 i.v and CD45-BV605 (total CD45⁺ cells) staining on lung AMs. **d.** Total number of AMs in the vasculature of the lung and in the lung parenchyma. **e.** Representative flow cytometry plots of CD45-BUV395 i.v and CD45-BV605 (total CD45⁺ cells) staining on lung neutrophils. **f.** Total number of neutrophils in the vasculature of the lung and in the lung parenchyma. Data in **b** are presented as the mean ±SEM of 5 (control) and 4 (FTY720) individual mice (blood) from one independent experiment. Data in **d** and **f** are presented as the mean ±SEM of 7 (control) and 4 (FTY720) individual mice (blood) from one independent experiment. Statistical significance of differences between groups in **b** was determined by unpaired, two-tailed Student's *t* test, and in **d** and **f** by one-way ANOVA with Tukey's post hoc test. *** $p \leq 0.001$.

Next, memory T cells in the lungs were assessed at day 4 post RSV re-challenge following FTY720 treatment to determine whether the gating strategy used correctly identifies $CD4^+$ and $CD8^+$ T_{RM} cells (Fig. 5.36 and Fig. 5.37). Airway and lung populations were quantified by flow cytometry and were gated as previously described (Fig. 4.3 for gating strategy). Immune cells in the vasculature of the lungs were defined as CD45-BUV395$^+$, CD45-BV605$^+$ while lung parenchyma immune cells were defined as CD45-BUV395$^-$, CD45-BV605$^+$. There was no significant difference between control and FTY720 treated mice in the total number of $CD4^+$ T cells observed in the lung during RSV re-challenge (Fig. 5.36a). Naïve $CD4^+$ T cells were completely absent from the lungs of FTY720 treated mice. In control treated, RSV/RSV infected mice, half of the naïve $CD4^+$ T cells detected were in the vasculature of the lung (Fig. 5.36b). $CD4^+$ T_{EM} cells were only present in the lung parenchyma and were absent from the vasculature of the lungs in both control and FTY720 treated RSV/RSV infected mice (Fig. 5.36c). There was a small but significant decrease in the number of $CD4^+$ T_{EM} cells in the lungs of mice treated with FTY720 compared to control treated mice (Fig. 5.36c). FTY720 treatment showed that there were no $CD4^+$ T_{RM} cells in the vasculature of the lungs of RSV re-challenged mice and that all $CD4^+$ T_{RM} cells were located in the lung parenchyma (Fig. 5.36d and Fig. 5.36e). Furthermore, there was no significant difference in the total number of $CD4^+$ T_{RM} cells in the lung between control treated and FTY720 treated RSV/RSV infected mice, confirming that this gating strategy correctly identifies $CD4^+$ T_{RM} in the lungs during the memory response to RSV.

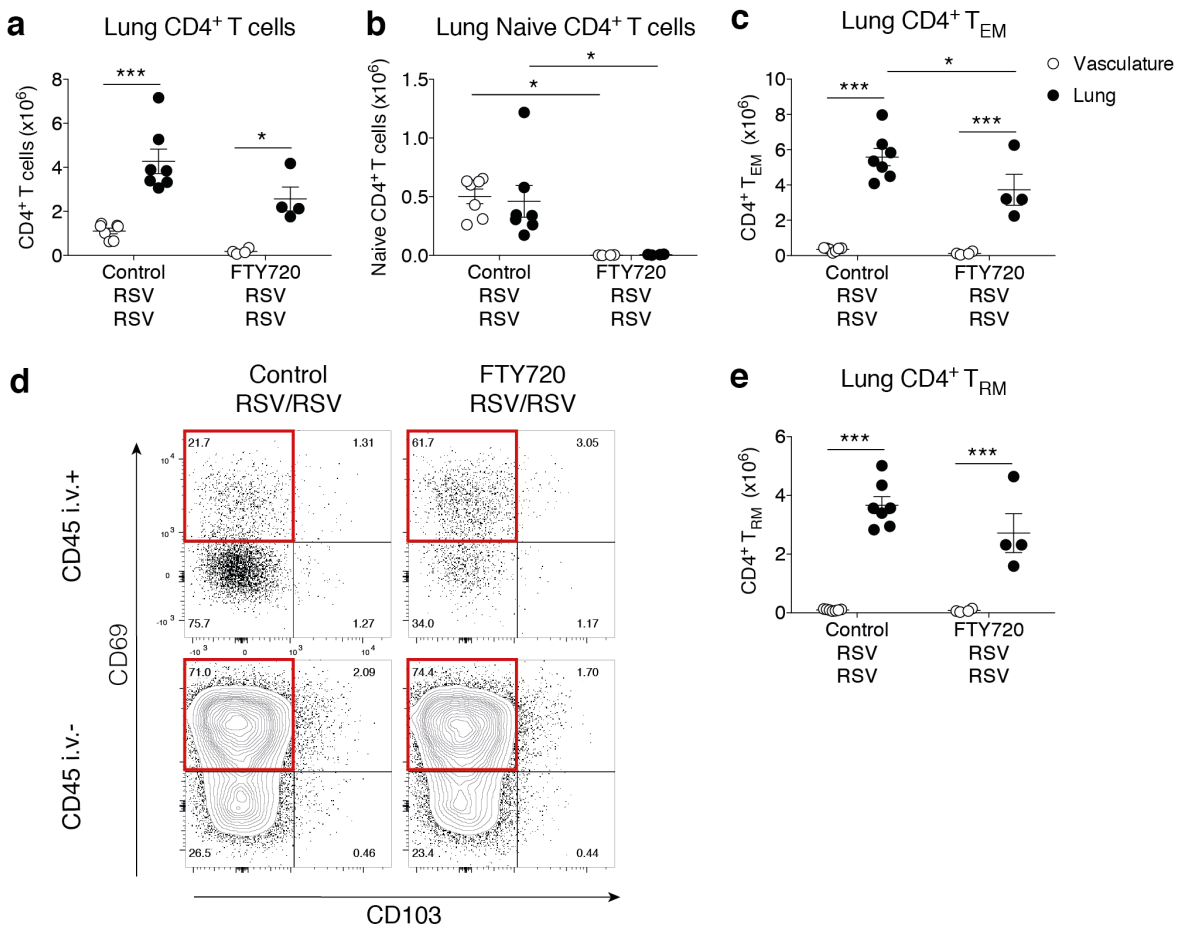

Figure 5.36. Lung CD4⁺ T_{RM} are unchanged following retention of circulating T cells in the LN by FTY720 treatment. Mice were infected with 7.5 x 10^6 FFU RSV i.n. and at 21 days p.i. mice were re-challenged with RSV. Mice were treated with 25 µg FTY720 i.p. administered daily from day -2 prior to re-challenge until day 3 post re-challenge. Lung cell populations were analysed by flow cytometry on day 4 post re-challenge (Fig. 4.3 for gating strategy). Mice were given CD45-BUV395 i.v. 5 min prior to euthanasia to distinguish cells in the vasculature of the lung (CD45-BUV395⁺) from resident lung cells (CD45-BUV395⁻). **a-c.** Total number of CD4⁺ T cells, naive CD4⁺ T cells and CD4⁺ T_{EM} cells in the vasculature of the lung and in the lung parenchyma. **d.** Representative flow cytometry plots of CD69 and CD103 expression on CD4⁺ T_{EM} cells, CD69⁺ CD103⁻ CD4⁺ T_{RM} highlighted in red. **e.** Total number of CD4⁺ T_{RM} cells in the vasculature of the lung and in the lung parenchyma. Data are presented as the mean ±SEM of 7 (control) and 4 (FTY720) individual mice, from one independent experiment. Statistical significance of differences between groups was determined by one-way ANOVA with Tukey's post hoc test. * $p \leq 0.05$, *** $p \leq 0.001$.

To assess whether the gating strategy also correctly identifies $CD8^+$ T_{RM} cells during RSV re-challenge, $CD8^+$ T cell populations were quantified in a similar manner by staining for cells in the vasculature of the lungs and in the lung parenchyma following FTY720 treatment of RSV re-challenged mice (Fig. 5.37). There was no difference in the total number of lung $CD8^+$ T cells between control and FTY720 treated mice (Fig. 5.37a). FTY720 treatment completely removed naïve $CD8^+$ T cells and $CD8^+$ T_{CM} cells from the vasculature of the lungs and from the lung parenchyma during RSV re-challenge (Fig. 5.37b – Fig. 5.37c). Both naïve $CD8^+$ T cells and $CD8^+$ T_{CM} cells were present in the vasculature of the lungs as well as in the lung itself in control treated, RSV re-challenged mice (Fig. 5.37b – Fig. 5.37c). There was no significant difference in the number of lung $CD8^+$ T_{EM} between control treated and FTY720 treated mice during RSV re-challenge (Fig. 5.37d). FTY720 treatment of mice confirmed that our gating strategy accurately identifies $CD8^+$ T_{RM} cells as there was no difference in the number of $CD8^+$ T_{RM} cells detected in the lung between control treated and FTY720 treated mice during RSV re-challenge (Fig. 5.37e and Fig. 5.37f). None of the $CD8^+$ T_{RM} cells detected in either control treated or FTY720 treated RSV/RSV infected mice were present in the vasculature of the lungs (Fig. 5.37e and Fig. 5.37f). As expected, all $CD45^+$ airway cells were negative for CD45-BUV395, indicating they were not detected in the vasculature of the lungs (Fig. 5.38a). In the airways, there was also no difference in the number of $CD4^+$ or $CD8^+$ T_{RM} cells detected between control and FTY720 treated mice following RSV re-challenge (Fig. 5.38b-c).

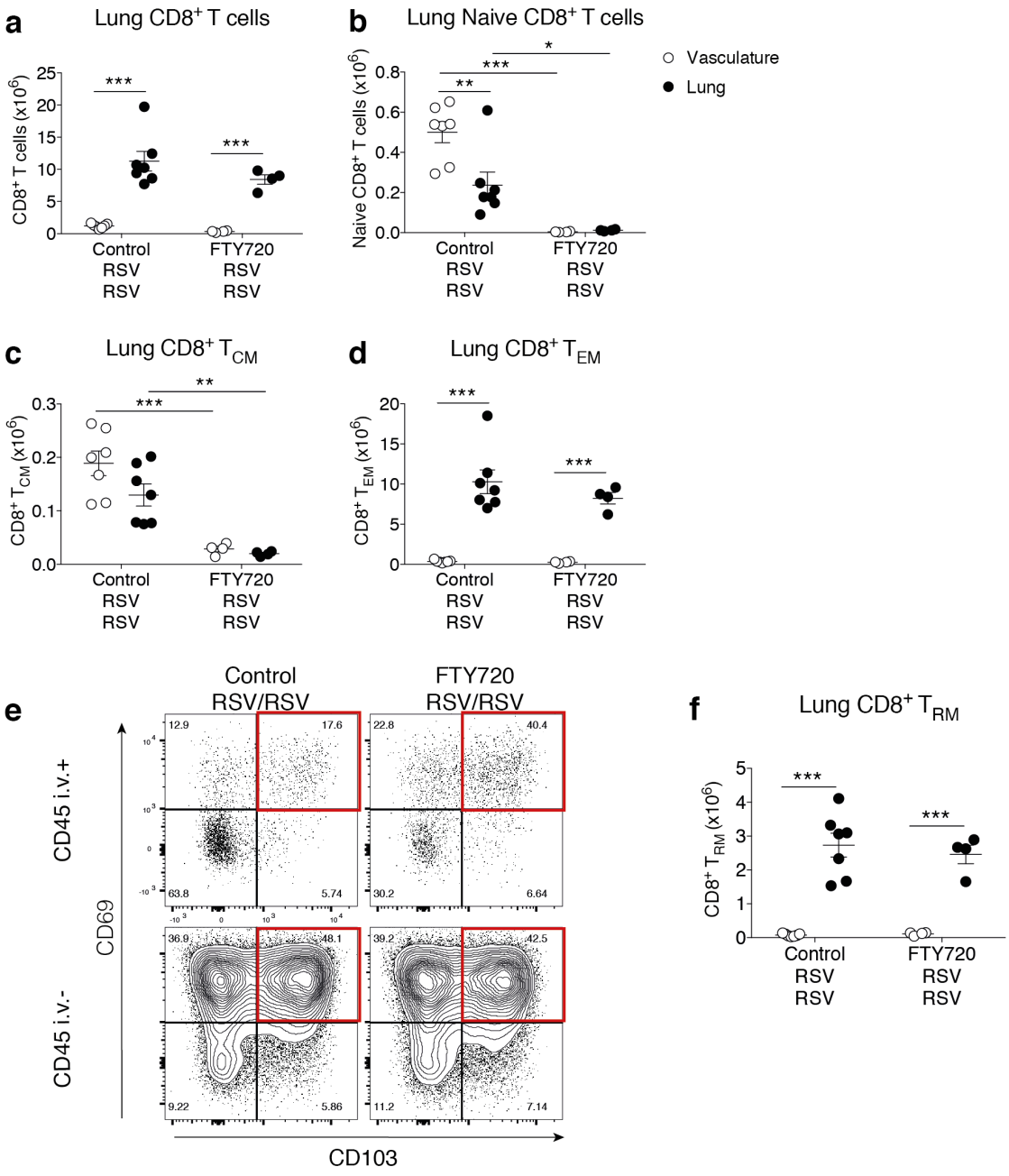

Figure 5.37. Lung CD8⁺ T_{RM} are unchanged following retention of circulating T cells in the LN by FTY720 treatment. Mice were infected with 7.5 x 10^6 FFU RSV i.n. and at 21 days p.i. mice were re-challenged with RSV. Mice were treated with 25 µg FTY720 i.p. administered daily from day -2 prior to re-challenge until day 3 post re-challenge. Lung cell populations were analysed by flow cytometry on day 4 post re-challenge (Fig. 4.3 for gating strategy). Mice were given CD45-BUV395 i.v. 5 min prior to euthanasia to distinguish cells in the vasculature of the lung (CD45-BUV395⁺) from resident lung cells (CD45-BUV395⁻). **a-d.** Total number of CD8⁺ T cells, naive CD8⁺ T cells, CD8⁺ T_{CM} cells and CD8⁺ T_{EM} cells in the vasculature of the lung and in the lung parenchyma. **e.** Representative flow cytometry plots of CD69 and CD103 expression on CD8⁺ T_{EM} cells; CD69⁺ CD103⁺ CD8⁺ T_{RM} highlighted in red. **f.** Total number of CD8⁺ T_{RM} cells in the vasculature of the lung and in the lung parenchyma. Data are presented as the mean ±SEM of 7 (control) and 4 (FTY720) individual mice, from one independent experiment. Statistical significance of differences between groups was determined by one-way ANOVA with Tukey's post hoc test. * $p \leq 0.05$, ** $p \leq 0.01$, *** $p \leq 0.001$.

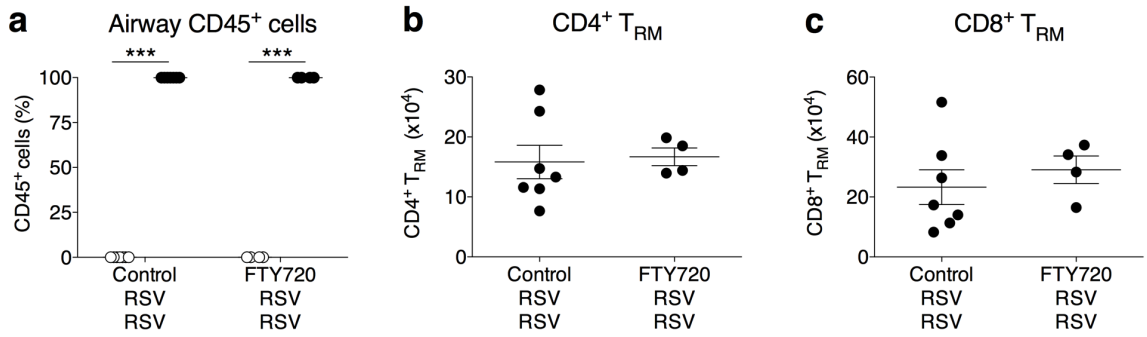

Figure 5.38. CD4⁺ and CD8⁺ T_{RM} cells in the airways are unchanged following retention of naïve T cells in the LN by FTY720 treatment. Mice were infected with 7.5 x 10^6 FFU RSV i.n. and at 21 days p.i. mice were re-challenged with RSV. Mice were treated with 25 µg FTY720 i.p. administered daily from day -2 prior to re-challenge until day 3 post re-challenge. Airway cell populations were analysed by flow cytometry on day 4 post re-challenge (Fig. 4.3 for gating strategy). Mice were given CD45-BUV395 i.v. 5 min prior to euthanasia to distinguish cells in the vasculature of the lung (CD45-BUV395⁺) from resident lung cells (CD45-BUV395⁻) **a.** Total number of CD45⁺ cells in the vasculature of the lung and in the airways of the lung. **b.** Total number of CD4⁺ T_{RM} in the airways. **c.** Total number of CD8⁺ T_{RM} cells in the airways. Data are presented as the mean ±SEM of 7 (control) and 4 (FTY720) individual mice, from one independent experiment. Statistical significance of differences between groups in **a** was determined by one-way ANOVA with Dunnett's post hoc test, and in **b** and **c** was determined by unpaired, two-tailed Student's *t* test. *** $p \leq 0.001$.

5.3.4 Neutrophil depletion during primary RSV infection does not influence the proliferation of T_{RM} cells in the lungs following RSV re-challenge

FTY720 treatment of mice during RSV infection confirmed that the gating strategy correctly identifies true CD4⁺ and CD8⁺ T_{RM} cells in the airways and in the lung (Fig. 5.36 and Fig. 5.37). In order to investigate whether lung neutrophilia during a primary RSV infection can influence the memory T cell response upon re-challenge, mice were treated with isotype control antibody or the neutrophil depleting antibody α-Ly6G every second day throughout the primary infection (Fig. 5.39a). Mice were then re-challenged with RSV on day 21 and memory responses in the lungs were investigated on day 4 post RSV re-challenge (Fig. 5.39a). As it had been observed that the isotype control antibody for α-Ly6G had some non-specific effects on the innate immune response to RSV (Fig. 5.18 – Fig. 5.19), a group of mice which were infected and re-challenged with RSV but did not receive any antibody throughout the primary infection were included as an additional control group. In both the airways and the lungs, α-Ly6G mediated neutrophil depletion did not affect the total numbers of CD4⁺ T cells (Fig. 5.39b), nor the total numbers of CD8⁺ T cells detected on day 4 post RSV re-challenge (Fig. 5.39c). In the airways, there was a slight increase in the number of CD8⁺ T cells detected in

isotype control treated, RSV/RSV infected mice as compared to untreated RSV/RSV infected mice (Fig. 5.39c). This difference was small and not detected in the total number of CD8⁺ T cells in the lungs between these two groups (Fig. 5.39c).

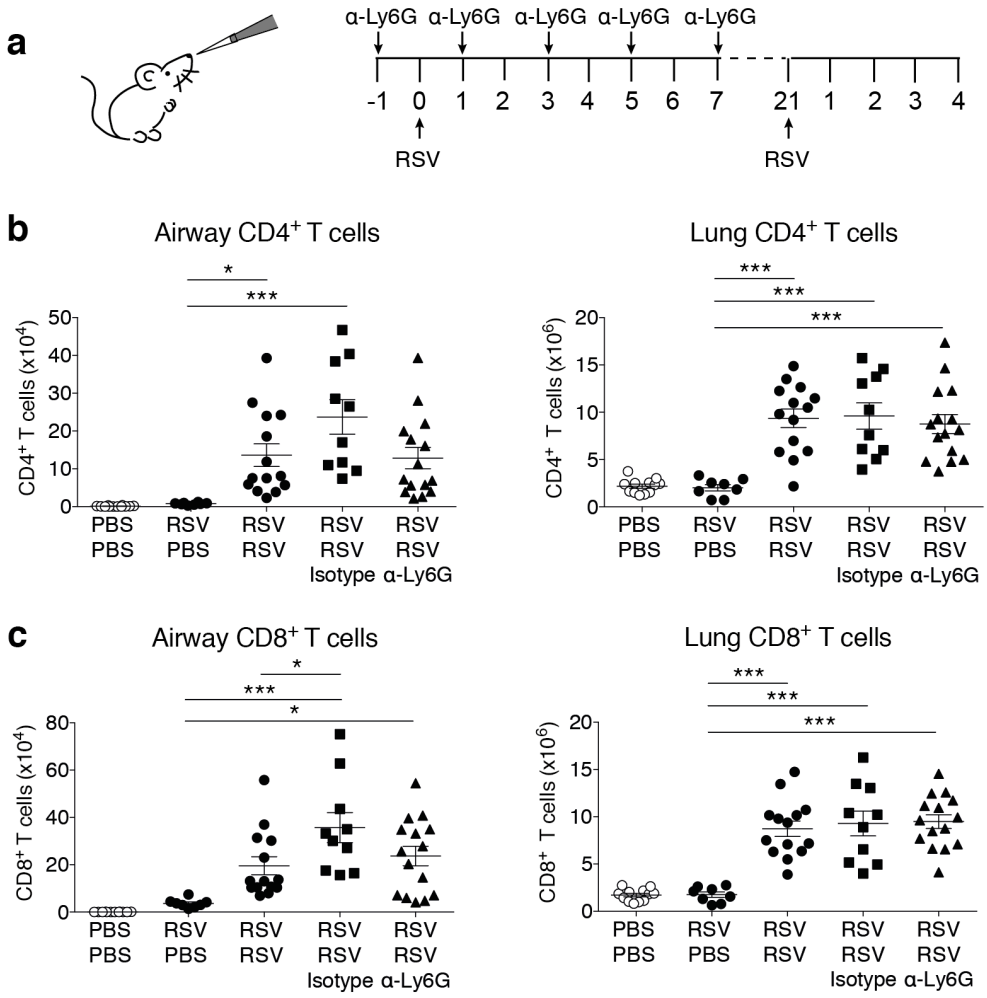

Figure 5.39. Lung neutrophilia during primary RSV infection does not affect T cell recruitment following RSV re-challenge. a. Mice were mock (PBS) infected or infected with 7.5 x 10^6 FFU RSV. To deplete neutrophils, 150 µg i.p. α-Ly6G or isotype control antibody was administered on days -1, 1, 3, 5 and 7 post primary RSV infection. Mice were re-challenged with RSV on day 21. Airway and lung cells were analysed by flow cytometry on day 4 post re-challenge (Fig. 4.3 for gating strategy). **b.** Total number of airway and lung CD4⁺ T cells. **c.** Total number of airway and lung CD8⁺ T cells. Data are presented as the mean ±SEM of 12 (PBS/PBS), 8 (RSV/PBS) and 10-15 (RSV/RSV) individual mice, pooled from two or three independent experiments. Statistical significance of differences was determined by one-way ANOVA with Tukey's post hoc test. Only differences between RSV infected groups are shown. * $p \leq 0.05$, *** $p \leq 0.001$.

Next, we assessed whether neutrophil depletion influences $CD4^+$ and $CD8^+$ T_{RM} cells in response to RSV re-challenge (Fig. 5.40). There were slightly fewer $CD4^+$ T_{RM} cells detected in the airways of α-Ly6G treated mice as compared to untreated or isotype control treated, RSV/RSV infected mice on day 4 post RSV re-challenge (Fig. 5.40a). However, this difference was not upheld in the lungs where there was no difference in the number of $CD4^+$ T_{RM} cells detected between untreated, isotype control treated or α-Ly6G treated RSV/RSV infected mice (Fig. 5.40a). There was also a slight decrease in the frequency of $CD8^+$ T_{RM} cells in the airways of α-Ly6G treated RSV/RSV mice as compared to isotype control treated RSV/RSV infected mice (Fig. 5.40b and Fig. 5.40c). This difference was not reflected in the total numbers of airway $CD8^+$ T_{RM} cells where there was no difference between the three groups of RSV/RSV infected mice (Fig. 5.40c). In the lungs, there was also no difference in either the frequency or total number of $CD8^+$ T_{RM} cells between untreated, isotype control treated or α-Ly6G treated RSV/RSV infected mice (Fig. 5.40d). These data indicate that neutrophil depletion during the primary RSV infection may have a small effect on the number of airway $CD4^+$ T_{RM} cells and on the frequency of airway $CD8^+$ T_{RM} cells during RSV re-challenge. However, these differences were not upheld in the lungs for either $CD4^+$ or $CD8^+$ T_{RM} cells during neutrophil depletion. We also confirmed that neutrophil depletion during the primary RSV infection did not affect the production of RSV-specific antibodies (Harriet Davenport, unpublished).

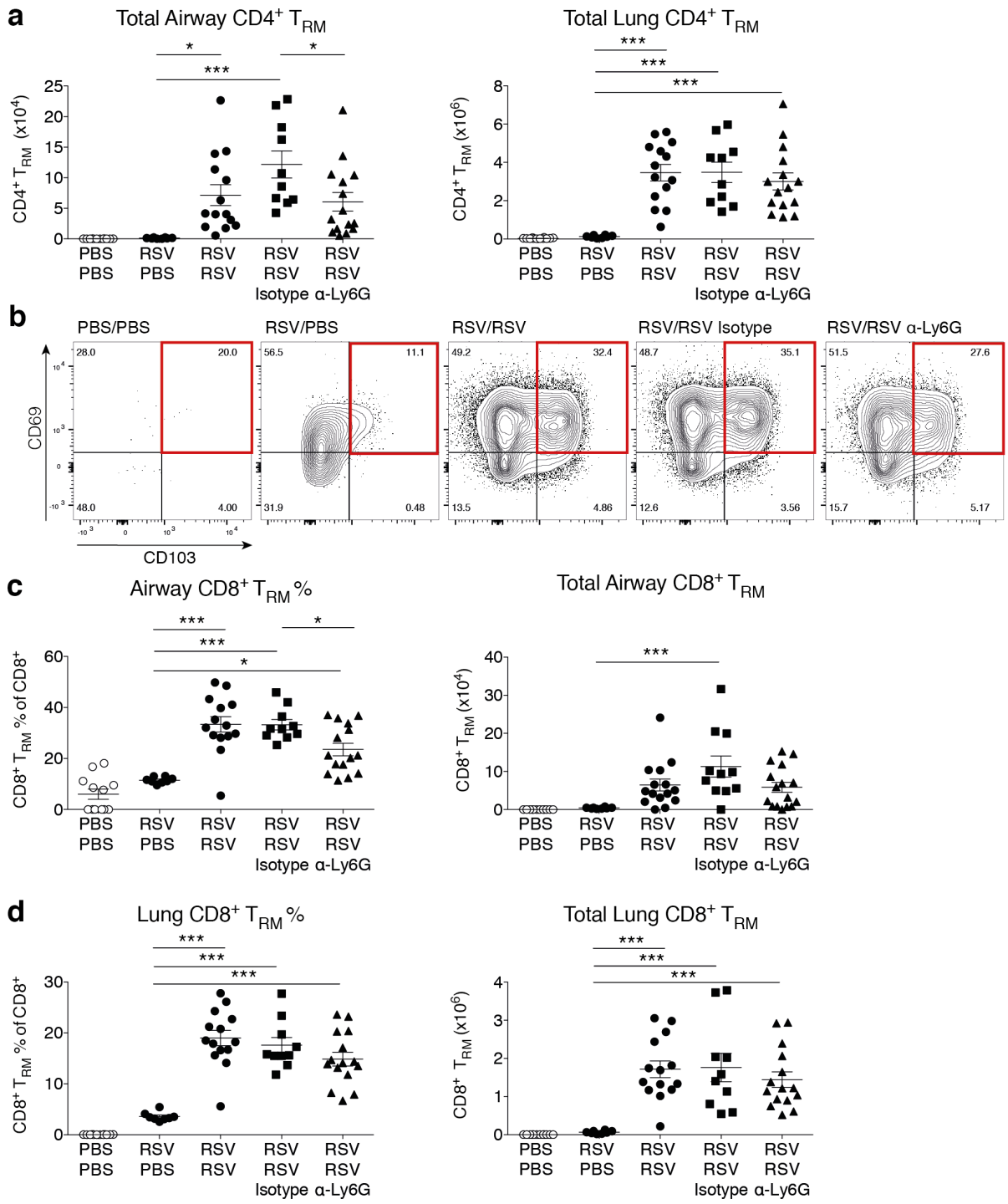

Figure 5.40. Lung neutrophilia during primary RSV infection does not affect the expansion of lung T_{RM} populations following RSV re-challenge. Mice were mock (PBS) infected or infected with 7.5 x 10^6 FFU RSV. To deplete neutrophils, 150 µg i.p. α-Ly6G or isotype control antibody was administered on days -1, 1, 3, 5 and 7 post primary RSV infection. Mice were re-challenged with RSV on day 21. Airway and lung cells were analysed by flow cytometry on day 4 post re-challenge (Fig. 4.3 for gating strategy). **a.** Total number of airway and lung $CD4^+$ T_{RM} cells. **b.** Representative flow cytometry plots of CD69 and CD103 expression on airway $CD8^+$ T_{EM} cells; $CD69^+$ $CD103^+$ $CD8^+$ T_{RM} highlighted in red. **c.** Frequency and total number of airway $CD8^+$ T_{RM} cells. **d.** Frequency and total number of lung $CD8^+$ T_{RM} cells. Data are presented as the mean ±SEM of 12 (PBS/PBS), 8 (RSV/PBS) and 10-15 (RSV/RSV) individual mice, pooled from two or three independent experiments. Statistical significance of differences was determined by one-way ANOVA with Tukey's post hoc test. Only differences between RSV infected groups are shown. * $p \leq 0.05$, *** $p \leq 0.001$.

To test whether neutrophil depletion during the primary RSV infection affects the functionality of the $CD8^+$ T_{RM} response, airway and lungs cells were stimulated *ex vivo* with an RSV-specific $CD8^+$ peptide and intracellular cytokine staining for IFN-γ and GrzmB was performed (Fig. 5.41). Overall, there was no difference in the ability of airway or lung $CD8^+$ T_{RM} cells from untreated, isotype control treated or α-Ly6G treated mice to produce IFN-γ or GrzmB after stimulation *ex vivo* 4 days post RSV re-challenge (Fig. 5.41a – Fig. 5.41c). Together, these data demonstrate that neutrophilia during the primary RSV infection does not have a role in the formation of functional $CD8^+$ T_{RM} cells in the lungs.

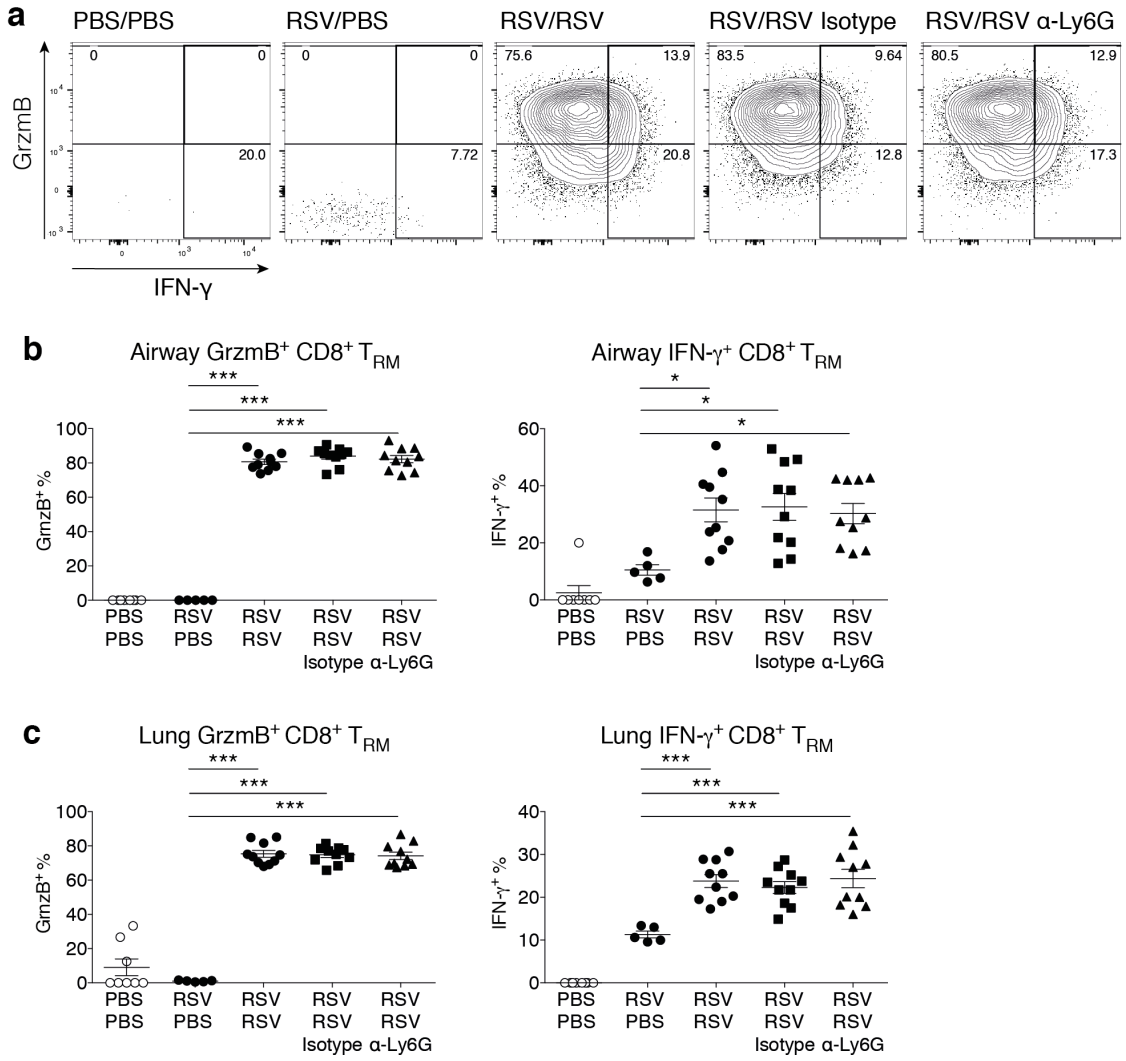

Figure 5.41. Lung neutrophilia during primary RSV infection does not affect the functionality of CD8+ T_{RM} cells following RSV re-challenge. Mice were mock (PBS) infected or infected with 7.5 x 10^6 FFU RSV. To deplete neutrophils, 150 µg i.p. α-Ly6G or isotype control antibody was administered on days -1, 1, 3, 5 and 7 post primary RSV infection. Mice were re-challenged with RSV on day 21 and airway and lung cells were analysed by flow cytometry on day 4 post re-challenge (Fig. 4.3 for gating strategy). For detection of intracellular cytokines, lung cells were stimulated with RSV M peptide. **a.** Representative flow cytometry plots of GrzmB and IFN-γ expression on airway CD8+ T_{RM} cells. **b.** Frequency of airway GrzmB+ and IFN-γ+ CD8+ T_{RM} cells. **c.** Frequency of lung GrzmB+ and IFN-γ+ CD8+ T_{RM} cells. Data are presented as the mean ±SEM of 8 (PBS/PBS), 5 (RSV/PBS) and 10 (RSV/RSV) individual mice, pooled from one or two independent experiments. Statistical significance of differences was determined by one-way ANOVA with Tukey's post hoc test. Only differences between RSV infected groups are shown. * $p \leq 0.05$, *** $p \leq 0.001$.

5.3.5 MAVS signalling is required for $CD4^+$ and $CD8^+$ T_{RM} cell responses during the memory immune response to RSV

To further explore how innate immunity and the PRR pathogen sensing pathways mediated by MAVS signalling might influence memory T cell responses during RSV infection and re-challenge, PRR knock-out mice unable to detect RSV in the cytosol via RIG-I or MDA5 (*Mavs*$^{-/-}$) were infected with RSV and then re-challenged with RSV 21 days later. Initially, viral load was assessed on days 2 and 4 post RSV re-challenge (Fig. 5.42a). *Mavs*$^{-/-}$ mice had higher viral loads at both day 2 and day 4 post RSV re-challenge, as compared to wt mice, indicating that these mice are impaired in their ability to restrict viral replication in the lungs following RSV re-challenge (Fig. 5.42a). Previous data from the lab has demonstrated that there is no difference in the concentration or neutralisation ability of RSV-specific antibodies produced by *Mavs*$^{-/-}$ mice following RSV infection (Nawamin Pinpathomrat and Harriet Davenport, unpublished). On day 2 post RSV re-challenge, there was no significant difference in the levels of *Cxcl9* or *Cxcl10* gene expression detected in the lungs of *Mavs*$^{-/-}$ mice as compared to wt mice (Fig. 5.42b).

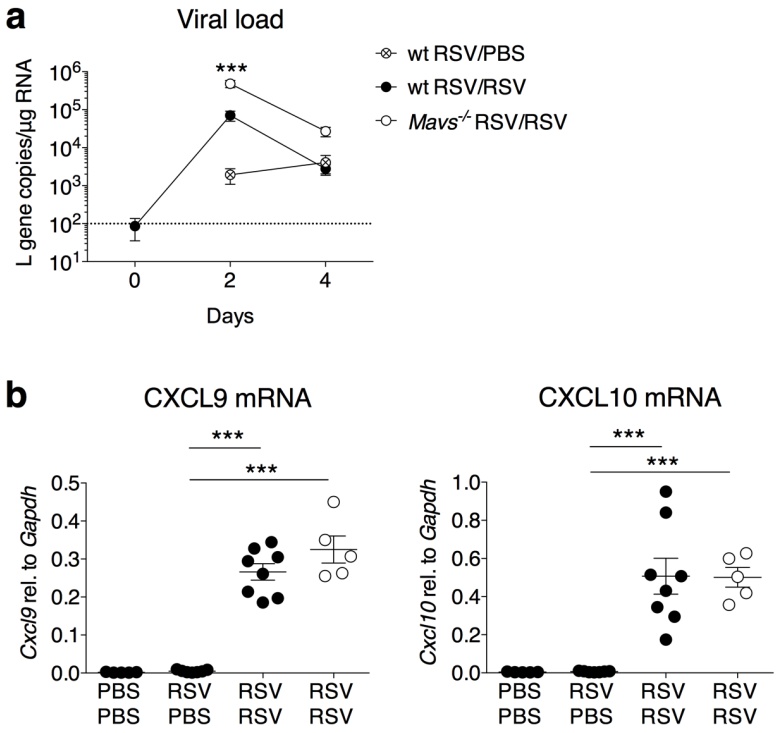

Figure 5.42. Viral load is elevated in *Mavs*$^{-/-}$ mice following RSV re-challenge. Wt and *Mavs*$^{-/-}$ mice were mock (PBS) infected or infected with 7.5 x 10^6 FFU RSV and re-challenged with RSV on day 21. RNA was isolated from lung tissue and gene expression was quantified by RT-qPCR. **a.** RSV L gene copy number was quantified using a DNA plasmid standard and normalised to *Gapdh* expression, at the indicated time points. Data are presented as the mean ±SEM of 9 (day 0, wt), 7 (day 2, wt RSV/PBS and wt RSV/RSV), 4 (day 2, *Mavs*$^{-/-}$), 7 (day 4, wt RSV/PBS), 9 (day 4, wt RSV/RSV) or 6 (day 4, *Mavs*$^{-/-}$) individual mice, pooled from one or two independent experiments. **b.** Expression levels of *Cxcl9* and *Cxcl10* were quantified relative to *Gapdh* on day 2 post re-challenge. Data are presented as the mean ±SEM of 5 (PBS/PBS), 7 (RSV/PBS) or 4-8 (RSV/RSV) individual mice, pooled from one or two independent experiments. Statistical significance of differences was determined by one-way ANOVA with Tukey's post hoc test. For **a,** * indicates statistical significance between wt RSV/RSV and *Mavs*$^{-/-}$ RSV/RSV. *** $p \leq 0.001$.

As antibody responses did not differ between the *Mavs*$^{-/-}$ mice and wt mice but the *Mavs*$^{-/-}$ mice were still impaired in their ability to control RSV replication during the memory response, memory T cell responses were investigated in *Mavs*$^{-/-}$ mice during RSV re-challenge (Fig. 5.43). Mice were mock (PBS) or RSV infected i.n., and then re-challenged with mock or RSV i.n. 21 days later. Wt mice were either mock infected twice (PBS/PBS), RSV infected then mock infected (RSV/PBS) or RSV infected twice (RSV/RSV). Memory immune responses were assessed on day 4 post RSV re-challenge. In the airways, there was no difference in the number of $CD4^+$ T cells between wt mice and *Mavs*$^{-/-}$ mice (Fig. 5.43a). There was no difference in the number of $CD8^+$ T cells in the airways of *Mavs*$^{-/-}$ mice but there was a decrease in the number of lung $CD8^+$ T cells in *Mavs*$^{-/-}$ mice, as compared to wt mice on day 4 post RSV re-challenge (Fig. 5.43b).

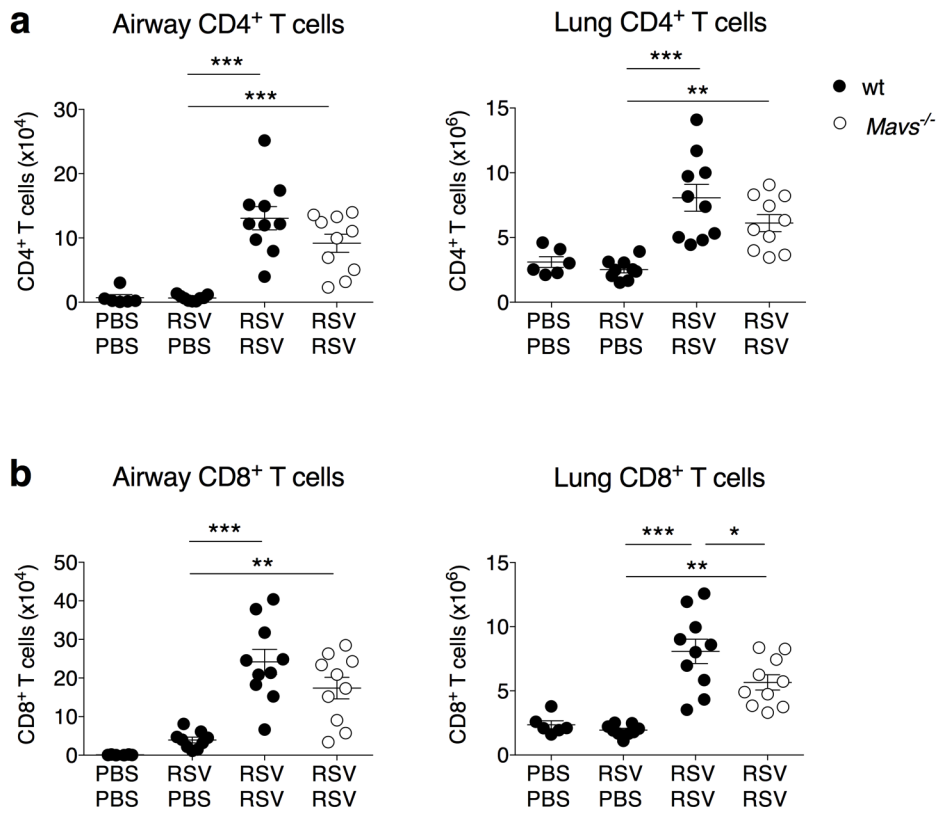

Figure 5.43. *Mavs*$^{-/-}$ mice have fewer lung CD8$^+$ T cells than wt mice following RSV re-challenge. Wt, *Mavs*$^{-/-}$ and *Myd88/Trif*$^{-/-}$ mice were mock (PBS) infected or infected with 7.5 x 10^6 FFU RSV and re-challenged with RSV on day 21. Airway and lung cell populations were analysed by flow cytometry on day 4 following re-challenge (Fig. 4.3 for gating strategy). **a.** Total number of airway and lung CD4$^+$ T cells. **b.** Total number of airway and lung CD8$^+$ T cells. Data are presented as the mean ±SEM of 6 (PBS/PBS), 9 (RSV/PBS) or 10 (RSV/RSV) individual mice, pooled from two independent experiments. Statistical significance of differences was determined by one-way ANOVA with Tukey's post hoc test. * $p \leq 0.05$, ** $p \leq 0.01$, *** $p \leq 0.001$.

Next, we assessed the CD4$^+$ T_{RM} cell response in *Mavs*$^{-/-}$ mice following RSV re-challenge (Fig. 5.44). There was no difference in the number of airway CD4$^+$ T_{RM} cells between the *Mavs*$^{-/-}$ mice and wt mice, however there were fewer CD4$^+$ T_{RM} cells in the lungs of both *Mavs*$^{-/-}$ mice than wt mice on day 4 post RSV re-challenge (Fig. 5.44a). Notably, in both the airways and the lung, the frequency and total number of CD8$^+$ T_{RM} cells detected in *Mavs*$^{-/-}$ mice was reduced as compared to wt mice (Fig. 5.44b – Fig. 5.44d). These data demonstrate that MAVS signalling is required either during the primary infection or secondary infection or both for adequate T_{RM} cell responses following RSV re-challenge.

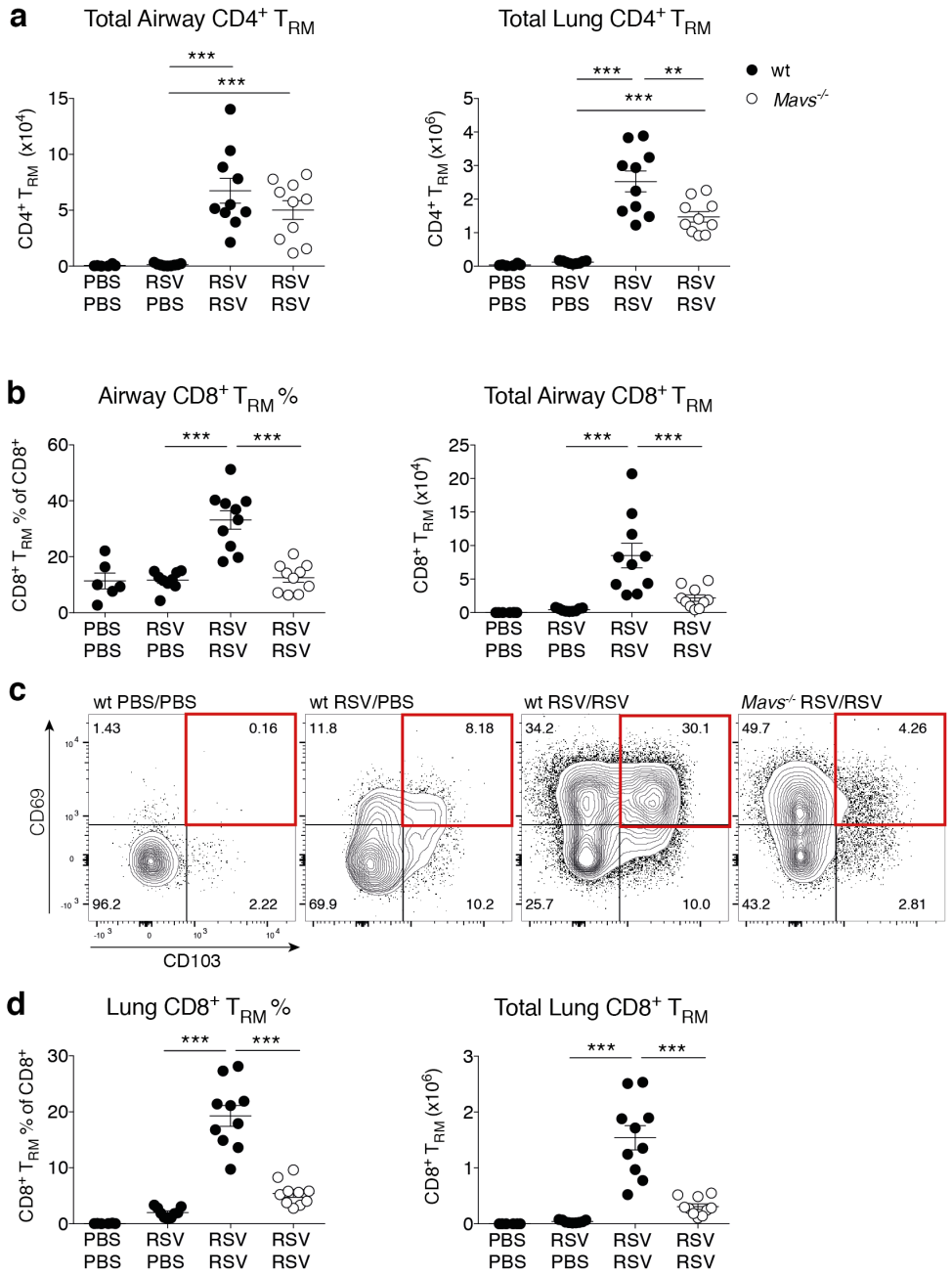

Figure 5.44. Signalling via MAVS is required for the establishment of CD4⁺ and CD8⁺ T_{RM} populations following RSV re-challenge. Wt and *Mavs*$^{-/-}$ mice were mock (PBS) infected or infected with 7.5 x 10^6 FFU RSV and re-challenged with RSV on day 21. Airway and lung cell populations were analysed by flow cytometry on day 4 following re-challenge (Fig. 4.3 for gating strategy). **a.** Total number of airway and lung CD4⁺ T_{RM} cells. **b.** Frequency and total number of airway CD8⁺ T_{RM} cells. **c.** Representative flow cytometry plots showing CD69 and CD103 expression on lung CD8⁺ T_{EM} cells; CD69⁺ CD103⁺ CD8⁺ T_{RM} highlighted in red. **d.** Frequency and total number of lung CD8⁺ T_{RM} cells. Data are presented as the mean ±SEM of 6 (PBS/PBS), 9 (RSV/PBS) or 10 (RSV/RSV) individual mice, pooled from two independent experiments. Statistical significance of differences was determined by one-way ANOVA with Tukey's post hoc test. ** $p \leq 0.01$, *** $p \leq 0.001$.

Sensing of pathogens by PRRs can have a multitude of downstream effects on the immune response. To investigate how MAVS deficiency affected CD45$^+$ cells globally in the lung during RSV infection, the flow cytometry data were analysed using the dimensionality reduction algorithm t-SNE (van der Maaten and Hinton 2008) (Fig. 5.45 and Fig. 5.46). The algorithm clearly identified distinct clusters of CD45$^+$ events. Manual gates (Fig. 4.3) were overlaid and confirmed that this approach identified similar cell populations to those which were defined using the manual gating strategy (Fig. 5.45 and Fig. 5.46). Furthermore, this approach illustrated that the major difference in the lung T cell populations in the *Mavs*$^{-/-}$ mice as compared to wt mice during RSV re-challenge was the reduction in the number of CD8$^+$ T_{RM} cells (Fig. 5.45 and Fig. 5.46). The other lung cell populations appeared similar between the *Mavs*$^{-/-}$ mice and the wt mice. When lung CD8$^+$ T cells were further analysed using t-SNE, this also clearly highlighted the reduction in CD8$^+$ T_{RM} cells in the lungs of *Mavs*$^{-/-}$ mice as compared to wt mice during RSV re-challenge (Fig. 5.46).

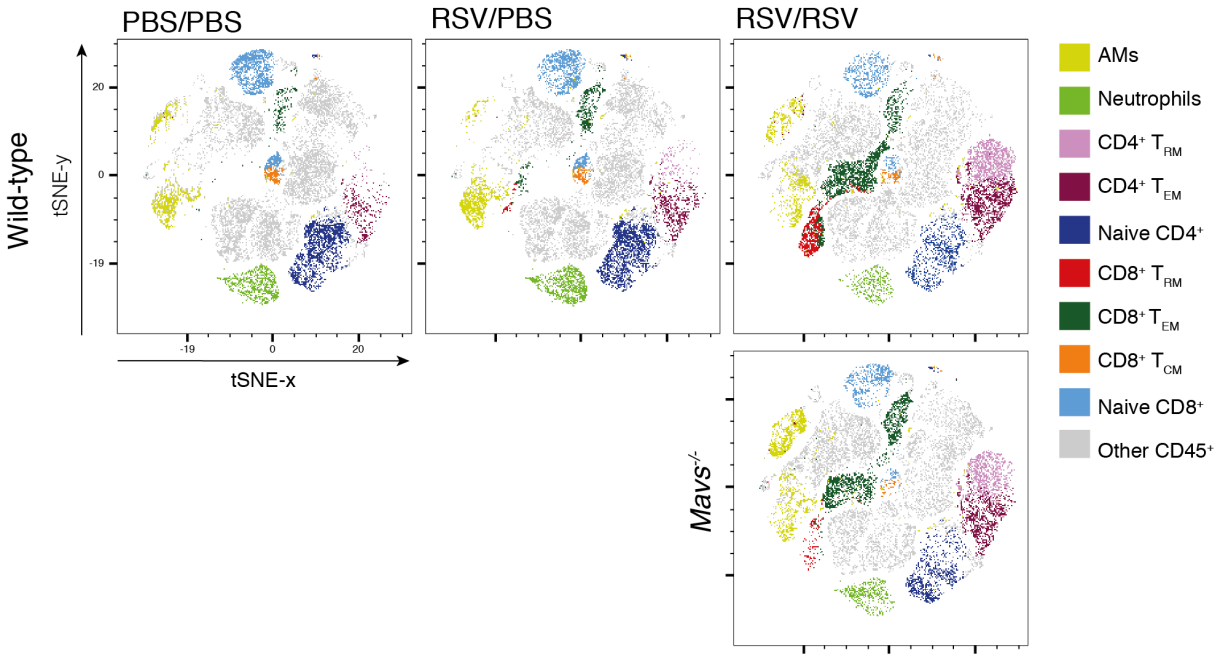

Figure 5.45. Dimensionality reduction algorithm t-SNE confirms manual gating strategy correctly identifies distinct memory T cell populations in wt and *Mavs*$^{-/-}$ mice during RSV re-challenge. Wt and *Mavs*$^{-/-}$ mice were mock (PBS) infected or infected with 7.5 x 10^6 FFU RSV and re-challenged with RSV on day 21. Lung cell populations were analysed by flow cytometry on day 4 following re-challenge (Fig. 4.3 for gating strategy). The t-SNE algorithm was used to analyse live, single, CD45$^+$ cells based on Ly6G, CD3, CD4, CD8, CD62L, CD44, CD69, CD103, IFN-γ and GrzmB expression. Manual gates (Fig. 4.3 for gating strategy) were overlaid onto clusters. Each plot represents 15,000 live, single, CD45$^+$ cells pooled from 3 individual mice per group, from one independent experiment.

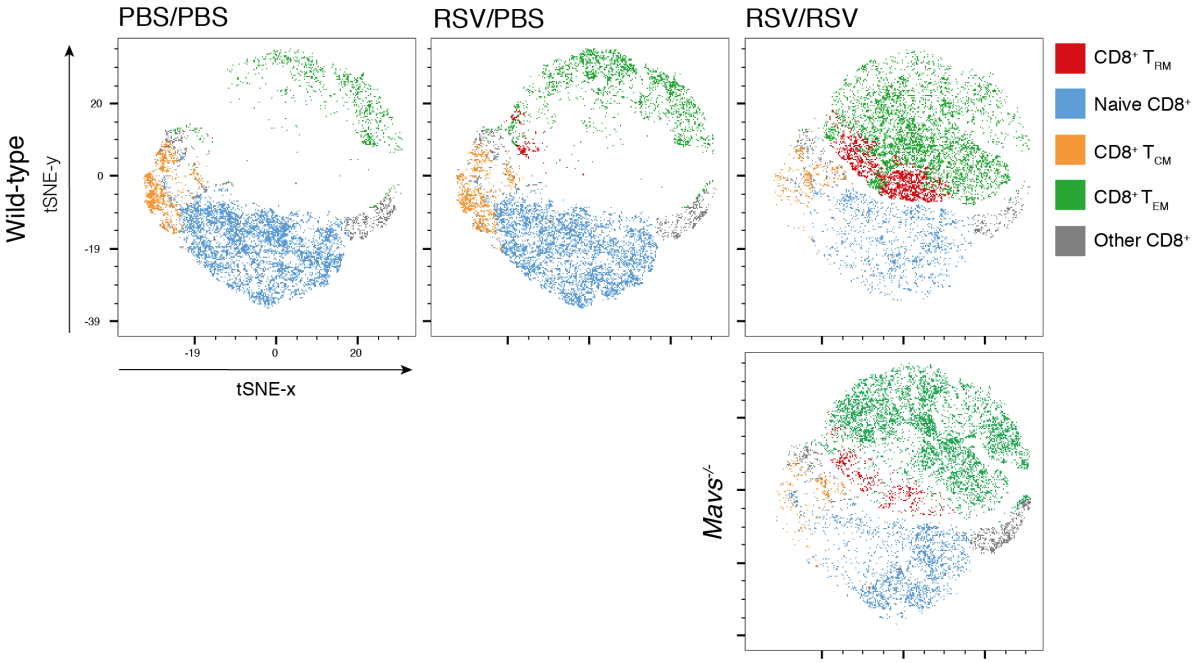

Figure 5.46. Dimensionality reduction algorithm t-SNE confirms that signalling via MAVS is required for the establishment of CD8⁺ T_{RM} cells following RSV re-challenge. Wt and *Mavs*$^{-/-}$ mice were mock (PBS) infected or infected with 7.5 x 10^6 FFU RSV and re-challenged with RSV on day 21. Lung cell populations were analysed by flow cytometry on day 4 following re-challenge (Fig. 4.3 for gating strategy). The t-SNE algorithm was used to analyse live, single, CD45⁺, CD3⁺, CD8⁺ cells based on CD62L, CD44, CD69, CD103, IFN-γ and GrzmB expression. Each plot represents 9000 live, single, CD45⁺, CD3⁺, CD8⁺ cells pooled from 3 individual mice per group, from one independent experiment.

To investigate whether MAVS signalling affected the functional ability T_{RM} cells to produce anti-viral cytokines following RSV re-challenge, airway and lung cells were stimulated *ex vivo* with an RSV-specific CD8⁺ T cell peptide and intracellular cytokine staining for IFN-γ and GrzmB was performed (Fig. 5.47). The airway CD8⁺ T_{RM} cells of *Mavs*$^{-/-}$ mice were impaired in their ability to produce both GrzmB and IFN-γ; there was a lower frequency of GrzmB⁺ and IFN-γ⁺ CD8⁺ T_{RM} cells in the airways of *Mavs*$^{-/-}$ mice on day 4 post RSV re-challenge following re-stimulated with RSV M peptide (Fig. 5.47a). In the lung, the CD8⁺ T_{RM} cells of *Mavs*$^{-/-}$ mice were not impaired in their ability to produce GrzmB following re-stimulation but were impaired in their ability to produce IFN-γ, as compared to wt RSV/RSV infected mice (Fig. 5.47b and Fig. 547c). Overall, there were much fewer GrzmB⁺ and IFN-γ⁺ CD8⁺ T_{RM} cells in total in the lungs of RSV/RSV infected *Mavs*$^{-/-}$ mice as compared to wt mice (Fig. 5.47d). This difference was largely driven by the fact there were fewer lung CD8⁺ T_{RM} cells present overall at this time point following RSV re-challenge (Fig. 5.44). Together, these data demonstrate that MAVS signalling is required for a functional T_{RM} cell response during RSV re-challenge.

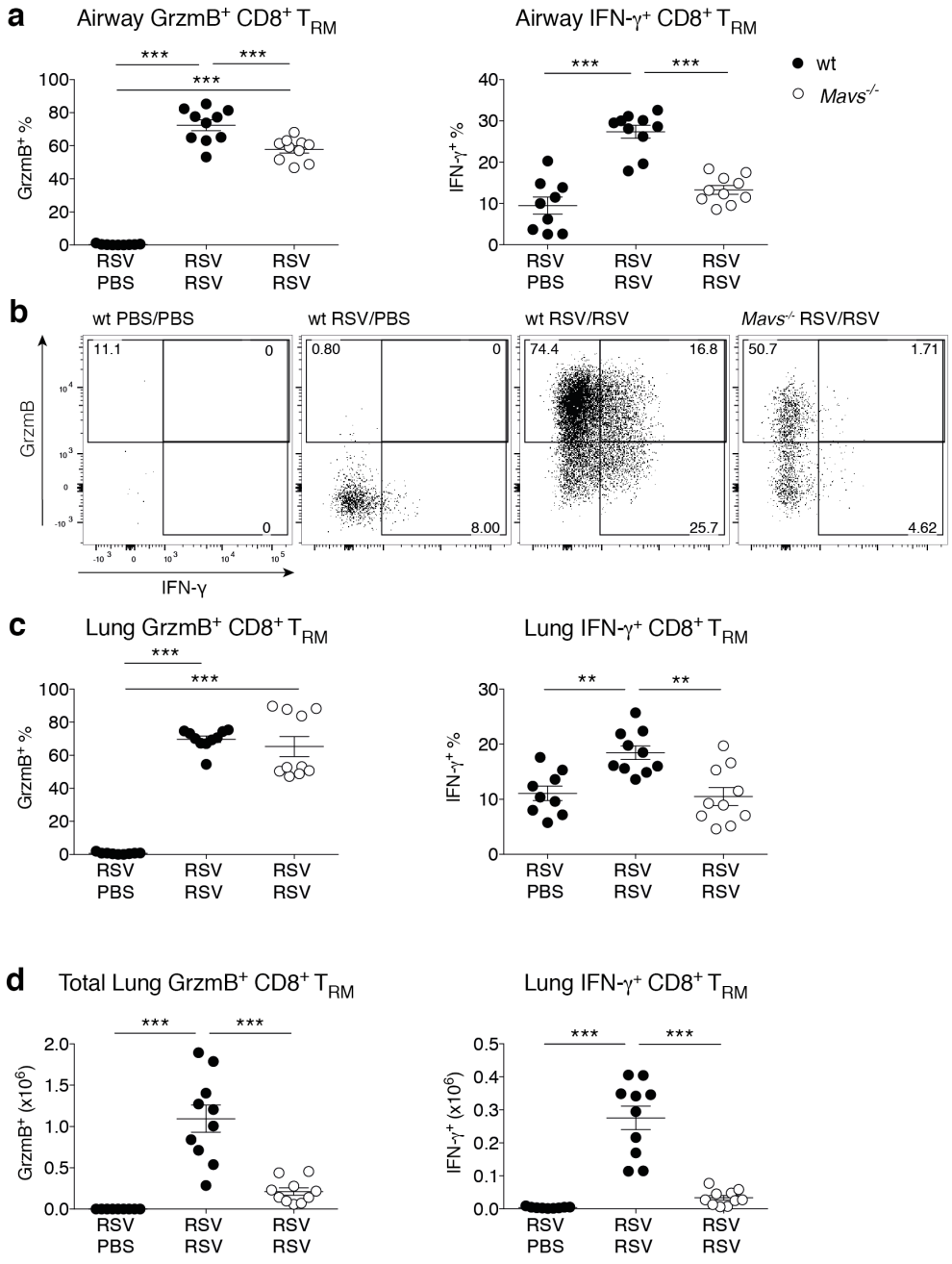

Figure 5.47. *Mavs*$^{-/-}$ mice have impaired CD8$^+$ T$_{RM}$ cytokine production following RSV re-challenge. Wt and *Mavs*$^{-/-}$ mice were mock (PBS) infected or infected with 7.5 x 10^6 FFU RSV and re-challenged with RSV on day 21. Airway and lung cell populations were analysed by flow cytometry on day 4 following re-challenge (Fig. 4.3 for gating strategy). For detection of intracellular cytokines, lung cells were stimulated with RSV M peptide. **a.** Frequency of GrzmB$^+$ and IFN-γ$^+$ airway CD8$^+$ T$_{RM}$ cells. **b.** Representative flow cytometry plots showing GrzmB and IFN-γ expression on lung CD8$^+$ T$_{RM}$ cells. **c.** Frequency of GrzmB$^+$ and IFN-γ$^+$ lung CD8$^+$ T$_{RM}$ cells. **d.** Total number of GrzmB$^+$ and IFN-γ$^+$ lung CD8$^+$ T$_{RM}$ cells. Data are presented as the mean ±SEM of 6 (PBS/PBS), 9 (RSV/PBS) or 10 (RSV/RSV) individual mice, pooled from two independent experiments. Statistical significance of differences was determined by one-way ANOVA with Tukey's post hoc test. Only significant differences between RSV re-challenged mice are shown. ** $p \leq 0.01$, *** $p \leq 0.001$.

5.3.6 Discussion

In this chapter, the role of innate immunity in shaping the development and functionality of the T_{RM} cell response was investigated during RSV infection. Neutrophil depletion throughout the primary RSV infection demonstrated that neutrophil recruitment during the primary infection does not have a major role in the development of functional $CD4^+$ or $CD8^+$ T_{RM} cells in the lung during RSV re-challenge. However, MAVS signalling was required for the formation of a functional $CD8^+$ T_{RM} cell response in the lung during memory immunity to RSV.

To study memory T cells, mice were infected with RSV and then re-challenged with RSV 21 days later. Previously published studies on memory T cell responses during RSV infection in mice have also allowed 21 days for the primary infection to resolve before re-infection (Kinnear *et al.* 2018). At 21 days post RSV infection there is no detectable replicating virus (Chávez-Bueno *et al.* 2005). Plaque assay titration of RSV in the BAL and in the lungs of RSV-infected mice has shown that replication-competent virus is undetectable from day 9 p.i. (Chávez-Bueno *et al.* 2005). Furthermore, the adaptive immune response is thought to have resolved as there is no difference in the number of RSV specific $CD8^+$ T cells in the airways or lungs between days 21 and 28 post RSV infection (Knudson *et al.* 2014; Lukens *et al.* 2010). In our experiments, the viral load did not increase from day 1 following RSV re-challenge and by day 4 the quantity of viral genome detectable by RT-qPCR was close to the detection limit of the assay and comparable to mice which had been infected 25 days earlier (Fig. 5.30b). However, we suspect live virus was cleared long before day 25 p.i. during the primary infection (RSV/PBS mice) and by day 4 post RSV re-challenge (RSV/RSV mice). The viral load did not increase from day 1 post re-challenge, unlike during a primary RSV infection (Goritzka *et al.* 2014). This suggests that viral replication was unable to occur during RSV re-challenge due to the efficiency of the humoral and cellular memory immune response (Shafagati and Williams 2018; Kinnear *et al.* 2018; Chiu and Openshaw 2015). It has previously been shown that RSV infection in a secondary infection is efficiently controlled (Kinnear *et al.* 2018). Mice develop an RSV-specific antibody response that will decrease the infection rate (Shafagati and Williams 2018; Kinnear *et al.* 2018; Chiu and Openshaw 2015). However, the infection is sufficient to elicit memory T cell responses (Kinnear *et al.* 2018).

Initially, AMs and neutrophils in the airways and lungs were characterised over time during RSV re-challenge. Notably, neutrophils were also recruited to the lungs early after re-infection but only half the number (1.5×10^6) were recruited as compared to during the primary RSV infection (3×10^6) at 24 h p.i. (Fig. 5.1). Both $CD4^+$ T_{EM} and $CD8^+$ T_{EM} cells drastically expanded

from day 3 following RSV re-challenge, with the greatest number observed in the lungs on day 4 post RSV re-challenge (Fig. 5.33 and Fig. 5.34). The gene expression of the T cell chemokines CXCL9 and CXCL10 peaked earlier, at day 1 post re-challenge. It has previously been shown that $CD8^+$ T cell depletion during RSV re-challenge heightens disease severity and that the transfer of $CD8^+$ airway cells from an RSV-experienced mouse can protect against RSV disease in the absence of RSV-specific antibodies (Kinnear *et al.* 2018). Although both $CD4^+$ and $CD8^+$ T_{RM} cells expanded from day 3 post re-challenge, with the greatest number of both subsets observed on day 4, the proliferation kinetics differed between these two T_{RM} cell subsets. There was no increase in the frequency of $CD8^+$ T_{RM} cells in RSV/RSV infected mice until after day 3 post re-challenge, when there was a drastic expansion of this population detected on day 4. Unlike $CD8^+$ T_{RM} cells, the frequency of $CD4^+$ T_{RM} cells expanded after day 1 post re-challenge as compared to RSV/PBS infected mice. Furthermore, the frequency of $CD4^+$ T_{RM} as a percentage of $CD4^+$ T_{EM} did not change drastically over time following RSV re-challenge. These data suggest that there is a population of $CD4^+$ T_{EM} cells which are not T_{RM} cells which also increase in number in the lung over time. However, these data are limited by the fact that $CD4^+$ T_{RM} cells are only distinguished from T_{EM} cells by the expression of CD69, which is also a T cell activation marker (Ziegler *et al.* 1994). Further cell surface markers of residency on $CD4^+$ T memory cells are needed to study this population fully. Nonetheless, these data may suggest that the initial proliferation of $CD4^+$ T_{RM} cells happens very rapidly within the first day of pathogen re-encounter. On the contrary, the increase in the number of $CD8^+$ T_{EM} cells was predominantly driven by the expansion of $CD8^+$ T_{RM} cells on day 4 post re-challenge suggesting $CD8^+$ T_{RM} cells make up the vast majority of $CD8^+$ T_{EM} cells in the lung during RSV re-challenge.

T_{RM} cells are classically defined by their location; these cells never re-enter the circulation instead they reside locally in the organ the infectious insult occurred within (Jiang *et al.* 2012; Masopust *et al.* 2010; Masopust *et al.* 2001). Upon pathogen re-encounter in these tissues, T_{RM} cells are able to rapidly exert antigen-specific effector functions to clear the pathogen (Pizzolla *et al.* 2017; Schenkel and Masopust 2014). We expected to detect the small population of inactive $CD4^+$ and $CD8^+$ T_{RM} cells in the lungs of RSV/PBS infected mice by flow cytometry. There was no difference in the frequency or number of $CD4^+$ or $CD8^+$ T_{RM} cells quantified from the lungs of RSV/PBS control infected mice when compared to PBS/PBS control infected mice but both T_{RM} cell populations could be observed visually by flow cytometry staining. Even though the populations could be observed, as both the $CD4^+$ and $CD8^+$ T_{RM} cell populations are so small prior to proliferation upon pathogen re-encounter, this

difference would have required a large number of mice per group to achieve statistical significance.

There is extensive debate in the literature about the appropriateness of the cell surface markers used to identify T_{RM} cells (Schenkel and Masopust 2014). CD69 is a transmembrane lectin-protein and a T cell activation marker (Ziegler *et al.* 1994) which inhibits S1P-mediated T cell migration into the blood. Gradients of S1P, a sphingolipid metabolite (Spiegel and Milstien 2011; Baeyens *et al.* 2015), regulate lymphocyte trafficking between the vasculature, lymph nodes and peripheral tissues by binding of the receptor S1PR1 (Skon *et al.* 2013; Spiegel and Milstien 2011). Cell surface expression of CD69 binds S1PR1 causing its internalisation from the cell surface membrane and degradation - this retains T cells in peripheral tissues by preventing migration towards S1P gradients in the blood (Mackay *et al.* 2015; Shiow *et al.* 2006; Bankovich *et al.* 2010). CD103 (integrin αE) is a receptor for E-cadherin which therefore tethers T cells to the epithelium (Karecla *et al.* 1995; Cepek *et al.* 1994). The challenge has been to distinguish T_{EM} cells in the tissue which may upregulate CD69 and CD103 during an infection from T_{RM} cells which never re-enter the circulation but expand locally. In the US, parabiosis experiments have been used to confirm CD69 and CD103 as appropriate cell surface markers to identify T_{RM} cells in various infectious diseases (Schenkel *et al.* 2014; Van Braeckel-Budimir *et al.* 2018; Fernandez-Ruiz *et al.* 2016). As parabiosis is not legal in the UK, an alternative experimental approach was adopted here using the drug FTY720 to confirm the gating strategy for both $CD4^+$ and $CD8^+$ T_{RM} cells in the lungs after RSV re-challenge. FTY720 removes T cells from the vasculature by internalisation of S1PR1, retaining circulating T cells in the lymph nodes. There is some disagreement in the literature over whether all T_{EM} cells express S1PR1, however it was recently shown during influenza virus infection that $CD44^+$, $CD69^-$ T_{EM} cells in the lungs do express *S1pr1* (Takamura *et al.* 2016).

Interestingly, FTY720 treatment also demonstrated that at day 4 post RSV re-challenge, when the numbers of lung neutrophils are comparable to naïve mice, all neutrophils were in the vasculature of the lung and not in the lung. This sheds light on the origin of the 5% lung neutrophils always observed in naïve mice throughout this work and highlights that perfusion of the lung during tissue harvest is not able to completely remove circulating cells. FTY720 treatment of mice during RSV re-challenge also demonstrated that the gating strategy used in this study correctly identifies both $CD4^+$ and $CD8^+$ T_{RM} cells. There was no difference in the total number of $CD4^+$ or $CD8^+$ T_{RM} cells detected in the airways or the lung of control treated mice as compared to FTY720 treated mice during RSV re-challenge. There were fewer $CD4^+$

T_{EM} cells in the lungs of FTY720 treated mice as compared to control treated mice during RSV re-challenge, supporting the earlier observation that there is a significant subset of $CD4^+$ T_{EM} cells recruited to the lung which are not T_{RM} cells. There was no difference in the total number of $CD8^+$ T_{EM} between drug and control treated RSV/RSV infected mice which also further strengthens the earlier observation that $CD8^+$ T_{RM} cells make up the vast majority of $CD8^+$ T_{EM} in the lungs during RSV re-challenge. However, the gating strategy used to identify $CD8^+$ T_{RM} cells is likely too conservative; there was a subset of $CD8^+$ T_{EM} cells which were $CD69^+$ and $CD103^-$ which were not removed from the lungs during RSV re-challenge by FTY720 treatment. These cells were also detected, albeit at a low frequency, in the lungs of RSV/PBS infected mice on day 4 following RSV re-challenge. CD103 expression has been demonstrated to be required for T_{RM} cell retention in the brain (Wakim *et al.* 2010), skin (Mackay *et al.* 2013), intestinal epithelium (Casey *et al.* 2012) and in the lung (Lee *et al.* 2011). However, distinct $CD103^+$ and $CD103^-$ $CD8^+$ T_{RM} cell populations have been described in the small intestine during *Yersinia pseudotuberculosis* infection (Bergsbaken and Bevan 2015). The two subsets of $CD8^+$ T_{RM} cells were shown to require different developmental signals and to localise to different locations in the intestine - $CD103^-$ T_{RM} cells were most abundant in the lamina propria. The development of a $CD103^-$ T_{RM} population in the lamina propria of the intestine was dependent on inflammatory signals, not antigen (Bergsbaken and Bevan 2015). However, CD103 expression on long-lived $CD8^+$ T cells in the lung was dependent on antigen presentation during influenza virus infection (Lee *et al.* 2011). It would be of great interest to further investigate whether the $CD103^-$ $CD69^+$ $CD8^+$ T_{EM} cell population identified in the lung in this study is a true T_{RM} cell population. During *Y. pseudotuberculosis* infection, this population was shown to be important for bacterial control and it would be of great interest to explore whether this population is also important in viral defence.

The molecular and immunological mechanisms underpinning T_{RM} cell formation and development remain poorly understood. It was only recently shown that T_{EM} cells develop from effector T cells which differentiate during the primary infection, as opposed to from naïve T cells (Youngblood *et al.* 2017; Akondy *et al.* 2017). However, the signals which determine whether a T_{EM} cell will differentiate into a circulating T_{EM} cell or a T_{RM} cell are still not known. Neutrophil depletion throughout the primary RSV infection had no major impact on the number of T_{RM} cells detected in the lung following RSV re-challenge, or on the quality of the $CD8^+$ T_{RM} cell response as assessed by cytokine production. This is perhaps not surprising as neutrophil depletion did not affect the number of $CD4^+$, $CD8^+$ or antigen-specific $CD8^+$ T cells recruited to the lung on day 8 during the primary infection (Fig. 5.23). Conversely, during influenza virus

infection, early lung neutrophilia did influence the recruitment of anti-viral $CD8^+$ T cells to the lung (Lim *et al.* 2015; Tate *et al.* 2012). However, although neutrophil depletion in influenza virus infection disrupted $CD8^+$ T cell recruitment, it did not disrupt the formation of a functional T_{RM} cell population (Reilly *et al.* 2016).

This project also found that even though *Mavs*$^{-/-}$ mice had higher viral loads during primary RSV infection (Fig. 5.24) they still had impaired T_{RM} cell responses during RSV re-challenge. Together, these studies show that the magnitude of virus in the lung during the primary infection does not necessarily translate to the formation of function T_{RM} cells and that additional signals are be required for T_{RM} cell development. It is not clear from this work whether MAVS signalling is required during the primary infection, secondary infection or both for appropriate T_{RM} cell responses during RSV re-challenge. In future work it would be interesting to determine whether the T_{RM} cell populations of RSV-experienced *Mavs*$^{-/-}$ mice are comparable to wt mice prior to RSV re-encounter, or whether the impairment is in the ability of these cells to proliferate during RSV re-encounter. During primary RSV infection, MAVS signalling is required for the production of type I IFNs which drives a downstream signalling cascade leading to the production of pro-inflammatory mediators such as IL-6 and TNF-α and the recruitment of $CD64^+$ inflammatory monocytes (Goritzka *et al.* 2014; Goritzka, Makris, *et al.* 2015; Bhoj *et al.* 2008; Demoor *et al.* 2012). The induction of the pro-inflammatory environment also provides the correct signals to activate lung neutrophils during RSV infection (Kirsebom *et al.* 2019). In future work it would be interesting to investigate whether the defect in T_{RM} cell responses in *Mavs*$^{-/-}$ mice is due to the lack of type I IFN responses during the primary infection.

Previously published work from the group has shown that even *Mavs/Myd88/Trif*$^{-/-}$ mice recruit T cells to the lung during RSV infection (Goritzka, Pereira, *et al.* 2015). A study by Bhoj *et al.* found that activated, $CD86^{high}$ cDCs were present in the mediastinal lymph nodes draining the lung even in the absence of MAVS and MyD88 signalling (Bhoj *et al.* 2008). Bhoj *et al.* hypothesise that this cell population most likely facilitates the recruitment of effector T cells to the lung in the absence of other innate immune signals (Bhoj *et al.* 2008). It is not known whether antigen presentation by DCs is involved in the differentiation pathways of functional T_{RM} cells but this would be interesting to investigate further in the future. In this study, *Mavs*$^{-/-}$ mice had increased viral loads on day 2 and day 4 post RSV re-challenge, as compared to wt mice. However, this study has not addressed whether the lack of viral control was due to the deficiency in the T_{RM} cell response. Previously in the lab, antibody production during RSV infection has been investigated in *Mavs*$^{-/-}$ mice and no differences have been observed in total RSV-specific IgG or IgA, or in the neutralising capacity of RSV-specific antibodies (Nawamin

Pinpathomrat and Harriet Davenport, unpublished). This would suggest that the T_{RM} cell deficiency may be responsible for the observed increase in viral load in the *Mavs*$^{-/-}$ mice. However, another study found that antibody production is defective in *Mavs*$^{-/-}$ mice during RSV infection (Bhoj *et al.* 2008). It is not clear why the data from our lab are not in agreement with this study but it is possible that these discrepancies are due to differences between viral batches. To our knowledge, antibody levels in *Mavs*$^{-/-}$ mice during RSV infection have not been investigated by other groups than Bhoj *et al.* and ourselves. In future studies, a causal relationship between T_{RM} cell deficiency and viral control during RSV re-challenge would need to be confirmed experimentally.

Together, this project demonstrates that innate PRR signalling pathways involved in the detection of RSV have important roles in the formation of appropriate T_{RM} cell responses. Further studies need to be undertaken to understand the mechanism between T_{RM} cell formation and development as this remains a major outstanding question in the field.

6 Discussion and Future work

6.1 Discussion

In this work, the regulation and role of neutrophils during RSV infection was investigated *in vivo*. Mice deficient in MAVS and in MyD88/TRIF signalling were used to investigate the innate signalling pathways regulating neutrophil recruitment and activation in the lung during RSV infection. This study found that these PRR signalling pathways collaborate and are both required for neutrophil recruitment and full activation to occur in the lung early during RSV infection. Furthermore, the role of neutrophils in viral control versus their contribution to disease severity was investigated using two complementary approaches. Neutrophil recruitment was abolished during RSV infection by antibody-mediated neutrophil depletion and was also augmented by treating mice with the neutrophil chemoattractant CXCL1 prior to and during RSV infection. This study demonstrated that neutrophils are not anti-viral but also demonstrated that they do not appear to be major drivers of pathogenesis during RSV infection of adult mice. However, treatment of mice with rCXCL1 prior to RSV infection did drive disease severity, likely in a manner dependent on pathogenic $CD8^+$ T cells. The biological relevance and immunological mechanism regulating this will be of great interest to investigate further in future work.

The first aim of this project was to investigate the mechanism regulating neutrophil recruitment in the lung during RSV infection *in vivo*. *Myd88/Trif*$^{-/-}$ mice, unable to detect RSV via the TLRs nor respond to signalling via the IL-1R or the IL-18R, were unable to recruit neutrophils to the lung during RSV infection demonstrating that signalling via MyD88/TRIF is essential for lung neutrophilia during RSV infection. RSV is thought to be detected by several TLRs including TLR2, TLR3, TLR4, TLR6 and TLR7 (Murawski *et al.* 2009; Kurt-Jones *et al.* 2000; Tal *et al.* 2004; Awomoyi *et al.* 2007) and it is likely recognition of RSV via one of these receptors which initiates neutrophil recruitment as CXCL1 production occurs very early, at 12 h following infection. However, from these data we cannot exclude the possibility that neutrophil recruitment occurs downstream of a DAMP or immune mediator triggering signalling via MyD88/TRIF. The IL-1R and IL-18R also signal via MyD88 however it is less likely that signalling via one of these receptors drives CXCL1 production as IL-1β and IL-1α peak at 12 h and 18 h following RSV infection, respectively (Goritzka *et al.* 2014). It is not clear whether signalling via MyD88 or TRIF is required for neutrophil recruitment but neutrophil impairment during RSV infection in *MyD88*$^{-/-}$ mice has previously been suggested (Murawski *et al.* 2009).

As the *Myd88/Trif*$^{-/-}$ mice are global knockouts, the cell type responsible for the recognition of RSV which then leads to CXCL1 production cannot be determined from this work. CD45^{-} non-epithelial, non-endothelial stromal cells were found to be the major source of CXCL1 during RSV infection. However, it is not necessarily the same cell type that recognises RSV which then goes on to produce CXCL1; there may be an intermediate mediator required. Data from the lab has found that mouse primary fibroblasts produce CXCL1 when stimulated with RSV *ex vivo* (Fahima Kausar, unpublished), however it is not yet known whether fibroblasts also produce CXCL1 in response to RSV *in vivo*. Furthermore, there are many other neutrophil chemoattractants which likely have a role in the recruitment of neutrophils to the lung during RSV infection in combination with CXCL1. This is evident as *Mavs*$^{-/-}$ mice recruited neutrophils but did not express high levels of *Cxcl1*, *Cxcl2* or *Cxcl5* in the airways during RSV infection.

It would be interesting in the future to expand on this work and investigate whether factors such as C5a, fMLP, PAF and LTB4 (Amulic *et al.* 2012; Kolaczkowska and Kubes 2013) also play a role in neutrophil recruitment during RSV infection. It would also be interesting to investigate whether the different MyD88/TRIF-dependent PRRs collaborate to induce chemoattractant production, whether the cellular source of other neutrophil chemoattractants is the same as for CXCL1 and which stromal cell type in the "other" stromal cell compartment is responsible for neutrophil recruitment. In this work, the involvement of the lung and gut microbiomes in shaping immune responses to RSV were not investigated. However, studies using germ-free mice have shown that commensal bacteria have an important role in shaping the expression of TLRs on intestinal epithelial cells (Huhta *et al.* 2016; Hörmann *et al.* 2015; Round and Mazmanian 2014). The microbiome in the lung has been less well studied than the gut microbiome, however it was also shown that the microbial composition in the lower airways can influence alveolar macrophage TLR4 responses (Segal *et al.* 2016). It would be interesting in future work to investigate whether commensal bacteria regulate PRR signalling in the airways in a manner which influences neutrophil recruitment and activation. It is well known that short-chain fatty acids, products of bacterial fermentation in the gut, have important roles in regulating different aspects of the immune response (Tan *et al.* 2014; Ríos-Covián *et al.* 2016). During influenza virus infection, it was shown in a mouse model of disease that a high-fibre diet restricted the production of CXCL1 in the lungs, leading to reduced neutrophil recruitment and limiting neutrophil-driven lung pathology (Trompette *et al.* 2018). Mice fed a high-fibre diet exhibited altered bone marrow haematopoiesis which enhanced the number of patrolling Ly6C^{-} monocytes. This in turn enhanced the number of alternatively activated macrophages which are the major producers of CXCL1 during influenza virus infection

(Trompette *et al.* 2018). Although macrophages do not appear to be the major source of CXCL1 in the lungs during RSV infection (Kirsebom *et al.* 2019), it would be interesting in future work to investigate whether short-chain fatty acids also regulate the immune response during RSV infection in a manner which influences neutrophil recruitment and/or activation.

The second aim of this project was to investigate the signals which are required to drive neutrophil activation in the lung during RSV infection. This study found that it is most likely a host-derived pro-inflammatory factor (or combination of factors) induced downstream of MAVS signalling which activates lung neutrophils during RSV infection. *Mavs*$^{-/-}$ mice, unable to detect RSV in the cytosol via the RLRs (Goritzka, Makris, *et al.* 2015; Bhoj *et al.* 2008; Demoor *et al.* 2012), were able to recruit neutrophils in response to RSV but the neutrophils recruited into the lungs of *Mavs*$^{-/-}$ mice did not become activated. Restoration of the pro-inflammatory environment in the lungs of *Mavs*$^{-/-}$ mice by treatment with rIFN-α following RSV infection was sufficient to at least partially activate neutrophils, as measured by the upregulation of cell surface CD64 and by the secretion of MPO into the airways. This suggests it is unlikely that signalling via MAVS on the neutrophils themselves is required for neutrophil activation during RSV infection. However, as these mice did not display significantly more MMP-9 and NE levels in the BAL than mock-treated *Mavs*$^{-/-}$ mice, it cannot be completely excluded that MAVS signalling is required on neutrophils for full neutrophil activation. These data also suggest that RSV itself does not directly activate neutrophils as *Mavs*$^{-/-}$ mice had higher viral loads than wt mice throughout the RSV infection but their neutrophils were not of an activated phenotype. As treatment of *Mavs*$^{-/-}$ mice with rIFN-α was sufficient to drive at least partial neutrophil activation, our data demonstrate that the lack of neutrophil activation was likely due to their inability to mount a pro-inflammatory immune environment as driven by the production of type I IFNs (Goritzka *et al.* 2014; Goritzka, Makris, *et al.* 2015; Bhoj *et al.* 2008; Demoor *et al.* 2012). This was further supported by the finding that neutrophils recruited into the lungs of *Myd88/Trif*$^{-/-}$ mice using rCXCL1 during RSV infection were able to become fully activated. Therefore, this study demonstrates that neutrophil activation during RSV infection is at least in part mediated by IFN-α or, more likely, by a factor or combination of the hundreds of factors induced downstream of type I IFN signalling via the IFNAR (Goritzka *et al.* 2014).

To investigate the precise factor required for neutrophil activation, bone marrow neutrophils were stimulated *ex vivo* with pro-inflammatory mediators, however no biologically relevant factor was able to induce neutrophil degranulation. Neutrophil activation is heavily regulated and requires multiple priming steps which occur during their extravasation from the circulation into the infected tissues (Amulic *et al.* 2012; Kolaczkowska and Kubes 2013). It is likely that

the bone marrow neutrophils used in this model system are too immature and un-primed to become activated. Neutrophil recruitment, priming and activation is a heavily regulated and complex process involving many contributing chemical and physical triggers (Amulic *et al.* 2012; Kolaczkowska and Kubes 2013). Many neutrophil chemokines can activate as well as recruit neutrophils, depending on their concentration gradient in the tissue (Amulic *et al.* 2012; Ley 2002). It is interesting that although *Mavs*$^{-/-}$ mice only recruited slightly fewer neutrophils into the lumen of the airways at 18 h post RSV infection than wt mice, no protein degranulation products were detected in the airways. This suggests that the neutrophil recruiting chemoattractants in *Mavs*$^{-/-}$ mice were not sufficient to initiate their degranulation and that there was an absolute requirement for a MAVS-dependent factor in the lung environment. It was not feasible to sort lung neutrophils from naïve mouse lungs as there are such few neutrophils present in a naïve lung, but it would be interesting to explore alternative experimental approaches to the *ex vivo* stimulation model in order to investigate the neutrophil-activating factor more fully in the future. IFN-α production requires MAVS signalling in AMs (Goritzka, Makris, *et al.* 2015), however AMs do not produce all the pro-inflammatory mediators induced in the lung during RSV infection (Makris *et al.* 2016). Following identification of the factor/s required for neutrophil activation, it would be interesting to investigate which cell types produce these mediators. It would also be interesting to investigate whether the production is dependent on the ability of these cells to respond to type I IFNs as would be expected from this work; this could be investigated in *Ifnar1*$^{-/-}$ mice.

The third and fourth aims of this project both relate to understanding the role of neutrophils during RSV infection *in vivo*. The third aim was to investigate whether neutrophils are anti-viral and the fourth aim was to investigate whether neutrophils contribute to disease severity. Neutrophil recruitment did not appear to be beneficial to the host during RSV infection as neutrophil depletion had no effect on viral load. Furthermore, neutrophil depletion did not impair the formation of memory immune responses. These data suggest that neutrophils are neither directly anti-viral, nor do they contribute indirectly to the anti-viral effector functions of other immune cells in the lung. Neutrophil depletion as a technique has the limitation that it removes all effects of neutrophils; some of which may be good and some which may be detrimental during the immune response. While neutrophils can contribute to disease, it is increasingly well appreciated that neutrophils can be beneficial - for example, during resolution (Mayadas *et al.* 2014; Deniset and Kubes 2016). As such, subtle effects of neutrophils may not be observed using neutrophil depletion. Nonetheless, overall these data suggest that the first hypothesis - that neutrophils are anti-viral and benefit the host, can be rejected in

agreement with existing literature (Stokes *et al.* 2013) as a large effect on viral load was not observed when neutrophils were removed.

The second hypothesis - that neutrophil recruitment to the lung during RSV infection drives disease severity, was more difficult to prove or disprove. Neither neutrophil depletion nor the augmentation of neutrophil recruitment to the lungs following RSV infection affected disease severity as measured by weight loss. Weight loss is a crude measure of disease severity and is it possible that lung damage occurred but was not reflected in the weight of the mice during RSV infection. Nonetheless, the results from this study suggest that the second hypothesis - that neutrophil activation in the lung heightens disease severity, can also be rejected for the adult mouse model of RSV disease. It must be considered that the mouse model of RSV infection may not recapitulate this aspect of RSV disease as observed in human infants. It is still possible that over-exuberant airway neutrophilia can contribute to disease severity during RSV-induced lower airway disease in infants, especially since neutrophils do not appear to benefit the host by contributing positively to anti-viral immunity, as shown in this work and by others (Stokes *et al.* 2013).

Despite the findings of this study that neutrophils do not drive disease severity, clinical observational studies of infants with severe RSV-induced lower airway disease have repeatedly demonstrated that neutrophils are extremely abundant in the lungs of infants (Abu-Harb *et al.* 1999; Marguet *et al.* 2008; Everard *et al.* 1994; McNamara 2003). Furthermore, whole blood transcriptomics have also suggested that genes regulated to neutrophil function are dysregulated during severe RSV disease in infants (Mejias *et al.* 2013) and that IL-8 alleles which pre-dispose individuals to heightened neutrophilia are associated with families in which an infant has been hospitalised with RSV-induced lower airway disease (Hull *et al.* 2000). Developmental differences likely affect disease susceptibility to RSV; age is the greatest risk factor in whether a person will develop severe disease (Hall *et al.* 2009; Murray *et al.* 2014; García *et al.* 2010; Lambert *et al.* 2014). More specifically, in new-born children, prematurity is a major risk factor for severe disease (Shi *et al.* 2015; Aujard and Fauroux 2002; Resch *et al.* 2019; Lambert *et al.* 2014). This may be due to the fact that the lungs are not fully developed at the time of birth (Narayanan *et al.* 2012; Herring *et al.* 2014). Neutrophils also continue to develop following birth; it is common for premature infants to experience transient neutropenia and this heightens their susceptibility to many infections (Nittala *et al.* 2012). Neutropenia has been observed in infants with RSV-induced disease, although it is not clear whether this is a cause or effect of the viral infection (Karavanaki *et al.* 2006). Unfortunately, the murine RSV infection model is very difficult to adapt to study disease in the context of developing immunity

as data from our lab and others has shown that neonatal mice are hyporesponsive to RSV during the primary infection (Spyridon Makris, unpublished). In line with this, neonatal mice do not elicit cytokine responses during stimulation with PRR agonists including poly(I:C), LPS or CpG (Spyridon Makris, unpublished). During primary RSV infection, neonatal mice do not develop disease as measured by weight loss and the infection does not recapitulate the extreme airway neutrophilia observed in severe disease of human infants (Tregoning *et al.* 2008; You *et al.* 2015). It is very challenging to conduct clinical studies of RSV infection, in part as infants are so difficult to obtain samples from, but more studies are needed to fully understand whether neutrophils contribute to disease severity during RSV-induced lower airway disease of human infants.

Together, the findings from this study suggest that neutrophil recruitment and activation in the lung has no beneficial effect on reducing RSV viral load in the lungs. Although we did not observe a pathogenic effect of neutrophil recruitment and activation in the adult mouse model of RSV infection, from this study we cannot rule out that neutrophils do not cause pathogenesis in human infants. It is possible that, in the future, therapies such as CXCR2 blockers could be used to restrict the over-exuberant influx of neutrophils into the airways which appears to overload the human infant lung during severe RSV disease. A difficulty with this approach would be the time point at which to give the treatment as neutrophil recruitment has usually already occurred at the point at which infants present with symptomatic disease. It would likely be very risky to give CXCR2 blockers prophylactically to infants at high risk of severe RSV disease as these drugs inhibit the inflammatory response. This would likely make infants very vulnerable to other bacterial and viral infections (Stadtmann and Zarbock 2012). An alternative approach could involve blocking neutrophil activation in the lung during severe disease to limit tissue pathology. The drug 6-hydroxy-5,7-dimethoxy-flavone (UFM24) was found to inhibit oxidative burst, but not NE release, by fMLP-stimulated human neutrophils (Tsai *et al.* 2017). In a mouse model of LPS-induced acute lung injury, UFM24 attenuated MPO activity (Tsai *et al.* 2017). Future work would be needed to understand which aspect of neutrophil activation is most likely to drive lung pathology in human infants in order to better be able to target the harmful effects of neutrophil activation.

An unexpected finding from this study, which does not relate to either of the two original hypotheses, was that instillation of the neutrophil chemoattractant rCXCL1 into the airways of mice prior to RSV infection heightened disease severity during the adaptive phase of the immune response (Habibi, Thwaites *et al.,* in review). This observation recapitulated the findings of a human challenge study (Habibi, Thwaites *et al.,* in review). In this study, the

immune environment in the nasal passage of volunteers was investigated prior to inoculation with RSV using transcriptomics. The volunteers who developed symptomatic disease following RSV inoculation had a number of DEGs as compared to the inoculated volunteers who did not become infected (as assessed by qPCR detection of RSV). Overwhelmingly, the DEGs which were upregulated in the group who developed symptomatic disease were associated with neutrophil recruitment and activation, suggesting that the observed phenomenon is likely conserved between mice and humans. Together, the data from these clinical and murine studies suggest that the presence of neutrophils in the airways at the point of infection may heighten RSV disease susceptibility and/or severity. It is well known that severe respiratory viral infections can compromise the lungs and can increase susceptibility to life-threatening bacterial lung infections (Thorburn *et al.* 2006; Hall *et al.* 1988; Hendaus *et al.* 2015). However, the data from this study could suggest that mild bacterial or fungal respiratory infections may also increase the susceptibility to and/or the severity of a secondary RSV infection.

It is not clear why some of the volunteers in the human challenge study had a baseline transcriptomic signature associated with neutrophil recruitment and activation from this study. All the volunteers were deemed to be healthy adults with no known underlying infections or symptoms of disease. However, neutrophil activation in the airways is not expected in health and neutrophils can be recruited rapidly in response to minor inflammatory triggers (Kolaczkowska and Kubes 2013). There were no major differences in the bacterial composition of the airways between the two groups, as assessed by 16S sequencing, but the fungal composition of the airways was not investigated (Habibi, Thwaites *et al.,* in review). It is possible that asymptomatic fungal infections or other inflammatory insults which induce low-level neutrophil recruitment to the airways are sufficient to heighten disease susceptibility to RSV, but further investigation into the cause of the airway neutrophilia observed at baseline in the volunteers is required to fully understand the mechanism driving the altered susceptibility to symptomatic disease following RSV inoculation between these two groups. These studies were performed in healthy adult volunteers and in mice; it is not known whether the phenomenon observed also occurs in human infants who develop severe RSV-induced lower airway disease. This would be of great interest to investigate but would be challenging as investigations would require phenotyping of the airways prior to RSV infection and infants are very rarely sampled until they present with severe disease.

Although more work is needed to confirm the cause of the phenotype observed and the immunological mechanism underlying the enhanced RSV disease, it is interesting to consider

this observation in a public health context. Should asymptomatic respiratory infections be able to drive disease susceptibility and/or severity during RSV infection, it is possible that low dose anti-fungal treatments or low dose antibiotics could be given prophylactically to susceptible individuals such as premature infants, the immunocompromised and the elderly, to prevent severe RSV-induced lower airway disease.

6.2 Future work

6.2.1 Further characterise the immunological mechanisms regulating neutrophil recruitment in RSV infection *in vivo*

Despite the fact that neutrophils do not contribute to disease severity in mice, it is still likely that neutrophils contribute to disease in human infants and therefore it is important to fully understand the immunological mechanisms regulating their recruitment and activation in the lung during RSV infection. In future work it would be interesting to expand on the finding that MyD88/TRIF signalling is required for neutrophil recruitment to the lung. Specifically, it would be of great interest to understand whether RSV itself is required to stimulate MyD88/TRIF for neutrophil recruitment. Furthermore, it would be interesting to investigate which PRR, on which cell type in the lung, is required for chemoattractant expression. These could be done investigated using knock-out mice of the TLRs known to detect RSV - TLR2, TLR3, TLR4, TLR6 and TLR7 (Murawski *et al.* 2009; Kurt-Jones *et al.* 2000; Tal *et al.* 2004; Awomoyi *et al.* 2007). Furthermore, it would also be interesting to fully investigate the other chemoattractants which contribute to neutrophil recruitment, especially to understand which factor/s are responsible for neutrophil recruitment in *Mavs*$^{-/-}$ mice. BAL supernatant could be assayed for factors including C5a, fMLP, PAF and LTB4 to assess this. It would also be interesting to confirm the specific cellular source of CXCL1 and other neutrophil chemoattractants. A larger stromal cell flow cytometry panel could be optimised, including markers such as Thy-1 (Baglole *et al.* 2005), to detect other subsets of epithelial cells and stromal cells including fibroblasts. Similar experiments could be performed where stromal cells are sorted and the gene expression of known neutrophil chemoattractants are quantified.

6.2.2 Determine the factor/s activating neutrophils in the lung during RSV infection

In this work, it was identified that a host-derived pro-inflammatory factor or combination of factors induced downstream of type I IFN signalling is likely the driver of neutrophil activation in the lung during RSV infection. However, the precise factor/s which activates neutrophils in the lung during RSV infection was not determined. The difficulty was in obtaining neutrophils which are biologically representative of neutrophils recruited into the lung in response to an infection and have received the priming signals which are necessary for their full activation and degranulation. Naïve mice have very few resident lung neutrophils, and their lung

neutrophils all appear to reside in the vasculature of the lungs, so it was not feasible to sort lung neutrophils from naïve mice. A strategy which still uses murine neutrophils to investigate this could involve recruiting neutrophils to the lung using a chemoattractant and then sorting and stimulating the lung neutrophils *ex vivo*. However, this approach has certain limitations. Firstly, the administration of any chemoattractant would cause some level of neutrophil activation. Furthermore, it is likely that the process of staining and sorting neutrophils either by FACS or by MACS would cause some physiological changes which may affect their activation status. It is also possible that human neutrophils could be isolated from peripheral blood and stimulated *in vitro* to investigate this. It would be interesting to separate the protein contents of the BAL supernatant by size and stimulate neutrophils *ex vivo* or *in vitro* with certain BAL fractions to determine what the protein or proteins which activate neutrophils is/are. As the factor appeared to be induced downstream of type I IFN signalling, an *in vivo* approach could involve using ISG knock out mice however, hundreds of ISGs are induced downstream of type I IFN signalling so this approach would be very expensive and time consuming. It is also likely that a combination of factors act on neutrophils to drive their activation. In this work, MAVS signalling was found to be required for neutrophil degranulation, but it would also be interesting to investigate whether neutrophils secrete NETs during RSV infection and whether this is also dependent on MAVS signalling. Ongoing work in the lab is investigating this by staining lung sections with fluorochrome-conjugated antibodies against cit H3, a specific marker of NETs.

6.2.3 Investigate how MAVS signalling supports the formation of memory T cell responses

Observational experiments from this project found that MAVS signalling impairs the formation of $CD8^+$ T_{RM} cells in the lung during RSV infection. In future work, it will be interesting to investigate the mechanism underlying this. It will be important to fully characterise how MAVS signalling affects the T cell response during the primary RSV infection. Previous work from the lab has demonstrated that MAVS mice have similar numbers if not more $CD8^+$ T cells recruited to the lung during the peak of RSV disease (Michelle Paulsen, unpublished), but this is perhaps unsurprising as these mice also have higher viral loads (Goritzka, Makris, *et al.* 2015). It will be interesting to investigate whether the deficiency observed in *Mavs*$^{-/-}$ mice is due to a problem with their ability to expand the T_{RM} pool in the lung upon re-challenge, or whether these mice are impaired in their ability to generate a pool of T cell memory cells. The $CD8^+$ T_{RM} cell pool at baseline would need to be studied in *Mavs*$^{-/-}$ mice infected with RSV and then

re-challenged with PBS. *Ifnar1*$^{-/-}$ mice could be used to investigate whether the formation of memory T cells is dependent on the induction of type I IFNs. It will also be interesting to investigate in more detail how MAVS signalling is required for memory T cell functionality, as measured by the production of cytokines in this study.

6.2.4 Determine the immunological mechanism mediating CD8$^+$ T cell driven disease when mice are given rCXCL1 pre-RSV infection

It will be of great interest in future work to investigate the surprising phenomenon that neutrophilia at baseline heightens disease susceptibility and/or disease severity, most likely in a manner driven by CD8$^+$ T cells. As the bacterial composition in the nasal passage did not explain the differences in neutrophilia, it would be interesting to use next generation sequencing to investigate whether differences in the fungal composition in the nasal passage of human volunteers could explain the distinct neutrophil-associated transcriptomic signature.

Future work should focus on determining the immunological mechanism underlying this phenotype. Using mice, antibody-mediated neutrophil depletion should be used to confirm that the effect observed is due to the neutrophils recruited into the airways by administration of rCXCL1. CXCL1 signals via CXCR2 which is also expressed on epithelial and endothelial cells in the lung (Stadtmann and Zarbock 2012; Addison *et al.* 2000) so it is possible the phenotype observed was due to effects of rCXCL1 on the immune response which were independent of neutrophil recruitment. Heightened disease was accompanied by an increase in the recruitment of CD8$^+$ T cells - known to be pathogenic during RSV infection (Cannon *et al.* 1988; Graham *et al.* 1991; Openshaw and Chiu 2013). Antibody-mediated CD8$^+$ T cell depletion should be used in this model system to confirm that the enhanced weight loss observed in mice treated with rCXCL1 prior to RSV infection was due to a pathogenic effect of CD8$^+$ T cells.

Future work should also fully investigate the immune environment in the lungs 12 h following rCXCL1 treatment; the point that RSV infection occurred in this model system. Neutrophil proteases may affect levels of surfactants in the airways or cleave anti-microbial peptides in the lung (Currie *et al.* 2016). It would be interesting to investigate whether rCXCL1 affects the concentrations of surfactants and anti-microbial peptides such as LL-37 in the airways. The number of AMs and monocytes was not affected by rCXCL1 treatment, but it would be

interesting to characterise the structural integrity of the lungs to quantify possible tissue damage caused by rCXCL1 driven neutrophilia prior to RSV infection.

Furthermore, it will be essential to investigate the recruitment of other innate immune cells following the RSV infection in this model. AMs, inflammatory monocytes, pDCs, cDCs and NK cells should all be enumerated to determine whether treatment of mice with rCXCL1 prior to RSV infection influences the recruitment or functionality of these immune cells which can help to shape the adaptive immune response. There is increasing evidence to show neutrophils can influence T cell responses, both directly and indirectly (Minns *et al.* 2019). It would be interesting to investigate whether the enhanced $CD8^+$ T cell driven weight loss occurs via enhanced antigen presentation. Neutrophils themselves have been shown to be capable of acting as APCs (Potter and Harding 2001; Culshaw *et al.* 2008; Hufford *et al.* 2012) and can also affect the antigen presentation capabilities of cDCs (Schuster *et al.* 2013; van Gisbergen *et al.* 2005; Bennouna and Denkers 2005; Charmoy *et al.* 2010). It will be particularly interesting to characterise whether antigen-presentation by $CD103^+$ cDCs to naïve T cells in the lymph nodes is affected. Interestingly, there was a decrease in the frequency of RSV-antigen specific $CD8^+$ T cells detected in the lung during severe disease when mice were treated with rCXCL1 prior to RSV infection. However, as the total number of $CD8^+$ T cells in the lung increased, as did the total number of RSV-antigen specific $CD8^+$ T cells. It is possible that the mechanism involves a signal which affects the proliferation capability of antigen-specific $CD8^+$ T cells recruited to the lung.

The situation as modelled in the mice is not representative of a mild infection; mice were given a very high dose of rCXCL1 pre-RSV infection and the number of neutrophils present in the lungs at the time of RSV infection would not be expected in the absence of a severe infectious insult or injury. In future work it would be interesting to titrate down the dose of rCXCL1 given to mice pre-RSV infection to determine what the lowest dose required is to maintain the phenotype in the murine model of disease. Furthermore, it would be interesting to develop a co-infection model in mice to test whether infection with a mild bacterial/fungal agent followed by RSV recapitulates the phenotype observed when mice are treated with rCXCL1 prior to RSV infection.

7 Bibliography

Abu-Harb, M., Bell, F., Finn, A., Rao, W.H., Nixon, L., Shale, D. and Everard, M.L. (1999). IL-8 and neutrophil elastase levels in the respiratory tract of infants with RSV bronchiolitis. *The European respiratory journal* **14**:139–143.

Addison, C.L., Daniel, T.O., Burdick, M.D., Liu, H., Ehlert, J.E., Xue, Y.Y., Buechi, L., *et al.* (2000). The CXC chemokine receptor 2, CXCR2, is the putative receptor for ELR+ CXC chemokine-induced angiogenic activity. *Journal of immunology* **165**:5269–5277.

Afonso, C.L., Amarasinghe, G.K., Bányai, K., Bào, Y., Basler, C.F., Bavari, S., Bejerman, N., *et al.* (2016). Taxonomy of the order Mononegavirales: update 2016. *Archives of virology* **161**:2351–2360.

Ajibade, A.A., Wang, H.Y. and Wang, R.-F. (2013). Cell type-specific function of TAK1 in innate immune signaling. *Trends in immunology* **34**:307–316.

Akira, S., Uematsu, S. and Takeuchi, O. (2006). Pathogen recognition and innate immunity. *Cell* **124**:783–801.

Akondy, R.S., Fitch, M., Edupuganti, S., Yang, S., Kissick, H.T., Li, K.W., Youngblood, B.A., *et al.* (2017). Origin and differentiation of human memory CD8 T cells after vaccination. *Nature* **552**:362–367.

Akthar, S., Patel, D.F., Beale, R.C., Peiró, T., Xu, X., Gaggar, A., Jackson, P.L., *et al.* (2015). Matrikines are key regulators in modulating the amplitude of lung inflammation in acute pulmonary infection. *Nature communications* **6**:8423.

Altamirano-Lagos, M.J., Díaz, F.E., Mansilla, M.A., Rivera-Pérez, D., Soto, D., McGill, J.L., Vasquez, A.E., *et al.* (2019). Current Animal Models for Understanding the Pathology Caused by the Respiratory Syncytial Virus. *Frontiers in microbiology* **10**:873.

Amulic, B., Cazalet, C., Hayes, G.L., Metzler, K.D. and Zychlinsky, A. (2012). Neutrophil Function: From Mechanisms to Disease. *Annual Review of Immunology* **30**:459–489.

Arnardottir, H.H., Freysdottir, J. and Hardardottir, I. (2012). Two circulating neutrophil populations in acute inflammation in mice. *Inflammation research* **61**:931–939.

Ascough, S., Paterson, S. and Chiu, C. (2018). Induction and Subversion of Human Protective Immunity: Contrasting Influenza and Respiratory Syncytial Virus. *Frontiers in immunology* **9**:323.

Asselin-Paturel, C., Boonstra, A., Dalod, M., Durand, I., Yessaad, N., Dezutter-Dambuyant, C., Vicari, A., *et al.* (2001). Mouse type I IFN-producing cells are immature APCs with plasmacytoid morphology. *Nature immunology* **2**:1144–1150.

Aujard, Y. and Fauroux, B. (2002). Risk factors for severe respiratory syncytial virus infection in infants. *Respiratory medicine* **96**:S9–14.

Awomoyi, A.A., Rallabhandi, P., Pollin, T.I., Lorenz, E., Sztein, M.B., Boukhvalova, M.S., Hemming, V.G., *et al.* (2007). Association of TLR4 polymorphisms with symptomatic respiratory syncytial virus infection in high-risk infants and young children. *Journal of immunology* **179**:3171–3177.

Baeyens, A., Fang, V., Chen, C. and Schwab, S.R. (2015). Exit Strategies: S1P Signaling and T Cell Migration. *Trends in immunology* **36**:778–787.

Baglole, C.J., Reddy, S.Y., Pollock, S.J., Feldon, S.E., Sime, P.J., Smith, T.J. and Phipps, R.P. (2005). Isolation and phenotypic characterization of lung fibroblasts. *Methods in molecular medicine* **117**:115–127.

Bakker, S.E., Duquerroy, S., Galloux, M., Loney, C., Conner, E., Eléouët, J.-F., Rey, F.A., *et al.* (2013). The respiratory syncytial virus nucleoprotein-RNA complex forms a left-handed helical nucleocapsid. *The Journal of general virology* **94**:1734–1738.

Bankovich, A.J., Shiow, L.R. and Cyster, J.G. (2010). CD69 suppresses sphingosine 1-phosophate receptor-1 (S1P1) function through interaction with membrane helix 4. *The Journal of biological chemistry* **285**:22328–22337.

Bardoel, B.W., Kenny, E.F., Sollberger, G. and Zychlinsky, A. (2014). The balancing act of neutrophils. *Cell host & microbe* **15**:526–536.

Barreda, D.R., Hanington, P.C. and Belosevic, M. (2004). Regulation of myeloid development and function by colony stimulating factors. *Developmental and comparative immunology* **28**:509–554.

Barreira, E.R., Precioso, A.R. and Bousso, A. (2011). Pulmonary surfactant in respiratory syncytial virus bronchiolitis: the role in pathogenesis and clinical implications. *Pediatric pulmonology* **46**:415–420.

Bataki, E.L., Evans, G.S. and Everard, M.L. (2005). Respiratory syncytial virus and neutrophil activation. *Clinical and Experimental Immunology* **140**:470–477.

Battles, M.B. and McLellan, J.S. (2019). Respiratory syncytial virus entry and how to block it. *Nature reviews. Microbiology* **17**:233–245.

Bächi, T. (1988). Direct observation of the budding and fusion of an enveloped virus by video microscopy of viable cells. *The Journal of Cell Biology* **107**:1689–1695.

Becker, S., Koren, H.S. and Henke, D.C. (1993). Interleukin-8 expression in normal nasal epithelium and its modulation by infection with respiratory syncytial virus and cytokines tumor necrosis factor, interleukin-1, and interleukin-6. *American journal of respiratory cell and molecular biology* **8**:20–27.

Belaaouaj, A., McCarthy, R., Baumann, M., Gao, Z., Ley, T.J., Abraham, S.N. and Shapiro, S.D. (1998). Mice lacking neutrophil elastase reveal impaired host defense against gram negative bacterial sepsis. *Nature Medicine* **4**:615–618.

Bem R. A., Domachowske, J. B., and Rosenberg, H. F. (2011). Animal models of human respiratory syncytial virus disease. *The American Journal of Physiology-Lung Cellular and Molecular Physiology* **301:**L148–L156.

Bennouna, S. and Denkers, E.Y. (2005). Microbial antigen triggers rapid mobilization of TNF-alpha to the surface of mouse neutrophils transforming them into inducers of high-level dendritic cell TNF-alpha production. *Journal of immunology* **174**:4845–4851.

Bergsbaken, T. and Bevan, M.J. (2015). Proinflammatory microenvironments within the intestine regulate the differentiation of tissue-resident $CD8^+$ T cells responding to infection. *Nature immunology* **16**:406–414.

Bermingham, A. and Collins, P.L. (1999). The M2-2 protein of human respiratory syncytial virus is a regulatory factor involved in the balance between RNA replication and transcription. *Proceedings of the National Academy of Sciences* **96**:11259–11264.

Bevilacqua, M.P., Stengelin, S., Gimbrone, M.A. and Seed, B. (1989). Endothelial leukocyte adhesion molecule 1: an inducible receptor for neutrophils related to complement regulatory proteins and lectins. *Science* **243**:1160–1165.

Bhattacharya, A., Wei, Q., Shin, J.N., Abdel Fattah, E., Bonilla, D.L., Xiang, Q. and Eissa, N.T. (2015). Autophagy Is Required for Neutrophil-Mediated Inflammation. *Cell Reports* **12**:1731–1739.

Bhoj, V.G., Sun, Q., Bhoj, E.J., Somers, C., Chen, X., Torres, J.-P., Mejias, A., *et al.* (2008). MAVS and MyD88 are essential for innate immunity but not cytotoxic T lymphocyte response against respiratory syncytial virus. *Proceedings of the National Academy of Sciences of the United States of America* **105**:14046–14051.

Bird, L. (2018). Asthma exacerbated by neutrophil ghosts. *Nature reviews. Immunology* **18**:602–603.

Blount, R.E., Morris, J.A. and Savage, R.E. (1956). Recovery of cytopathogenic agent from chimpanzees with coryza. *Proceedings of the Society for Experimental Biology and Medicine* **92**:544–549.

Bohmwald, K., Gálvez, N.M.S., Canedo-Marroquín, G., Pizarro-Ortega, M.S., Andrade-Parra, C., Gómez-Santander, F. and Kalergis, A.M. (2019). Contribution of Cytokines to Tissue Damage During Human Respiratory Syncytial Virus Infection. *Frontiers in immunology* **10**:452.

Boo, K.-H. and Yang, J.-S. (2010). Intrinsic cellular defenses against virus infection by antiviral type I interferon. *Yonsei medical journal* **51**:9–17.

Borchers, A.T., Chang, C., Gershwin, M.E. and Gershwin, L.J. (2013). Respiratory syncytial virus--a comprehensive review. *Clinical reviews in allergy & immunology* **45**:331–379.

Borjesson, D.L., Simon, S.I., Hodzic, E., Ballantyne, C.M. and Barthold, S.W. (2002). Kinetics of CD11b/CD18 up-regulation during infection with the agent of human granulocytic ehrlichiosis in mice. *Laboratory Investigation* **82**:303–311.

Borregaard, N. and Cowland, J.B. (1997). Granules of the human neutrophilic polymorphonuclear leukocyte. *Blood* **89**:3503–3521.

Bossert, B. and Conzelmann, K.-K. (2002). Respiratory syncytial virus (RSV) nonstructural (NS) proteins as host range determinants: a chimeric bovine RSV with NS genes from human RSV is attenuated in interferon-competent bovine cells. *Journal of Virology* **76**:4287–4293.

Bossert, B., Marozin, S. and Conzelmann, K.-K. (2003). Nonstructural proteins NS1 and NS2 of bovine respiratory syncytial virus block activation of interferon regulatory factor 3. *Journal of Virology* **77**:8661–8668.

Bournazou, I., Pound, J.D., Duffin, R., Bournazos, S., Melville, L.A., Brown, S.B., Rossi, A.G., *et al.* (2009). Apoptotic human cells inhibit migration of granulocytes via release of lactoferrin. *Journal of Clinical Investigation* **119**:20–32.

Bowdish, D.M.E., Davidson, D.J., Scott, M.G. and Hancock, R.E.W. (2005). Immunomodulatory activities of small host defense peptides. *Antimicrobial agents and chemotherapy* **49**:1727–1732.

Braciale, T.J., Sun, J. and Kim, T.S. (2012). Regulating the adaptive immune response to respiratory virus infection. *Nature reviews. Immunology* **12**:295–305.

Bradley, L.M., Douglass, M.F., Chatterjee, D., Akira, S. and Baaten, B.J.G. (2012). Matrix metalloprotease 9 mediates neutrophil migration into the airways in response to influenza virus-induced toll-like receptor signaling. *PLoS Pathogens* **8**:e1002641.

Bramley, T.J., Lerner, D. and Sames, M. (2002). Productivity losses related to the common cold. *Journal of occupational and environmental medicine* **44**:822–829.

Brandau, S. and Hartl, D. (2017). Lost in neutrophil heterogeneity? CD10! *Blood* **129**:1240–1241.

Branzk, N. and Papayannopoulos, V. (2013). Molecular mechanisms regulating NETosis in infection and disease. *Seminars in Immunopathology* **35**:513–530.

Branzk, N., Lubojemska, A., Hardison, S.E., Wang, Q., Gutierrez, M.G., Brown, G.D. and Papayannopoulos, V. (2014). Neutrophils sense microbe size and selectively release neutrophil extracellular traps in response to large pathogens. *Nature immunology* **15**:1017–1025.

Brinkmann, V., Reichard, U., Goosmann, C., Fauler, B., Uhlemann, Y., Weiss, D.S., Weinrauch, Y., *et al.* (2004). Neutrophil Extracellular Traps Kill Bacteria. *Science* **303**:1532–1535.

Brown, A.P. and Ganey, P.E. (1995). Neutrophil degranulation and superoxide production induced by polychlorinated biphenyls are calcium dependent. *Toxicology and applied pharmacology* **131**:198–205.

Buckle, A.M. and Hogg, N. (1989). The effect of IFN-gamma and colony-stimulating factors on the expression of neutrophil cell membrane receptors. *Journal of immunology* **143**:2295–2301.

Bukreyev, A., Yang, L. and Collins, P.L. (2012). The secreted G protein of human respiratory syncytial virus antagonizes antibody-mediated restriction of replication involving macrophages and complement. *Journal of Virology* **86**:10880–10884.

Bukreyev, A., Yang, L., Fricke, J., Cheng, L., Ward, J.M., Murphy, B.R. and Collins, P.L. (2008). The secreted form of respiratory syncytial virus G glycoprotein helps the virus evade antibody-mediated restriction of replication by acting as an antigen decoy and through effects on Fc receptor-bearing leukocytes. *Journal of Virology* **82**:12191–12204.

Burotto, M., Chiou, V.L., Lee, J.-M. and Kohn, E.C. (2014). The MAPK pathway across different malignancies: a new perspective. *Cancer* **120**:3446–3456.

Canedo-Marroquín, G., Acevedo-Acevedo, O., Rey-Jurado, E., Saavedra, J.M., Lay, M.K., Bueno, S.M., Riedel, C.A., *et al.* (2017). Modulation of Host Immunity by Human Respiratory Syncytial Virus Virulence Factors: A Synergic Inhibition of Both Innate and Adaptive Immunity. *Frontiers in Cellular and Infection Microbiology* **7**:367.

Cannon, M.J., Openshaw, P.J. and Askonas, B.A. (1988). Cytotoxic T cells clear virus but augment lung pathology in mice infected with respiratory syncytial virus. *The Journal of Experimental Medicine* **168**:1163–1168.

Cannon, M.J., Stott, E.J., Taylor, G. and Askonas, B.A. (1987). Clearance of persistent respiratory syncytial virus infections in immunodeficient mice following transfer of primed T cells. *Immunology* **62**:133–138.

Carman, C.V. (2009). Mechanisms for transcellular diapedesis: probing and pathfinding by 'invadosome-like protrusions'. *Journal of cell science* **122**:3025–3035.

Carmona-Rivera, C. and Kaplan, M.J. (2013). Low-density granulocytes: a distinct class of neutrophils in systemic autoimmunity. *Seminars in Immunopathology* **35**:455–463.

Casey, K.A., Fraser, K.A., Schenkel, J.M., Moran, A., Abt, M.C., Beura, L.K., Lucas, P.J., *et al.* (2012). Antigen-independent differentiation and maintenance of effector-like resident memory T cells in tissues. *Journal of immunology* **188**:4866–4875.

Castanheira, F.V.S. and Kubes, P. (2019). Neutrophils and NETs in modulating acute and chronic inflammation. *Blood* **133**:2178–2185.

Cepek, K.L., Shaw, S.K., Parker, C.M., Russell, G.J., Morrow, J.S., Rimm, D.L. and Brenner, M.B. (1994). Adhesion Between Epithelial-Cells and T-Lymphocytes Mediated by E-Cadherin and the Alpha(E)Beta(7) Integrin. *Nature* **372**:190–193.

Cerutti, A., Puga, I. and Magri, G. (2013). The B cell helper side of neutrophils. *Journal of Leukocyte Biology* **94**:677–682.

Chanock, R., Roizman, B. and Myers, R. (1957). Recovery from infants with respiratory illness of a virus related to chimpanzee coryza agent (CCA). I. Isolation, properties and characterization. *American journal of hygiene* **66**:281–290.

Charmoy, M., Brunner-Agten, S., Aebischer, D., Auderset, F., Launois, P., Milon, G., Proudfoot, A.E.I., *et al.* (2010). Neutrophil-derived CCL3 is essential for the rapid recruitment of dendritic cells to the site of Leishmania major inoculation in resistant mice. *PLoS Pathogens* **6**:e1000755.

Chávez-Bueno, S., Mejias, A., Gomez, A.M., Olsen, K.D., Ríos, A.M., Fonseca-Aten, M., Ramilo, O., *et al.* (2005). Respiratory syncytial virus-induced acute and chronic airway disease is independent of genetic background: an experimental murine model. *Virology journal* **2**:46.

Chen, G.Y. and Nuñez, G. (2010). Sterile inflammation: sensing and reacting to damage. *Nature reviews. Immunology* **10**:826–837.

Chen, K. and Kolls, J.K. (2013). T cell-mediated host immune defenses in the lung. *Annual review of immunology* **31**:605–633.

Chen, L. and Flies, D.B. (2013). Molecular mechanisms of T cell co-stimulation and co-inhibition. *Nature reviews. Immunology* **13**:227–242.

Chiba, K., Yanagawa, Y., Masubuchi, Y., Kataoka, H., Kawaguchi, T., Ohtsuki, M. and Hoshino, Y. (1998). FTY720, a novel immunosuppressant, induces sequestration of circulating mature lymphocytes by acceleration of lymphocyte homing in rats. I. FTY720 selectively decreases the number of circulating mature lymphocytes by acceleration of lymphocyte homing. *Journal of immunology* **160**:5037–5044.

Chiu, C. and Openshaw, P.J. (2015). Antiviral B cell and T cell immunity in the lungs. *Nature immunology* **16**:18–26.

Christiaansen, A.F., Knudson, C.J. and Weiss, K.A. (2014). The CD4 T cell response to respiratory syncytial virus infection. *Immunologic research* **59**:109–117.

Chtanova, T., Schaeffer, M., Han, S.-J., van Dooren, G.G., Nollmann, M., Herzmark, P., Chan, S.W., *et al.* (2008). Dynamics of neutrophil migration in lymph nodes during infection. *Immunity* **29**:487–496.

Collins, P.L. and Graham, B.S. (2008). Viral and host factors in human respiratory syncytial virus pathogenesis. *Journal of Virology* **82**:2040–2055.

Colman, P.M. and Lawrence, M.C. (2003). The structural biology of type I viral membrane fusion. *Nature reviews. Molecular cell biology* **4**:309–319.

Colonna, M. and Trinchieri, G. (2004). Plasmacytoid dendritic cells in immunity. *Nature immunology* **5**:1219–1226.

Colotta, F., Re, F., Polentarutti, N., Sozzani, S. and Mantovani, A. (1992). Modulation of granulocyte survival and programmed cell death by cytokines and bacterial products. *Blood* **80**:2012–2020.

Condliffe, A.M., Kitchen, E. and Chilvers, E.R. (1998). Neutrophil priming: pathophysiological consequences and underlying mechanisms. *Clinical science* **94**:461–471.

Cortjens, B., de Boer, O.J., de Jong, R., Antonis, A.F., Sabogal Piñeros, Y.S., Lutter, R., van Woensel, J.B., *et al.* (2016). Neutrophil extracellular traps cause airway obstruction during respiratory syncytial virus disease. *The Journal of pathology* **238**:401–411.

Costa, S., Bevilacqua, D., Cassatella, M.A. and Scapini, P. (2019). Recent advances on the crosstalk between neutrophils and B or T lymphocytes. *Immunology* **156**:23–32.

Cowland, J.B. and Borregaard, N. (2016). Granulopoiesis and granules of human neutrophils. *Immunological reviews* **273**:11–28.

Crotta, S., Davidson, S., Mahlakõiv, T., Desmet, C.J., Buckwalter, M.R., Albert, M.L., Staeheli, P., *et al.* (2013). Type I and type III interferons drive redundant amplification loops to induce a transcriptional signature in influenza-infected airway epithelia. *PLoS Pathogens* **9**:e1003773.

Cua, D.J. and Tato, C.M. (2010). Innate IL-17-producing cells: the sentinels of the immune system. *Nature reviews. Immunology* **10**:479–489.

Culshaw, S., Millington, O.R., Brewer, J.M. and McInnes, I.B. (2008). Murine neutrophils present Class II restricted antigen. *Immunology letters* **118**:49–54.

Currie, S.M., Findlay, E.G., McHugh, B.J., Mackellar, A., Man, T., Macmillan, D., Wang, H., *et al.* (2013). The human cathelicidin LL-37 has antiviral activity against respiratory syncytial virus. *PloS one* **8**:e73659.

Currie, S.M., Gwyer Findlay, E., McFarlane, A.J., Fitch, P.M., Böttcher, B., Colegrave, N., Paras, A., *et al.* (2016). Cathelicidins Have Direct Antiviral Activity against Respiratory Syncytial Virus In Vitro and Protective Function In Vivo in Mice and Humans. *Journal of immunology* **196**:2699–2710.

Curtsinger, J.M., Schmidt, C.S., Mondino, A., Lins, D.C., Kedl, R.M., Jenkins, M.K. and Mescher, M.F. (1999). Inflammatory cytokines provide a third signal for activation of naive CD4+ and CD8+ T cells. *Journal of immunology* **162**:3256–3262.

Curtsinger, J.M., Valenzuela, J.O., Agarwal, P., Lins, D. and Mescher, M.F. (2005). Type I IFNs provide a third signal to CD8 T cells to stimulate clonal expansion and differentiation. *Journal of immunology* **174**:4465–4469.

Dang, A.T. and Marsland, B.J. (2019). Microbes, metabolites, and the gut-lung axis. *Mucosal Immunology* **12**:843–850.

Dang, P.M., Fontayne, A., Hakim, J., Benna, El, J. and Périanin, A. (2001). Protein kinase C zeta phosphorylates a subset of selective sites of the NADPH oxidase component p47phox and participates in formyl peptide-mediated neutrophil respiratory burst. *Journal of immunology* **166**:1206–1213.

Dang, P.M.-C., Stensballe, A., Boussetta, T., Raad, H., Dewas, C., Kroviarski, Y., Hayem, G., *et al.* (2006). A specific p47phox -serine phosphorylated by convergent MAPKs mediates neutrophil NADPH oxidase priming at inflammatory sites. *Journal of Clinical Investigation* **116**:2033–2043.

Das, S., Palmer, O.P., Leight, W.D., Surowitz, J.B., Pickles, R.J., Randell, S.H. and Buchman, C.A. (2005). Cytokine amplification by respiratory syncytial virus infection in human nasal epithelial cells. *The Laryngoscope* **115**:764–768.

Davidson, S., McCabe, T.M., Crotta, S., Gad, H.H., Hessel, E.M., Beinke, S., Hartmann, R., *et al.* (2016). IFNλ is a potent anti-influenza therapeutic without the inflammatory side effects of IFNα treatment. *EMBO molecular medicine* **8**:1099–1112.

De Weerd, W., Twilhaar, W.N. and Kimpen, J.L. (1998). T cell subset analysis in peripheral blood of children with RSV bronchiolitis. *Scandinavian journal of infectious diseases* **30**:77–80.

Demoor, T., Petersen, B.C., Morris, S., Mukherjee, S., Ptaschinski, C., De Almeida Nagata, D.E., Kawai, T., *et al.* (2012). IPS-1 signaling has a nonredundant role in mediating antiviral responses and the clearance of respiratory syncytial virus. *Journal of immunology* **189**:5942–5953.

Deniset, J.F. and Kubes, P. (2016). Recent advances in understanding neutrophils. *F1000Research* **5**:2912.

Deniset, J.F., Surewaard, B.G., Lee, W.-Y. and Kubes, P. (2017). Splenic Ly6Ghigh mature and Ly6Gint immature neutrophils contribute to eradication of S. pneumoniae. *The Journal of Experimental Medicine* **214**:1333–1350.

Desai, P., Tahiliani, V., Stanfield, J., Abboud, G. and Salek-Ardakani, S. (2018). Inflammatory monocytes contribute to the persistence of CXCR3hi CX3CR1lo circulating and lung-resident memory CD8+ T cells following respiratory virus infection. *Immunology and cell biology* **96**:370–378.

Desch, A.N., Randolph, G.J., Murphy, K., Gautier, E.L., Kedl, R.M., Lahoud, M.H., Caminschi, I., *et al.* (2011). CD103+ pulmonary dendritic cells preferentially acquire and present apoptotic cell-associated antigen. *The Journal of Experimental Medicine* **208**:1789–1797.

Devi, S., Wang, Y., Chew, W.K., Lima, R., A-González, N., Mattar, C.N.Z., Chong, S.Z., *et al.* (2013). Neutrophil mobilization via plerixafor-mediated CXCR4 inhibition arises from lung demargination and blockade of neutrophil homing to the bone marrow. *The Journal of Experimental Medicine* **210**:2321–2336.

DeVincenzo, J.P., El Saleeby, C.M. and Bush, A.J. (2005). Respiratory syncytial virus load predicts disease severity in previously healthy infants. *Journal of infectious diseases* **191:**1861-1868.

Dickson, R.P., Erb-Downward, J.R., Martinez, F.J. and Huffnagle, G.B. (2016). The Microbiome and the Respiratory Tract. *Annual review of physiology* **78**:481–504.

Dudek, M., Puttur, F., Arnold-Schrauf, C., Kühl, A.A., Holzmann, B., Henriques-Normark, B., Berod, L., *et al.* (2016). Lung epithelium and myeloid cells cooperate to clear acute pneumococcal infection. *Mucosal Immunology* **9**:1288–1302.

Dumas, A., Bernard, L., Poquet, Y., Lugo-Villarino, G. and Neyrolles, O. (2018). The role of the lung microbiota and the gut-lung axis in respiratory infectious diseases. *Cellular microbiology* **20**:e12966.

Durant, L.R., Makris, S., Voorburg, C.M., Loebbermann, J., Johansson, C. and Openshaw, P.J.M. (2013). Regulatory T cells prevent Th2 immune responses and pulmonary eosinophilia during respiratory syncytial virus infection in mice. *Journal of Virology* **87**:10946–10954.

Ehl, S., Bischoff, R., Ostler, T., Vallbracht, S., Schulte-Mönting, J., Poltorak, A. and Freudenberg, M. (2004). The role of Toll-like receptor 4 versus interleukin-12 in immunity to respiratory syncytial virus. *European journal of immunology* **34**:1146–1153.

El-Benna, J., Dang, P.M.-C. and Gougerot-Pocidalo, M.-A. (2008). Priming of the neutrophil NADPH oxidase activation: role of p47phox phosphorylation and NOX2 mobilization to the plasma membrane. *Seminars in Immunopathology* **30**:279–289.

Emboriadou, M., Hatzistilianou, M., Magnisali, C., Sakelaropoulou, A., Exintari, M., Conti, P. and Aivazis, V. (2007). Human neutrophil elastase in RSV bronchiolitis. *Annals of clinical and laboratory science* **37**:79–84.

Empey, K.M., Orend, J.G., Peebles, R.S., Egaña, L., Norris, K.A., Oury, T.D. and Kolls, J.K. (2012). Stimulation of immature lung macrophages with intranasal interferon gamma in a novel neonatal mouse model of respiratory syncytial virus infection. *PloS one* **7**:e40499.

Escobar, G.J., Ragins, A., Li, S.X., Prager, L., Masaquel, A.S. and Kipnis, P. (2010). Recurrent Wheezing in the Third Year of Life Among Children Born at 32 Weeks' Gestation or Later Relationship to Laboratory-Confirmed, Medically Attended Infection With Respiratory Syncytial Virus During the First Year of Life. *Archives of Pediatrics & Adolescent Medicine* **164**:915–922.

Everard, M.L., Swarbrick, A., Wrightham, M., McIntyre, J., Dunkley, C., James, P.D., Sewell, H.F., *et al.* (1994). Analysis of cells obtained by bronchial lavage of infants with respiratory syncytial virus infection. *Archives of Disease in Childhood* **71**:428–432.

Falsey, A.R. and Walsh, E.E. (2005). Respiratory syncytial virus infection in elderly adults. *Drugs & aging* **22**:577–587.

Faurschou, M. and Borregaard, N. (2003). Neutrophil granules and secretory vesicles in inflammation. *Microbes and infection* **5**:1317–1327.

Fearns, R. and Collins, P.L. (1999). Role of the M2-1 transcription antitermination protein of respiratory syncytial virus in sequential transcription. *Journal of Virology* **73**:5852–5864.

Fedechkin, S.O., George, N.L., Wolff, J.T., Kauvar, L.M. and DuBois, R.M. (2018). Structures of respiratory syncytial virus G antigen bound to broadly neutralizing antibodies. *Science Immunology* **3**:eaar3534.

Feng, D., Nagy, J.A., Pyne, K., Dvorak, H.F. and Dvorak, A.M. (1998). Neutrophils emigrate from venules by a transendothelial cell pathway in response to FMLP. *Journal of Experimental Medicine* **187**:903–915.

Fernandez-Ruiz, D., Ng, W.Y., Holz, L.E., Ma, J.Z., Zaid, A., Wong, Y.C., Lau, L.S., *et al.* (2016). Liver-Resident Memory CD8+ T Cells Form a Front-Line Defense against Malaria Liver-Stage Infection. *Immunity* **45**:889–902.

Foxman, E.F., Campbell, J.J. and Butcher, E.C. (1997). Multistep navigation and the combinatorial control of leukocyte chemotaxis. *The Journal of Cell Biology* **139**:1349–1360.

Fridlender, Z.G., Sun, J., Kim, S., Kapoor, V., Cheng, G., Ling, L., Worthen, G.S., *et al.* (2009). Polarization of Tumor-Associated Neutrophil Phenotype by TGF-β: “N1” versus “N2” TAN. *Cancer Cell* **16**:183–194.

Fuchs, T.A., Abed, U., Goosmann, C., Hurwitz, R., Schulze, I., Wahn, V., Weinrauch, Y., *et al.* (2007). Novel cell death program leads to neutrophil extracellular traps. *The Journal of Cell Biology* **176**:231–241.

Fuentes, S., Tran, K.C., Luthra, P., Teng, M.N. and He, B. (2007). Function of the respiratory syncytial virus small hydrophobic protein. *Journal of Virology* **81**:8361–8366.

Fulton, R.B. and Meyerholz, D.K. (2010). Foxp3+ CD4 regulatory T cells limit pulmonary immunopathology by modulating the CD8 T cell response during respiratory syncytial virus infection. *Journal of immunology* **185**:2382–2392.

Funchal, G.A., Jaeger, N., Czepielewski, R.S., Machado, M.S., Muraro, S.P., Stein, R.T., Bonorino, C.B.C., *et al.* (2015). Respiratory syncytial virus fusion protein promotes TLR-4-dependent neutrophil extracellular trap formation by human neutrophils. *PloS one* **10**:e0124082.

Furze, R.C. and Rankin, S.M. (2008). Neutrophil mobilization and clearance in the bone marrow. *Immunology* **125**:281–288.

Fuxman Bass, J.I., Alvarez, M.E., Gabelloni, M.L., Vermeulen, M.E., Amaral, M.M., Geffner, J.R. and Trevani, A.S. (2008). GM-CSF enhances a CpG-independent pathway of neutrophil activation triggered by bacterial DNA. *Molecular immunology* **46**:37–44.

Gack, M.U., Shin, Y.C., Joo, C.-H., Urano, T., Liang, C., Sun, L., Takeuchi, O., *et al.* (2007). TRIM25 RING-finger E3 ubiquitin ligase is essential for RIG-I-mediated antiviral activity. *Nature* **446**:916–920.

Galani, I.E. and Andreakos, E. (2015). Neutrophils in viral infections: Current concepts and caveats. *Journal of Leukocyte Biology* **98**:557–564.

Gan, S.-W., Tan, E., Lin, X., Yu, D., Wang, J., Tan, G.M.-Y., Vararattanavech, A., *et al.* (2012). The small hydrophobic protein of the human respiratory syncytial virus forms pentameric ion channels. *The Journal of biological chemistry* **287**:24671–24689.

García, C.G., Bhore, R., Soriano-Fallas, A., Trost, M., Chason, R., Ramilo, O. and Mejias, A. (2010). Risk factors in children hospitalized with RSV bronchiolitis versus non-RSV bronchiolitis. *Pediatrics* **126**:e1453–60.

García, J., García-Barreno, B., Vivo, A. and Melero, J.A. (1993). Cytoplasmic inclusions of respiratory syncytial virus-infected cells: formation of inclusion bodies in transfected cells that coexpress the nucleoprotein, the phosphoprotein, and the 22K protein. *Virology* **195**:243–247.

Garcia-Mauriño, C., Moore-Clingenpeel, M., Thomas, J., Mertz, S., Cohen, D.M., Ramilo, O. and Mejias, A. (2019). Viral load dynamics and clinical disease severity in infants with respiratory syncytial virus infection. *Journal of infectious diseases* **219:**1207-1215.

Garofalo, R.P., Patti, J., Hintz, K.A., Hill, V., Ogra, P.L. and Welliver, R.C. (2001). Macrophage inflammatory protein-1alpha (not T helper type 2 cytokines) is associated with severe forms of respiratory syncytial virus bronchiolitis. *The Journal of infectious diseases* **184**:393–399.

Gaudry, M., Brégerie, O., Andrieu, V., Benna, El, J., Pocidalo, M.A. and Hakim, J. (1997). Intracellular pool of vascular endothelial growth factor in human neutrophils. *Blood* **90**:4153–4161.

Geerdink, R.J., Hennus, M.P., Westerlaken, G.H.A., Abrahams, A.C., Albers, K.I., Walk, J., Wesselink, E., *et al.* (2017). LAIR-1 limits neutrophil extracellular trap formation in viral bronchiolitis. *The Journal of allergy and clinical immunology* **141**:811–814.

Geginat, J., Lanzavecchia, A. and Sallusto, F. (2003). Proliferation and differentiation potential of human CD8+ memory T-cell subsets in response to antigen or homeostatic cytokines. *Blood* **101**:4260–4266.

Gill, M.A., Palucka, A.K., Barton, T., Ghaffar, F., Jafri, H., Banchereau, J. and Ramilo, O. (2005). Mobilization of plasmacytoid and myeloid dendritic cells to mucosal sites in children with respiratory syncytial virus and other viral respiratory infections. *The Journal of infectious diseases* **191**:1105–1115.

Glezen, W.P., Taber, L.H., Frank, A.L. and Kasel, J.A. (1986). Risk of primary infection and reinfection with respiratory syncytial virus. *American journal of diseases of children* **140**:543–546.

Gong, Y. and Koh, D.-R. (2010). Neutrophils promote inflammatory angiogenesis via release of preformed VEGF in an in vivo corneal model. *Cell and tissue research* **339**:437–448.

Goritzka, M., Durant, L.R., Pereira, C., Salek-Ardakani, S., Openshaw, P.J.M. and Johansson, C. (2014). Alpha/Beta Interferon Receptor Signaling Amplifies Early Proinflammatory Cytokine Production in the Lung during Respiratory Syncytial Virus Infection. *Journal of Virology* **88**:6128–6136.

Goritzka, M., Makris, S., Kausar, F., Durant, L.R., Pereira, C., Kumagai, Y., Culley, F.J., *et al.* (2015). Alveolar macrophage-derived type I interferons orchestrate innate immunity to RSV through recruitment of antiviral monocytes. *The Journal of Experimental Medicine* **212**:699–714.

Goritzka, M., Pereira, C., Makris, S., Durant, L.R. and Johansson, C. (2015). T cell responses are elicited against Respiratory Syncytial Virus in the absence of signalling through TLRs, RLRs and IL-1R/IL-18R. *Scientific reports* **5**:18533.

Graça-Souza, A.V., Arruda, M.A.B., de Freitas, M.S., Barja-Fidalgo, C. and Oliveira, P.L. (2002). Neutrophil activation by heme: implications for inflammatory processes. *Blood* **99**:4160–4165.

Graham, B.S., Bunton, L.A., Wright, P.F. and Karzon, D.T. (1991). Role of T lymphocyte subsets in the pathogenesis of primary infection and rechallenge with respiratory syncytial virus in mice. *Journal of Clinical Investigation* **88**:1026–1033.

Guerrero-Plata, A., Casola, A., Suarez, G., Yu, X., Spetch, L., Peeples, M.E. and Garofalo, R.P. (2006). Differential response of dendritic cells to human metapneumovirus and respiratory syncytial virus. *American journal of respiratory cell and molecular biology* **34**:320–329.

Guthrie, L.A., McPhail, L.C., Henson, P.M. and Johnston, R.B. (1984). Priming of neutrophils for enhanced release of oxygen metabolites by bacterial lipopolysaccharide. Evidence for increased activity of the superoxide-producing enzyme. *Journal of Experimental Medicine* **160**:1656–1671.

Habibi, M.S., Jozwik, A., Makris, S., Dunning, J., Paras, A., DeVincenzo, J.P., de Haan, C.A.M., *et al.* (2015). Impaired Antibody-mediated Protection and Defective IgA B-Cell Memory in Experimental Infection of Adults with Respiratory Syncytial Virus. *American Journal of Respiratory and Critical Care Medicine* **191**:1040–1049.

Halfhide, C.P., Flanagan, B.F., Brearey, S.P., Hunt, J.A., Fonceca, A.M., McNamara, P.S., Howarth, D., *et al.* (2011). Respiratory syncytial virus binds and undergoes transcription in neutrophils from the blood and airways of infants with severe bronchiolitis. *The Journal of infectious diseases* **204**:451–458.

Hall, C.B., Powell, K.R., Schnabel, K.C., Gala, C.L. and Pincus, P.H. (1988). Risk of secondary bacterial infection in infants hospitalized with respiratory syncytial viral infection. *The Journal of pediatrics* **113**:266–271.

Hall, C.B., Walsh, E.E., Long, C.E. and Schnabel, K.C. (1991). Immunity to and Frequency of Reinfection with Respiratory Syncytial Virus. *The Journal of infectious diseases* **163**:693–698.

Hall, C.B., Weinberg, G.A., Iwane, M.K., Blumkin, A.K., Edwards, K.M., Staat, M.A., Auinger, P., *et al.* (2009). The burden of respiratory syncytial virus infection in young children. *The New England journal of medicine* **360**:588–598.

Harding, M.G., Zhang, K., Conly, J. and Kubes, P. (2014). Neutrophil crawling in capillaries; a novel immune response to Staphylococcus aureus. *PLoS Pathogens* **10**:e1004379.

Haynes, L.M., Moore, D.D., Kurt-Jones, E.A., Finberg, R.W., Anderson, L.J. and Tripp, R.A. (2001). Involvement of toll-like receptor 4 in innate immunity to respiratory syncytial virus. *Journal of Virology* **75**:10730–10737.

Hägglund, S., Blodörn, K., Näslund, K., Vargmar, K., Lind, S.B., Mi, J., Araínga, M., *et al.* (2017). Proteome analysis of bronchoalveolar lavage from calves infected with bovine respiratory syncytial virus-Insights in pathogenesis and perspectives for new treatments. *PloS one* **12**:e0186594.

Heidema, J., Lukens, M.V., van Maren, W.W.C., van Dijk, M.E.A., Otten, H.G., van Vught, A.J., van der Werff, D.B.M., *et al.* (2007). CD8+ T cell responses in bronchoalveolar lavage

fluid and peripheral blood mononuclear cells of infants with severe primary respiratory syncytial virus infections. *Journal of immunology* **179**:8410–8417.

Hendaus, M.A., Jomha, F.A. and Alhammadi, A.H. (2015). Virus-induced secondary bacterial infection: a concise review. *Therapeutics and clinical risk management* **11**:1265–1271.

Henderson, J., Hilliard, T.N., Sherriff, A., Stalker, D., Shammari, N.A. and Thomas, H.M. (2005). Hospitalization for RSV bronchiolitis before 12 months of age and subsequent asthma, atopy and wheeze: A longitudinal birth cohort study. *Pediatric allergy and immunology* **16**:386–392.

Hendricks, D.A., Baradaran, K., McIntosh, K. and Patterson, J.L. (1987). Appearance of a soluble form of the G protein of respiratory syncytial virus in fluids of infected cells. *The Journal of general virology* **68**:1705–1714.

Hendricks, D.A., McIntosh, K. and Patterson, J.L. (1988). Further characterization of the soluble form of the G glycoprotein of respiratory syncytial virus. *Journal of Virology* **62**:2228–2233.

Henning, G., Ohl, L., Junt, T., Reiterer, P., Brinkmann, V., Nakano, H., Hohenberger, W., *et al.* (2001). CC chemokine receptor 7-dependent and -independent pathways for lymphocyte homing: modulation by FTY720. *Journal of Experimental Medicine* **194**:1875–1881.

Herbold, W., Maus, R., Hahn, I., Ding, N., Srivastava, M., Christman, J.W., Mack, M., *et al.* (2010). Importance of CXC chemokine receptor 2 in alveolar neutrophil and exudate macrophage recruitment in response to pneumococcal lung infection. *Infection and immunity* **78**:2620–2630.

Herring, M.J., Putney, L.F., Wyatt, G., Finkbeiner, W.E. and Hyde, D.M. (2014). Growth of alveoli during postnatal development in humans based on stereological estimation. *American journal of physiology. Lung cellular and molecular physiology* **307**:L338–44.

Hetzel, M., Walcher, D., Grüb, M., Bach, H., Hombach, V. and Marx, N. (2003). Inhibition of MMP-9 expression by PPARgamma activators in human bronchial epithelial cells. *Thorax* **58**:778–783.

Hidalgo, A., Peired, A.J., Wild, M., Vestweber, D. and Frenette, P.S. (2007). Complete identification of E-selectin ligands on neutrophils reveals distinct functions of PSGL-1, ESL-1, and CD44. *Immunity* **26**:477–489.

Hijano, D.R., Maron, G. and Hayden, R.T. (2018). Respiratory Viral Infections in Patients With Cancer or Undergoing Hematopoietic Cell Transplant. *Frontiers in microbiology* **9**:3097.

Hildreth, A.D. and O'Sullivan T.E. (2019). Tissue-resident innate and innate-like lymphocyte responses to viral infection. *Viruses* **11**:272.

Hirahara, K., Poholek, A., Vahedi, G., Laurence, A., Kanno, Y., Milner, J.D. and O'Shea, J.J. (2013). Mechanisms underlying helper T-cell plasticity: implications for immune-mediated disease. *The Journal of allergy and clinical immunology* **131**:1276–1287.

Ho, A.W.S., Prabhu, N., Betts, R.J., Ge, M.Q., Dai, X., Hutchinson, P.E., Lew, F.C., *et al.* (2011). Lung CD103+ dendritic cells efficiently transport influenza virus to the lymph node and load viral antigen onto MHC class I for presentation to CD8 T cells. *Journal of immunology* **187**:6011–6021.

Hoeksema, M., Tripathi, S., White, M., Qi, L., Taubenberger, J., van Eijk, M., Haagsman, H., *et al.* (2015). Arginine-rich histones have strong antiviral activity for influenza A viruses. *Innate immunity* **21**:736–745.

Hogan, R.J., Usherwood, E.J., Zhong, W., Roberts, A.A., Dutton, R.W., Harmsen, A.G. and Woodland, D.L. (2001). Activated antigen-specific CD8+ T cells persist in the lungs following recovery from respiratory virus infections. *Journal of immunology* **166**:1813–1822.

Hong, C.-W. (2017). Current Understanding in Neutrophil Differentiation and Heterogeneity. *Immune network* **17**:298–306.

Hörmann, N., Brandão, I., Jäckel, S., Ens, N,, Lillich, M., Walter, U. and Reinhardt, C. (2014). Gut microbial colonization orchestrates TLR2 expression, signaling and epithelial proliferation in the small intestinal mucosa. *PLoS One* **9:**e113080.

Hornung, V., Schlender, J., Guenthner-Biller, M., Rothenfusser, S., Endres, S., Conzelmann, K.-K. and Hartmann, G. (2004). Replication-dependent potent IFN-alpha induction in human plasmacytoid dendritic cells by a single-stranded RNA virus. *Journal of immunology* **173**:5935–5943.

Houben, M.L., Coenjaerts, F.E., Rossen, J.W., Belderbos, M.E., Hofland, R.W., Kimpen, J.L. and Bont, L. (2010). Disease severity and viral load are correlated in infants with primary respiratory syncytial virus infection in the community. *Journal of medical virology* **82:**1266-1271.

Hozumi, A., Nishimura, Y., Nishiuma, T., Kotani, Y. and Yokoyama, M. (2001). Induction of MMP-9 in normal human bronchial epithelial cells by TNF-alpha via NF-kappa B-mediated pathway. *American journal of physiology. Lung cellular and molecular physiology* **281**:L1444–52.

Huang, S., Wei, W. and Yun, Y. (2009). Upregulation of TLR7 and TLR3 gene expression in the lung of respiratory syncytial virus infected mice. *Wei Sheng Wu Xue Bao* **49**:239–245.

Hufford, M.M., Richardson, G., Zhou, H., Manicassamy, B., García-Sastre, A., Enelow, R.I. and Braciale, T.J. (2012). Influenza-infected neutrophils within the infected lungs act as antigen presenting cells for anti-viral CD8(+) T cells. *PloS one* **7**:e46581.

Huhta, H., Helminen, O., Kauppila, J.H., Salo, T., Porvari, K., Saarnio, J., Lehenkari, P.P. and Karttunen T.J. (2016). The expression of Toll-like receptors in normal human and murine gastrointestinal organs and the effect of microbiome and cancer. *Journal of histochemistry and cytochemistry* **64:**470-482.

Hull, J., Thomson, A. and Kwiatkowski, D. (2000). Association of respiratory syncytial virus bronchiolitis with the interleukin 8 gene region in UK families. *Thorax* **55**:1023–1027.

Hussell, T. and Bell, T.J. (2014). Alveolar macrophages: plasticity in a tissue-specific context. *Nature reviews. Immunology* **14**:81–93.

Hussell, T. and Openshaw, P.J. (1998). Intracellular IFN-gamma expression in natural killer cells precedes lung CD8+ T cell recruitment during respiratory syncytial virus infection. *The Journal of general virology* **79**:2593–2601.

Hyde, D.M., Miller, L.A., McDonald, R.J., Stovall, M.Y., Wong, V., Pinkerton, K.E., Wegner, C.D., *et al.* (1999). Neutrophils enhance clearance of necrotic epithelial cells in ozone-induced lung injury in rhesus monkeys. *The American journal of physiology* **277**:L1190–8.

Iborra, S., Martínez-López, M., Khouili, S.C., Enamorado, M., Cueto, F.J., Conde-Garrosa, R., Del Fresno, C., *et al.* (2016). Optimal Generation of Tissue-Resident but Not Circulating Memory T Cells during Viral Infection Requires Crosspriming by DNGR-1+ Dendritic Cells. *Immunity* **45**:847–860.

Ichinohe, T., Lee, H.K., Ogura, Y., Flavell, R. and Iwasaki, A. (2009). Inflammasome recognition of influenza virus is essential for adaptive immune responses. *The Journal of Experimental Medicine* **206**:79–87.

Iijima, N. and Iwasaki, A. (2014). T cell memory. A local macrophage chemokine network sustains protective tissue-resident memory CD4 T cells. *Science* **346:**93-98.

Isaacs, A. and Lindemann, J. (1957). Virus interference. I. The interferon. *Proceedings of the Royal Society of London. Series B, Biological sciences* **147**:258–267.

Ito, M., Nishio, M., Kawano, M., Kusagawa, S., Komada, H., Ito, Y. and Tsurudome, M. (1997). Role of a single amino acid at the amino terminus of the simian virus 5 F2 subunit in syncytium formation. *Journal of Virology* **71**:9855–9858.

Ivashkiv, L.B. and Donlin, L.T. (2014). Regulation of type I interferon responses. *Nature reviews. Immunology* **14**:36–49.

Jameson, S.C. and Masopust, D. (2018). Understanding Subset Diversity in T Cell Memory. *Immunity* **48**:214–226.

Janssen, R., Bont, L., Siezen, C.L.E., Hodemaekers, H.M., Ermers, M.J., Doornbos, G., Van't Slot, R., *et al.* (2007). Genetic susceptibility to respiratory syncytial virus bronchiolitis is

predominantly associated with innate immune genes. *The Journal of infectious diseases* **196**:826–834.

Jessen, B., Faller, S., Krempl, C.D. and Ehl, S. (2011). Major histocompatibility complex-dependent cytotoxic T lymphocyte repertoire and functional avidity contribute to strain-specific disease susceptibility after murine respiratory syncytial virus infection. *Journal of Virology* **85**:10135–10143.

Jewell, N.A., Vaghefi, N., Mertz, S.E., Akter, P., Peebles, R.S., Bakaletz, L.O., Durbin, R.K., *et al.* (2007). Differential type I interferon induction by respiratory syncytial virus and influenza a virus in vivo. *Journal of Virology* **81**:9790–9800.

Jia, S.H., Li, Y., Parodo, J., Kapus, A., Fan, L., Rotstein, O.D. and Marshall, J.C. (2004). Pre-B cell colony-enhancing factor inhibits neutrophil apoptosis in experimental inflammation and clinical sepsis. *Journal of Clinical Investigation* **113**:1318–1327.

Jiang, X., Clark, R.A., Liu, L., Wagers, A.J., Fuhlbrigge, R.C. and Kupper, T.S. (2012). Skin infection generates non-migratory memory CD8+ T(RM) cells providing global skin immunity. *Nature* **483**:227–231.

Jin, H.S., Suh, H.W., Kim, S.J. and Jo, E.K. (2017). Mitochondrial Control of Innate Immunity and Inflammation. *Immune network* **17**:77–88.

Johansson, C. (2016). Respiratory syncytial virus infection: an innate perspective. *F1000Research* **5**:2898.

Johnson, J.E., Gonzales, R.A., Olson, S.J, Wright, P.F. and Graham, B.S. (2007). The histopathology of fatal untreated human respiratory syncytial virus infection. *Modern Pathology* **20:**108–119.

Johnson, S.M., McNally, B.A., Ioannidis, I., Flano, E., Teng, M.N., Oomens, A.G., Walsh, E.E., *et al.* (2015). Respiratory Syncytial Virus Uses CX3CR1 as a Receptor on Primary Human Airway Epithelial Cultures. *PLoS Pathogens* **11**:e1005318.

Jones, H.G., Ritschel, T., Pascual, G., Brakenhoff, J.P.J., Keogh, E., Furmanova-Hollenstein, P., Lanckacker, E., *et al.* (2018). Structural basis for recognition of the central conserved region of RSV G by neutralizing human antibodies. *PLoS Pathogens* **14**:e1006935.

Jozwik, A., Habibi, M.S., Paras, A., Zhu, J., Guvenel, A., Dhariwal, J., Almond, M., *et al.* (2015). RSV-specific airway resident memory CD8+T cells and differential disease severity after experimental human infection. *Nature communications* **6**:10224.

Kaiko, G.E., Phipps, S., Angkasekwinai, P., Dong, C. and Foster, P.S. (2010). NK cell deficiency predisposes to viral-induced Th2-type allergic inflammation via epithelial-derived IL-25. *Journal of immunology* **185**:4681–4690.

Karavanaki, K., Polychronopoulou, S., Giannaki, M., Haliotis, F., Sider, B., Brisimitzi, M., Dimitriou, C., *et al.* (2006). Transient and chronic neutropenias detected in children with different viral and bacterial infections. *Acta paediatrica* **95**:565–572.

Karecla, P.I., Bowden, S.J., Green, S.J. and Kilshaw, P.J. (1995). Recognition of E-cadherin on epithelial cells by the mucosal T cell integrin alpha M290 beta 7 (alpha E beta 7). *European journal of immunology* **25**:852–856.

Kato, T. and Kitagawa, S. (2006). Regulation of neutrophil functions by proinflammatory cytokines. *International journal of hematology* **84**:205–209.

Kawai, T. and Akira, S. (2010). The role of pattern-recognition receptors in innate immunity: update on Toll-like receptors. *Nature immunology* **11**:373–384.

Kawasaki, T. and Kawai, T. (2014). Toll-like receptor signaling pathways. *Frontiers in immunology* **5**:461.

Keane, M.P., Belperio, J.A., Xue, Y.Y., Burdick, M.D. and Strieter, R.M. (2004). Depletion of CXCR2 inhibits tumor growth and angiogenesis in a murine model of lung cancer. *Journal of immunology* **172**:2853–2860.

Keck, T., Balcom, J.H., Fernández-del Castillo, C., Antoniu, B.A. and Warshaw, A.L. (2002). Matrix metalloproteinase-9 promotes neutrophil migration and alveolar capillary leakage in pancreatitis-associated lung injury in the rat. *Gastroenterology* **122**:188–201.

Kho, S., Minigo, G., Andries, B., Leonardo, L., Prayoga, P., Poespoprodjo, J.R., Kenangalem, E., *et al.* (2019). Circulating Neutrophil Extracellular Traps and Neutrophil Activation Are Increased in Proportion to Disease Severity in Human Malaria. *The Journal of infectious diseases* **219**:1994–2004.

Kienle, K. and Lämmermann, T. (2016). Neutrophil swarming: an essential process of the neutrophil tissue response. *Immunological reviews* **273**:76–93.

Killip, M.J., Fodor, E. and Randall, R.E. (2015). Influenza virus activation of the interferon system. *Virus Research* **209**:11–22.

Kim, H.W., Canchola, J.G., Brandt, C.D., Pyles, G., Chanock, R.M., Jensen, K. and Parrott, R.H. (1969). Respiratory syncytial virus disease in infants despite prior administration of antigenic inactivated vaccine. *American journal of epidemiology* **89**:422–434.

Kim, T.H. and Lee, H.K. (2014). Innate immune recognition of respiratory syncytial virus infection. *BMB reports* **47**:184–191.

Kim, T.S. and Braciale, T.J. (2009). Respiratory dendritic cell subsets differ in their capacity to support the induction of virus-specific cytotoxic CD8+ T cell responses. *PloS one* **4**:e4204.

Kinnear, E., Lambert, L., McDonald, J.U., Cheeseman, H.M., Caproni, L.J. and Tregoning, J.S. (2018). Airway T cells protect against RSV infection in the absence of antibody. *Mucosal Immunology* **11**:249–256.

Kirsebom, F.C.M., Kausar, F., Nuriev, R., Makris, S. and Johansson, C. (2019). Neutrophil recruitment and activation are differentially dependent on MyD88/TRIF and MAVS signaling during RSV infection. *Mucosal Immunology* **12**:1244–1255.

Kiss, G., Holl, J.M., Williams, G.M., Alonas, E., Vanover, D., Lifland, A.W., Gudheti, M., *et al.* (2014). Structural analysis of respiratory syncytial virus reveals the position of M2-1 between the matrix protein and the ribonucleoprotein complex. *Journal of Virology* **88**:7602–7617.

Kjeldsen, L., Sengeløv, H., Lollike, K., Nielsen, M.H. and Borregaard, N. (1994). Isolation and characterization of gelatinase granules from human neutrophils. *Blood* **83**:1640–1649.

Knudson, C.J., Weiss, K.A. and Hartwig, S.M. (2014). The pulmonary localization of virus-specific T lymphocytes is governed by the tissue tropism of infection. *Journal of Virology* **88**:9010–9016.

Kolaczkowska, E. and Kubes, P. (2013). Neutrophil recruitment and function in health and inflammation. *Nature reviews. Immunology* **13**:159–175.

Kościuczuk, E.M., Lisowski, P., Jarczak, J., Strzałkowska, N., Jóźwik, A., Horbańczuk, J., Krzyżewski, J., *et al.* (2012). Cathelicidins: family of antimicrobial peptides. A review. *Molecular biology reports* **39**:10957–10970.

Kotenko, S.V., Gallagher, G., Baurin, V.V., Lewis-Antes, A., Shen, M., Shah, N.K., Langer, J.A., *et al.* (2003). IFN-lambdas mediate antiviral protection through a distinct class II cytokine receptor complex. *Nature immunology* **4**:69–77.

Krishnamoorthy, N., Douda, D.N., Brüggemann, T.R., Ricklefs, I., Duvall, M.G., Abdulnour, R.-E.E., Martinod, K., *et al.* (2018). Neutrophil cytoplasts induce TH17 differentiation and skew inflammation toward neutrophilia in severe asthma. *Science Immunology* **3**:eaao4747.

Kurt-Jones, E.A., Popova, L., Kwinn, L., Haynes, L.M., Jones, L.P., Tripp, R.A., Walsh, E.E., *et al.* (2000). Pattern recognition receptors TLR4 and CD14 mediate response to respiratory syncytial virus. *Nature immunology* **1**:398–401.

Lambert, L., Sagfors, A.M., Openshaw, P.J.M. and Culley, F.J. (2014). Immunity to RSV in Early-Life. *Frontiers in immunology* **5**:466.

Lamborn, I.T., Jing, H., Zhang, Y., Drutman, S.B., Abbott, J.K., Munir, S., Bade, S., *et al.* (2017). Recurrent rhinovirus infections in a child with inherited MDA5 deficiency. *The Journal of Experimental Medicine* **214**:1949–1972.

Lawrence, M.B. and Springer, T.A. (1993). Neutrophils roll on E-selectin. *Journal of immunology* **151**:6338–6346.

Lawrence, M.B., Bainton, D.F. and Springer, T.A. (1994). Neutrophil tethering to and rolling on E-selectin are separable by requirement for L-selectin. *Immunity* **1**:137–145.

Lawrence, S.M., Corriden, R. and Nizet, V. (2018). The Ontogeny of a Neutrophil: Mechanisms of Granulopoiesis and Homeostasis. *Microbiology and molecular biology reviews* **82**:25.

Lämmermann, T. (2016). In the eye of the neutrophil swarm-navigation signals that bring neutrophils together in inflamed and infected tissues. *Journal of Leukocyte Biology* **100**:55–63.

Lämmermann, T., Afonso, P.V., Angermann, B.R., Wang, J.M., Kastenmüller, W., Parent, C.A. and Germain, R.N. (2013). Neutrophil swarms require LTB4 and integrins at sites of cell death in vivo. *Nature* **498**:371–375.

Lee, D., Schultz, J.B., Knauf, P.A. and King, M.R. (2007). Mechanical shedding of L-selectin from the neutrophil surface during rolling on sialyl Lewis x under flow. *The Journal of biological chemistry* **282**:4812–4820.

Lee, D.C.P., Harker, J.A.E., Tregoning, J.S., Atabani, S.F., Johansson, C., Schwarze, J. and Openshaw, P.J.M. (2010). CD25+ natural regulatory T cells are critical in limiting innate and adaptive immunity and resolving disease following respiratory syncytial virus infection. *Journal of Virology* **84**:8790–8798.

Lee, Y.T., Suarez-Ramirez, J.E., Wu, T., Redman, J.M., Bouchard, K., Hadley, G.A. and Cauley, L.S. (2011). Environmental and antigen receptor-derived signals support sustained surveillance of the lungs by pathogen-specific cytotoxic T lymphocytes. *Journal of Virology* **85**:4085–4094.

Lefrançois, L. and Marzo, A.L. (2006). The descent of memory T-cell subsets. *Nature* **6**:618–623.

Legg, J.P., Hussain, I.R., Warner, J.A., Johnston, S.L. and Warner, J.O. (2003). Type 1 and type 2 cytokine imbalance in acute respiratory syncytial virus bronchiolitis. *American Journal of Respiratory and Critical Care Medicine* **168**:633–639.

Leliefeld, P.H.C., Koenderman, L. and Pillay, J. (2015). How Neutrophils Shape Adaptive Immune Responses. *Frontiers in immunology* **6**:471.

LeVine, A.M., Elliott, J., Whitsett, J.A., Srikiatkhachorn, A., Crouch, E., DeSilva, N. and Korfhagen, T. (2004). Surfactant protein-d enhances phagocytosis and pulmonary clearance of respiratory syncytial virus. *American journal of respiratory cell and molecular biology* **31**:193–199.

Ley, K. (2002). Integration of inflammatory signals by rolling neutrophils. *Immunological reviews* **186**:8–18.

Ley, K., Hoffman, H.M., Kubes, P., Cassatella, M.A., Zychlinsky, A., Hedrick, C.C. and Catz, S.D. (2018). Neutrophils: New insights and open questions. *Science Immunology* **3**:eaat4579.

Li, F., Zhu, H., Sun, R., Wei, H. and Tian, Z. (2012). Natural killer cells are involved in acute lung immune injury caused by respiratory syncytial virus infection. *Journal of Virology* **86**:2251–2258.

Li, S., Strelow, A., Fontana, E.J. and Wesche, H. (2002). IRAK-4: a novel member of the IRAK family with the properties of an IRAK-kinase. *Proceedings of the National Academy of Sciences* **99**:5567–5572.

Liesman, R.M., Buchholz, U.J., Luongo, C.L., Yang, L., Proia, A.D., DeVincenzo, J.P., Collins, P.L., *et al.* (2014). RSV-encoded NS2 promotes epithelial cell shedding and distal airway obstruction. *The Journal of clinical investigation* **124**:2219–2233.

Liljeroos, L., Krzyzaniak, M.A., Helenius, A. and Butcher, S.J. (2013). Architecture of respiratory syncytial virus revealed by electron cryotomography. *Proceedings of the National Academy of Sciences of the United States of America* **110**:11133–11138.

Lim, K., Hyun, Y.-M., Lambert-Emo, K., Capece, T., Bae, S., Miller, R., Topham, D.J., *et al.* (2015). Neutrophil trails guide influenza-specific $CD8^+$ T cells in the airways. *Science* **349**:aaa4352.

Lindemans, C.A., Coffer, P.J., Schellens, I.M.M., de Graaff, P.M.A., Kimpen, J.L.L. and Koenderman, L. (2006). Respiratory syncytial virus inhibits granulocyte apoptosis through a phosphatidylinositol 3-kinase and NF-kappaB-dependent mechanism. *Journal of immunology* **176**:5529–5537.

Ling, Z., Tran, K.C. and Teng, M.N. (2009). Human respiratory syncytial virus nonstructural protein NS2 antagonizes the activation of beta interferon transcription by interacting with RIG-I. *Journal of Virology* **83**:3734–3742.

Liu, F., Wu, H.Y., Wesselschmidt, R., Kornaga, T. and Link, D.C. (1996). Impaired production and increased apoptosis of neutrophils in granulocyte colony-stimulating factor receptor-deficient mice. *Immunity* **5**:491–501.

Liu, J., Ruckwardt, T.J., Chen, M., Johnson, T.R. and Graham, B.S. (2009). Characterization of respiratory syncytial virus M- and M2-specific CD4 T cells in a murine model. *Journal of Virology* **83**:4934–4941.

Liu, P., Jamaluddin, M., Li, K., Garofalo, R.P., Casola, A. and Brasier, A.R. (2007). Retinoic acid-inducible gene I mediates early antiviral response and Toll-like receptor 3 expression in respiratory syncytial virus-infected airway epithelial cells. *Journal of Virology* **81**:1401–1411.

Loebbermann, J., Thornton, H., Durant, L., Sparwasser, T., Webster, K.E., Sprent, J., Culley, F.J., *et al.* (2012). Regulatory T cells expressing granzyme B play a critical role in controlling lung inflammation during acute viral infection. *Mucosal Immunology* **5**:161–172.

Loo, Y.M., Fornek, J., Crochet, N., Bajwa, G., Perwitasari, O., Martinez-Sobrido, L., Akira, S., *et al.* (2008). Distinct RIG-I and MDA5 signaling by RNA viruses in innate immunity. *Journal of Virology* **82**:335–345.

Ludwig, A., Petersen, F., Zahn, S., Götze, O., Schröder, J.M., Flad, H.D. and Brandt, E. (1997). The CXC-chemokine neutrophil-activating peptide-2 induces two distinct optima of neutrophil chemotaxis by differential interaction with interleukin-8 receptors CXCR-1 and CXCR-2. *Blood* **90**:4588–4597.

Lukacs, N.W., Moore, M.L., Rudd, B.D., Berlin, A.A., Collins, R.D., Olson, S.J., Ho, S.B., *et al.* (2006). Differential immune responses and pulmonary pathophysiology are induced by two different strains of respiratory syncytial virus. *The American journal of pathology* **169**:977–986.

Lukacs, N.W., Smit, J.J., Mukherjee, S., Morris, S.B., Nuñez, G. and Lindell, D.M. (2010). Respiratory virus-induced TLR7 activation controls IL-17-associated increased mucus via IL-23 regulation. *Journal of immunology* **185**:2231–2239.

Lukens, M.V., Kruijsen, D., Coenjaerts, F.E.J., Kimpen, J.L.L. and van Bleek, G.M. (2009). Respiratory syncytial virus-induced activation and migration of respiratory dendritic cells and subsequent antigen presentation in the lung-draining lymph node. *Journal of Virology* **83**:7235–7243.

Lukens, M.V., van de Pol, A.C., Coenjaerts, F.E.J., Jansen, N.J.G., Kamp, V.M., Kimpen, J.L.L., Rossen, J.W.A., *et al.* (2010). A systemic neutrophil response precedes robust CD8(+) T-cell activation during natural respiratory syncytial virus infection in infants. *Journal of Virology* **84**:2374–2383.

Mackay, L.K., Braun, A., Macleod, B.L., Collins, N., Tebartz, C., Bedoui, S., Carbone, F.R., *et al.* (2015). Cutting edge: CD69 interference with sphingosine-1-phosphate receptor function regulates peripheral T cell retention. *Journal of immunology* **194**:2059–2063.

Mackay, L.K., Wynne-Jones, E., Freestone, D., Pellicci, D.G., Mielke, L.A., Newman, D.M., Braun, A., Masson, F. *et al.* (2015). T-box transcription factors combine with the cytokines TGF-β and IL-15 to control tissue-resident memory T cell fate. *Immunity* **43:**1101-1111.

Mackay, L.K., Rahimpour, A., Ma, J.Z., Collins, N., Stock, A.T., Hafon, M.-L., Vega-Ramos, J., *et al.* (2013). The developmental pathway for CD103(+)CD8+ tissue-resident memory T cells of skin. *Nature immunology* **14**:1294–1301.

Makris, S., Bajorek, M., Culley, F.J., Goritzka, M. and Johansson, C. (2016). Alveolar Macrophages Can Control Respiratory Syncytial Virus Infection in the Absence of Type I Interferons. *Journal of Innate Immunity* **8**:452–463.

Man, W.H., de Steenhuijsen Piters, W.A.A. and Bogaert, D. (2017). The microbiota of the respiratory tract: gatekeeper to respiratory health. *Nature reviews. Microbiology* **15**:259–270.

Mani, V., Bromley, S.K., Äijö, T., Mora-Buch, R., Carrizosa, E., Warner, R.D., Hamze, M., Sen, D.R. *et al.* (2019). Migratory DCs activate TGF-β to precondition naïve $CD8^+$ T cells for tissue-resident memory fate. *Science* **366:** eaav5728.

Mantovani, A., Cassatella, M.A., Costantini, C. and Jaillon, S. (2011). Neutrophils in the activation and regulation of innate and adaptive immunity. *Nature* **11**:519–531.

Marguet, C., Bocquel, N., Benichou, J., Basuyau, J.P., Hellot, M.F., Couderc, L., Mallet, E., *et al.* (2008). Neutrophil but not eosinophil inflammation is related to the severity of a first acute epidemic bronchiolitis in young infants. *Pediatric allergy and immunology* **19**:157–165.

Marini, O., Costa, S., Bevilacqua, D., Calzetti, F., Tamassia, N., Spina, C., De Sabata, D., *et al.* (2017). Mature CD10+ and immature CD10- neutrophils present in G-CSF-treated donors display opposite effects on T cells. *Blood* **129**:1343–1356.

Marr, N., Turvey, S.E. and Grandvaux, N. (2013). Pathogen recognition receptor crosstalk in respiratory syncytial virus sensing: a host and cell type perspective. *Trends in microbiology* **21**:568–574.

Marsland, B.J., Trompette, A. and Gollwitzer, E.S. (2015). The Gut-Lung Axis in Respiratory Disease. *Annals of the American Thoracic Society* **12**:S150–6.

Masopust, D., Choo, D., Vezys, V., Wherry, E.J., Duraiswamy, J., Akondy, R., Wang, J., et al. (2010). Dynamic T cell migration program provides resident memory within intestinal epithelium. *The Journal of Experimental Medicine* **207:**553–564.

Masopust, D. and Soerens, A.G. (2019). Tissue-resident T cells and other resident leukocytes. *Annual Review of Immunology* **37:**521-546.

Masopust, D., Vezys, V., Marzo, A.L. and Lefrançois, L. (2001). Preferential localization of effector memory cells in nonlymphoid tissue. *Science* **291**:2413–2417.

Massena, S., Christoffersson, G., Hjertström, E., Zcharia, E., Vlodavsky, I., Ausmees, N., Rolny, C., *et al.* (2010). A chemotactic gradient sequestered on endothelial heparan sulfate induces directional intraluminal crawling of neutrophils. *Blood* **116**:1924–1931.

Matloubian, M., Lo, C.G., Cinamon, G., Lesneski, M.J., Xu, Y., Brinkmann, V., Allende, M.L., *et al.* (2004). Lymphocyte egress from thymus and peripheral lymphoid organs is dependent on S1P receptor 1. *Nature* **427**:355–360.

Mayadas, T.N., Cullere, X. and Lowell, C.A. (2014). The Multifaceted Functions of Neutrophils. *Annual Review of Pathology: Mechanisms of Disease* **9**:181–218.

McColl, S.R. and Clark-Lewis, I. (1999). Inhibition of murine neutrophil recruitment in vivo by CXC chemokine receptor antagonists. *Journal of immunology* **163**:2829–2835.

McNamara, P.S. (2003). Bronchoalveolar lavage cellularity in infants with severe respiratory syncytial virus bronchiolitis. *Archives of Disease in Childhood* **88**:922–926.

McNamara, P.S., Fonceca, A.M., Howarth, D., Correia, J.B., Slupsky, J.R., Trinick, R.E., Turaiki, Al, W., *et al.* (2013). Respiratory syncytial virus infection of airway epithelial cells, in vivo and in vitro, supports pulmonary antibody responses by inducing expression of the B cell differentiation factor BAFF. *Thorax* **68**:76–81.

Mejias, A., Dimo, B., Suarez, N.M., Garcia, C., Suarez-Arrabal, M.C., Jartti, T., Blankenship, D., *et al.* (2013). Whole blood gene expression profiles to assess pathogenesis and disease severity in infants with respiratory syncytial virus infection. *PLoS medicine* **10**:e1001549.

Melendez, A.J. and Tay, H.K. (2008). Phagocytosis: a repertoire of receptors and Ca(2+) as a key second messenger. *Bioscience reports* **28**:287–298.

Melero, J.A. and Moore, M.L. (2013). Influence of Respiratory Syncytial Virus Strain Differences on Pathogenesis and Immunity. *Current Topics in Microbiology and Immunology* **372**:59–82.

Meylan, E., Burns, K., Hofmann, K., Blancheteau, V., Martinon, F., Kelliher, M. and Tschopp, J. (2004). RIP1 is an essential mediator of Toll-like receptor 3-induced NF-kappa B activation. *Nature immunology* **5**:503–507.

Middleton, J., Neil, S., Wintle, J., Clark-Lewis, I., Moore, H., Lam, C., Auer, M., *et al.* (1997). Transcytosis and surface presentation of IL-8 by venular endothelial cells. *Cell* **91**:385–395.

Miller, L.S., O'Connell, R.M., Gutierrez, M.A., Pietras, E.M., Shahangian, A., Gross, C.E., Thirumala, A., *et al.* (2006). MyD88 mediates neutrophil recruitment initiated by IL-1R but not TLR2 activation in immunity against Staphylococcus aureus. *Immunity* **24**:79–91.

Minns, D., Smith, K.J. and Findlay, E.G. (2019). Orchestration of Adaptive T Cell Responses by Neutrophil Granule Contents. *Mediators of inflammation* **2019**:8968943–15.

Miralda, I., Uriarte, S.M. and McLeish, K.R. (2017). Multiple Phenotypic Changes Define Neutrophil Priming. *Frontiers in Cellular and Infection Microbiology* **7**:217.

Mitra, R., Baviskar, P., Duncan-Decocq, R.R., Patel, D. and Oomens, A.G.P. (2012). The human respiratory syncytial virus matrix protein is required for maturation of viral filaments. *Journal of Virology* **86**:4432–4443.

Morabito, K.M., Erez, N., Graham, B.S. and Ruckwardt, T.J. (2016). Phenotype and Hierarchy of Two Transgenic T Cell Lines Targeting the Respiratory Syncytial Virus KdM282-90 Epitope Is Transfer Dose-Dependent. *PloS one* **11**:e0146781.

Moore, M.L., Chi, M.H., Luongo, C., Lukacs, N.W., Polosukhin, V.V., Huckabee, M.M., Newcomb, D.C., Buchholz, U.J. *et al.* (2009). A chimeric A2 strain of respiratory syncytial virus (RSV) with the fusion protein of RSV strain line 19 exhibits enhanced viral load, mucus, and airway dysfunction. *Journal of Virology* **83:**4185-4194.

Mueller, S.N., Gebhardt, T., Carbone, F.R. and Heath, W.R. (2013). Memory T cell subsets, migration patterns, and tissue residence. *Annual review of immunology* **31**:137–161.

Mufson, M.A., Orvell, C., Rafnar, B. and Norrby, E. (1985). Two distinct subtypes of human respiratory syncytial virus. *The Journal of general virology* **66**:2111–2124.

Muraro, S.P., De Souza, G.F., Gallo, S.W., Da Silva, B.K., De Oliveira, S.D., Vinolo, M.A.R., Saraiva, E.M., *et al.* (2018). Respiratory Syncytial Virus induces the classical ROS-dependent NETosis through PAD-4 and necroptosis pathways activation. *Scientific reports* **8**:14166.

Murawski, M.R., Bowen, G.N., Cerny, A.M., Anderson, L.J., Haynes, L.M., Tripp, R.A., Kurt-Jones, E.A., *et al.* (2009). Respiratory syncytial virus activates innate immunity through Toll-like receptor 2. *Journal of Virology* **83**:1492–1500.

Murray, J., Bottle, A., Sharland, M., Modi, N., Aylin, P., Majeed, A., Saxena, S., *et al.* (2014). Risk factors for hospital admission with RSV bronchiolitis in England: a population-based birth cohort study. *PloS one* **9**:e89186.

Muruganandah, V., Sathkumara, H.D., Navarro, S. and Kupz, A. (2018). A Systematic Review: The Role of Resident Memory T Cells in Infectious Diseases and Their Relevance for Vaccine Development. *Frontiers in immunology* **9**:1574.

Nair, H., Nokes, D.J., Gessner, B.D., Dherani, M., Madhi, S.A., Singleton, R.J., O'Brien, K.L., *et al.* (2010). Global burden of acute lower respiratory infections due to respiratory syncytial virus in young children: a systematic review and meta-analysis. *Lancet* **375**:1545–1555.

Narasaraju, T., Yang, E., Samy, R.P., Ng, H.H., Poh, W.P., Liew, A.-A., Phoon, M.C., *et al.* (2011). Excessive neutrophils and neutrophil extracellular traps contribute to acute lung injury of influenza pneumonitis. *The American journal of pathology* **179**:199–210.

Narayanan, M., Owers-Bradley, J., Beardsmore, C.S., Mada, M., Ball, I., Garipov, R., Panesar, K.S., *et al.* (2012). Alveolarization continues during childhood and adolescence: new evidence from helium-3 magnetic resonance. *American Journal of Respiratory and Critical Care Medicine* **185**:186–191.

Nauseef, W.M. and Borregaard, N. (2014). Neutrophils at work. *Nature immunology* **15**:602–611.

Neyt, K. and Lambrecht, B.N. (2013). The role of lung dendritic cell subsets in immunity to respiratory viruses. *Immunological reviews* **255**:57–67.

Ng, L.G., Ostuni, R. and Hidalgo, A. (2019). Heterogeneity of neutrophils. *Nature reviews. Immunology* **19**:255–265.

Nguyen, G.T., Green, E.R. and Mecsas, J. (2017). Neutrophils to the ROScue: Mechanisms of NADPH Oxidase Activation and Bacterial Resistance. *Frontiers in Cellular and Infection Microbiology* **7**:373.

Nicolás-Ávila, J.Á., Adrover, J.M. and Hidalgo, A. (2017). Neutrophils in Homeostasis, Immunity, and Cancer. *Immunity* **46**:15–28.

Nittala, S., Subbarao, G.C. and Maheshwari, A. (2012). Evaluation of neutropenia and neutrophilia in preterm infants. *The journal of maternal-fetal & neonatal medicine* **25**:100–103.

Noah, T.L. and Becker, S. (1993). Respiratory syncytial virus-induced cytokine production by a human bronchial epithelial cell line. *The American journal of physiology* **265**:L472–8.

O'Dwyer, D.N., Dickson, R.P. and Moore, B.B. (2016). The Lung Microbiome, Immunity, and the Pathogenesis of Chronic Lung Disease. *Journal of immunology* **196**:4839–4847.

O'Shea, J.J. and Paul, W.E. (2010). Mechanisms underlying lineage commitment and plasticity of helper CD4+ T cells. *Science* **327**:1098–1102.

Odobasic, D., Kitching, A.R. and Holdsworth, S.R. (2016). Neutrophil-Mediated Regulation of Innate and Adaptive Immunity: The Role of Myeloperoxidase. *Journal of immunology research* **2016**:2349817–11.

Oliveira-Nascimento, L., Massari, P. and Wetzler, L.M. (2012). The Role of TLR2 in Infection and Immunity. *Frontiers in immunology* **3**:79.

Openshaw, P.J. and Chiu, C. (2013). Protective and dysregulated T cell immunity in RSV infection. *Current opinion in virology* **3**:468–474.

Openshaw, P.J.M., Chiu, C., Culley, F.J. and Johansson, C. (2017). Protective and Harmful Immunity to RSV Infection. *Annual Review of Immunology* **35**:501–532.

Otten, M.A., Bakema, J.E., Tuk, C.W., Glennie, M.J., Tutt, A.L., Beelen, R.H.J., van de Winkel, J.G.J., *et al.* (2012). Enhanced FcαRI-mediated neutrophil migration towards tumour colonies in the presence of endothelial cells. *European journal of immunology* **42**:1815–1821.

Paiva, C.N. and Bozza, M.T. (2014). Are reactive oxygen species always detrimental to pathogens? *Antioxidants & redox signaling* **20**:1000–1037.

Papadopoulos, N.G., Gourgiotis, D., Javadyan, A., Bossios, A., Kallergi, K., Psarras, S., Tsolia, M.N., *et al.* (2004). Does respiratory syncytial virus subtype influences the severity of acute bronchiolitis in hospitalized infants? *Respiratory medicine* **98**:879–882.

Papayannopoulos, V. (2018). Neutrophil extracellular traps in immunity and disease. *Nature reviews. Immunology* **18**:134–147.

Papayannopoulos, V. (2015). Sweet NETs, Bitter Wounds. *Immunity* **43**:223–225.

Papayannopoulos, V., Metzler, K.D., Hakkim, A. and Zychlinsky, A. (2010). Neutrophil elastase and myeloperoxidase regulate the formation of neutrophil extracellular traps. *The Journal of Cell Biology* **191**:677–691.

Peiró, T., Patel, D.F., Akthar, S., Gregory, L.G., Pyle, C.J., Harker, J.A., Birrell, M.A., *et al.* (2018). Neutrophils drive alveolar macrophage IL-1β release during respiratory viral infection. *Thorax* **73**:546–556.

Peiseler, M. and Kubes, P. (2019). More friend than foe: the emerging role of neutrophils in tissue repair. *The Journal of clinical investigation* **130**:553.

Peñaloza, H.F., Salazar-Echegarai, F.J. and Bueno, S.M. (2018). Interleukin 10 modulation of neutrophil subsets infiltrating lungs during Streptococcus pneumoniae infection. *Biochemistry and biophysics reports* **13**:12–16.

Petri, B., Phillipson, M. and Kubes, P. (2008). The physiology of leukocyte recruitment: an in vivo perspective. *Journal of immunology* **180**:6439–6446.

Phillipson, M., Kaur, J., Colarusso, P., Ballantyne, C.M. and Kubes, P. (2008). Endothelial domes encapsulate adherent neutrophils and minimize increases in vascular permeability in paracellular and transcellular emigration. *PloS one* **3**:e1649.

Pillai, P.S., Molony, R.D., Martinod, K., Dong, H., Pang, I.K., Tal, M.C., Solis, A.G., *et al.* (2016). Mx1 reveals innate pathways to antiviral resistance and lethal influenza disease. *Science* **352**:463–466.

Pillay, J., Braber, den, I., Vrisekoop, N., Kwast, L.M., de Boer, R.J., Borghans, J.A.M., Tesselaar, K., *et al.* (2010). In vivo labeling with 2H2O reveals a human neutrophil lifespan of 5.4 days. *Blood* **116**:625–627.

Pilsczek, F.H., Salina, D., Poon, K.K.H., Fahey, C., Yipp, B.G., Sibley, C.D., Robbins, S.M., *et al.* (2010). A novel mechanism of rapid nuclear neutrophil extracellular trap formation in response to Staphylococcus aureus. *Journal of immunology* **185**:7413–7425.

Pittman, K. and Kubes, P. (2013). Damage-associated molecular patterns control neutrophil recruitment. *Journal of Innate Immunity* **5**:315–323.

Pizzolla, A., Nguyen, T.H.O., Smith, J.M., Brooks, A.G., Kedzieska, K., Heath, W.R., Reading, P.C., *et al.* (2017). Resident memory CD8+ T cells in the upper respiratory tract prevent pulmonary influenza virus infection. *Science Immunology* **2**:eaam6970.

Potera, R.M., Jensen, M.J., Hilkin, B.M., South, G.K., Hook, J.S., Gross, E.A. and Moreland, J.G. (2016). Neutrophil azurophilic granule exocytosis is primed by TNF-α and partially regulated by NADPH oxidase. *Innate immunity* **22**:635–646.

Potter, N.S. and Harding, C.V. (2001). Neutrophils process exogenous bacteria via an alternate class I MHC processing pathway for presentation of peptides to T lymphocytes. *Journal of immunology* **167**:2538–2546.

Pribul, P.K., Harker, J., Wang, B., Wang, H., Tregoning, J.S., Schwarze, J. and Openshaw, P.J.M. (2008). Alveolar macrophages are a major determinant of early responses to viral lung infection but do not influence subsequent disease development. *Journal of Virology* **82**:4441–4448.

Prince, G.A., Jenson, A.B., Horswood, R.L., Camargo, E. and Chanock, R.M. (1978). The pathogenesis of respiratory syncytial virus infection in cotton rats. *The American Journal of Pathology* **93:**771–791.

Puga, I., Cols, M., Barra, C.M., He, B., Cassis, L., Gentile, M., Comerma, L., *et al.* (2012). B cell-helper neutrophils stimulate the diversification and production of immunoglobulin in the marginal zone of the spleen. *Nature immunology* **13**:170–180.

Pugin, J., Widmer, M.C., Kossodo, S., Liang, C.M., Preas HL2nd and Suffredini, A.F. (1999). Human neutrophils secrete gelatinase B in vitro and in vivo in response to endotoxin and proinflammatory mediators. *American journal of respiratory cell and molecular biology* **20**:458–464.

Randall, R.E. and Goodbourn, S. (2008). Interferons and viruses: an interplay between induction, signalling, antiviral responses and virus countermeasures. *The Journal of general virology* **89**:1–47.

Rankin, S.M. (2010). The bone marrow: a site of neutrophil clearance. *Journal of Leukocyte Biology* **88**:241–251.

Rehwinkel, J., Tan, C.P., Goubau, D., Schulz, O., Pichlmair, A., Bier, K., Robb, N., *et al.* (2010). RIG-I detects viral genomic RNA during negative-strand RNA virus infection. *Cell* **140**:397–408.

Reilly, E.C., Lambert-Emo, K. and Topham, D.J. (2016). The Effects of Acute Neutrophil Depletion on Resolution of Acute Influenza Infection, Establishment of Tissue Resident Memory (T-RM), and Heterosubtypic Immunity. *PloS one* **11**: e0164247.

Resch, B., Wörner, C., Özdemir, S., Hubner, M., Puchas, C. and Urlesberger, B. (2019). Respiratory Syncytial Virus Associated Hospitalizations in Infants of 33 to 42 Weeks' Gestation: Does Gestational Age Matter? *Klinische Padiatrie* **231**:206–211.

Richards, M.K., Liu, F., Iwasaki, H., Akashi, K. and Link, D.C. (2003). Pivotal role of granulocyte colony-stimulating factor in the development of progenitors in the common myeloid pathway. *Blood* **102**:3562–3568.

Ríos-Covián, D., Ruas-Madiedo, P., Margolles, A., Gueimonde, M., de los Reyes-Gavilán, C.G., and Salazar, N. (2016). Intestinal short chain fatty acids and their link with diet and human health. *Frontiers in microbiology* **7:**185.

Rose, E.B., Wheatley, A., Langley, G., Gerber, S. and Haynes, A. (2018). Respiratory Syncytial Virus Seasonality - United States, 2014-2017. *Morbidity and mortality weekly report* **67**:71–76.

Round, J.L. and Mazmanian, S.K. (2009). The gut microbiome shapes intestinal immune responses during health and disease. *Nature reviews immunology* **9:**313-323.

Ruckwardt, T.J., Malloy, A.M.W., Morabito, K.M. and Graham, B.S. (2014). Quantitative and qualitative deficits in neonatal lung-migratory dendritic cells impact the generation of the CD8+ T cell response. *PLoS Pathogens* **10**:e1003934.

Rudd, B.D., Smit, J.J., Flavell, R.A., Alexopoulou, L., Schaller, M.A., Gruber, A., Berlin, A.A., *et al.* (2006). Deletion of TLR3 alters the pulmonary immune environment and mucus production during respiratory syncytial virus infection. *Journal of immunology* **176**:1937–1942.

Rørvig, S., Østergaard, O., Heegaard, N.H.H. and Borregaard, N. (2013). Proteome profiling of human neutrophil granule subsets, secretory vesicles, and cell membrane: correlation with transcriptome profiling of neutrophil precursors. *Journal of Leukocyte Biology* **94**:711–721.

Sacco, R.E., Durbin, R.K. and Durbin, J.E. (2015). Animal models of respiratory syncytial virus infection and disease. *Current Opinion in Virology* **13:** 117–122.

Sabbah, A., Chang, T.H., Harnack, R., Frohlich, V., Tominaga, K., Dube, P.H., Xiang, Y., *et al.* (2009). Activation of innate immune antiviral responses by Nod2. *Nature immunology* **10**:1073–1080.

Sadik, C.D., Kim, N.D. and Luster, A.D. (2011). Neutrophils cascading their way to inflammation. *Trends in immunology* **32**:452–460.

Sallusto, F., Geginat, J. and Lanzavecchia, A. (2004). Central memory and effector memory T cell subsets: function, generation, and maintenance. *Annual Review of Immunology* **22**:745–763.

Sallusto, F., Lenig, D., Förster, R., Lipp, M. and Lanzavecchia, A. (1999). Two subsets of memory T lymphocytes with distinct homing potentials and effector functions. *Nature* **401**:708–712.

Savage, D.C. (1977). Microbial ecology of the gastrointestinal tract. *Annual review of microbiology* **31**:107–133.

Schaefer, L. (2014). Complexity of danger: the diverse nature of damage-associated molecular patterns. *The Journal of biological chemistry* **289**:35237–35245.

Schenkel, J.M. and Masopust, D. (2014). Tissue-Resident Memory T Cells. *Immunity* **41**:886–897.

Schenkel, J.M., Fraser, K.A. and Masopust, D. (2014). Resident memory CD8 T cells occupy frontline niches in secondary lymphoid organs. *Journal of immunology* **192**:2961–2964.

Schenkel, J.M., Fraser, K.A., Vezys, V. and Masopust, D. (2014). Sensing and alarm function of resident memory $CD8^+$ T cells. *Nature immunology* **14:**509-513.

Schmidt, M.E. (2018). Cytokines and CD8 T cell immunity during respiratory syncytial virus infection. *Cytokine* **S1043-4666**:30297–30297.

Schneider, W.M., Chevillotte, M.D. and Rice, C.M. (2014). Interferon-stimulated genes: a complex web of host defenses. *Annual review of immunology* **32**:513–545.

Schoggins, J.W. (2018). Recent advances in antiviral interferon-stimulated gene biology. *F1000Research* **7**:309.

Schoggins, J.W., MacDuff, D.A., Imanaka, N., Gainey, M.D., Shrestha, B., Eitson, J.L., Mar, K.B., *et al.* (2014). Pan-viral specificity of IFN-induced genes reveals new roles for cGAS in innate immunity. *Nature* **505**:691–695.

Schönrich, G. and Raftery, M.J. (2016). Neutrophil Extracellular Traps Go Viral. *Frontiers in immunology* **7**:366.

Schroder, K., Hertzog, P.J., Ravasi, T. and Hume, D.A. (2004). Interferon-gamma: an overview of signals, mechanisms and functions. *Journal of Leukocyte Biology* **75**:163–189.

Schuster, S., Hurrell, B. and Tacchini-Cottier, F. (2013). Crosstalk between neutrophils and dendritic cells: a context-dependent process. *Journal of Leukocyte Biology* **94**:671–675.

Science, M., Akseer, N., Asner, S. and Allen, U. (2019). Risk stratification of immunocompromised children, including pediatric transplant recipients at risk of severe respiratory syncytial virus disease. *Pediatric transplantation* **23**:e13336.

Segal, L.N., Clemente, J.C., Tsay, J.C., Koralov, S.B., Keller, B.C., Wu, B.G., Li, Y., Shen, N. *et al.* (2016). Enrichment of the lung microbiome with oral taxa is associated with lung inflammation of a Th17 phenotype. *Nature microbiology* **1:**16031.

Selvaggi, C., Pierangeli, A., Fabiani, M., Spano, L., Nicolai, A., Papoff, P., Moretti, C., *et al.* (2014). Interferon lambda 1-3 expression in infants hospitalized for RSV or HRV associated bronchiolitis. *The Journal of infection* **68**:467–477.

Selvatici, R., Falzarano, S., Mollica, A. and Spisani, S. (2006). Signal transduction pathways triggered by selective formylpeptide analogues in human neutrophils. *European journal of pharmacology* **534**:1–11.

Sen, G.C. (2001). Viruses and interferons. *Annual review of microbiology* **55**:255–281.

Seth, R.B., Sun, L., Ea, C.-K. and Chen, Z.J. (2005). Identification and characterization of MAVS, a mitochondrial antiviral signaling protein that activates NF-kappaB and IRF 3. *Cell* **122**:669–682.

Shafagati, N. and Williams, J. (2018). Human metapneumovirus - what we know now. *F1000Research* **7**:135.

Shi, T., Balsells, E., Wastnedge, E., Singleton, R., Rasmussen, Z.A., Zar, H.J., Rath, B.A., *et al.* (2015). Risk factors for respiratory syncytial virus associated with acute lower respiratory infection in children under five years: Systematic review and meta-analysis. *Journal of global health* **5**:020416.

Shi, T., Denouel, A., Tietjen, A.K., Campbell, I., Moran, E., Li, X., Campbell, H., *et al.* (2019). Global Disease Burden Estimates of Respiratory Syncytial Virus-Associated Acute Respiratory Infection in Older Adults in 2015: A Systematic Review and Meta-Analysis. *The Journal of infectious diseases* **352**:1749.

Shi, T., McAllister, D.A., O'Brien, K.L., Simões, E.A.F., Madhi, S.A., Gessner, B.D., Polack, F.P., *et al.* (2017). Global, regional, and national disease burden estimates of acute lower respiratory infections due to respiratory syncytial virus in young children in 2015: a systematic review and modelling study. *Lancet* **390**:946–958.

Shigeta, S., Hinuma, Y., Suto, T. and Ishida, N. (1968). The cell to cell infection of respiratory syncytial virus in HEp-2 monolayer cultures. *The Journal of general virology* **3**:129–131.

Shiow, L.R., Rosen, D.B., Brdicková, N., Xu, Y., An, J., Lanier, L.L., Cyster, J.G., *et al.* (2006). CD69 acts downstream of interferon-alpha/beta to inhibit S1P1 and lymphocyte egress from lymphoid organs. *Nature* **440**:540–544.

Siezen, C.L.E., Bont, L., Hodemaekers, H.M., Ermers, M.J., Doornbos, G., Van't Slot, R., Wijmenga, C., *et al.* (2009). Genetic susceptibility to respiratory syncytial virus bronchiolitis in preterm children is associated with airway remodeling genes and innate immune genes. *The Pediatric infectious disease journal* **28**:333–335.

Sigurs, N., Aljassim, F., Kjellman, B., Robinson, P.D., Sigurbergsson, F., Bjarnason, R. and Gustafsson, P.M. (2010). Asthma and allergy patterns over 18 years after severe RSV bronchiolitis in the first year of life. *Thorax* **65**:1045–1052.

Simoes, E.A. (1999). Respiratory syncytial virus infection. *Lancet* **354**:847–852.

Simon, S.I. and Kim, M.-H. (2010). A day (or 5) in a neutrophil's life. *Blood* **116**:511–512.

Skon, C.N., Lee, J.-Y., Anderson, K.G., Masopust, D., Hogquist, K.A. and Jameson, S.C. (2013). Transcriptional downregulation of S1pr1 is required for the establishment of resident memory CD8+ T cells. *Nature immunology* **14**:1285–1293.

Smolen, J.E., Petersen, T.K., Koch, C., O'Keefe, S.J., Hanlon, W.A., Seo, S., Pearson, D., *et al.* (2000). L-selectin signaling of neutrophil adhesion and degranulation involves p38 mitogen-activated protein kinase. *The Journal of biological chemistry* **275**:15876–15884.

Smyth, R.L. and Openshaw, P.J.M. (2006). Bronchiolitis. *Lancet* **368**:312–322.

Soehnlein, O. and Lindbom, L. (2010). Phagocyte partnership during the onset and resolution of inflammation. *Nature reviews. Immunology* **10**:427–439.

Spiegel, S. and Milstien, S. (2011). The outs and the ins of sphingosine-1-phosphate in immunity. *Nature reviews. Immunology* **11**:403–415.

Stadtmann, A. and Zarbock, A. (2012). CXCR2: From Bench to Bedside. *Frontiers in immunology* **3**:263.

Stark, M.A., Huo, Y., Burcin, T.L., Morris, M.A., Olson, T.S. and Ley, K. (2005). Phagocytosis of apoptotic neutrophils regulates granulopoiesis via IL-23 and IL-17. *Immunity* **22**:285–294.

Stein, R., Sherrill, D., Morgan, W.J., Holberg, C.J., Halonen, M., Taussig, L.M., Wright, A.L., *et al.* (1999). Respiratory syncytial virus in early life and risk of wheeze and allergy by age 13 years. *Lancet* **354**:541–545.

Steinert, E.M., Schenkel, J.M., Fraser, K.A., Beura, L.K., Manlove, L.S., Igyártó, B.Z., Southern, P.J. and Masopust, D. (2015). Quantifying memory CD8 T cells reveals regionalization of immunosurveillance. *Cell* **161:**737-749.

Stensballe, L.G., Ravn, H., Kristensen, K., Meakins, T., Aaby, P. and Simões, E.A.F. (2009). Seasonal variation of maternally derived respiratory syncytial virus antibodies and association with infant hospitalizations for respiratory syncytial virus. *The Journal of pediatrics* **154**:296–298.

Stier, M.T., Bloodworth, M.H., Toki, S., Newcomb, D.C., Goleniewska, K., Boyd, K.L., Quitalig, M., *et al.* (2016). Respiratory syncytial virus infection activates IL-13-producing group 2 innate lymphoid cells through thymic stromal lymphopoietin. *The Journal of allergy and clinical immunology* **138**:814–824.e11.

Stokes, K.L., Chi, M.H., Sakamoto, K., Newcomb, D.C., Currier, M.G., Huckabee, M.M., Lee, S., Goleniewska, K. *et al.* (2011). Differential pathogenesis of respiratory syncytial virus (RSV) clinical isolates in BALB/c mice. *Journal of Virology* **85:**5782–5793.

Stokes, K.L., Currier, M.G., Sakamoto, K., Lee, S., Collins, P.L., Plemper, R.K. and Moore, M.L. (2013). The respiratory syncytial virus fusion protein and neutrophils mediate the airway

mucin response to pathogenic respiratory syncytial virus infection. *Journal of Virology* **87**:10070–10082.

Sullender, W.M. (2000). Respiratory syncytial virus genetic and antigenic diversity. *Clinical microbiology reviews* **13**:1–15.

Summers, C., Rankin, S.M., Condliffe, A.M., Singh, N., Peters, A.M. and Chilvers, E.R. (2010). Neutrophil kinetics in health and disease. *Trends in immunology* **31**:318–324.

Sun, L., Wu, J., Du, F., Chen, X. and Chen, Z.J. (2013). Cyclic GMP-AMP synthase is a cytosolic DNA sensor that activates the type I interferon pathway. *Science* **339**:786–791.

Suzuki, K., Hino, M., Kutsuna, H., Hato, F., Sakamoto, C., Takahashi, T., Tatsumi, N., *et al.* (2001). Selective activation of p38 mitogen-activated protein kinase cascade in human neutrophils stimulated by IL-1beta. *Journal of immunology* **167**:5940–5947.

Sykes, D.A., Riddy, D.M., Stamp, C., Bradley, M.E., McGuiness, N., Sattikar, A., Guerini, D., *et al.* (2014). Investigating the molecular mechanisms through which FTY720-P causes persistent S1P(1) receptor internalization. *British Journal of Pharmacology* **171**:4797–4807.

Sørensen, O.E., Follin, P., Johnsen, A.H., Calafat, J., Tjabringa, G.S., Hiemstra, P.S. and Borregaard, N. (2001). Human cathelicidin, hCAP-18, is processed to the antimicrobial peptide LL-37 by extracellular cleavage with proteinase 3. Blood 97:3951-3959.

Tabarani, C.M., Bonville, C.A., Suryadevara, M., Branigan, P., Wang, D., Huang, D., Rosenberg, H.F., *et al.* (2013). Novel inflammatory markers, clinical risk factors and virus type associated with severe respiratory syncytial virus infection. *The Pediatric infectious disease journal* **32**:e437–42.

Tak, T., Rygiel, T.P., Karnam, G., Bastian, O.W., Boon, L., Viveen, M., Coenjaerts, F.E., *et al.* (2018). Neutrophil-mediated Suppression of Influenza-induced Pathology Requires CD11b/CD18 (MAC-1). *American journal of respiratory cell and molecular biology* **58**:492–499.

Takamura, S., Yagi, H., Hakata, Y., Motozono, C., McMaster, S.R., Masumoto, T., Fujisawa, M., *et al.* (2016). Specific niches for lung-resident memory CD8 +T cells at the site of tissue regeneration enable CD69-independent maintenance. *Journal of Experimental Medicine* **213**:3057–3073.

Takeuchi, O. and Akira, S. (2010). Pattern recognition receptors and inflammation. *Cell* **140**:805–820.

Tal, G., Mandelberg, A., Dalal, I., Cesar, K., Somekh, E., Tal, A., Oron, A., *et al.* (2004). Association between common Toll-like receptor 4 mutations and severe respiratory syncytial virus disease. *The Journal of infectious diseases* **189**:2057–2063.

Tan, J., McKenzie, C., Potamitis, M., Thorburn, A.N., Mackay, C.R. and Macia, L. (2014). The role of short-chain fatty acids in health and disease. *Advances in immunology* **121:**91-119.

Tate, M.D., Brooks, A.G. and Reading, P.C. (2008). The role of neutrophils in the upper and lower respiratory tract during influenza virus infection of mice. *Respiratory Research* **9**:932–13.

Tate, M.D., Brooks, A.G., Reading, P.C. and Mintern, J.D. (2012). Neutrophils sustain effective CD8(+) T-cell responses in the respiratory tract following influenza infection. *Immunology and cell biology* **90**:197–205.

Tate, M.D., Deng, Y.-M., Jones, J.E., Anderson, G.P., Brooks, A.G. and Reading, P.C. (2009). Neutrophils ameliorate lung injury and the development of severe disease during influenza infection. *Journal of immunology* **183**:7441–7450.

Tate, M.D., Ioannidis, L.J., Croker, B., Brown, L.E., Brooks, A.G. and Reading, P.C. (2011). The role of neutrophils during mild and severe influenza virus infections of mice. *PloS one* **6**:e17618.

Tay, S.P., Cheong, S.K., Hamidah, N.H. and Ainoon, O. (1998). Flow cytometric analysis of intracellular myeloperoxidase distinguishes lymphocytes, monocytes and granulocytes. *The Malaysian journal of pathology* **20**:91–94.

Taylor, G. (2017). Animal models of respiratory syncytial virus infection. *Vaccine* **35:**469-480.

Tayyari, F., Marchant, D., Moraes, T.J., Duan, W., Mastrangelo, P. and Hegele, R.G. (2011). Identification of nucleolin as a cellular receptor for human respiratory syncytial virus. *Nature Medicine* **17**:1132–1135.

Teijaro, J.R., Turner, D., Pham, Q., Wherry, E.J., Lefrançois, L. and Farber, D.L. (2011). Cutting edge: Tissue-retentive lung memory CD4 T cells mediate optimal protection to respiratory virus infection. *Journal of immunology* **187:**5510-5514.

Teng, T.S., Ji, A.L., Ji, X.Y. and Li, Y.Z. (2017). Neutrophils and Immunity: From Bactericidal Action to Being Conquered. *Journal of immunology research* **2017**:9671604–14.

Thomas, C.J. and Schroder, K. (2013). Pattern recognition receptor function in neutrophils. *Trends in immunology* **34**:317–328.

Thomas, J.M., Pos, Z., Reinboth, J., Wang, R.Y., Wang, E., Frank, G.M., Lusso, P., *et al.* (2014). Differential responses of plasmacytoid dendritic cells to influenza virus and distinct viral pathogens. *Journal of Virology* **88**:10758–10766.

Thompson, W.W., Shay, D.K., Weintraub, E., Brammer, L., Cox, N., Anderson, L.J. and Fukuda, K. (2003). Mortality associated with influenza and respiratory syncytial virus in the United States. *JAMA* **289**:179–186.

Thomsen, S.F., van der Sluis, S., Stensballe, L.G., Posthuma, D., Skytthe, A., Kyvik, K.O., Duffy, D.L., *et al.* (2009). Exploring the Association between Severe Respiratory Syncytial Virus Infection and Asthma A Registry-based Twin Study. *American Journal of Respiratory and Critical Care Medicine* **179**:1091–1097.

Thorburn, K., Harigopal, S., Reddy, V., Taylor, N. and van Saene, H.K.F. (2006). High incidence of pulmonary bacterial co-infection in children with severe respiratory syncytial virus (RSV) bronchiolitis. *Thorax* **61**:611–615.

Tian, J., Huang, K., Krishnan, S., Svabek, C., Rowe, D.C., Brewah, Y., Sanjuan, M., *et al.* (2013). RAGE inhibits human respiratory syncytial virus syncytium formation by interfering with F-protein function. *The Journal of general virology* **94**:1691–1700.

Tofts, P.S., Chevassut, T., Cutajar, M., Dowell, N.G. and Peters, A.M. (2011). Doubts concerning the recently reported human neutrophil lifespan of 5.4 days. *Blood* **117**:6050–6054.

Tognarelli, E.I., Bueno, S.M. and González, P.A. (2019). Immune-Modulation by the Human Respiratory Syncytial Virus: Focus on Dendritic Cells. *Frontiers in immunology* **10**:810.

Toussaint, M., Jackson, D.J., Swieboda, D., Guedan, A., Tsourouktsoglou, T.-D., Ching, Y.M., Radermecker, C., *et al.* (2017). Host DNA released by NETosis promotes rhinovirus-induced type-2 allergic asthma exacerbation. *Nature Medicine* **23**:681–691.

Tregoning, J.S., Yamaguchi, Y., Harker, J., Wang, B. and Openshaw, P.J.M. (2008). The role of T cells in the enhancement of respiratory syncytial virus infection severity during adult reinfection of neonatally sensitized mice. *Journal of Virology* **82**:4115–4124.

Triantafilou, K., Vakakis, E., Kar, S., Richer, E., Evans, G.L. and Triantafilou, M. (2012). Visualisation of direct interaction of MDA5 and the dsRNA replicative intermediate form of positive strand RNA viruses. *Journal of cell science* **125**:4761–4769.

Trompette, A., Gollwitzer, E.S., Pattaroni, C., Lopez-Mejia, I.C., Riva, E., Pernot, J., Ubags, N., Fajas, L. *et al.* (2018). Dietary fiber confers protection against flu by shaping $Ly6C^-$ patrolling monocyte hematopoiesis and $CD8^+$ T cell metabolism. *Immunity* **48:**992-1005.

Tsai, Y.F., Chu, T.C., Chang, W.Y., Wu, Y.C., Chang, F.R., Yang, S.C., Wu, T.Y., Hsu, Y.M. *et al.* (2017). 6-Hydroxy-5,7-dimethoxy-flavone suppresses the neutrophil respiratory burst via selective PDE4 inhibition to ameliorate acute lung injury. *Free radical biology and medicine* **106:**379-392.

Urban, C.F. and Nett, J.E. (2019). Neutrophil extracellular traps in fungal infection. *Seminars in cell & developmental biology* **89**:47–57.

Van Braeckel-Budimir, N., Badovinac, V.P. and Harty, J.T. (2018). Repeated Antigen Exposure Extends the Durability of Influenza-Specific Lung-Resident Memory CD8+ T Cells and Heterosubtypic Immunity. *Cell Reports* **24**:3374–3382.e3.

van der Maaten, L. and Hinton, G. (2008). Visualizing Data using t-SNE. *Journal of Machine Learning Research* **9**:2579–2605.

van Gisbergen, K.P.J.M., Sanchez-Hernandez, M., Geijtenbeek, T.B.H. and van Kooyk, Y. (2005). Neutrophils mediate immune modulation of dendritic cells through glycosylation-dependent interactions between Mac-1 and DC-SIGN. *Journal of Experimental Medicine* **201**:1281–1292.

van Schaik, S.M., Enhorning, G., Vargas, I. and Welliver, R.C. (1998). Respiratory syncytial virus affects pulmonary function in BALB/c mice. *The Journal of infectious diseases* **177**:269–276.

Villenave, R., Thavagnanam, S., Sarlang, S., Parker, J., Douglas, I., Skibinski, G., Heaney, L.G., *et al.* (2012). In vitro modeling of respiratory syncytial virus infection of pediatric bronchial epithelium, the primary target of infection in vivo. *Proceedings of the National Academy of Sciences of the United States of America* **109**:5040–5045.

Vivier, E., Artis, D., Colonna, M., Diefenbach, A., Di Santo, J.P., Eberl, G., Koyasu, S., Locksley, R.M., *et al.* (2018). Innate lymphoid cells: 10 years on. *Cell* **174:**1054-1066.

Wack, A., Terczyńska-Dyla, E. and Hartmann, R. (2015). Guarding the frontiers: the biology of type III interferons. *Nature immunology* **16**:802–809.

Wakim, L.M., Gupta, N., Mintern, J.D. and Villadangos, J.A. (2013). Enhanced survival of lung tissue-resident memory CD8$^+$ T cells during infection with influenza virus due to selective expression of IFITM3. *Nature immunology* **14**:238–245.

Wakim, L.M., Woodward-Davis, A. and Bevan, M.J. (2010). Memory T cells persisting within the brain after local infection show functional adaptations to their tissue of residence. *Proceedings of the National Academy of Sciences of the United States of America* **107**:17872–17879.

Wang, H., Peters, N. and Schwarze, J. (2006). Plasmacytoid dendritic cells limit viral replication, pulmonary inflammation, and airway hyperresponsiveness in respiratory syncytial virus infection. *Journal of immunology* **177**:6263–6270.

Wang, J. (2018). Neutrophils in tissue injury and repair. *Cell and tissue research* **371**:531–539.

Wang, J., Hossain, M., Thanabalasuriar, A., Gunzer, M., Meininger, C. and Kubes, P. (2017). Visualizing the function and fate of neutrophils in sterile injury and repair. *Science* **358**:111–116.

Warnatsch, A., Tsourouktsoglou, T.-D., Branzk, N., Wang, Q., Reincke, S., Herbst, S., Gutierrez, M., *et al.* (2017). Reactive Oxygen Species Localization Programs Inflammation to Clear Microbes of Different Size. *Immunity* **46**:421–432.

Weber, M.W., Mulholland, E.K. and Greenwood, B.M. (1998). Respiratory syncytial virus infection in tropical and developing countries. *Tropical medicine & international health* **3**:268–280.

Welliver, T.P., Garofalo, R.P., Hosakote, Y., Hintz, K.H., Avendano, L., Sanchez, K., Velozo, L., *et al.* (2007). Severe human lower respiratory tract illness caused by respiratory syncytial virus and influenza virus is characterized by the absence of pulmonary cytotoxic lymphocyte responses. *The Journal of infectious diseases* **195**:1126–1136.

Wherry, E.J., Teichgräber, V., Becker, T.C., Masopust, D., Kaech, S.M., Antia, R., Andrian, von, U.H., *et al.* (2003). Lineage relationship and protective immunity of memory CD8 T cell subsets. *Nature immunology* **4**:225–234.

Williams, M.R., Azcutia, V., Newton, G., Alcaide, P. and Luscinskas, F.W. (2011). Emerging mechanisms of neutrophil recruitment across endothelium. *Trends in immunology* **32**:461–469.

Wills-Karp, M. (2018). Neutrophil ghosts worsen asthma. *Science Immunology* **3**:eaau0112.

Wimley, W.C., Selsted, M.E. and White, S.H. (1994). Interactions between human defensins and lipid bilayers: evidence for formation of multimeric pores. *Protein science* **3**:1362–1373.

Wu, J., Sun, L., Chen, X., Du, F., Shi, H., Chen, C. and Chen, Z.J. (2013). Cyclic GMP-AMP is an endogenous second messenger in innate immune signaling by cytosolic DNA. *Science* **339**:826–830.

Wu, T., Hu, Y., Lee, Y.T., Bouchard, K.R., Benechet, A., Khanna, K. and Cauley, L.S. (2014). Lung-resident memory CD8 T cells (TRM) are indispensable for optimal cross-protection against pulmonary virus infection. *Journal of Leukocyte Biology* **95**:215–224.

Yanagawa, Y., Sugahara, K., Kataoka, H., Kawaguchi, T., Masubuchi, Y. and Chiba, K. (1998). FTY720, a novel immunosuppressant, induces sequestration of circulating mature lymphocytes by acceleration of lymphocyte homing in rats. II. FTY720 prolongs skin allograft survival by decreasing T cell infiltration into grafts but not cytokine production in vivo. *Journal of immunology* **160**:5493–5499.

Yang, D., Chen, Q., Chertov, O. and Oppenheim, J.J. (2000). Human neutrophil defensins selectively chemoattract naive T and immature dendritic cells. *Journal of Leukocyte Biology* **68**:9–14.

Yao, Y., Matsushima, H., Ohtola, J.A., Geng, S., Lu, R. and Takashima, A. (2015). Neutrophil priming occurs in a sequential manner and can be visualized in living animals by monitoring IL-1β promoter activation. *Journal of immunology* **194**:1211–1224.

Yipp, B.G., Petri, B., Salina, D., Jenne, C.N., Scott, B.N.V., Zbytnuik, L.D., Pittman, K., *et al.* (2012). Infection-induced NETosis is a dynamic process involving neutrophil multitasking in vivo. *Nature Medicine* **18**:1386–1393.

You, D., Siefker, D.T., Shrestha, B., Saravia, J. and Cormier, S.A. (2015). Building a better neonatal mouse model to understand infant respiratory syncytial virus disease. *Respiratory Research* **16**:91.

Youngblood, B., Hale, J.S., Kissick, H.T., Ahn, E., Xu, X., Wieland, A., Araki, K., *et al.* (2017). Effector CD8 T cells dedifferentiate into long-lived memory cells. *Nature* **552**:404–409.

Zanin, M., Baviskar, P., Webster, R. and Webby, R. (2016). The Interaction between Respiratory Pathogens and Mucus. *Cell host & microbe* **19**:159–168.

Zeilhofer, H.U. and Schorr, W. (2000). Role of interleukin-8 in neutrophil signaling. *Current Opinion in Hematology* **7**:178–182.

Zhang, L., Peeples, M.E., Boucher, R.C., Collins, P.L. and Pickles, R.J. (2002). Respiratory syncytial virus infection of human airway epithelial cells is polarized, specific to ciliated cells, and without obvious cytopathology. *Journal of Virology* **76**:5654–5666.

Ziegler, S.F., Ramsdell, F. and Alderson, M.R. (1994). The activation antigen CD69. *Stem cells* **12**:456–465.